TU Delft

Delft University of Technology

Remote sensing-based prediction of forest fire characteristics

Maffei, C.

DOI
10.4233/uuid:8938bc7b-27e7-4b72-b744-1d8a1b0928a5

Publication date
2022

Document Version
Final published version

Citation (APA)
Maffei, C. (2022). *Remote sensing-based prediction of forest fire characteristics*. [Dissertation (TU Delft), Delft University of Technology]. https://doi.org/10.4233/uuid:8938bc7b-27e7-4b72-b744-1d8a1b0928a5

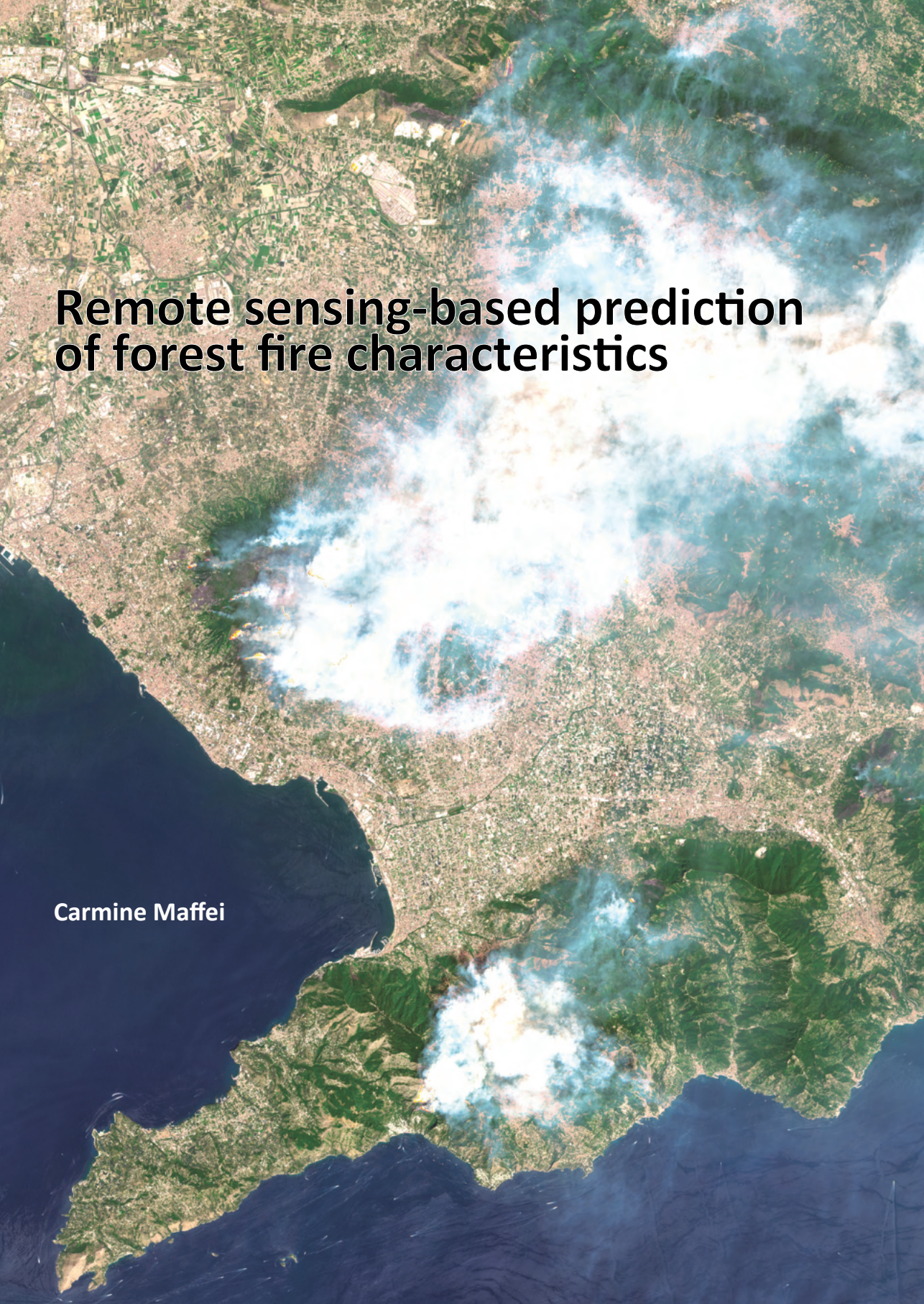
Important note
To cite this publication, please use the final published version (if applicable).
Please check the document version above.

Copyright
Other than for strictly personal use, it is not permitted to download, forward or distribute the text or part of it, without the consent of the author(s) and/or copyright holder(s), unless the work is under an open content license such as Creative Commons.

Takedown policy
Please contact us and provide details if you believe this document breaches copyrights.
We will remove access to the work immediately and investigate your claim.

This work is downloaded from Delft University of Technology.
For technical reasons the number of authors shown on this cover page is limited to a maximum of 10.

Remote sensing-based prediction of forest fire characteristics



Carmine Maffei

Remote sensing-based prediction of forest fire characteristics

Remote sensing-based prediction of forest fire characteristics

Dissertation

for the purpose of obtaining the degree of doctor

at Delft University of Technology

by the authority of the Rector Magnificus Prof.dr.ir. T.H.J.J. van der Hagen

Chair of the Board for Doctorates

to be defended publicly on

Tuesday 11, January 2022 at 10:00 o'clock

by

Carmine MAFFEI

Diploma di Laurea in Ingegneria Aerospaziale
Università degli Studi di Napoli Federico II, Italy

born in Pozzuoli, Italy

This dissertation has been approved by the promotors.

Composition of the doctoral committee:

Rector Magnificus,	chairperson
Dr. R.C. Lindenbergh,	Delft University of Technology, *promotor*
Prof.dr. M. Menenti,	Chinese Academy of Sciences, *promotor*
Independent members:	
Prof.dr.ing. W.G.M. Bastiaanssen,	Delft University of Technology
Prof R. Minciardi,	Università degli Studi di Genova
Dr. J. San-Miguel-Ayanz,	Joint Research Centre
Prof.dr. K. Tansey,	University of Leicester
Prof.dr.ir. B.J.H. van de Wiel,	Delft University of Technology
Prof.dr.ir. R.F. Hanssen	Delft University of Technology, *reserve*

TU Delft Delft University of Technology

Front & back: Sentinel-2B natural colour image of the Bay of Naples acquired on 12 July 2017 during the large fires affecting Mount Vesuvius and Sorrento Peninsula. Image processing and cover composition by Prof. Pasquale Argenziano and Ar. Teresa Patriziano.

Printed by: Ridderprint, Ohmweg 21, 2952 BD, Alblasserdam. https://www.ridderprint.nl/

© 2022 by Carmine Maffei

This work is licensed under CC BY-SA 4.0. To view a copy of this license, visit https://creativecommons.org/licenses/by-sa/4.0/.

ISBN 978-94-6384-275-4 ISBN 978-94-6384-276-1 (eBook)

An electronic version of this dissertation is available at https://repository.tudelft.nl.

In loving memory of my dad, Giuseppe (1937-2021)

Table of contents

Acknowledgements xiii
Summary xv
Samenvatting xix
List of acronyms xxiii
1. Introduction 1
1.1. Background 1
1.2. Fire management terminology 4
1.2.1. Fire hazard and fire danger 5
1.2.2. Fire risk 6
1.2.3. Fire terminology in the context of this study 7
1.3. Biophysical observables related to forest fire danger 8
1.4. Fire danger rating systems 10
1.4.1. The McArthur Forest Fire Danger Index (FFDI) 10
1.4.2. The National Fire Danger Rating System (NFDRS) of the United States 11
1.4.3. The Fire Weather Index (FWI) System 11
1.5. Contribution of remote sensing to fire danger mapping 13
1.5.1. Meteorological vs remote sensing estimation of DFMC 13
1.5.2. Meteorological vs remote sensing estimation of LFMC 14
1.5.3. Earth Observation applications in fire danger mapping 17
1.6. Research objectives and thesis outline 18
2. Campania study area and its fire regime 21
2.1. Introduction 21

2.2. Materials and methods 23
2.2.1. Study area 23
2.2.2. Fire data 27
2.2.3. Land cover and topography maps 29
2.2.4. Bubble plots 29
2.2.5. Bar charts and box plots 31
2.3. Results 31
2.3.1. Fire seasonality and inter-annual variations 31
2.3.2. Understanding spatial patterns of fire occurrence 33
2.3.3. Effect of land cover 34
2.3.4. Effect of topography 37
2.4. Discussion 39
2.4.1. Seasonality, inter-annual variation, and spatial consistency of fires 40
2.4.2. Understanding spatial patterns of fire occurrence 42
2.4.3. Influence of land cover on fire occurrence and total burned area 43
2.4.4. Influence of topography on fire occurrence and total burned area 44
2.4.5. Influence of topography and land cover on fire behaviour characteristics 45
2.5. Conclusions 45
3. Relating spatiotemporal patterns of forest fires burned area and duration to diurnal land surface temperature anomalies 47
3.1. Introduction 48
3.2. Materials and Methods 50
3.2.1. Study Area 50
3.2.2. Data 50
3.2.3. Modelling temporal patterns of LST 52
3.2.4. Evaluation of land surface temperature anomaly 53
3.2.5. Parametric distributions of burned area and fire duration 55
3.2.6. Conditional distribution of fire characteristics 56
3.3. Results 56
3.3.1. Evaluation of land surface temperature anomaly 56

3.3.2. Statistical models of burned area and fire duration 57
3.3.3. Conditional distribution of burned area and fire duration 59
3.4. Discussion 61
3.5. Conclusions 65
4. A MODIS-based perpendicular moisture index to retrieve leaf moisture content of forest canopies 67
4.1. Introduction 68
4.2. Materials and methods 70
4.2.1. Simulation of canopy reflectance spectra with PROSPECT and SAIL 70
4.2.2. Simulation of MODIS reflectance data 71
4.2.3. Development and validation of a spectral index 71
4.3. Results 75
4.3.1. Exploration of simulated MODIS reflectance data 75
4.3.2. Sensitivity of MODIS spectral reflectance to vegetation moisture 76
4.3.3. Development and validation of a spectral index sensitive to LFMC 77
4.4. Discussion 78
4.5. Conclusions 81
5. Predicting forest fires burned area and rate of spread from pre-fire multispectral satellite measurements 83
5.1. Introduction 84
5.2. Materials and methods 86
5.2.1. Study area 86
5.2.2. Data 86
5.2.3. The Perpendicular Moisture Index 88
5.2.4. Parametric distributions of fire characteristics 89
5.2.5. Conditional distributions of fire characteristics 89
5.2.6. Probability of extreme events conditional to ignition 89
5.3. Results 90
5.3.1. Temporal and spatial variability of PMI 90
5.3.2. Probability models of fire characteristics 90
5.3.3. Conditional distributions of fire characteristics 90

5.3.4. Probability of extreme events conditional to ignition 94
5.4. Discussion 95
5.5. Conclusions 105
6. Combining multi-spectral and thermal remote sensing to predict forest fire characteristics 107
6.1. Introduction 108
6.2. Materials and methods 110
6.2.1. Study area 110
6.2.2. Data 110
6.2.3. Retrieval of land surface temperature anomaly 111
6.2.4. The Perpendicular Moisture Index (PMI) 112
6.2.5. Conditional distributions of fire characteristics 112
6.2.6. Probability of extreme events conditional to ignition 113
6.3. Results 113
6.3.1. Comparing LST anomaly and PMI performance in predicting fire characteristics 113
6.3.2. Assessing the performance of LST anomaly and PMI against the FWI System components 114
6.3.3. Predicting the probability of extreme events conditional to ignition 117
6.4. Discussion 119
6.4.1. Considerations on spatial and temporal granularity of satellite data 120
6.4.2. LST anomaly and PMI as predictors of fire characteristics 122
6.4.3. Comparing the predictive performance of LST anomaly and PMI against the FWI System components 124
6.4.4. Interpreting results against combustion and propagation processes 124
6.4.5. Joint use of LST anomaly and PMI for the prediction of extreme events . 125
6.5. Conclusion 126
7. Conclusions and recommendations 129
7.1. From research questions to results 129
7.2. Novelty and impact 134
7.3. Outlook and recommendations 135

References 137
About the author 173
List of publications 175
Articles in peer-reviewed journals 175
Book chapters 176
Articles in international conference proceedings 176

Acknowledgements

This dissertation marks the end of an unbelievably long journey. It has been my night job for years and a source of opportunities to expand my knowledge, gather research independence, develop invaluable technical skills, and work with fantastic scientists and professionals. This achievement would have never been possible without the support of many people to whom goes my infinite gratitude.

The first I would like to mention is Prof. Massimo Menenti. We started discussing the potential of using remote sensing observations of forest condition to predict fire danger many years ago, well before starting this PhD venture. He has always been an inspiring scientist and a welcoming promotor. His guidance has been as essential as his review of the ideas I was proposing. Put simply, his supervision has been a firm point for the success of this study. My gratitude also goes to Dr Roderik Lindenbergh. He joined as a promotor later along the way. Nevertheless, his "helicopter view" on the material I was producing has been invaluable, allowing me to clarify concepts and improve the manuscript. In truth, interactions with him date way back in time since I started the PhD programme at Delft University of Technology. He has always been present when I needed a review, provided feedback on analytical approaches, and introduced me to scientists in his network.

I express all my gratitude to Dr Antonio Leone. I learned so much about remote sensing from him, soon after graduation. He was the first to suggest that I should be pursuing a PhD programme and introduced me to Massimo. A life changing suggestion indeed. In this study his support has been essential in characterising the fire regime in the study area. I express my gratitude to Dr Ben Gorte for his guidance on interpreting data simulated by means of radiative transfer models. A huge thank you goes to Dr Marc Schleiss for his review of some of the statistical considerations in this study and for his recommendations to further explore relationships among data.

I would like to thank Prof. Ramon Hanssen for encouraging me to complete the PhD research and for following up the progress with flexibility and support. I am immensely grateful to all Secretary staff, and specifically to Suzanne de Hoog, Lidwien de Jong, Rebeca Domingo, Debbie Rietdijk, and Irma Zomerdijk for having managed with professionalism and kindness my hospitality at TU Delft.

Special gratitude goes to those that shared, directly or indirectly, the development of this research through contributions, exchange of ideas and cups of coffee in the corridors. I am

referring to Dr Silvia Alfieri, Dr Lorenzo Iannini, Dr Hamid Ghafarian, Dr Jiaguang Li, and Dr Ali Mousivand. Their professionalism, commitment, support, and passion have been inspirational.

This study saw the support of the *Carabinieri* (Italian national gendarmerie) Forest Fire Protection Information Unit (*Nucleo Informativo Antincendio Boschivo*). They provided, in collaboration with *Dipartimento della Protezione Civile* (Italian Civil Protection Department), the fire data used in this study. However, their contribution was not just about the data, but also about a productive exchange of ideas. In this sense I am grateful to Col Angelo Marciano, Col Marco Di Fonzo, Engr Fabrizio di Liberto and Col Mauro Capone for their hospitality in warm and welcoming meetings, their time in reviewing the material I was sharing with them, the openness toward my research ideas and their constructive feedback. I am also grateful to the specialists of the Entente Valabre Dr Adrien Mangiavillano (now at Nîmes Métropole) and Col Claude Picard for the precious insights into their activities. They raised my attention on the need to predict emergencies. This later drove my efforts to translate remote sensing observations of forest condition into probabilities of extreme forest fires.

I already mentioned that this study has been my night job for a few years. Yet it would not have been possible without the flexibility of my employers and of my line managers. I am grateful to Rajinder Bhuhi, Prof. Stephan Reiff-Marganiec, Roberto Tartaglia Polcini and Anjuu Trevedi MBE for all the support they were able to provide. I would also express a special thank you to Prof. Heiko Balzter, Dr Mariano Focareta, Engr Giuseppe Meoli, and John Roberts. The exchange of ideas with them has been part of the successful recipe of this dissertation.

This study was entirely based on the use of open-source software: GDAL/OGR (GDAL/OGR Contributors, 2021), GNU Octave (Eaton et al., 2020) with HANTS (Abouali, 2021), GRASS GIS (GRASS Development Team, 2020), Python (van Rossum and de Boer, 1991), QGIS (QGIS Development Team, 2021), and R (R Core Team, 2020) with packages caret (Kuhn, 2021), evd (Stephenson, 2002), fitdistrplus (Delignette-Muller and Dutang, 2015), ggplot2 (Wickham, 2016), trend (Pohlert, 2020). The silent work of their respective communities is a powerful enabler of research and innovation.

Afar from computers, journal papers and books, I found strength and support in my partner Andrea, my family, and my friends. Without their encouragement and love I could have never made it. Among my friends, I want to mention Dr Anna Tedeschi, who has been fiercely pushing me to never give up, Marcello Bellavista, much quieter supporter but also an essential language reviewer of wide parts of this manuscript, Prof. Pasquale Argenziano and Ar. Teresa Patriziano for being always by my side and for the time spent in preparing the cover of this dissertation.

Finally, I am grateful to the past me for having decided to go this route at the expense of some other ways to employ leisure time. It was worth it, for the journey, not the end.

Summary

Forest fires are a major ecosystem disturbance at global scale, put pressure on agencies in charge of citizens and infrastructure security and cause unvaluable human losses. Fires are controlled by multiple static and dynamic drivers related to topography, land cover, climate, weather, and anthropic activity. Among these, weather is an active driver of live and dead fuel moisture, which has a direct effect on fire occurrence and behaviour. As a result, in areas experiencing prolonged droughts and heat waves, altered meteorological patterns lead to increased frequency and intensity of forest fires.

The operational response of governments, local authorities, forest managers and civil protection agencies in charge of managing forest fires is informed by the assessment of factors controlling fire occurrence and behaviour, often synthesised in maps of fire danger. Danger is defined as the resultant of all factors affecting the inception, spread, and difficulty of control of fires, and it is typically expressed in the form of an index.

Key contributors to fire danger are fuel type, amount, and conditions, notably with respect to moisture content. Remote sensing measurements in the shortwave infrared are sensitive to water content of live fuels, while measurements in the thermal infrared allow the detection of vegetation stress conditions due to vapour pressure deficit. In fact, several scholars proved that satellite estimates of vegetation water content and of land surface temperature could be effectively used to predict fire occurrence. Nevertheless, to the best of this author's knowledge, no research was previously published connecting pre-fire remote sensing measurements to fire behaviour characteristics. This clearly identifies a knowledge gap which needs further investigation and that can be translated in the following research question: to what extent can remote sensing of forest condition be used to predict fire behaviour characteristics and assess the probability of extreme events?

The research described in this dissertation aimed at developing methods based on pre-fire optical and thermal remote sensing observations of forests for the prediction of fire behaviour characteristics. The study was carried out in Campania, Italy (13595 km^2), one of the most densely populated and fire affected regions in the Mediterranean. Data on all fire events recorded between 2002 and 2011 was provided by Carabinieri (Italian national gendarmerie) forest fire preparedness unit (*Nucleo Informativo Antincendio Boschivo*, NIAB). The study made use of MODIS land surface temperature (LST) and surface

reflectance collection 6 products, which are publicly available on the USGS Land Processes Distributed Active Archive Center (LP DAAC). Approach was probabilistic in nature, trying to relate pre-fire satellite observations of vegetation conditions to the probability distributions of burned area, fire duration and rate of spread.

Efforts initially focussed on assessing LST anomaly and its effect on fire behaviour characteristics. LST anomaly is a measure of excess enthalpy stored in fuels. It controls the probability of flames extinction and thus fire duration. First, a climatology of LST was constructed from the longest available time series of daily MODIS LST by means of the Harmonic Analysis of Time Series (HANTS) algorithm. HANTS was then used to construct annual models of daily LST. Finally, the daily LST anomaly was evaluated as the difference between the annual model and the climatology. Fires in the database were then associated with LST anomaly values recorded at their corresponding location on the day prior to the event. Probability distribution functions of log-transformed burned area (normal), log-transformed fire duration (generalised extreme value, GEV) and log-transformed rate of spread (Weibull) where then determined in ten decile bins of LST anomaly. The mean and the standard deviation of the normal distribution of log-transformed burned area showed a clear linear dependence on LST anomaly (r^2=0.81, $p<0.001$ and r^2=0.52, $p<0.05$ respectively), indicating an increase in the probability of large fires with increasing LST anomaly. Similarly, a marked linear dependence on LST anomaly was found for the location (r^2=0.78, $p<0.001$), scale (r^2=0.79, $p<0.001$) and shape (r^2=0.87, $p<0.001$) of the GEV distribution of log-transformed fire duration, favouring longer fire duration with increasing LST anomaly. Conversely, the LST anomaly had a limited effect on the Weibull distribution of log-transformed rate of spread, with scale and shape showing slightly decreasing trends (r^2=0.50, $p<0.05$ and r^2=0.54, $p<0.05$ respectively). A likelihood ratio test showed that the probability models of log-transformed burned area, fire duration and rate of spread conditional to LST anomaly (alternative models) allowed the rejection of the corresponding unconditional models fitting all data (null models), confirming that LST anomaly is a covariate of burned area, fire duration and, to a lesser extent, rate of spread. These results are in line with expectations from models of the combustion process.

Following a similar line of reasoning, this study further focussed on remote sensing of live fuel moisture content (LFMC). This vegetation property controls ignition delay, and thus affects flames propagation. The first step was the construction of a novel spectral index, the perpendicular moisture index (PMI), specifically designed to be sensitive to LFMC. The PMI was developed from simulated vegetation spectral data convolved to MODIS bands by noting that in the spectral reflectance subspace of MODIS bands 2 (0.86 μm) and 5 (1.24 μm) isolines of LFMC can be identified, and that these isolines are straight and parallel. By taking as a reference the line corresponding to LFMC=0 (completely dry vegetation), the PMI was calculated as the distance of measured reflectance from the reference line. The PMI is thus a measure of LFMC, and higher values of PMI correspond to higher moisture content. The index was found to be linearly related to LFMC, especially for dense vegetation cover (r^2=0.70 when leaf area index is larger than 2, r^2=0.87 when larger than 4). When vegetation cover is less dense, the contribution of soil background to the measured reflectance increases, and the PMI underestimates LFMC.

PMI maps were produced from the MODIS 8-day composited reflectance product, and fires in the database were associated with the corresponding PMI value at the fire location in the pre-fire compositing period. Using the same approach adopted for LST anomaly, the probability distribution functions of log-transformed burned area, fire duration and rate of spread were determined in ten decile bins of PMI. The mean of the normal distribution of log-transformed burned area showed a clear linear dependence on PMI (r^2=0.80, p<0.001), while no trend could be observed for standard deviation. A clear linear dependence on PMI was also found for scale and shape of the Weibull distribution of log-transformed rate of spread (r^2=0.97, p<0.001 and r^2=0.82, p<0.001 respectively). These results were further confirmed by a likelihood ratio test where the probability models of log-transformed burned area and rate of spread conditional to PMI allowed the rejection of the corresponding unconditional models fitting all data. Location and shape of the GEV distribution of log-transformed fire duration showed no significant linear trend with PMI, whereas scale showed a weak trend (r^2=0.55, p<0.05). However, in the likelihood ratio test the probability model of log-transformed fire duration conditional to PMI failed to reject the corresponding unconditional model. These results showed that PMI is a covariate of burned area and rate of spread, as expected from flames propagation models, but not of fire duration.

Predictions of fire characteristics based on concurrent observations of LST anomaly and PMI were compared with predictions based on the Fire Weather Index (FWI) System. This fire danger rating tool proved to be effective in several areas worldwide, including Europe. FWI values from weather reanalysis data were associated with fires in the database and were analysed with the same approach adopted for LST anomaly and PMI. It was found that parameters of the probability distribution function of log-transformed burned area and fire duration conditional to FWI System components followed clear linear trends, with increasing danger values leading to higher probabilities of large burned areas and long fire durations. Conversely, FWI System components were unrelated to the rate of spread. Trend analysis (coefficient of determination and p-value of the linear fit, Sen's slope and Mann-Kendall test) and likelihood ratio tests were used to compare the trends in the parameters of the probability distributions of fire characteristics. It was shown that remote sensing predictions of burned area and fire duration were comparable or better than those from FWI, and that PMI is a good predictor of the rate of spread whereas FWI System components are not.

The identified linear trends in the dependence of the parameters of the probability distribution of log-transformed burned area, fire duration and rate of spread on LST anomaly and on PMI allow the prediction of the probability of extreme events, conditional to ignition, as a function of pre-fire remote sensing observations. As both LST anomaly and PMI are good covariates of burned area, these two remote sensing observations of vegetation conditions can be used jointly to improve the prediction of the probability of fires larger than say, the 95th percentile of all events recorded in the study area (30 ha). It was found that the probability of a fire resulting in a burned area larger than 30 ha increases from 0.9% to 9.2% with pre-fire LST anomaly increasing from -2.1 to 4.3 K and increases from 1.8% to 7.4% with pre-fire PMI decreasing from 0.052 to -0.032. When the probability of fires exceeding 30.0 ha is modelled as a function of both LST anomaly and PMI, the

probability increases from 0.5% to 12.7%. This confirms that the joint use of LST anomaly and PMI leads to improved predictions.

The scientific community showed a consensus on the need to improve fire danger prediction through a more accurate assessment of live fuel condition. Existing fire danger rating systems estimate fuel moisture content from meteorological variables, which results in an undesired approximated solution due to underlying assumptions. Consequently, any direct observation of fuel moisture content has the potential to enable a better evaluation of fire occurrence and fire danger indices. From a remote sensing perspective, these considerations are translated in the research question on the need to understand to what extent can satellite measurements be used to predict forest fire behaviour characteristics. This research showed that remote sensing of vegetation in the optical and thermal domains allows the prediction of the probability distributions of fire behaviour characteristics such as burned area, duration, and rate of spread. These can be further used to evaluate the probability of extreme events, conditional to ignition, as a function of pre-fire remote sensing measurements, contributing to predict danger. It should be noted once more that this result was achieved by using pre-fire remote sensing observations, allowing the prediction of fire characteristics. In perspective, results showed in this dissertation can support the development of operational tools for forest managers and civil protection agencies in their fire preparedness activities.

Samenvatting

Bosbranden zijn verantwoordelijk voor wereldwijde verstoringen van het ecosysteem, leggen druk op instanties die burgers en infrastructuur beveiligen en veroorzaken veel menselijk leed en hoge kosten. De ontwikkeling van bosbranden wordt bepaald door meerdere statische en dynamische factoren zoals topografie, bodembedekking, klimaat, weer en menselijke activiteiten. Het weer is een actieve aanjager van de hoeveelheid vocht in levende en dode brandstof, wat een direct effect heeft op het begin en de ontwikkeling van een brand. In het bijzonder leiden meteorologische veranderingen, zoals het vaker optreden van langdurige droogte en hittegolven tot een verhoogde frequentie en intensiteit van bosbranden.

Mogelijke acties van landelijke en lokale autoriteiten, bosbeheerders en andere instanties verantwoordelijk voor bosbrand beheersing, worden gebaseerd op de beoordeling van factoren die het optreden en het gedrag van branden karakteriseren. Vaak worden zulke factoren samengevat in brandgevaar kaarten. Gevaar wordt gedefinieerd als de uitkomst van alle factoren die van invloed zijn op het ontstaan, de verspreiding en de moeilijkheidsgraad van het beheersen van branden, en wordt doorgaans uitgedrukt in de vorm van een index.

De belangrijkste factoren die bijdragen aan brandgevaar zijn het brandstoftype, de hoeveelheid en de omstandigheden, met name met betrekking tot de hoeveelheid vocht. Remote sensing-metingen in het kortgolvig-infrarood zijn gevoelig voor het watergehalte van levende brandstoffen, terwijl metingen in het thermische infrarood de detectie van vegetatiestress mogelijk maken. Verschillende wetenschappers hebben zelfs bewezen dat satellietschattingen van het watergehalte van de vegetatie en van de temperatuur van het landoppervlak effectief kunnen worden gebruikt om het optreden van brand te voorspellen. Desalniettemin is er, voor zover deze auteur weet, nog geen onderzoek gepubliceerd dat remote sensing-metingen van voor een brand koppelt aan het gedrag van een brand. Deze kennislacune wordt vertaald in de volgende onderzoeksvraag: in hoeverre kunnen satellietmetingen van de conditie van bossen gebruikt worden om brandgedrag te voorspellen en de waarschijnlijkheid van extreme gebeurtenissen te beoordelen?

Het onderzoek in dit proefschrift is gericht op het ontwikkelen van methoden gebruik makend van optische en thermische satellietwaarnemingen van onverbrande bossen voor

de karakterisatie van brandgedrag. Het onderzoek werd uitgevoerd in Campania, Italië een van de dichtstbevolkte en meest door brand getroffen regio's rond de Middellandse Zee. Gegevens over alle geregistreerde branden tussen 2002 en 2011 zijn verstrekt door de Carabinieri (Italiaanse nationale politie) afdeling voor bosbranden (*Nucleo Informativo Antincendio Boschivo*, NIAB). De studie maakte gebruik van openbare satelliet producten bestaande uit MODIS-landoppervlaktetemperatuur (LST) en gecorrigeerde spectrale reflecties in 6 golflengtes. De aanpak is probabilistisch van aard en relateert satellietwaarnemingen van de vegetatieomstandigheden vóór de brand aan verschillende waarschijnlijkheidsverdelingen met betrekking tot het verbrande gebied, de brandduur en de verspreidingssnelheid van de brand

Het onderzoek was aanvankelijk gericht op het beoordelen van LST-afwijkingen en de relatie met brandgedrag. LST-afwijking is een maat voor overtollige enthalpie opgeslagen in brandstof. Kort gezegd, bepaalt enthalpie in grote mate de kans op het doven van vlammen en dus de brandduur. Eerst werd het langdurig verloop van LST geconstrueerd uit de langst beschikbare tijdreeksen van dagelijkse MODIS LST door middel van het Harmonic Analysis of Time Series (HANTS) algoritme. HANTS werd vervolgens gebruikt om jaarlijkse modellen van dagelijkse LST te construeren. Ten slotte werd de dagelijkse LST-afwijking geëvalueerd als het verschil tussen het jaarmodel en de klimatologie. Branden in de database werden vervolgens gerelateerd aan LST-afwijkingswaarden geregistreerd op de dag voorafgaand aan de brand. Vervolgens werden kansverdelingsfuncties van log-getransformeerd verbrand gebied (normaal), log-getransformeerde brandduur (gegeneraliseerde extreme waarde, GEV) en log-getransformeerde verspreidingssnelheid (Weibull) bepaald. Het gemiddelde en de standaardafwijking van de normale verdeling van het log-getransformeerde verbrande gebied vertoonde een duidelijke lineair verband met de LST-afwijking wat wijst op een toename van de kans op grote branden met toenemende LST-afwijking. Evenzo werd een duidelijke lineaire afhankelijkheid van de LST-anomalie gevonden voor locatie, schaal en vorm van de GEV-verdeling van log-getransformeerde brandduur, wat een langere brandduur suggereert met toenemende LST-afwijking. Omgekeerd had de LST-afwijking een beperkt effect op de Weibull-verdeling van de log-getransformeerde spreidingssnelheid, waarbij schaal en vorm licht afnemende trends vertoonden. Een waarschijnlijkheidsverhoudingstest toonde aan dat de LST-afwijking een zogenaamde covariabele is van verbrand gebied, brandduur en, in mindere mate, verspreidingssnelheid. Deze resultaten zijn in lijn met wat verwacht kan worden op grond van modellen van het verbrandingsproces.

Op een vergelijkbare manier is ook satellietdata van het vochtgehalte van levende brandstof (LFMC) bestudeerd. Deze vegetatie-eigenschap regelt de ontstekingsvertraging en beïnvloedt dus de verspreiding van vlammen. De eerste stap was de constructie van een nieuwe spectrale index, de zogenaamde verticale vochtindex (PMI), speciaal ontworpen om gevoelig te zijn voor LFMC. PMI is ontwikkeld door gesimuleerde spectrale vegetatiegegevens te relateren aan de respons in 2 spectrale MODIS-banden. Door als referentie de lijn te nemen die overeenkomt met LFMC=0 (volledig droge vegetatie), werd de PMI berekend als de afstand van de gemeten reflectie tot de referentielijn. De PMI is dus een maat voor LFMC, en hogere PMI-waarden komen overeen met een hoger vochtgehalte. De index bleek lineair gerelateerd te zijn aan LFMC, vooral in het geval van

dichte vegetatiebedekking. Wanneer de vegetatiebedekking minder dicht is, neemt de bijdrage van de bodem onder de vegetatie aan de gemeten reflectie toe en onderschat de PMI de LFMC.

PMI-kaarten werden geproduceerd op basis van het MODIS 8-daagse samengestelde reflectieproduct. Vervolgens werden branden in de database geassocieerd met de overeenkomstige PMI-waarde op de brandlocatie in de periode vóór de brand. Met dezelfde benadering als voor LST-afwijkingen, werden de kansverdelingsfuncties van log-getransformeerd verbrand gebied, brandduur en verspreidingssnelheid bepaald. Het gemiddelde van de normale verdeling van het log-getransformeerde verbrande gebied vertoonde een duidelijke lineaire afhankelijkheid van, terwijl er geen trend kon worden waargenomen voor de standaardafwijking. Er werd ook een duidelijke lineaire afhankelijkheid van PMI gevonden voor schaal en vorm van de Weibull-verdeling van de log-getransformeerde spreidingssnelheid. Deze resultaten werden verder bevestigd door een waarschijnlijkheidsratio-test. Locatie en vorm van de GEV-verdeling van log-getransformeerde brandduur vertoonden geen significante lineaire trend met PMI, terwijl schaal een zwakke trend vertoonde. Deze resultaten toonden aan dat PMI een covariabele is van het verbrande gebied en de verspreidingssnelheid, zoals verwacht van vlamvoortplantingsmodellen, maar niet van brandduur.

Voorspellingen van brandkenmerken op basis van gelijktijdige waarnemingen van LST-afwijkingen en PMI werden vergeleken met voorspellingen op basis van het Fire Weather Index (FWI)-systeem. Deze applicatie voor het beoordelen van brandgevaar bleek effectief te zijn in verschillende gebieden wereldwijd, waaronder Europa. FWI-waarden uit gegevens uit de weeranalyse werden geassocieerd met branden in de database en werden geanalyseerd met dezelfde benadering die werd gebruikt voor LST-afwijkingen en PMI. Er werd gevonden dat parameters van de kansverdelingsfunctie van log-getransformeerd verbrand gebied en brandduur afhankelijk van FWI-componenten duidelijke lineaire trends volgden, waarbij toenemende gevaarwaarden effectief leidden tot hogere kansen op grote verbrande gebieden en lange brandduur. Omgekeerd waren de FWI-componenten niet gerelateerd aan de verspreidingssnelheid. Statistische trendanalyse werd gebruikt om de trends in de parameters van de kansverdelingen van brandkenmerken te vergelijken. Er werd aangetoond dat satelliet gebaseerde voorspellingen van verbrande oppervlakte en brandduur vergelijkbaar of beter waren dan die van FWI, en dat PMI een goede voorspeller is van de verspreidingssnelheid, terwijl FWI-componenten dat niet zijn.

De geïdentificeerde lineaire afhankelijkheden maken het mogelijk om de kans op extreme brand-gerelateerde gebeurtenissen, te voorpellen als functie van satellietwaarnemingen. Aangezien zowel de LST-afwijking als de PMI goede covariaten zijn van het verbrande gebied, kunnen deze twee satellietwaarnemingen van de vegetatieomstandigheden samen worden gebruikt om de voorspelling van de kans op branden te verbeteren die groter zijn dan bijvoorbeeld het 95^{e} percentiel van alle gebeurtenissen in een studiegebied. De resultaten laten zien dat de kans op een brand met een verbrand gebied groter dan 30 ha toeneemt van 0,9% tot 9,2% wanneer de LST-afwijking toeneemt van -2,1 tot 4,3 K terwijl die kans toeneemt van 1,8% tot 7,4% wanneer PMI daalt van 0,052 naar -0,032. Wanneer de LST-afwijking als de PMI samen worden gebruikt, neemt de kans op zo'n grote brand toe

van 0,5% naar 12,7%. Dit bevestigt dat het gezamenlijke gebruik van LST-afwijking en PMI tot betere voorspellingen leidt.

Er is consensus over de noodzaak om de voorspelling van brandgevaar te verbeteren door een nauwkeurigere beoordeling van de toestand van levende brandstof. Bestaande classificatiesystemen voor brandgevaar schatten het brandstofvochtgehalte op basis van alleen meteorologische metingen, wat vaak resulteert in minder goede schattingen. Elke directe waarneming van het brandstofvochtgehalte kan een betere evaluatie mogelijk maken van het optreden van brand en van de brandgevaarindices. Daarom was het doel van de onderzoeksvraag om te begrijpen in hoeverre satellietmetingen kunnen worden gebruikt om kenmerken van bosbrandgedrag te voorspellen. Dit onderzoek toonde aan dat remote sensing van vegetatie in het optische en thermische domein brandgedragskenmerken zoals verbrand oppervlak, duur en verspreidingssnelheid kan voorspellen. Deze voorspellingen kunnen worden gebruikt om de waarschijnlijkheid van extreme gebeurtenissen te evalueren, afhankelijk van ontsteking, als een functie van remote sensing-metingen vooraf, wat effectief bijdraagt aan het voorspellen van gevaar. Hierbij moet nogmaals worden opgemerkt dat dit resultaat is bereikt door gebruik te maken van remote sensing-waarnemingen voordat een band plaats vindt, en dat daarmee brandkarakteristieken kunnen worden voorspeld. De resultaten in dit proefschrift kunnen daarom bijdragen aan het verbeteren van operationele instrumenten voor bosbeheerders en beschermingsinstanties bij hun dagelijks werk om kwetsbare gebieden en hun bewoners te beschermen.

List of acronyms

BUI	Build-Up Index
CLC	Coordination of Information on the Environment (CORINE) Land Cover
DC	Drought Code
DEM	Digital elevation model
DFMC	Dry fuel moisture content
DMC	Duff Moisture Code
DOD	Degree of over determinedness
EWT	Equivalent water thickness
FET	Fit error tolerance
FFDI	McArthur Forest Fire Danger Index
FFMC	Fine Fuel Moisture Code
FWI	Fire Weather Index
GEV	Generalised extreme value
GVMI	Global vegetation moisture index
HANTS	Harmonic analysis of time series
ISI	Initial Spread Index
JM	Jeffries-Matusita (distance)
KBDI	Keetch-Byram drought index
LAI	Leaf area index
LFMC	Live fuel moisture content
LOOCV	Leave-one-out cross-validation
LP DAAC	Land Processes Distributed Active Archive Center
LST	Land surface temperature

NDVI	Normalised difference vegetation index
NDWI	Normalised difference water index
NFDRS	National Fire Danger Rating System of the United States
NIR	Near infrared
PMI	Perpendicular moisture index
PROSPECT	Leaf optical properties model
QA	Quality assurance
RTM	Radiative transfer model
SAIL	Scattering by Arbitrarily Inclined Leaves radiative transfer model
SNR	Signal-to-noise ratio
SWIR	Shortwave infrared
TIR	Thermal infrared
TOC	Top of the canopy

1. Introduction

1.1. Background

Forest fires (Figure 1.1) are a major driver of ecosystem disturbance at global scale (Bond et al., 2005; Krebs et al., 2010; Pyne et al., 1996), affect the biogeochemical cycle (Thonicke et al., 2008), are a source of atmospheric emissions (Lehsten et al., 2009; Parker et al., 2016; van der Werf et al., 2010), alter the net carbon balance (Lasslop et al., 2019; Seidl et al., 2014), disturb forest structure (Harvey et al., 2016), and cause long-term changes in soil properties (Bowd et al., 2019; Certini, 2005). Fires also condition anthropic activities as they threaten human lives (Viegas, 2009), have a negative effect on quality of life (FAO, 2007; Reisen et al., 2015), and cause substantial economic loss (Montagné-Huck and Brunette, 2018; Pellegrini et al., 2018). Several habitats are characterised by recurring fires, with vegetation communities depending on fires to maintain biodiversity and productivity (Morgan et al., 2001; Parra and Moreno, 2017; Pugh et al., 2019). Globally, a decline in burned areas in savannas and grasslands has been observed, essentially driven by change in land use, although patterns in reduction vary substantially across different regions (Andela et al., 2017; Turco et al., 2016). Reversely, increasing trends in burned area have been reported in forest ecosystems (Abatzoglou et al., 2019; Andela et al., 2017; Liu et al., 2010), and evidence supports the hypothesis that climate change may be altering fire dynamics (Anderegg et al., 2020; Lozano et al., 2010; Stevens-Rumann et al., 2018) through the direct and indirect effects that weather variability exerts on fuel moisture and availability (Pausas and Ribeiro, 2013; Seidl et al., 2017; Williams and Abatzoglou, 2016) and ultimately on spatial and temporal patterns of fire occurrence and on fire behaviour (Flannigan et al., 2016; Podschwit et al., 2018; Syphard et al., 2018).

Fires are controlled by multiple static and dynamic drivers related to topography, land cover, climate, weather and anthropic activity (Lasslop and Kloster, 2017; Littell et al., 2016; Mhawej et al., 2015). Among these, weather is an active driver of live and dead fuel moisture (Trenberth et al., 2014; Ustin et al., 2009; Williams and Abatzoglou, 2016). Fuel moisture has in turn a direct effect on fire occurrence and behaviour, as the proportion of water in live and dead fuels controls ignition delay, probability of extinction and rate of spread (Chuvieco et al., 2009; Finney et al., 2013; Rothermel, 1972; Wilson, 1985). As a result, in areas experiencing prolonged droughts and heat waves, such as the Mediterranean basin, altered meteorological patterns create the preconditions for



Figure 1.1. Forest fire in Maiella National Park, Italy, 20th August 2017. Photo © 2017 by Salvatore Mancini, CC BY-SA 4.0.

increased frequency and intensity of forest fires (Gudmundsson et al., 2014; Lindner et al., 2010).

Society is faced with the need to manage forest fires with preparedness and response efforts aimed at increasing the security of citizens and properties, and at preserving the services and the natural development of the biomes being affected. Such efforts encompass mitigation, preparedness, response and recovery (Gunes and Kovel, 2000; Mohamed Shaluf, 2008; Oliveira et al., 2017), and are summarized in the fire management cycle (Figure 1.2).

Mitigation refers to prevention activities aimed at the reduction of the probability of a fire to spread and of the damage caused by those fires that actually occur (Brenkert–Smith et al., 2006; Burns and Cheng, 2007; Fernandes, 2013; Gunes and Kovel, 2000; McFarlane et al., 2011). Preparedness encompasses all initiatives aimed at developing operational response capabilities in case of a fire, including exercises and training (Gunes and Kovel, 2000; Minas et al., 2012; Mohamed Shaluf, 2008). It is informed by the assessment, among the others, of factors contributing to the spatial and temporal variability of fire risk, e.g. through maps of fuel type, amount and condition, weather, vulnerability and value of natural resources and anthropic assets (Oliveira et al., 2017; Thompson et al., 2015). Response is the ensemble of actions undertaken at the moment a fire breakout is identified, towards the containment of flames and the minimisation of damages (Gunes and Kovel, 2000; North et al., 2015). It mainly involves the activation of resources for the suppression of fires and the securing of population and infrastructures (Calkin et al., 2015). Recovery

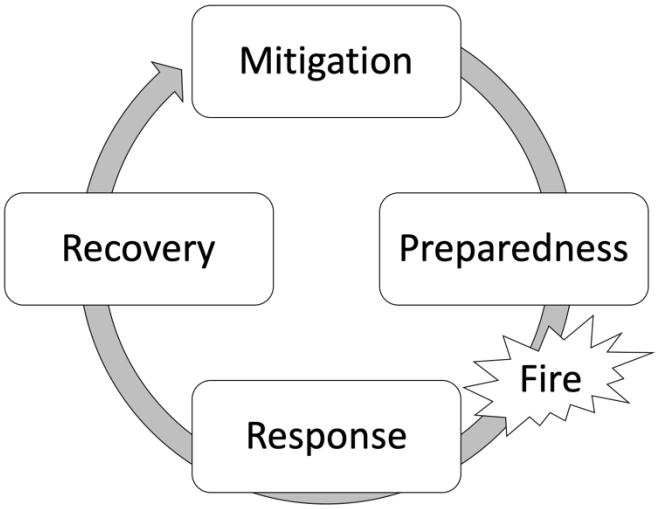


Figure 1.2. The forest fire management cycle includes prevention and response.

refers to strategies and interventions aimed at the short term recovery and long term restoration of areas affected by fires (Gunes and Kovel, 2000). This goes through the assessment of damage, the restoration/reconstruction of infrastructures and the forest management practices aimed at facilitating the return of forest functions to normality (Shive et al., 2013). Damage assessment is typically enabled by the production of maps of burnt scars, damage severity, soil erosion susceptibility and post-fire vegetation recovery (Hurteau and North, 2010; Oliveira et al., 2017; Parson et al., 2010).

Each phase of the fire management cycle involves a different ensemble of stakeholders, each bearing its own set of responsibilities, interests, and ultimately needs. This is reflected in the requirements of support tools and services, which show a significant diversity even for the same type of information. Fuel condition, for example, is relevant to fire managers in the preparedness stage for the advance deployment of resources (Mhawej et al., 2015; Miller and Ager, 2013), to fire suppression teams in the response phase to run flames propagation models and decide attack strategies (Ager et al., 2011; Papadopoulos and Pavlidou, 2011), and to forest managers in the mitigation phase to sectorize forests by clear-cutting to limit fire spread (Fernandes, 2015; Fernandes and Botelho, 2003). Information on fuel condition would be needed at two diverse spatial and temporal scales: for preparedness purposes, fortnightly or weekly regional scale assessments are sufficient, while the application of flames propagation models and the planning of fire breaks would need to rely on the most recent local scale information (Carlson and Burgan, 2003).

The Remote Sensing scientific community has long been working on the development of assessment methods relevant to all phases of the fire management cycle (Chuvieco, 2009, 2003; Chuvieco et al., 2016; Leblon, 2005; Leblon et al., 2016; Tansey et al., 2004), thus serving the needs of diverse stakeholders. With regards to preparedness, forest managers and civil protection agencies work with concepts like fire hazard, danger, and risk. Hazard

refers to fuel available for burning, i.e. fuel type, amount, and condition. Risk is a measure of the probability of a fire to ignite and spread. Danger is a measure of the difficulty to control fires, and thus refers to fire occurrence and behaviour (FAO, 1986). Personal conversations with managers of *Carabinieri* (Italian national gendarmerie) Forest Fire Protection Information Unit (*Nucleo Informativo Antincendio Boschivo*, NIAB, previously a separate entity as *Corpo Forestale dello Stato*, National Forestry Corps), the Italian Civil Protection Department (*Dipartimento della Protezione Civile*), and the *Entente Valabre* (the coordinating organisation of several South France and Corsica departments and departmental fire services) highlighted a clear need for improved fire prevention support services allowing the prediction of fire occurrence and fire behaviour, or more specifically the prediction of emergency conditions (Mazzetti et al., 2009).

Several fire danger rating systems exist worldwide, evaluating in a combined manner biophysical and environmental factors that control fire occurrence and behaviour by applying time-dependent indices, often represented as maps, to support the decision-making process (Allgöwer et al., 2003; Sirca et al., 2018). Among these factors fuel condition, and specifically its moisture content, can be assessed by means of satellite Earth Observation (Ma et al., 2019; Yebra et al., 2013). Operationally, the prediction of emergency conditions is translated into the prediction of the probability of either exceptional fire occurrence or extreme fire events (Finney, 2005; Flannigan et al., 2016; Podschwit et al., 2018; Syphard et al., 2018). In fact, several studies showed how optical and thermal remote sensing of forests can be used to predict fire occurrence (Abdollahi et al., 2018; Bajocco et al., 2015; Dasgupta et al., 2006). However, fire danger also refers to fire behaviour (Ruffault et al., 2018) and, to the best of author's knowledge, no prior research was published that uses remote sensing measurements to predict fire behaviour characteristics. In broader terms, it is not yet known to what extent remote sensing of forest condition may be used to predict fire behaviour characteristics and to assess the probability of extreme events.

To further specify this knowledge gap and identify clear and concise research questions, these considerations will be further developed in the following sections. First, relevant fire management terminology will be detailed, discussing the most used definitions of fire hazard, danger, and risk. Further, the biophysical observables determining fire danger will be highlighted, and it will be clarified how fuel moisture content controls fire occurrence and fire behaviour. The most widely used fire danger rating systems will be introduced, noting how they ingest meteorological inputs to evaluate moisture content of live and dead fuels and ultimately predict fire behaviour. A review of methods based on remote sensing for the estimation of live and dead fuel moisture content will be proposed, and these will be compared to corresponding methods based on meteorological inputs. This review will finally lead to the identification of the specific research questions that are the subject of this study.

1.2. Fire management terminology

In common language, the words risk, danger and hazard refer to the chance of negative events, the amount of loss deriving from an unexpected event, or to objects or situations

that might be harmful. In technical communities more objective definitions have been adopted that do not consider the negative perception of the event and relate to specific observable quantities. Nevertheless, definitions may vary across different communities, and even within the same technical group. This is notably the case in the wildfire management community, where some governmental and non-governmental agencies set out glossaries that are often not consistent with each other (Hardy, 2005; Miller and Ager, 2013). To ensure a consistent language in this study and to clarify terms, the following paragraphs focus on the definitions of fire hazard, danger, and risk, while the next section highlights the key observable properties needed to characterise them.

1.2.1. Fire hazard and fire danger

The terms danger and hazard are prone to misinterpretation due to both the semantic meaning of these two words and the fact that in many languages these are translated with the same expression (for example in Italian, German and Portuguese). FAO reports two definitions of fire hazard, differentiated by geographical area (FAO, 1986).

> *"North America: A fuel complex, defined by volume, type, condition, arrangement, and location, that determines the degree both of ease of ignition and of fire suppression difficulty".*

> *"Non-U.S. English speaking world: A measure of that part of the fire danger contributed by fuels available for burning, worked out from their relative amount, type, and condition, particularly their moisture content".*

Both highlight hazard as a precondition to fire, essentially determined by fuel presence and its condition. The non-U.S. English speaking world definition is more operational, as it clearly identifies hazard as a measurable component of fire danger and explains how it is evaluated, highlighting the specific role of moisture content. Fuels available for burning are further defined as (FAO, 1986):

> *"The portion of the total fuel that would actually burn under various specified conditions".*

The amount of fuel available for combustion is a proportion of all fuels in a given area, and it is determined by their moisture content. Fuels with high moisture content are difficult to ignite, inefficient in sustaining combustion, and slow in propagating flames. This clearly implies that fire hazard is fully quantified as long as fuel amount and type are mapped together with its moisture content. The latter is measured as a percentage of the oven dry fuel mass. Depending on specific conditions, dead fuels moisture content (DFMC) may range from a few percent to 300%, while live fuels moisture content (LFMC) may range from 50% to more than 1000% (Pyne et al., 1996).

FAO defines fire danger as (FAO, 1986):

"The resultant, often expressed as an index, of both constant and variable factors affecting the inception, spread, and difficulty of control of fires and the damage they cause".

There is clearly a level of subjectivity in defining the difficulty of control, and indeed the concept of danger is semantically related to a human perception (Bachmann and Allgöwer, 2000). Nevertheless, this definition clarifies that fire danger is the resultant of several factors affecting fire behaviour, as opposed to fire hazard which only relates to fuel condition (Allgöwer et al., 2003). With an example limited to winds (a variable factor) and topography (a constant factor), danger in an area characterised by steep slopes in a windy day would be considered higher than in a flat area with no winds with the same level of hazard, as winds facilitate flames propagation while topographic constraints might limit ease of access by suppression crews.

The FAO definition of danger includes a reference to fire damage, which is defined as (FAO, 1986):

"The detrimental effects of fires expressed in monetary or other units, including the unfavourable effects of fire-caused changes in the resource base on the attainment of organisational goals".

This definition suggests that several different measures of fire damage might be used. In fact, approaches to the evaluation of fire impact may vary significantly across different stakeholders. Nevertheless, from a preparedness point of view, focus is not on the evaluation of fire damage, but only on the prediction of fire occurrence and behaviour. This is widely reflected in the indices being produced by fire danger monitoring tools available to fire managers (Allgöwer et al., 2003; Sirca et al., 2018).

1.2.2. Fire risk

FAO introduced two definitions of fire risk (FAO, 1986):

"The chance of fire starting, as affected by the nature and incidence of causative agencies; an element of the fire danger in any area".

"Any causative agency".

The latter definition refers to any possible ignition source of a fire (unintentional or intentional human action, or a natural event such as lightning). More relevant to this study is the first definition, essentially describing risk as a probability, whose value is dependent on the nature and the incidence of ignition sources. From an operational point of view, the risk would then be defined as the probability of a fire to spread in a specific location (expressed e.g. per square kilometre) within a specific period of time (e.g. in a week).

The quantification of fire risk requires the evaluation of all possible ignition causes, taking into consideration their variation with space and time, along with the probability of ignition.

Indeed, for a fire to occur, the presence of a heat source is not sufficient, as fuels available for burning must be present. Fire risk is thus quantified as:

$$R = P_{ignition} \cdot P_{precondition} \quad (1.1)$$

where $P_{ignition}$ is the probability of any fire cause to materialize, while $P_{precondition}$ is the probability that the fuel allows the ignition of a fire. This clearly implies that hazard is an inherent component of fire risk (Allgöwer et al., 2003).

The most widespread natural heat source allowing the ignition of fires is lightning (Ganteaume et al., 2013; Latham and Williams, 2001). Its probability of occurrence is normally evaluated as an element of weather forecasts. The quantification of the anthropic component of fire risk requires an understanding of the way in which human activities are related to fire occurrence. Elements like road network and traffic circulation patterns, presence of settlements and production facilities, recreational activities and several others need to be mapped along with their seasonality, and their contribution to probability of ignition needs to be identified (Bachmann and Allgöwer, 2000).

From a risk management perspective, the FAO definition of fire risk is not exhaustive, as it does not consider the exposure to loss, and thus the potential damage that a fire might produce. FAO considers potential damage as a component of fire danger instead but, as discussed, this use of the terminology is not reflected in the fire management community (Bachmann and Allgöwer, 2000). In this context, risk is better defined as the probability of a wildfire to occur at a specific location and under given circumstances, and its expected outcome as defined by the impact on the affected objects (Allgöwer et al., 2003). Quantitatively, this is expressed as:

$$R = P_{ignition} \cdot P_{precondition} \cdot V \quad (1.2)$$

where *V* is a measure for the expected loss due to the fire. A comprehensive approach for the evaluation of the potential damage deriving from a fire requires the analysis of the structure underlying risk and the integrated quantification of wildfire effects, behaviour and occurrence (Bachmann and Allgöwer, 2000).

1.2.3. Fire terminology in the context of this study

The rest of this thesis will make wide reference to the terms fire hazard and fire danger. The proposed summary of how these terms are defined in literature highlighted contradicting definitions across and within technical communities. To avoid confusion, it is worth clarifying the nomenclature adopted throughout this dissertation.

The term fire hazard will be used to refer to fuel type, amount, and condition. Remote sensing observations of land surface temperature and of fuel moisture content are treated as being related to fire hazard when they refer to fuel condition with no reference to fire occurrence or behaviour. In this sense, fire hazard is a measure of the preconditions needed for a fire to start and spread.

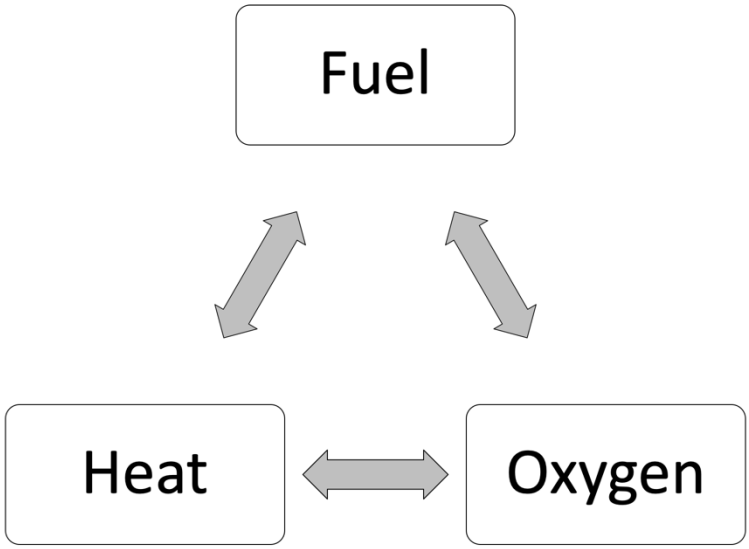


Figure 1.3. Fire fundamentals triangle. Forest fires only occur when all these three fundamentals are present.

The term fire danger will be used to refer to the resultant of all factors affecting the inception, spread, and difficulty of control of fires. Remote sensing observations of land surface temperature and of fuel moisture content will be considered contributors to fire danger when they are analysed along actual forest fire data to identify relationships with fire occurrence and fire behaviour characteristics.

1.3. Biophysical observables related to forest fire danger

Forest fires occur when all three fire fundamentals are present: fuel, heat and oxygen (Figure 1.3) (Pyne et al., 1996). Fuels are conveniently classified in live and dead, the former essentially being vegetation, and the latter composed by the organic elements of forest litter such as dry leaves, small twigs and compacted organic material in the topsoil. The combustion process starts off with the pre-ignition, when a heat source inducts the endothermic reaction leading to dehydration and pyrolysis, with release of volatiles. Through dehydration, fuel temperature of ignition lowers. If the presence of the heat source persists to the point when fuel temperature reaches the temperature of ignition, transition to combustion occurs. At this stage, volatiles produced during preignition form a visible flame. Extinction occurs when one of the fire fundamentals is removed.

Granted the presence of fuels, both live and dead, and oxygen, time to ignition in the presence of a heat source substantially depends on the moisture content of fuels, otherwise referred to as fuel condition or state, which in turns determines the fuel available for burning. As the occurrence and duration of heat sources are stochastic processes determined by natural or anthropic activities, either unintentional or not, fuel moisture

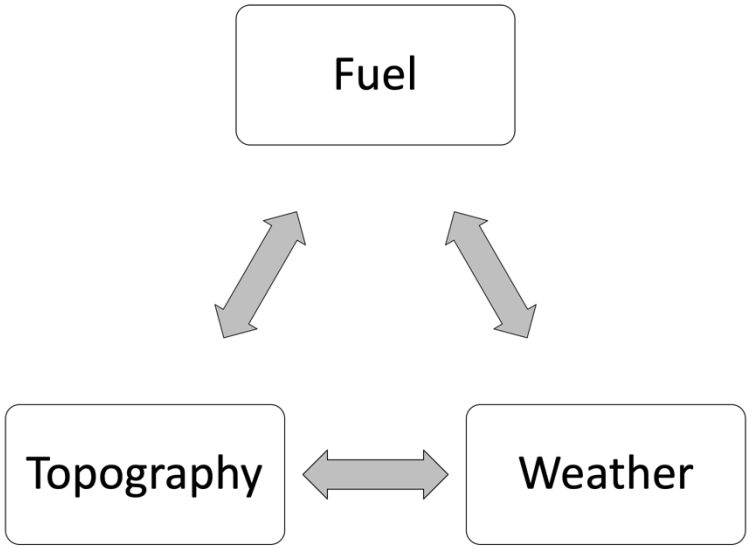


Figure 1.4. Fire environment triangle. The three elements of the triangle drive fire behaviour, and thus control fire danger.

content controls the probability of ignition, and thus fire occurrence (Finney, 2005; Finney et al., 2011; Hardy, 2005).

Fire behaviour is the resultant of the environment in which the fire is burning (Rothermel, 1972), and it is controlled by three elements (fire environment triangle): fuel, topography and weather (Figure 1.4) (Pyne et al., 1996). The presence of fuel, both live and dead, is widely determined by land use/land cover. Its spatial distribution, amount and condition directly affect combustion properties and flame propagation. Topography determines fire behaviour directly through the effect of slope steepness on flame length and rate of spread. Indeed, upslope fuels are exposed to more radiation from flames than downslope fuels, resulting in a quicker propagation in their direction. Topography also affects fire behaviour indirectly. Elevation controls fuel distribution and condition through the influence it exerts on fuel availability, rainfall patterns, temperature, relative humidity, green-up, and curing dates. Aspect determines the irradiance, the latter being higher on south and southwest facing slopes in the northern hemisphere (north and northwest facing slopes in the southern hemisphere), this resulting in lower relative humidity and higher air temperature. Finally, topography has a direct influence on the local wind field. Weather determines fire behaviour directly through the action of winds. These increase contact between flames and fuels and facilitate transport of heat through convection, creating the conditions for a quicker spread in the wind direction. Weather variability also affects fire behaviour indirectly, through the effect it has on fuel moisture. Temperature, relative humidity, rainfall and winds control the evaporation process of dead fuels, determining the variability of their moisture content (Aguado et al., 2007; Liu, 2017; Viney, 1991). The same meteorological variables affect, through their contribution to transpiration, the moisture content of live fuels (Arnold et al., 1998; Douglass, 1967; Swift et al., 1975). Fuel moisture

content then ultimately controls fire behaviour, as it can inhibit or promote the propagation of flames (Jolly, 2007; Rossa et al., 2016; Rossa and Fernandes, 2017; Ustin et al., 2009).

Optical, thermal and microwave remote sensing can play a key role in mapping factors contributing to fire occurrence and behaviour, and thus to the quantification of fire danger. Researchers worldwide have developed approaches for mapping land cover (Wulder et al., 2018), fuel amount (Lu et al., 2016), fuel condition (Ma et al., 2019; Yebra et al., 2013), and topography (van Zyl, 2001). A literature review of how this potential has been translated into the assessment of fire danger is proposed in §1.5. However, next section will first explore what tools are currently available to forest manager to predict fire danger. This will help contextualise the role of remote sensing in fire danger mapping and identify knowledge gaps.

1.4. Fire danger rating systems

Fire occurrence and behaviour are both controlled by fuel moisture content, which in turn is the result of fuel interaction with the environment, i.e. weather and topography (Andrews, 2007; Finney, 1998; Rothermel, 1991, 1972; Van Wagner, 1987; Yebra et al., 2013). Theoretically, all factors contributing to the evolution of moisture content over time should be quantified, and all processes should be accurately modelled, to predict fire danger. In practice, fire danger modelling tools developed so far rely on simplified assumptions on the involved biophysical processes, to evaluate fuel moisture content and represent fire danger against a conventional scale. Weather is the most variable factor driving live and dead fuels moisture content, and all fire danger indices developed so far share their common dependence on meteorological inputs. The three most cited danger rating systems are discussed in the following subsections.

1.4.1. The McArthur Forest Fire Danger Index (FFDI)

The McArthur Forest Fire Danger Index (FFDI) is a measure of forest fire danger developed by the Commonwealth Scientific and Industrial Research Organisation (CSIRO) and used by Australian fire authorities (Dowdy et al., 2009; McArthur, 1967). It was initially developed on an experimental basis and conceived as a card meter operated by hand to provide a forecast of expected fire occurrence and behaviour as expressed by a single indicator. Use of the card required an evaluation of air temperature, rainfall, relative humidity, wind speed and days since last rain. The meters were later translated into equations to allow numerical computation (Griffiths, 1999; McArthur, 1967; Noble et al., 1980).

FFDI is partially based on the Keetch-Byram drought index (KBDI), a measure of drought conditions (Keetch and Byram, 1968). KBDI was developed through the modelling of the evaporation process for the evaluation of water deficit in deep duff and upper soil layers. As such, it is also a model of the moisture content of the largest size classes of dead fuels.

1.4.2. The National Fire Danger Rating System (NFDRS) of the United States

The National Fire Danger Rating System (NFDRS) used in the United States is a collection of fuel condition and fire behaviour indices computed from weather station measurements, fuel models, climate class and slope (Burgan, 1988; Deeming et al., 1977). The system was conceived to support the planning of staffing level for the potential response to the fire behaviour that could be expected in case of a fire breakout (Bradshaw et al., 1984; Walding et al., 2018). NFDRS indices are further integrated with maps of vegetation relative greenness derived from time series of remote sensing data to produce the Fire Potential Index (FPI), a predictor of fire occurrence (Chowdhury and Hassan, 2015a; Preisler et al., 2009).

From an operational point of view, the NFDRS ingests daily observations of temperature, relative humidity, precipitation, and wind speed from automated weather stations, optionally the moisture content of a standardised fuel stick (measured from its weight), and information on slope, latitude, climate class and fuel model to compute the KBDI and the moisture content of four classes of dead fuels and two classes of live fuels (woody and herbaceous). In this computation, previous values of the moisture content of the two classes of largest dead fuels are carried over from the previous day. Input parameters and computed moisture values are further processed to produce four output indices (Schlobohm and Brain, 2002). The Spread Component (SC), computed from fuel model, slope, wind speed and dead fuel moisture content, is an estimate of the rate of spread of the frontline of a fire. The Ignition Component (IC) is the probability of a fire to spread, thus requiring suppression action. It is essentially computed from the moisture content of fine fuels and from SC. The Energy Release Component (ERC), an estimate of the energy release of the flaming zone of a fire, is contributed from the modelled moisture content of both live and dead fuels. The Burning Index (BI), computed from IC and ERC, is a measure of difficulty of control of a fire due to its expected behaviour.

1.4.3. The Fire Weather Index (FWI) System

The Fire Weather Index (FWI) System is a collection of six indicators, computed from daily readings of temperature, relative humidity, wind speed, and 24-hour cumulated precipitation to represent the effect of moisture content of three classes of forest fuel and of wind speed on fire behaviour in a standardised fuel type and in no slope conditions (Van Wagner, 1987). Their evaluation is progressive, in the sense that their current values do not only depend on current day values of the named meteorological variables, but also on the previous day value of the same indicators, so that their temporal evolution is characterised by a time lag with respect to meteorological events. The FWI System was initially developed to provide a fire danger rating in Canada. Nevertheless, it proved to be a robust mean to effectively map fire danger in several other areas worldwide, including Europe (de Groot and Flannigan, 2014; Dowdy et al., 2009; San-Miguel-Ayanz et al., 2012; Taylor and Alexander, 2006).

In detail, the FWI System is composed of three moisture codes and three fire behaviour indices (Figure 1.5). The Fine Fuel Moisture Code (FFMC) is computed from precipitation,

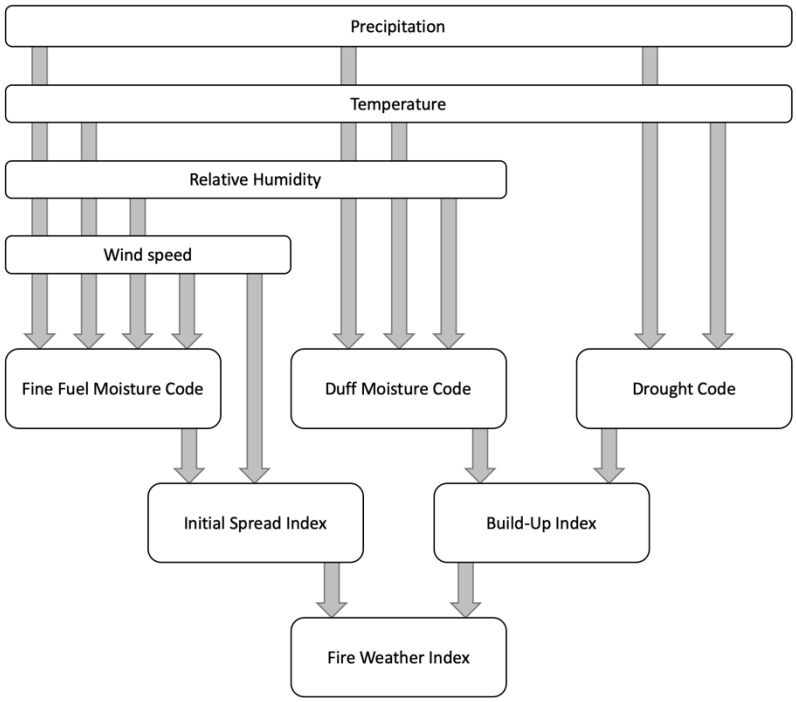


Figure 1.5. Schematic representation of the Fire Weather Index (FWI) System, that provides three moisture codes and three fire behaviour indices.

relative humidity, wind speed and air temperature to represent a measure of moisture content of litter and dead fine fuels. The Duff Moisture Code (DMC) is computed from precipitation, relative humidity, and air temperature. It is related to the moisture content of loosely compacted, decomposing organic matter. The Drought Code (DC) represents water content of deeper layers of compact organic matter and heavy surface dead fuels and is computed from precipitation and air temperature only. The Initial Spread Index (ISI) is computed from FFMC and wind speed to provide a measure of the rate of spread, independently of the amount of fuel. The Build-Up Index (BUI) is a combination of DMC and DC representing the fuel available for combustion. The Fire Weather Index (FWI) combines ISI and BUI to provide a measure of the intensity of a spreading fire, i.e. the energy output rate per unit length of fire front.

These indicators develop over different ranges of values, and danger thresholds are usually identified locally based on fire history (Van Wagner, 1987). Each component of the FWI System carries a different layer of information on fire danger. FFMC provides a measure of ease of fire inception and flammability of the top fuel layer, where initial ignition usually occurs. DMC and DC are rather related to fuel consumption of medium and large sized woody material. ISI is generally related to burned area, as it combines fine fuel moisture content and wind speed, both relevant to this fire characteristic. BUI is a good predictor of

fire behaviour and fuel consumption. FWI, as a synthesis of the other five indices, is generally related to several descriptors of fire behaviour.

1.5. Contribution of remote sensing to fire danger mapping

At the core of all three fire danger rating systems above and of fire danger rating systems in general is the modelling of fuel moisture content from meteorological measurements. Fuel moisture content is then used to compute one or more danger indices that serve as descriptors of fire occurrence and behaviour. The level of sub-classification of fuels varies widely across models, with the examples previously discussed ranging from the single indicator provided by the FFDI to the four classes of dead fuels and two classes of live fuels of the NFDRS. Apart from the NFDRS, which optionally uses the hand-measured weight of a standardised fuel stick to measure moisture content of the 10-hour time lag dead fuel class, no direct evaluation of moisture content is used. This is common also to other fire danger models not discussed here (Chuvieco, 2003).

Modelling fuel moisture content from meteorological variables results in a degree of approximation, as opposed to direct measurement, due to the simplifying assumptions this implies (Ruffault et al., 2018; Schunk et al., 2017). In fact, evaluations are computed either from point weather measurements, e.g. automated weather stations, and as such are only valid in a limited area around the point of data collection (Schlobohm and Brain, 2002; Walding et al., 2018), or from coarse resolution weather maps (~10 km resolution). This leads to a scale of representation that might or might not be suitable for management purposes depending on the extent of the area being monitored by the local firefighting services (San-Miguel-Ayanz et al., 2012). As a consequence, any direct observation of fuel moisture content has the potential to enable a better evaluation of fire occurrence and fire behaviour danger indices (Jolly, 2007; Rossa and Fernandes, 2017; Ruffault et al., 2018). As field measurements are not a viable option, this outlines a clear opportunity for Earth Observation technologies, as they provide repeated and frequent observations of land surface conditions and processes (Allgöwer et al., 2003; Ma et al., 2019; Yebra et al., 2013).

1.5.1. Meteorological vs remote sensing estimation of DFMC

The estimation of DFMC from meteorological measurements is broadly supported by literature. Reviews of empirical and process based models, including those adopted in the fire danger rating systems discussed in §1.4, confirm that a certain degree of accuracy can be achieved, especially for fine fuels (Matthews, 2014; Viney, 1991). The research focus on fine fuels is explained by their prominent role, as compared to classes of larger dead fuels, in determining ignition probability and flames propagation (Pyne et al., 1996; Schunk et al., 2014). Indeed, the FFMC of the FWI System and its adaptations proved to be good predictors of the moisture content of fine fuels and dead grass in diverse conditions (Aguado et al., 2007; Bianchi and Defossé, 2014; Slijepcevic et al., 2015), albeit its poor capacity to predict rapid moisture content variations is acknowledged (Anderson and

Anderson, 2009). Similar observations are reported for the 10-hour time lag dead fuel class of the NFDRS (Aguado et al., 2007; Carlson et al., 2007; Nelson, 2000).

Dead fuels are often covered by the overlaying canopy, and their direct observation with optical and thermal remote sensing instruments may be unfeasible. This led to the development of indirect estimation methods based either on empirical approaches or on process-based methods using satellite-derived proxies. Empirical methods rely on regression or on artificial neural networks to separate canopy and background components in optical satellite measurements and assess moisture content of litter (Adab et al., 2016; Yang et al., 2018) or the value of the corresponding weather-based dead fuel moisture indices (Merzouki and Leblon, 2011). These methods lack generality, as derived models are site-specific. Process based approaches model vapour pressure deficit and equilibrium moisture content from satellite estimates of air temperature and relative humidity (Nieto et al., 2010; Nolan et al., 2016b). However, results tend to be biased (Nieto et al., 2010), especially in areas with low vegetation density (Nolan et al., 2016b).

Opportunities for the direct estimation of DFMC are allowed by the proven sensitivity of radar backscatter to litter moisture (Bourgeau-Chavez et al., 2007; Leblon et al., 2016). As opposed to optical and thermal sensors, radar sensors penetrate cloud cover and have the advantage of acquiring surface information in any weather condition. Experiments demonstrated that seasonal trends of radar backscatter in forests are correlated with DMC, DC, BUI and FWI of the Fire Weather Index System (Abbott et al., 2007; Leblon et al., 2002), which in turn are related to DFMC. However, other factors affect radar backscatter, including forest structure, biomass and vegetation water content (Leblon et al., 2016). Retrievals of soil moisture from passive microwave sensors were found to be linearly related to vegetation moisture spectral indices (Hunt et al., 2011).

1.5.2. Meteorological vs remote sensing estimation of LFMC

Estimation of the moisture content of live fuels from meteorological observations can be based on the modelling of the evapotranspiration process, as is the is the case for the two live fuel moisture codes of the NFDRS (Burgan, 1988; Deeming et al., 1977). More often, empirical correlations have been reported, linking meteorological drought indices, such as the KBDI and the FWI System moisture codes DMC and DC, to the moisture content of vegetation, at least for species most sensitive to meteorological conditions (Dimitrakopoulos and Bemmerzouk, 2003; Ganatsas et al., 2011; Pellizzaro et al., 2007a; Viegas et al., 2001). However, results are ambiguous and lack general applicability, as any link between LFMC and weather forcing is dependent on site-specific weather patterns and on structural and physiological characteristics of plants, which are species-specific (Jolly and Johnson, 2018; Nolan et al., 2018; Pellizzaro et al., 2007b; Ruffault et al., 2018). In fact, it was acknowledged that meteorological estimation of LFMC does not perform as well as with DFMC, and thus this parameter is not adequately represented by fire danger models (Ruffault et al., 2018), although it is essential in predicting fire behaviour (Jolly, 2007; Rossa et al., 2016; Rossa and Fernandes, 2017; Ustin et al., 2009).

As opposed to DFMC, there is a wide literature demonstrating remote sensing applications for either the direct or the indirect estimation of water amount in live fuels (Ma et al., 2019; Veraverbeke et al., 2018; Yebra et al., 2013; Yool, 2009). This is supported by biophysical processes determining the radiometric properties of leaves as a function of water content and water stress conditions (Leblon, 2005; Stow et al., 2006; Yebra et al., 2018, 2013). Indeed, leaves and small twigs are the parts of living plants that most contribute to fire behaviour of woody vegetation (Piñol et al., 1998; Viegas et al., 2001), and their moisture content are closely correlated (Castro et al., 2003; Piñol et al., 1998; Saura-Mas and Lloret, 2007; Viegas et al., 2001).

The evaluation of vegetation moisture from remote sensing measurements in the optical domain relies on detailed studies of the optical properties of leaves (Gates et al., 1965; Gausman and Allen, 1973; Tucker, 1980; Woolley, 1971). The concept of equivalent water thickness (EWT) was introduced in these studies, denoting the mass of water in leaf tissues per unit leaf area:

$$EWT = \frac{M_f - M_d}{A} \quad (1.3)$$

where M_f is the mass of the fresh leaf as measured in the field, M_d is the corresponding mass of the same leaf that has been oven dried, and A is leaf area. The name of this measure of leaf water originates from the observation that in the shortwave infrared (SWIR) range of the electromagnetic spectrum (1.1-2.5 μm) the absorption of solar radiation from a compact leaf can be approximated by the absorption of an equivalent layer of water (Gausman and Allen, 1973). EWT is scaled to canopy level by simple multiplication by leaf area index (LAI) (Ceccato et al., 2002a):

$$EWT_c = EWT \cdot LAI \quad (1.4)$$

EWT_c is thus the total amount of water in the canopy per unit ground area. Having a direct effect on the optical properties of vegetation, EWT is a parameter of leaf radiative transfer models such as PROSPECT (Feret et al., 2008; Jacquemoud and Baret, 1990), justifying its popularity in the remote sensing scientific community. However, this measure of water content differs substantially from LFMC, the latter being a measure of percentage water relative to the mass of leaf dry matter:

$$LFMC = \frac{M_f - M_d}{M_d} \cdot 100 \quad (1.5)$$

Being a measure of water relative to dry mass, LFMC is not scaled to canopy level through LAI. Clearly, a single LFMC value can correspond to various EWT values, depending on leaf dry mass.

The demonstrated sensitivity of leaf spectral signature to leaf structure and to dry matter content (DMC, M_f per leaf unit area) in the near infrared (NIR, 0.7-1.1 μm), and to leaf structure, EWT and DMC in the SWIR (Ceccato et al., 2001; Seelig et al., 2008) led to the development of several broadband spectral indices that used NIR reflectance as a normalising factor against leaf structure and DMC towards the estimation of EWT (Ceccato et al., 2002a; Gao, 1996; Hardisky et al., 1983; Hunt and Rock, 1989). It should be observed

that, when computed from satellite remote sensing measurements, spectral indices of vegetation moisture are actually sensitive to EWT_c, and thus they are inherently responsive to LAI (Colombo et al., 2008; Dasgupta and Qu, 2009). The sensitivity to LAI is indeed a general characteristic of spectral indices based on SWIR wavelengths (Bowyer and Danson, 2004; Dawson et al., 1999; Wang et al., 2008; Zarco-Tejada et al., 2003).

Spectral indices for the estimation of EWT generally do not achieve the same accuracy in estimating LFMC (Caccamo et al., 2012; Carlson and Burgan, 2003; Danson and Bowyer, 2004; Davidson et al., 2006; Maki et al., 2004; Yilmaz et al., 2008), although some exceptions are reported in literature, depending on species-specific conditions (Sow et al., 2013; Verbesselt et al., 2007, 2002). Indeed, LFMC does not cause spectral features in vegetation reflectance as is with EWT (Gao and Goetz, 1990; Peñuelas et al., 1993). This led to the development of alternative strategies based on the inversion of radiative transfer models exploiting the independent effect of EWT and DMC on vegetation reflectance (Jacquemoud et al., 2000; Zarco-Tejada et al., 2003) to retrieve them separately and compute LFMC directly. The applicability of this method is limited in scale and resolution by the fact that it relies on retrieval strategies where DMC values are constrained by prior knowledge of observed vegetation species (Quan et al., 2016, 2015; Riaño et al., 2005; Yebra et al., 2018; Yebra and Chuvieco, 2009a, 2009b). Approaches not based on prior information of the observed surface exploited the high dimensionality of hyperspectral measurements to retrieve LFMC with partial least squares regression (Li et al., 2007) and with wavelet analysis (Cheng et al., 2011). A computationally simpler approach is the Water Index (Peñuelas et al., 1997, 1993). It was proved to be generally more effective than broadband indices in retrieving LFMC (Danson and Bowyer, 2004), but its operational use is unfeasible as operational hyperspectral optical sensors providing global frequent revisits are currently not available.

In ecosystems where prolonged droughts and heat waves are the preconditions for increases in frequency and intensity of forest fires, an indirect approach may be adopted to evaluate LFMC from remote sensing observations in the thermal infrared (TIR) domain. The underlaying biophysical mechanism is the vegetation transpiration regulation mechanism which reacts to water stress conditions by reducing stomatal conductance, thus leading to an increase of canopy temperature (Hsiao, 1973; Schulze et al., 1973; Zweifel et al., 2009). Indeed, this has been widely used to map vegetation stress conditions from satellite estimates of land surface temperature (LST) (Jackson et al., 1981; Kalma et al., 2008; Karnieli et al., 2010; Liu et al., 2016; Nemani and Running, 1989).

In the microwave domain, the sensitivity of radar backscatter to vegetation moisture (Leblon et al., 2016) led to the identification of empirical methods for the evaluation of EWT (Konings et al., 2019). Several microwave indices were proved to be correlated with EWT and LFMC (Fan et al., 2018; Hunt et al., 2011; Tanase et al., 2015), but indices from measurements in the optical domain generally outperform microwave indices (Fan et al., 2018). This is justified by the typically complex relationships linking LFMC to radar measurements (Abbott et al., 2007; Leblon et al., 2002; Saatchi and Moghaddam, 2000).

1.5.3. Earth Observation applications in fire danger mapping

LFMC and DFMC are parameters in fire propagation models (Andrews et al., 2013; Finney, 1998; Rothermel, 1991, 1972). In principle, this would open to the use of remote sensing in the simulation of flames propagation. Clearly, the significance of simulations produced by such models heavily relies on the quality of input data (Dasgupta et al., 2007), and in the case of biophysical quantities retrieved through remote sensing based methods accuracy may be typically assessed against field measurements (Gao et al., 2015; Ullah et al., 2014). Yet, the applicability of remote sensing observations of fuel condition in the simulation of flames propagation relies on the availability of measurements in useful wavelengths at a spatial and temporal resolution adequate for this application. Spatial resolution currently appears to be the most stringent requirement, as flame propagation models may only provide meaningful information when used at fine-scale (Finney, 2001, 2000, 1998).

Approaches for the use of remote sensing data in fire danger mapping rather focussed on relating LST, broadband spectral indices of vegetation moisture content, such as the Normalised Difference Water Index (NDWI) (Gao, 1996) and the Global Vegetation Moisture Index (GVMI) (Ceccato et al., 2002a), radar backscatter or indirect measures of plant stress to forest fires. NDWI was used along with remotely sensed LST and atmospheric columnar water vapour to predict fire danger (Abdollahi et al., 2018), while time series of this index documented the seasonality of fire occurrence and demonstrated good forecasting capabilities (Huesca et al., 2014, 2009). GVMI was used in combination with LST, normalised difference vegetation index (NDVI), topography, land cover and maps of human settlements to predict fire occurrence (Pan et al., 2016), although in specific land cover types other spectral indices had a better performance (Cao et al., 2013). Radar backscatter was related to fire danger (Abbott et al., 2007; Leblon et al., 2002) and vegetation moisture (Hunt et al., 2011), although it is also affected by many other surface properties (Leblon et al., 2016).

Other approaches related indirect estimates of plant water stress to fire occurrence, e.g. through the analysis of time series of optical vegetation spectral indices as a measure of greenness, either alone (Bajocco et al., 2015; Burgan et al., 1998; Maselli et al., 2003) or in conjunction with LTS (Abdollahi et al., 2018; Chowdhury and Hassan, 2015b). Some researchers used LST to model energy budgets (Leblon, 2005; Nolan et al., 2016b; Vidal et al., 1994) or to estimate heat energy of pre-ignition (Dasgupta et al., 2006), and predict fire occurrence. Fire occurrence was also related to LST anomalies, although no shared definition of such parameter exists (Manzo-Delgado et al., 2004; Matin et al., 2017; Pan et al., 2016).

Cited approaches essentially focus on fire occurrence. However, fire danger models are meant not only to predict fire occurrence, but also to provide a measure of expected fire behaviour. In this sense, to respond to the identified need to improve fire danger models (Ruffault et al., 2018), it would be relevant to understand the potential of remote sensing in predicting fire behaviour characteristics either deterministically (Dasgupta et al., 2007) or probabilistically (Flannigan et al., 2016; Podschwit et al., 2018). The latter would be more suitable for fire managers, who are used to concepts like the probability of extreme events. As discussed, fire behaviour is controlled by fuel moisture content, and this in turn

determines radiometric properties of vegetation and soil. There are grounds to hypothesise that remote sensing observations of live fuel condition may be used to predict forest fire behaviour. Nevertheless, to the best of author's knowledge, no research was previously published in literature connecting remote sensing measurements to fire characteristics. This clearly identifies a knowledge gap which needs further investigation.

1.6. Research objectives and thesis outline

Considerations so far lead to the following overall research question:

To what extent can remote sensing of forest condition be used to predict fire behaviour characteristics and assess the probability of extreme events?

Focussing on optical and thermal remote sensing, the response to this research question requires the following steps: identify appropriate remote sensing metrics of live fuel condition, relate these metrics to probability distributions of some fire behaviour characteristics, and compare the predictive performance of these remote sensing derived metrics against traditional fire danger rating systems. These steps and the relevant research sub-questions they raise are detailed as follows.

Q1. Which characteristics of fire behaviour are probabilistically related to pre-fire LST anomalies? Remote sensing of LST allows the evaluation of vegetation water stress. As plant water stress is related to LFMC, both LST and LST anomalies have been successfully used to predict fire occurrence. However, no research has been reported so far linking pre-fire LST or LST anomaly to fire behaviour characteristics.

Q2. To what extent can LFMC be retrieved by means of a broadband spectral index? Methods proposed so far for the estimation of LFMC rely on the inversion of radiative transfer models to retrieve water and dry mass content and the further computation of LFMC. In addition to the inherent uncertainty of model inversion, LFMC retrieval accuracy depends on constrained values of model parameters and thus on extensive field work. A simpler approach would be to use broadband spectral indices. Nonetheless, indices proposed so far are sensitive to EWT, not to LFMC.

Q3. Which characteristics of fire behaviour are probabilistically related to pre-fire remote sensing estimates of LFMC? Remote sensing of vegetation moisture in the optical domain has been related to fire occurrence and to some fire danger indices. However, this does not meet fire managers' need to predict the probability of extreme events. Indeed, fire danger is a measure of the difficulty of controlling a fire, which in turn is a consequence of fire behaviour. Further research is thus needed to link remote sensing estimates of LFMC to probability distribution of fire behaviour characteristics.

Q4. To what extent may pre-fire remote sensing estimations of LST anomaly and LFMC be used synergistically to improve predictions of extreme events? Several studies demonstrated the joint use of optical and thermal remote sensing for the prediction of fire occurrence or the evaluation of fire danger. Once remote sensing of LFMC and of LST

anomalies have been proved to predict fire behaviour, it would be relevant to investigate opportunities for their joint use.

Q5. How do remote sensing predictions of fire behaviour compare against predictions enabled by traditional, meteorological fire danger models such as the Fire Weather Index (FWI) System (Van Wagner, 1987)? Satellite remote sensing measurements of live fuel condition have been found to be related to fire danger indices based on meteorological input. To build towards an integration of existing fire danger models and remote sensing retrievals it would be relevant to compare the performance of these two in the prediction of fire behaviour characteristics.

The specific objectives of the study to address these research questions are thus to:

- Develop a method to evaluate remote sensing measurements of LST anomalies and demonstrate that these can be used to predict fire characteristics.
- Improve the generality of existing remote sensing approaches for the assessment of LFMC through the definition of an appropriate optical broadband spectral index.
- Demonstrate that remote sensing estimates of LFMC can be used to predict fire characteristics.
- Develop a framework for the joint use of optical and thermal remote sensing observation of live fuel condition and the prediction of extreme events.
- Assess remote sensing performance against the FWI System components.

For this research, a dataset on forest fires occurred in Campania, Italy, was provided by the Natural Resources Unit of Carabinieri. This Italian law enforcement agency is in charge, among other responsibilities, of burned area inventorying. Available data is thus to be considered official. Fire data was combined with pre-fire remote sensing measurements by the MODIS instrument on board the Aqua satellite. The focus on this sensor was suggested by the availability on the same instrument of spectral bands covering the near infrared, shortwave infrared, and thermal infrared domains. It further allows, with its long time series, to cover the entire span of available fire data. Aqua-MODIS (MODIS FM1) was preferred to its Terra counterpart (MODIS PFM) as its daytime overpasses are in the early afternoon, a time of the day when vapour pressure deficit is at a maximum. This would allow capturing vegetation conditions in the moment of the day when maximum stress occurs.

The thesis will develop along the following outline. Chapter 2 will describe the study area, introduce the available dataset of forest fires, and discuss the fire regime in the region. Chapter 3 will develop a methodology for the evaluation of land surface temperature anomaly and for its use in predicting the probability distribution of some fire behaviour characteristics (Maffei et al., 2018). Chapter 4 will introduce a new broadband spectral index for the evaluation of LFMC (Maffei and Menenti, 2014). Chapter 5 will evaluate the probability distribution functions of some fire behaviour characteristics and develop an approach to predict the probability of extreme events as a function of the spectral index introduced in chapter 4 (Maffei and Menenti, 2019). Chapter 6 will compare the performance of optical remote sensing of LFMC and of thermal remote sensing of LST anomaly in predicting fire behaviour characteristics against the six FWI System components.

It will further develop a framework for the joint use optical and thermal remote sensing for the prediction of the probability of extreme events. Chapter 7 will contextualise results proposed in chapters 3 to 6, discuss novelty and impact, propose an outlook of possible developments and future applications, and provide some recommendations.

2. Campania study area and its fire regime

2.1. Introduction

The characterisation of the fire regime, i.e. of the spatial and temporal patterns of fire events occurring in a specific region over a given period of time, is an essential step towards the knowledge to support informed management of forests (Bajocco et al., 2009; Carmo et al., 2011; Díaz-Delgado et al., 2004; Fiorucci et al., 2008; Morgan et al., 2001; Rodrigues et al., 2019). It is also needed to understand the resilience and sensitivity of vegetation communities to fires and how and to what extent the fire phenomenon controls forest functionality and land cover change at regional scale (Díaz-Delgado et al., 2004, 2002; Lloret et al., 2002; Morgan et al., 2001; Pausas et al., 2008).

A wide array of landscape features affects fire regime. Climate drives spatial and seasonal variation of fire occurrence (Flatley et al., 2011). Weather patterns determine both fire occurrence and burned area (Oliveira et al., 2012; Salis et al., 2019). Topography controls both fire frequency (Cyr et al., 2007) and total burned area (Dickson et al., 2006), although its effect might be modulated by climate (Flatley et al., 2011). Population density and other socio-economic factors determine both burned area and fire frequency (Carlucci et al., 2019; Catry et al., 2009; Ferrara et al., 2019; Moreira et al., 2010). Land cover is a strong predictor of variability in fire regime (Bajocco and Ricotta, 2008; Carmo et al., 2011; Wells et al., 2004), with shrublands, grasslands and forest areas influencing fire patterns, burned area and fire frequency (Moreira et al., 2010; Mouillot et al., 2003).

The named landscape factors do not exhaust all possible drivers of spatial variability of fire events (Parisien and Moritz, 2009). Nevertheless, it would be relevant to develop an understanding of fire regime in the study area to support the interpretation of the results presented in this dissertation (Moreira et al., 2009; Nicholls and Lucas, 2007). In fact, generalisation from other areas and scales might be misleading (Telesca et al., 2007b), as the specific combinations of factors affecting fire regime tend to be quite unique to different regions and sub-regions (Wells et al., 2004; Zumbrunnen et al., 2008), and the role of some drivers are more evident when studied at regional scale (Rollins et al., 2002).

The research outlined in this dissertation focussed on the study area of Campania, Italy. The interest in this area is given by its position in the middle of the Mediterranean, by the diversity of the landscape and land use/land cover it embraces, and by the high anthropic

pressure that leads to almost all fires being triggered by human activities (Lovreglio et al., 2010; Michetti and Pinar, 2019). Campania is a NUTS2 region. In Italy, this administrative level bears responsibilities in terms of planning, prevention, and fight against forest fires (Italian Law no. 353/2000).

While Italy is among the European Countries the most affected by fires (San-Miguel-Ayanz et al., 2019), the forest fire phenomenon has not been studied evenly across the Italian peninsula, and most scholarly papers report analyses at regional or local scale. Fire selectivity against land cover was verified in Sardinia (Bajocco et al., 2019; Bajocco and Ricotta, 2008). Further studies in Sardinia and Tuscany showed that a relationship exists between temporal variability of fire events, climate and phenology (Bajocco et al., 2010a, 2010b, 2009; Cardil et al., 2014; Telesca and Lasaponara, 2006). Recurrent fire ignitions were related to distance to roads and land cover in Apulia (Elia et al., 2020). Fire zoning was produced at regional level in Piedmont and Veneto based on fire statistics in mountainous administrative sub-regions (Bovio and Camia, 1997). Fire occurrence in Aosta Valley were related to land cover, air temperature, precipitation and proximity to infrastructures (Vacchiano et al., 2018). A practical procedure to produce fire zoning based on the aggregation of small administrative units was proposed and tested in Liguria (Fiorucci et al., 2008). Fire occurrence and burned area were evaluated against socio-economic factors in the whole of Italy (Carlucci et al., 2019).

A few papers provided evidence of self-organised criticality of the fire phenomenon in Italy. Fire size appears to follow a power-law distribution in Liguria, Tuscany, Cilento (part of Campania), Molise and Simbruini Mountains (Ricotta et al., 2001, 1999; Telesca et al., 2007a). Temporal clustering of fire events was verified at regional and national scale (Bajocco et al., 2017; Corral et al., 2008; Lasaponara et al., 2005; Ricotta et al., 2006; Telesca et al., 2005; Telesca and Lasaponara, 2010, 2006). Spatial clustering was confirmed in Liguria and Tuscany (Telesca et al., 2007b; Tuia et al., 2008, 2007).

The cited literature provides an important contribution towards the understanding of spatial and temporal characteristics of fire occurrence and of its spatial drivers in some Italian regions. Yet a comprehensive analysis describing fire regime in the study area of this research is missing, despite its being among the most fire prone regions in the Mediterranean (Modugno et al., 2016; San-Miguel-Ayanz et al., 2019). More relevantly, while some studies focussed on burned area, no research has been performed in Italy to infer spatial drivers of other fire characteristics such as fire duration and rate of spread.

Specific spatial drivers being investigated in this chapter are land cover and topography. This selection of factors is far from being comprehensive (Parisien and Moritz, 2009). Indeed, the objective is not the creation of models for the prediction of spatial patterns of fire occurrence or of fire behaviour, but rather the creation of a minimum knowledge base for the interpretation of research results proposed in chapters 3, 5 and 6 of this dissertation. In more detail, the objectives of this chapter are to provide a thorough description of the study area, describe in detail fire data being used in chapters 3, 5 and 6, understand seasonal and interannual variability of fire occurrence, total burned area, and of some fire behaviour characteristics such as burned area, duration and rate of spread, and review how

land cover and topography determine spatial patterns of fire occurrence, total burned area, and fire behaviour.

In the following section the study area is introduced, and its landscape is described in terms of physical and environmental resources. Further, available fire data is presented along with methods used to interpret it. Section 2.3 reports results in terms of fire occurrence maps, synthesis statistics and graphs with the aim of describing the fire regime in Campania. Section 2.4 comments on reported results, interpreting them against physical and environmental characteristics of the region. A conclusive section summarises findings and contextualises them with respect to the wider content of this dissertation.

2.2. Materials and methods

In this section the study area is introduced and described in terms of its physical and environmental resources. Available fire data, land cover and topography maps are subsequently presented. Finally, methods used to interpret the interaction between fires and landscape characteristics of the study area are outlined.

2.2.1. Study area

Campania, Italy (40.83°N, 14.13°E, 13595 km^2, Figure 2.1), is one of the most densely populated and fire affected regions in Mediterranean Europe (Modugno et al., 2016; San-Miguel-Ayanz et al., 2018). Landscape is divided in two main geomorphological areas. Western Campania alternates rocky coasts and alluvial plains. The climate is typically Mediterranean, with average yearly rainfall between 800 and 1000 mm. Summers are hot and dry, while maximum rainfall is recorded in winter. The eastern part of the region comprises mountains and hills. Temperature patterns are determined by altitude, while yearly rainfall reaches 1500 mm, with a maximum in autumn and a minimum in summer (Amato and Valletta, 2017; Ducci and Tranfaglia, 2008; Fratianni and Acquaotta, 2017). Land cover (Figure 2.2) is dominated by agricultural lands (56% of the region), forests and semi-natural areas (38%). Among agricultural lands, arable fields are prevalent, followed by fruit trees, olive groves and vineyards. Among forest and semi-natural areas, broad leaved forest largely dominates.

A comprehensive approach to interpret the landscape traits that affect fire occurrence (see §1.3) is through the land systems map (Di Gennaro, 2002), an overall inventory of physical-environmental resources in the region (Figure 2.3). This map was constructed using an integrated physiographic approach which identifies geographic areas, thereby named land systems, that can be considered homogeneous in terms of environmental factors influencing their land use and eventually their degradation processes (FAO, 1995). In this sense, land systems are environmental structures that are linked to the integrated action of climate, morphology, biotic communities and permanent anthropic modifications, and it is expected that the corresponding specificity of these factors affects fire distribution (Biermann et al., 2016; Dube, 2009; Harrison et al., 2010; Lavorel et al., 2006; Pausas and Paula, 2012).

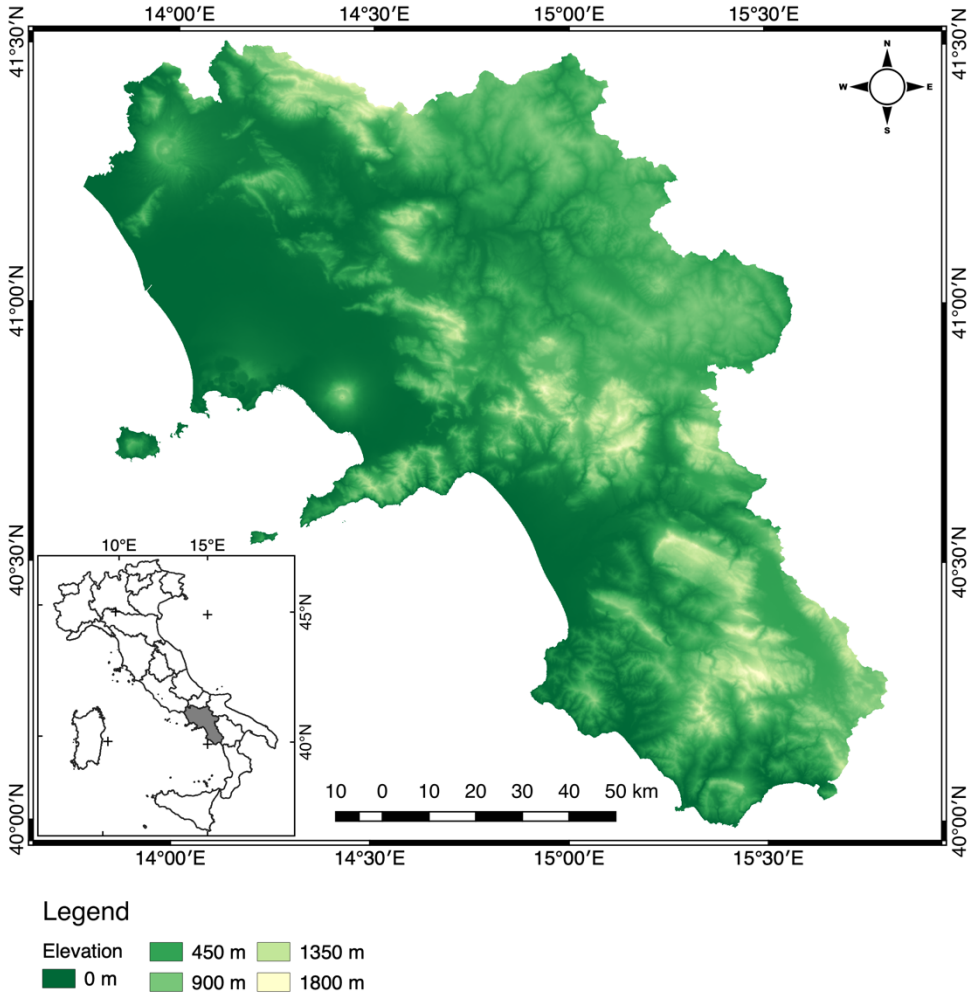


Figure 2.1. Elevation map of Campania, the study area of this research. Landscape is divided along the longitudinal gradient in two main geomorphologically and climatically different areas.

Campanian landscape is classified into ten land systems: high mountain, calcareous mountain, marly-arenaceous and marly-calcareous mountain, inland hill, coastal hill, volcanic complex, footslope plain, alluvial terrace, alluvial plain, coastal plain. Within each land system, a few sub-systems can be identified.

The most prevalent land systems in the region (about 30% of the surface) are the inland hills of Irpinia, Sannio, the upper basin of Sele, and Cilento (labels D1, D2 and D3 in Figure 2.3). Lithology in these areas is dominated by sandstones and Campanian grey tuff. Climatic interference (i.e. the limitation to the potential crop production due to climatic conditions) is low to moderate, while the risk of summer water deficit is moderate to high. Agricultural lands cover about 80% of the total surface of this system, while the remaining part is

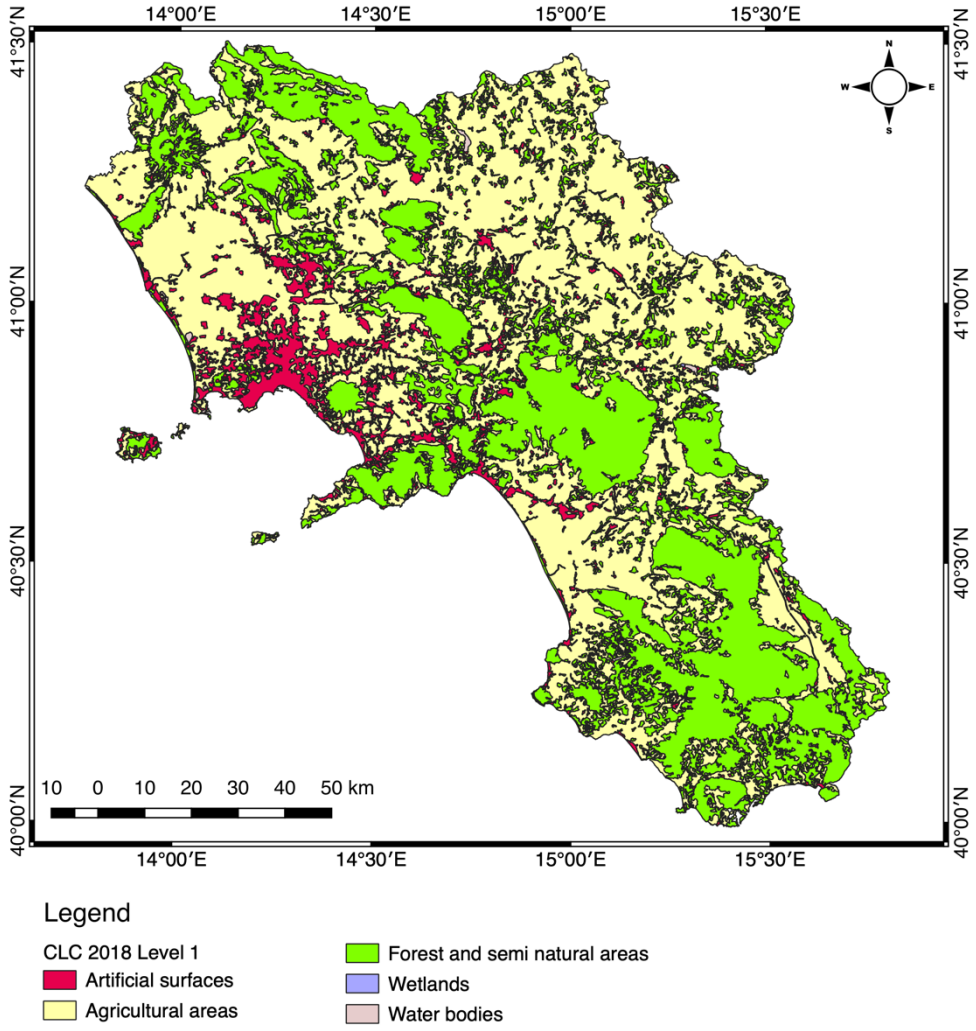
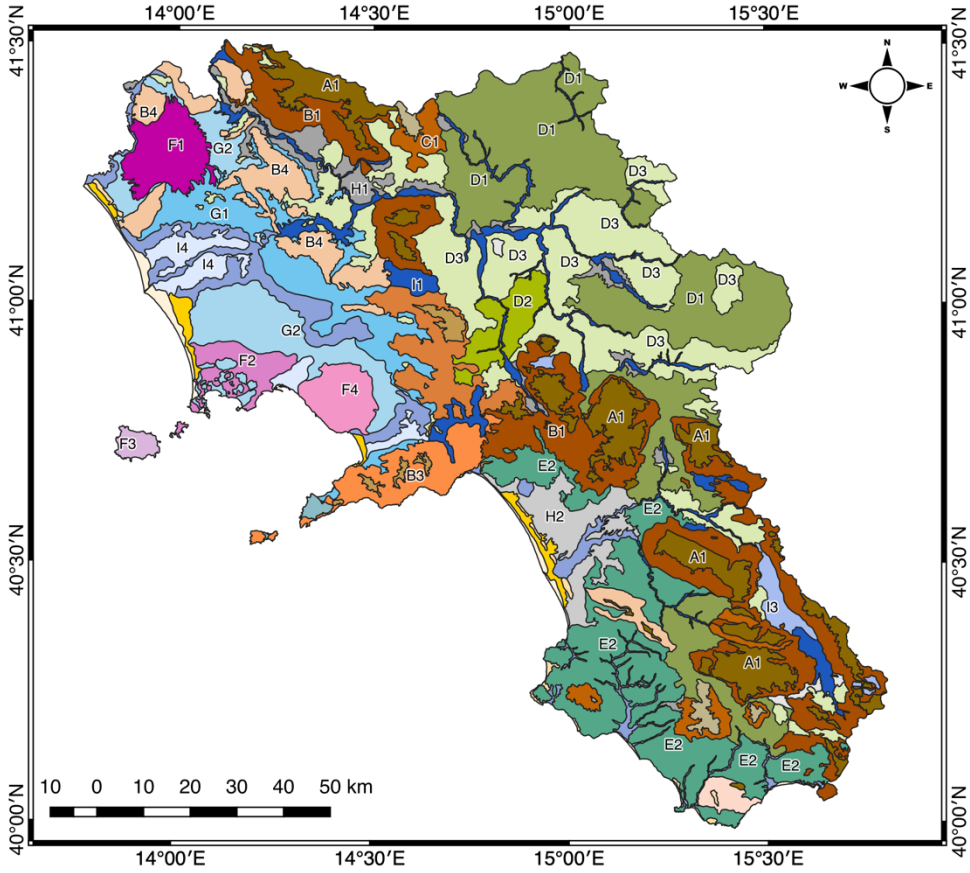


Figure 2.2. CORINE Land Cover (CLC) 2018 Level 1 map of Campania. Dominant land cover types are agricultural lands (56% of the region), forests and semi-natural areas (38%).

occupied by natural and semi-natural vegetation. The infrastructural and urban density is low.

Calcareous mountains represent 20% of the regional surface through the land systems of Montevergine and Sarno, Sorrento-Amalfi peninsula, and Mts. Massico and Tifatini (labels B1, B2, B3, B4 and B5 in Figure 2.3). These areas undergo moderate climatic interference and comprise about 40% of the areas covered by forests and natural vegetation in Campania.



Land Systems

- A1 - Calcareous high mountain with pyroclastic cover
- A2 - Calcareous high mountain of Montevergine and Sarno with pyroclastic cover
- A3 - Marly-arenaceous and marly-calcareous high mountain
- B1 - Internal calcareous reliefs with pyroclastic cover
- B2 - Calcareous reliefs of Montevergine and Sarno with pyroclastic cover
- B3 - Calcareous reliefs of the Sorrento and Amalfi peninsula with pyroclastic cover
- B4 - Calcareous reliefs with pyroclastic cover
- B5 - Calcareous coastal reliefs of Mount Bulgheria
- C1 - Marly-arenaceous and marly-calcareous mountain reliefs
- D1 - Clay hill
- D2 - Clay hill with pyroclastic cover
- D3 - Marly-arenaceous, marly-calcareous and conglomeratic hill
- E1 - Coastal hill of the Sorrento-Amalfi peninsula
- E2 - Cilento coastal hill
- F1 - Roccamonfina volcanic complex
- F2 - Volcanic reliefs of the Phlegraean Fields
- F3 - Volcanic reliefs of the island of Ischia
- F4 - Somma-Vesuvio volcanic complex
- G1 - Foothills of the calcareous reliefs
- G2 - Foothills of volcanic reliefs
- H1 - Alluvial terraces of the upper and middle Volturno river and of the Apennine rivers
- H2 - Alluvial terraces of the Sele river plain
- H3 - Terraced basins of the ancient lakes
- I1 - Alluvial plains in the upper and middle Volturno river and in the Apennine rivers
- I2 - Alluvial plains in the lower Garigliano, Volturno and Apennine rivers
- I3 - Morphologically depressed areas of the internal alluvial plains
- I4 - Morphologically depressed areas of the alluvial plains, in the lower Volturno river and of the smaller streams
- L1 - Retro-dune depressions
- L2 - Ancient dunes and marine terraces
- L3 - Dune systems and beaches

Figure 2.3. Land systems map of Campania (from Di Gennaro, 2002).

Alluvial plain is about 10% of regional landscape, and includes the land systems around Volturno, Sele and Garigliano rivers and several inland, morphologically depressed alluvial areas (labels I1, I2, I3 and I4 in Figure 2.3). Campanian alluvial plains are characterised by slight or negligible climatic interference (i.e. there is no climatic limitation to agricultural and forest production), with moderate to high summer water deficit. The land is mainly occupied by high value crops, with a relevant presence of infrastructural and urban areas.

Coastal hills include the coastal reliefs of Cilento, Eboli and of the Sorrento-Amalfi peninsula, totalling 9% of regional surface (labels E1 and E2 in Figure 2.3). Climatic interference is low and summer water deficit risk is high. The land use is mainly comprised of natural vegetation (about 40% of the total area) and high value agricultural systems.

Footslope plains (9% of the region) include the areas around the calcareous and volcanic reliefs and are essentially located in north-west Campania (labels G1 and G2 in Figure 2.3). These have no or slight climatic interference and moderate to high risk of summer water deficit. Infrastructures and urban areas cover about 21% of this land system, the remaining part being mainly occupied by orchards, vineyards, hazel groves, and horticultural crops.

High mountain (8% of Campania) embraces the summit areas and the higher slopes of the calcareous, marly-arenaceous and marly-calcareous reliefs (labels A1, A2 and A3 in Figure 2.3). It crosses the whole central portion of the region from north-west to south-east and is characterised by high to very high climatic interference. About 92% of this land system is covered by natural and semi-natural vegetation.

The volcanic complex land system plays an important role in Campania, both in terms of landscape and high agricultural and forest productivity, while only being 5% of its surface. It includes the volcanic complex of Roccamonfina, the volcanic reliefs of the Phlegraean Fields, the volcanic island of Ischia and the volcanic complex of Somma-Vesuvius (labels F1, F2, F3 and F4 in Figure 2.3). The urban density of the latter is high to very high on the lower parts of slopes, while it is low to moderate at higher elevations, where forests, chestnut wood and coppice dominate the land use.

Alluvial terraces (5% of regional surface) include the upper and medium Volturno and Sele rivers (labels H1, H2 and H3 in Figure 2.3). These areas are morphologically raised above the base of the alluvial plain, with no or slight climatic interference, and moderate to high risk of summer water deficit. The dominant land uses are high value agriculture (orchards, vineyards, and hazel groves), forage, cereals, and horticultural crops.

The remaining land systems occupy altogether less than 4% of the Campania surface and are not discussed herein.

2.2.2. Fire data

The fire data used in this research was provided by the Forest Fire Protection Information Unit of Carabinieri. This law enforcement agency is in charge, among other responsibilities, of forest fires prevention, firefighting, arson investigations and prosecution, and burned area inventorying. Available data is thus to be considered official and correct.

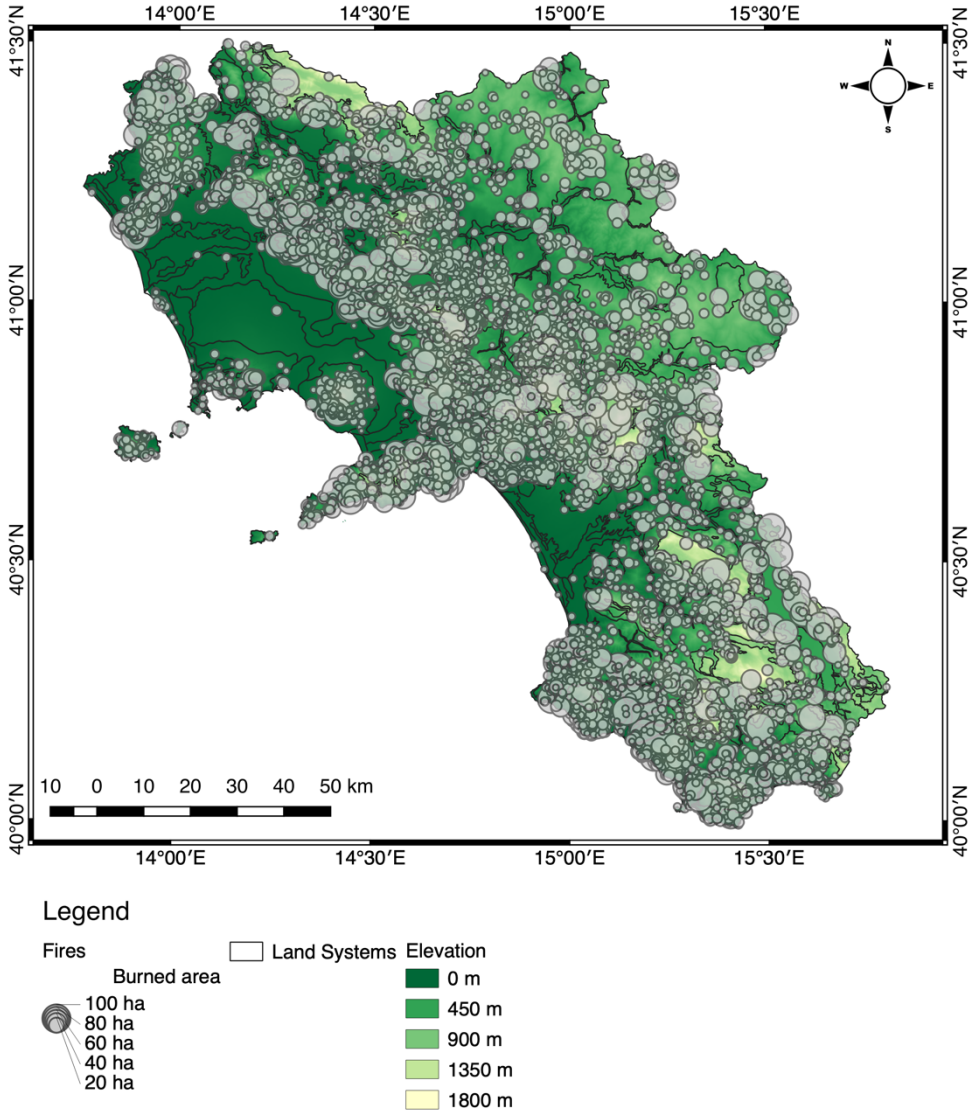


Figure 2.4. Fires recorded in 1998-2011 in Campania and their burned area.

The database reports details of all the 11731 fires occurred in Campania between 1998 and 2011 (Figure 2.4). While Carabinieri record burnt scar perimeters on a fire-by-fire basis, according to conventional practices of field surveying with GPS receivers and desk digital cartography, these were not provided for this research.

The dataset details for each event: cartographic coordinates of the centroid of burned area, date and time of initial spread and fire extinction, final burned area, and presumed causes. Further to burned area, additional fire behaviour attributes that can be retrieved from the

dataset are fire duration and rate of spread. Fire duration was evaluated as the difference, in hours, between fire inception and extinction. Rate of spread was calculated from burned area and fire duration in the simplified assumption of a circular fire growing at a constant rate in every direction throughout its duration on a flat and uniform surface. Fires in the dataset were further intersected with land cover and topography maps so that each event was associated with the corresponding land cover class, terrain slope and aspect.

On average, 838 fires were recorded every year. Mean burned area was 6.5 ha, mean fire duration was 9.6 hours and mean rate of spread 22.1 m/h. 99.7% of fires had an anthropic cause: 73.9% were due to arson, 10.0% to unintentional anthropic activity, while 15.8% were reported as unclassified anthropic (either arson or unintentional). Personal communications with Carabinieri officials clarified that the latter classification substantially includes anthropic fires for which a proof confirming them as either arson or unintentional was not identified.

2.2.3. Land cover and topography maps

Fires in the database were intersected with land cover and topographic maps to understand how these factors drive fire occurrence. The Coordination of Information on the Environment (CORINE) land cover (CLC) map is an inventory of land cover in European countries initiated in 1985 (European Environment Agency, 2007). CLC maps are produced at a nominal scale of 1:100.000, with a minimum mapping unit of 25 ha and minimum width of linear elements of 100 m. The first CLC map was produced in 1990, and since 2000 is updated every six years. As fires in the database span a 14-year period, events were associated with the closest prior CLC version. The latest level 1 CLC map of Campania is plotted in Figure 2.2. The level 2 and level 3 descriptions of CLC classes affected by fires in the study area are reported in Table 2.1.

Elevation for each fire data point was extracted from the Digital Elevation Model over Europe (EU-DEM) v1.0 (Bashfield and Keim, 2011). EU-EM is a digital surface model developed by the European Environment Agency (EEA) as part of the Copernicus Land Monitoring Service. This product is a fusion of ASTER Global Digital Elevation Model (GDEM) and Shuttle Radar Topographic Mission (SRTM) data by means of a weighted averaging approach. The EU-DEM v1.0 was produced at a resolution of 25 m, and its validation reported a relatively unbiased (-0.56 m) overall vertical accuracy of 2.9 m RMSE (Tøttrup, 2014). Slope and aspect were computed from the EU-DEM using standard GIS tools (Hofierka et al., 2009). Slope was classified in seven bins of 5° between 0° and 35°, and in a further eighth bin including all values above 35°. Aspect was classified in the eight cardinal and intercardinal directions, plus a ninth class including all points with slope less than 5° and for which aspect was not computed.

2.2.4. Bubble plots

To identify spatial and temporal patterns of fire occurrence, bubble plots were used as an alternative to a series of maps. The objective was to join spatial and temporal information

in a single plot, at the expense of one of the spatial dimensions (for example latitude). The diagram was constructed as a scatterplot of fire events with longitude plotted along the x axis and date along the y axis; each fire was represented in the diagram with a circle, whose size is representative of burnt area (Bartlein et al., 2008). Burned area was reported in four classes: fires smaller than 1 ha, fires between 1 and 10 ha, fires between 10 and 100 ha, and fires larger than 100 ha.

The study area extends for about 170 km in both the South-North and the West-East directions; latitude and longitude are not a strong surrogate for a specific set of landscape

Table 2.1. CORINE Land Cover (CLC) classes affected by fires in the study area.

Level 2 code	*Description*	*Level 3 code*	*Description*
21	Arable land	211	Non-irrigated arable land
		212	Permanently irrigated land
22	Permanent crops	221	Vineyards
		222	Fruit trees and berry plantations
		223	Olive groves
23	Pastures	231	Pastures
24	Heterogeneous agricultural areas	241	Annual crops associated with permanent crops
		242	Complex cultivation patterns
		243	Land principally occupied by agriculture, with significant areas of natural vegetation
31	Forest	311	Broad-leaved forest
		312	Coniferous forest
		313	Mixed forest
32	Shrub and/or herbaceous vegetation associations	321	Natural grassland
		323	Sclerophyllous vegetation
		324	Transitional woodland/shrub
33	Open spaces with little or no vegetation	333	Sparsely vegetated areas
		334	Burnt areas

attributes, so it is here underlined that there is no reason to prefer one of them to produce the plot. Indeed, the advantage in using the bubble plot lies in its potential to show spatial and temporal continuities in fire regime, and to disclose relationships eventually existing between them.

2.2.5. Bar charts and box plots

Bar charts were used to provide a quantitative description of fire occurrence and total burned area versus land cover and topography. Box plots were produced to evaluate the dispersion of burned area, fire duration and rate of spread year to year and across land cover, slope, and aspect classes.

An approach to the production of bar charts is to just report the counts of occurred fires and the sums of burned area for each class of land cover, slope, and aspect. This would merely report repartition of all fires across landscape features. However, in this study a different approach was adopted, reporting fire occurrence and burned area in terms of annual densities, i.e. number of fires and burned area per square kilometre per year (Kharuk et al., 2007). More specifically, relative number of fires n_c in a landscape feature (land cover, slope, or aspect) class c was computed as:

$$n_c = \frac{N_c}{A_c \cdot Y} \quad (2.1)$$

where N_c is the number of fires in the dataset falling within landscape feature class c, A_c is the area of landscape feature class c in the study area, and Y is the number of years covered by the dataset (14 in this study). Similarly, relative burned area b_c was computed as:

$$b_c = \frac{B_c}{A_c \cdot Y} \quad (2.2)$$

where B_c is the total burned area within landscape feature class c. Using relative values rather than total values has the advantage of providing a more objective mean to compare results within the study area and potentially across other regions and ecosystems.

2.3. Results

This section first reports an assessment of fire seasonality and inter-annual variability based on information retrieved from the fires database. It then reports findings derived by intersecting fire data with land systems, land cover and topography maps.

2.3.1. Fire seasonality and inter-annual variations

Fire occurrence shows a marked year to year variation in the number of fires, total burnt area, and average burned area of individual fires (Table 2.2). Years where the phenomenon appears to be severe alternate with those where it is more limited. Year 2007 stands out as exceptional in terms of total burnt area. This is further reflected in the dispersion of burned

area of individual fires (Figure 2.5a), which is the highest among the other years for its larger fires. A similar observation may be drawn for burned area in 2000, and indeed this year is characterised by the second largest total burned area in the dataset. The dispersion of fire duration (Figure 2.5b) shows an annual variability mimicking that of burned area. Conversely, rate of spread shows a more limited annual variability (Figure 2.5c).

Fires exhibit a marked seasonality (Figure 2.6), peaking in the summer season, with 82% of fires and 89% of burned area recorded between June and September. A second peak, although less relevant, is observed in March. This double seasonality is also evident in the bubble plot in Figure 2.7, and it occurs every year. Summer fires spread throughout all longitudes in the region, while there is a lack of such spatial continuity in late winter/early spring fires. A notable exception is year 2002 where the lack of longitudinal and temporal continuity of summer fires is reflected by the small number of recorded events and a relatively low mean fire size (Table 2.2). The bubble plot also shows that the years exhibiting the largest number of events, i.e. 2000, 2001, 2003, 2007 and 2011 (Table 2.2), are characterised by a prolonged summer fire season (thicker summer bubble cluster).

Table 2.2. Annual synthesis of all fires recorded in the study area between 1998 and 2011.

Year	*Number of fires*	*Total burned area (km^2)*	*Average fire size (ha)*
1998	497	35.7	7.2
1999	280	18.2	6.5
2000	843	86.7	10.3
2001	984	51.0	5.2
2002	310	11.7	3.8
2003	1323	54.8	4.1
2004	803	31.2	3.9
2005	669	19.4	2.9
2006	423	17.2	4.1
2007	1757	257.4	14.7
2008	776	34.3	4.4
2009	895	51.4	5.8
2010	537	19.6	3.7
2011	1634	69.2	4.2

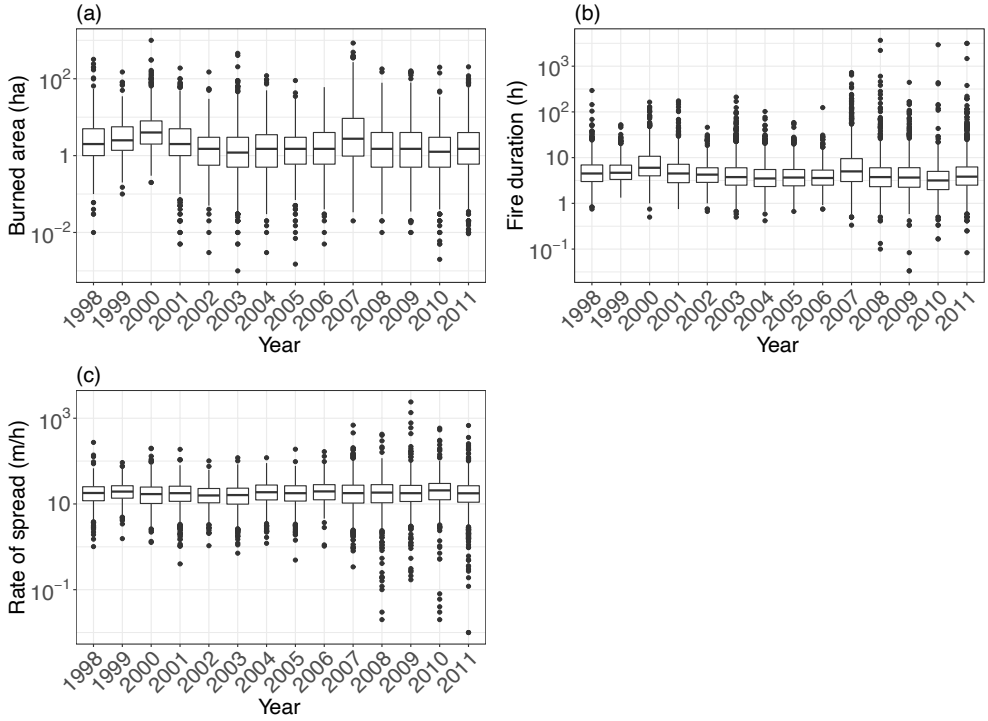


Figure 2.5. Box plots of annual burned area (a), fire duration (b), and rate of spread (c). Burned area and fire duration show a marked annual variability.

2.3.2. Understanding spatial patterns of fire occurrence

An assessment of the spatial distribution of forest fires against the Campanian land systems map showed that annual patterns of fire occurrence are substantially consistent over time (Figure 2.8) and tend to be spatially distributed according to the characteristics of the landscape. The land systems most affected by fires are:

- The calcareous mountains of Montevergine and Sarno, the calcareous reliefs of the Sorrento-Amalfi peninsula, the Apennine reliefs with pyroclastic cover of Massico and Tifatini, and the calcareous reliefs of Cilento;
- Cilento coastal hills, and specifically its sub-systems of the marly-arenaceous hills and of the clayey hills;
- All the main volcanic areas, and namely those corresponding to the land systems of Somma-Vesuvius, Phlegraean Fields and Roccamonfina;
- The inland hills, limited to those areas dominated by broad-leaved forests.

Fires had no impact on the remaining land systems, basically corresponding to the two main coastal plains of Campania (alluvial plains of Volturno and Sele rivers).

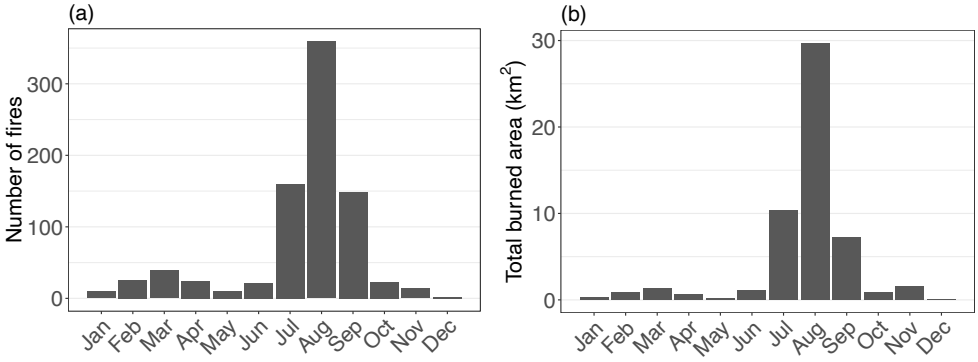


Figure 2.6. Seasonality of fire occurrence in the observation period 1998-2011: (a) average number of fires; (b) average total burnt area. Most fires and the largest proportion of burned area are recorded between June and September.

2.3.3. Effect of land cover

The land cover class most affected by fires in terms of both total number of fires and total burnt area is broad-leaved forest (CLC class 311 in Table 2.3), with an average of 298 fires recorded, and 21.2 km^2 burnt each year. Shrub and herbaceous vegetation associations (CLC classes 321, 323 and 324) report 166 events per year, and a total burned area of 15.2 km^2/year. Conversely, heterogeneous agricultural areas (CLC classes 241, 242 and 243) report a larger number of fires (193 per year), but a lower total burned area (8.6 km^2/year). Olive groves (CLC class 223) are affected by 56 fires per year, resulting in a loss of 2.7 km^2/year. Significantly affected by fires is also non-irrigated arable land (CLC class 211) with 65 fires reported each year and a burned area of 2.1 km^2/year.

Bar charts of the density of number of fires and total burned area per land cover class (Figure 2.9) show that areas reported under the CLC class of burned areas (code 334) exhibit the highest number of fires and burned area per km^2 per year. However, it is worth noting that this land cover class has a limited extent in the study area. Sclerophyllous vegetation (CLC class 323) is the land cover type most affected by fires, both in terms of number of ignitions and total burnt area (about 1.6 ha per km^2 burnt each year). Natural grassland (class 321) exhibits comparable levels of burned area (about 1.5 ha/km^2/year), although a lower number of events is recorded. In more general terms, fire occurrence and total burned area is most relevant in shrub and herbaceous vegetation associations (classes 321, 323, 324).

Heterogeneous agricultural areas, represented in Campania by CLC classes 241, 242 and 243 (Table 2.1) show a lower annual density of number of fires and total burned area, as compared to forests, shrubs, and herbaceous vegetation associations. Similar lower values are recorded also by pastures (CLC class 231). Among permanent crops, olive groves (CLC class 223) are considerably affected by fires.

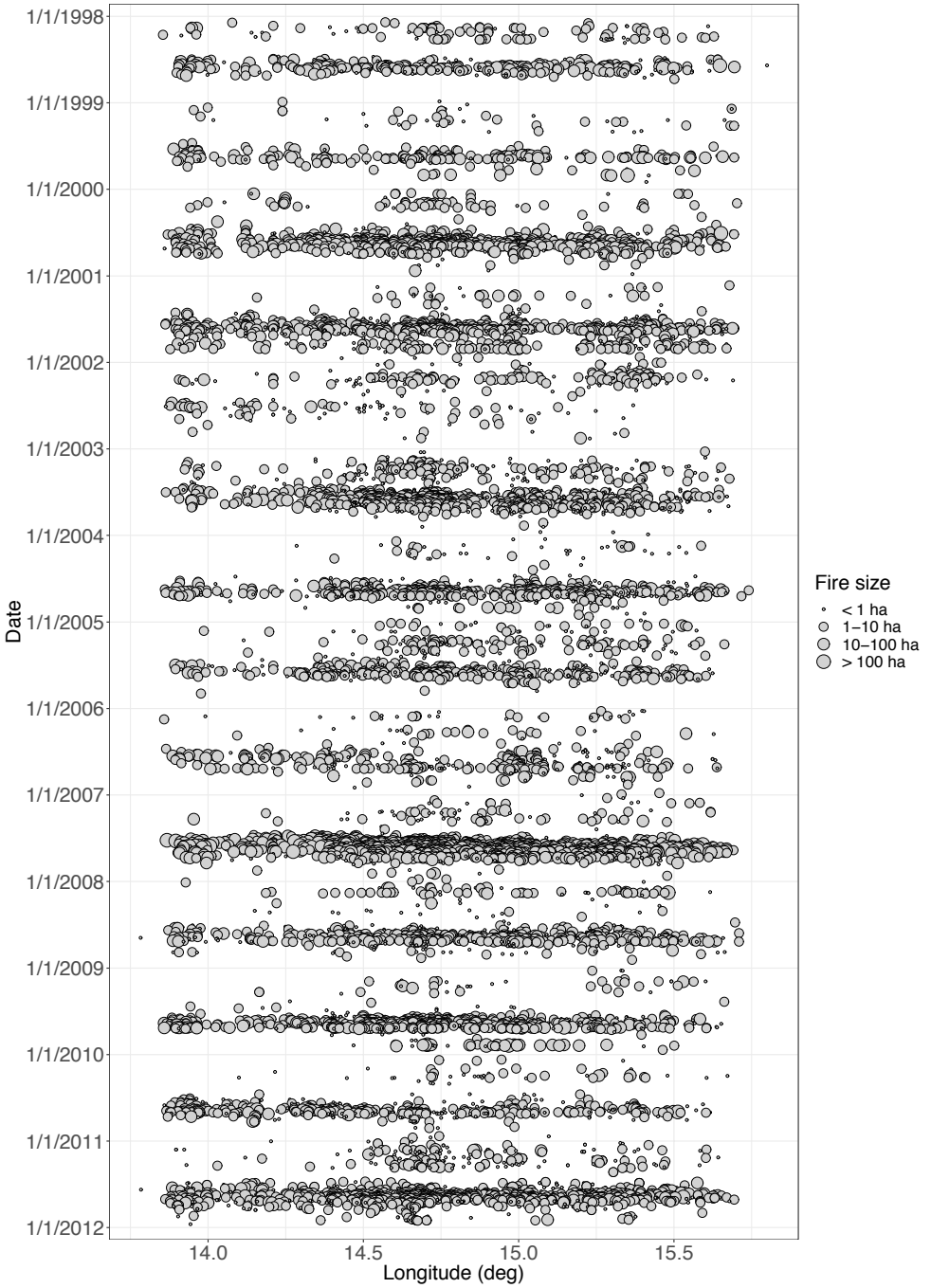


Figure 2.7. Bubble plot reporting fire size vs date and longitude in the study area.

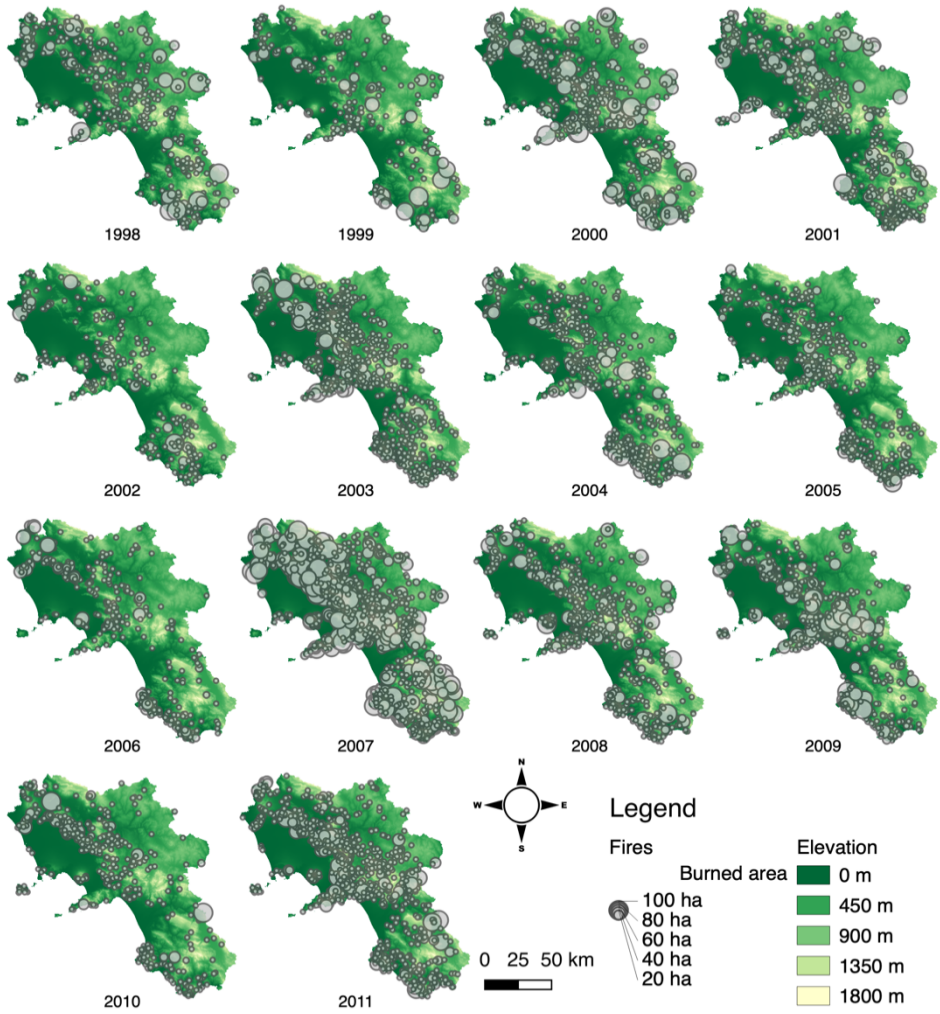


Figure 2.8. Annual spatial patterns of fires and their burned area. Year 2007 stands out in terms of both number of fires and of burned area.

Box plots show considerable variability of burned area across CLC classes (Figure 2.10a). Burned area in shrub and herbaceous vegetation associations (CLC classes 321, 323 and 324) tends to be larger than in forests (CLC classes 311, 312, 313). Similarly, non-irrigated arable land (CLC class 211) and pastures (CLC class 231) are characterised by larger fires as compared to other classes among agricultural areas. Within forests, fires in broad-leaved forest (class 311) are larger than in coniferous and mixed forests (classes 312 and 313 respectively).

Dispersion of fire duration shows little variability across CLC classes (Figure 2.10b). A similar consideration can be drawn for rate of spread (Figure 2.10c), although coniferous forest and mixed forest (CLC classes 312 and 313) show slightly lower values against all other land cover classes.

2.3.4. Effect of topography

Bar charts of the density of number of fires and total burned area in bins of terrain slope show that topography is a strong driver of fire occurrence (Figure 2.11). A marked increase in the number of ignitions up to a slope of 20-30° is observed, then followed by a decrease, whereas total burned area steadily increases throughout the computed slope ranges. Likewise, slope appears to affect fire behaviour characteristics. The box plot of burned area (Figure 2.12a) shows increasing values with increasing slope. Similarly, fires tend to have a

Table 2.3. Synthesis of fires by land cover class in the study area between 1998 and 2011. Keys for class codes are reported in Table 2.1.

CLC class	*Number of fires*	*Total burned area (km^2)*
211	510	29.9
212	2	0.1
221	6	0.4
222	273	10.8
223	787	38.3
231	98	9.9
241	327	15.7
242	1123	52.8
243	1249	52.3
311	4176	296.2
312	148	4.7
313	99	5.1
321	861	102.7
323	572	38.7
324	894	70.7
333	60	6.5
334	22	1.6

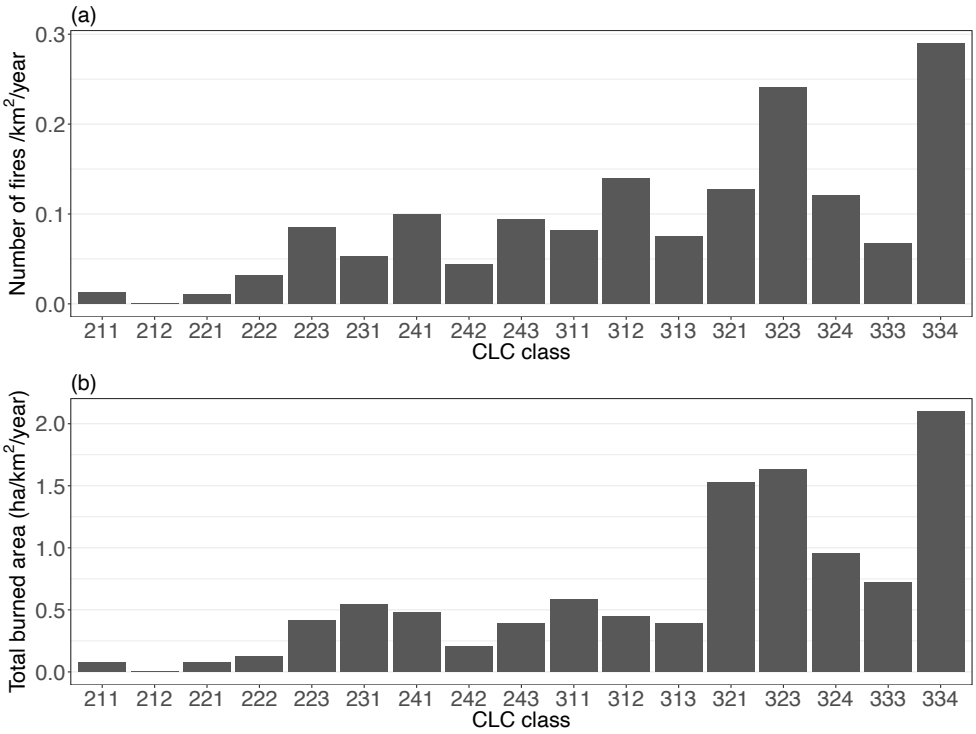


Figure 2.9. Bar charts of fire occurrence in CORINE land cover class: a) number of fires per square kilometre per year; b) total burnt area in hectares per square kilometre per year. Keys for class codes are reported in Table 2.1.

longer duration with increasing slope (Figure 2.12b). Rate of spread shows a slight increase as slope increases up to 10-15°, then followed by a slight decrease with increasing slopes (Figure 2.12c).

Aspect is a clear factor determining both fire occurrence and total burned area (Figure 2.13). Southwest- to south- and east-facing slopes show a higher fire occurrence per year per square kilometre as compared to northeast- to north- and west-facing slopes. A much lower fire occurrence is recorded in substantially horizontal terrain. Slightly different results are observed when the total burnt area is considered instead, with a more marked prominence of southwest- south- and southeast-facing slopes as opposed to other aspect values. Like fire occurrence, total burned area shows significantly lower values on horizontal terrain. Fire behaviour characteristics do not vary with aspect, with burned area, fire duration and rate of spread all showing even dispersion across all aspect classes (Figure 2.14).

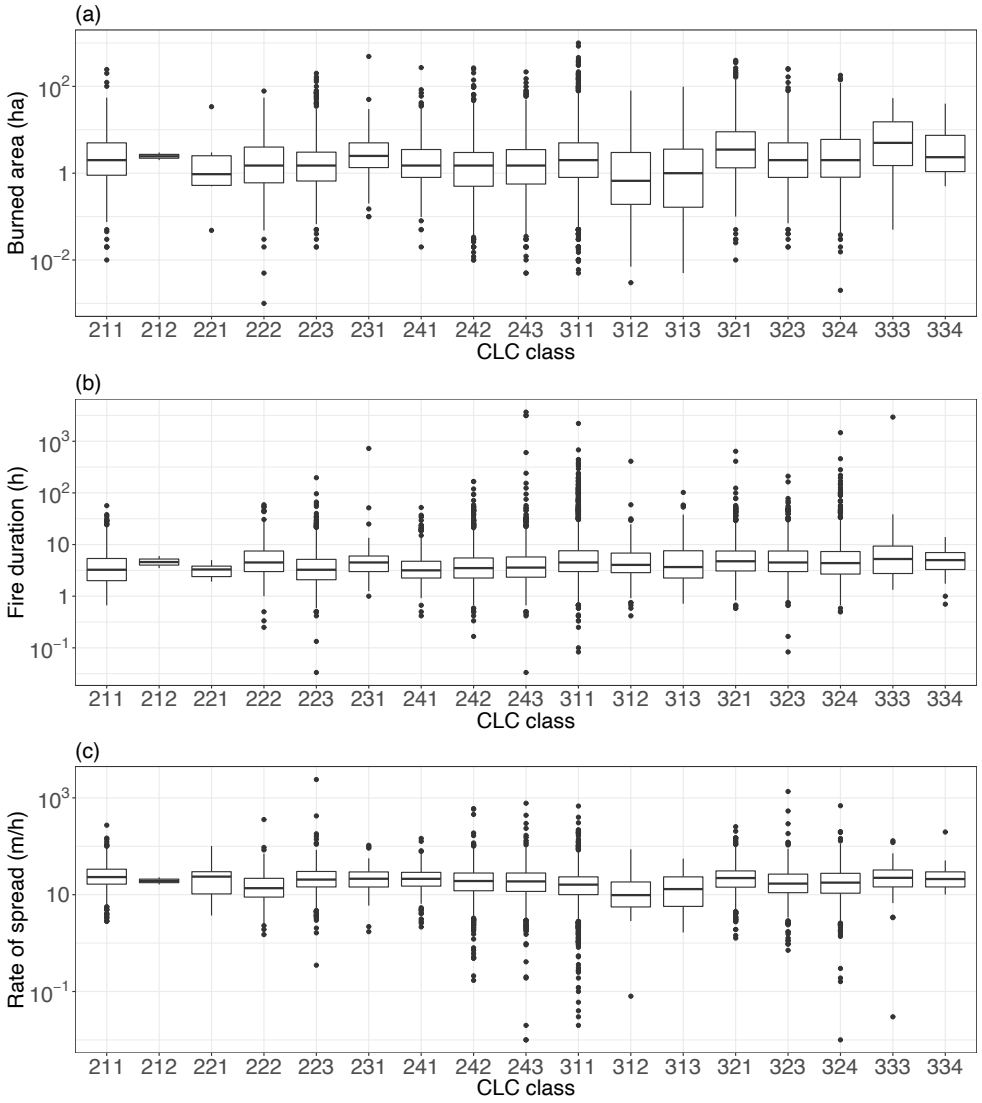


Figure 2.10. Box plots of burned area (a), fire duration (b), and rate of spread (c) in CLC land cover classes. Keys for class codes are reported in Table 2.1.

2.4. Discussion

In this section results on fires seasonality and annual variability are first discussed. Spatial patterns of fire occurrence are then reviewed against the biophysical and anthropic factors characterising land systems. A more quantitative assessment follows, discussing the effect of land cover and topography on both fire occurrence and fire behaviour characteristics.

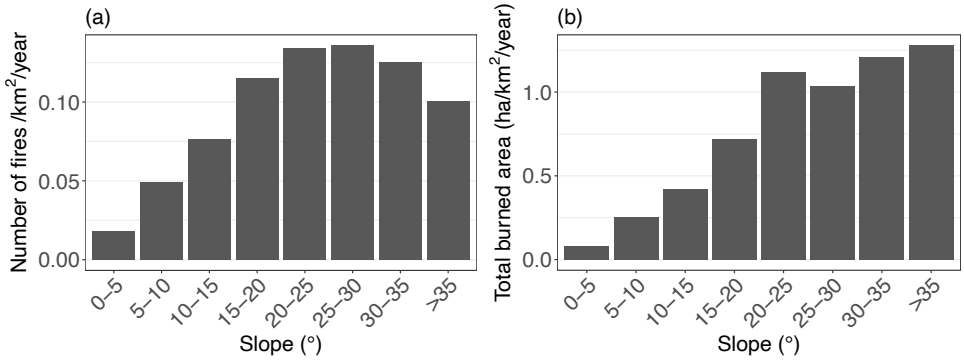


Figure 2.11. Bar charts of fire occurrence in slope classes: a) number of fires per square kilometre per year; b) total burnt area in hectares per square kilometre per year.

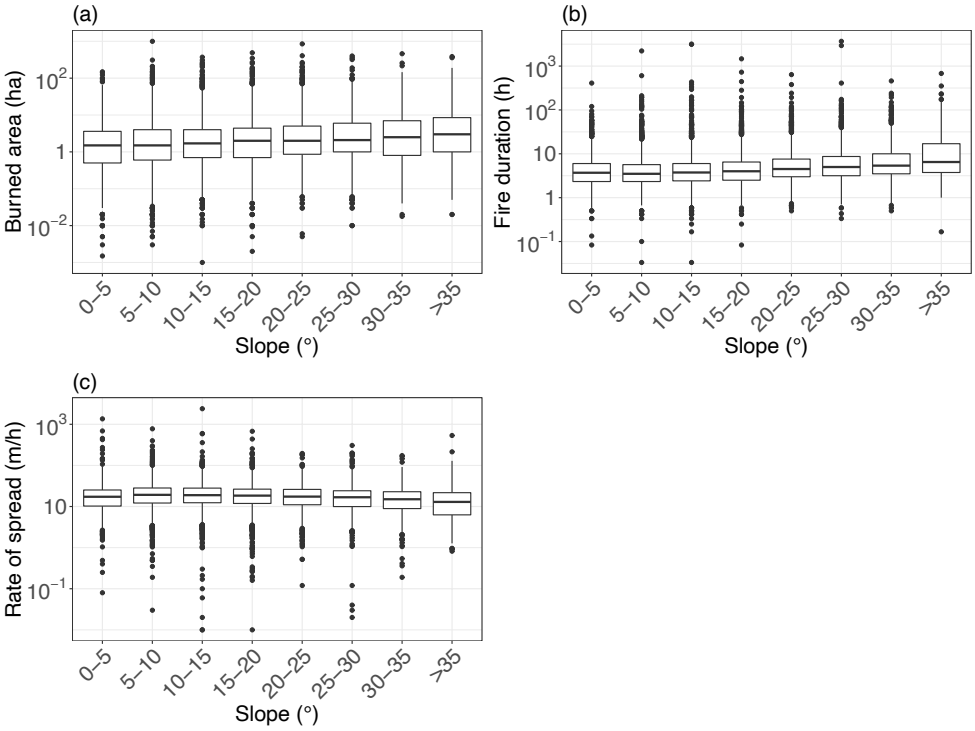


Figure 2.12. Box plots of burned area (a), fire duration (b), and rate of spread (c) in slope classes.

2.4.1. Seasonality, inter-annual variation, and spatial consistency of fires

Fire occurrence and total burned area show a marked seasonality, with most events being recorded between June and September (Figure 2.6). This seasonality is evident also in the bubble plot reporting fire size against longitude and date (Figure 2.7). Years characterised

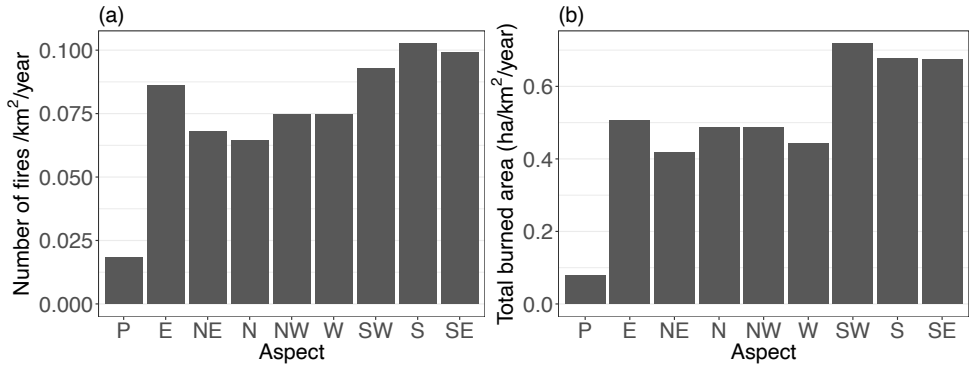


Figure 2.13. Bar charts of fire occurrence in aspect classes: a) number of fires per square kilometre per year; b) total burnt area in hectares per square kilometre per year. Label P (plain) refers to fires occurring on areas with slope less than 5°, where aspect was not computed.

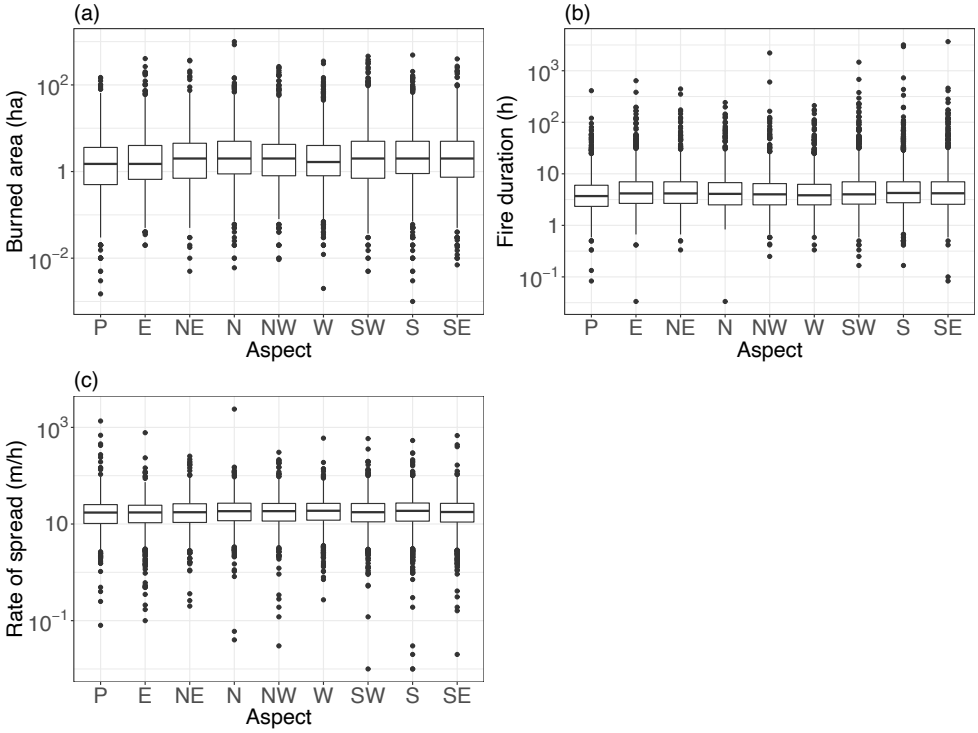


Figure 2.14. Box plots of burned area (a), fire duration (b), and rate of spread (c) in aspect classes. Label P (plain) refers to fires occurring on areas with slope less than 5°, where aspect was not computed.

by a peak in fire occurrences, i.e. 2000, 2001, 2003, 2007 and 2011 (Table 2.2), show a markedly longer fire season. Years 2000 and 2007 also stand out for the distribution of burned area and fire duration being dispersed towards larger values (Figure 2.5). The observed seasonality and annual variability are in line with the wider context of

Mediterranean European countries, where summers are characterised by low precipitation and high temperature leading to the build-up of preconditions favouring fire ignition and propagation (Ganteaume et al., 2013; San-Miguel-Ayanz et al., 2013).

The fire phenomenon exhibits a clear interannual variability in terms of number of fires, total burned area, and average fire size (Table 2.2). This variability is common in the Mediterranean and it is determined by the corresponding interannual variability in weather conditions (Pausas and Paula, 2012; San-Miguel-Ayanz et al., 2013; Turco et al., 2013; Viegas and Viegas, 1994). Fires peaked in 2007, especially in terms of total burned area and average fire size. Indeed, summer 2007 in Italy is noted for being exceptional in terms of unusually large fires spreading throughout Central and Southern Italy and causing loss of lives (Milazzo and Capone, 2010).

Annual spatial patterns of fire occurrence are substantially consistent over time (Figure 2.8), despite the observed interannual variability (Table 2.2). This is true also for year 2002, albeit the bubble plot in Figure 2.7 highlighted its lack of longitudinal and temporal continuity of summer fires, as compared to all other years in the dataset. This suggests that, beyond interannual variability in the number of fires and burned area controlled by variable factors such as weather (Ganteaume et al., 2013; Viegas and Viegas, 1994), the spatial patterns of fire occurrence in the study area are determined by landscape characteristics (Barbati et al., 2015; Duane et al., 2015; Lavorel et al., 2006; Ruffault and Mouillot, 2017).

2.4.2. Understanding spatial patterns of fire occurrence

The intersection of forest fires on the land systems map highlighted a clear relationship between the spatial patterns of fire occurrence and landscape characteristics. Land systems of the medium and low calcareous mountain of Montevergine and Sarno, the Sorrento-Amalfi peninsula, and Mounts Massico and Tifatini (labels B1, B2, B3, B4 and B5 in Figure 2.3) were affected by forest fires on an almost yearly basis. Indeed, these land systems are characterised by a moderate to high climatic interference (see §2.2.1). Moreover, natural vegetation (hereby comprising about 40% of the entire natural vegetation cover in the region) is dominated by fire sensitive species such as chestnut, mixed forests of mesophyte broad-leaved species, holm oak, xerophyte prairie and shrubs at different levels of degradation.

Fire occurrence in Cilento coastal reliefs (label E2 in Figure 2.3), characterised by low climatic interference, is rather due the high risk of summer water deficit and to land use. The latter is dominated by olive groves, cereal crops, and natural vegetation, with prevalence of thermophile broad-leaved forests, holm oak, shrubs, garrigue and xerophyte prairies. Anthropic pressure might exert a role in driving fire occurrence, as it is particularly high in July and August due to summer tourism, matching the observed seasonality (Figure 2.6). Similar considerations justify the high fire occurrence in the Roccamonfina, Campi Flegrei, Ischia Island and Somma-Vesuvio volcanic complexes (labels F1, F2, F3 and F4 in Figure 2.3). These land-systems are characterised by low to moderate climatic interference and moderate to high risk of summer water deficit. Agricultural and forest land uses are highly productive, thanks to the high fertility of the volcanic soils, and are dominated by

chestnut, hazel groves, fruit trees, scrubs, vineyards, and olive groves. Anthropic pressure is moderate to high.

In internal areas, fires occur on the hill land-systems of Irpinia, Sannio, the upper basin of Sele, and Cilento (labels D1, D2 and D3 in Figure 2.3). While land use is mainly agricultural (80% of the total area of these land-systems), and the infrastructural and urban density is low, fires are recorded in the remaining natural surfaces, characterised by sparse and relatively small broad-leaved forests. Yet, soil fertility leads to a significant development of biomass which, associated with the moderate to high risk of summer water deficit, leads to high fuel availability (§1.2.1) during the dry season.

Fires had no impact on the remaining land systems, basically corresponding to the two main coastal plains of Campania (alluvial plains of Volturno and Sele rivers), which are essentially devoted to orchards and horticulture under widespread irrigation.

Across land systems a clear link between patterns of fire occurrence (or the lack thereof) and some landscape characteristics emerges. Indeed, climatic conditions, land cover and anthropic pressure appear consistently to be drivers of fire occurrence. In this sense, fire may be considered a landscape-shaping process in some of the land systems in the study area (Biermann et al., 2016; Dube, 2009; Harrison et al., 2010).

2.4.3. Influence of land cover on fire occurrence and total burned area

The considerations discussed in the previous section were further developed to quantitatively understand the effects of land cover and topography on fire regime and, in the following section, on fire behaviour characteristics. Indeed, fire occurrence and fire behaviour are determined by a large number of factors, essentially falling into five groups: topography, land cover, climate, weather, and anthropic activity (Barrett et al., 2016; Costafreda-Aumedes et al., 2016; Faivre et al., 2016, 2014; Falk et al., 2007; Fernandes et al., 2016; Fischer et al., 2015; Gustafson et al., 2011; Lasslop and Kloster, 2017; Littell et al., 2016; Viegas and Viegas, 1994). Clearly, the considerations proposed in this chapter are far from being exhaustive. The intended objective is to have a grasp of how the proposed subset of static factors controlling the fire phenomenon in the region determines the spatial variability of fire occurrence, total burned area, and fire behaviour. In this sense, the proposed analysis serves as a background information supporting the interpretation of satellite observations of fuel condition (chapters 3, 5 and 6).

The land cover class that most contributed to fire phenomenon in terms of total number of fires and total burnt area is broad-leaved forest (CLC class 311, Table 2.3). However annual densities, i.e. values normalised against land cover area and number of years covered by the dataset (Figure 2.9), show that forests are less affected by fires than shrubs and herbaceous vegetation (CLC classes 321, 323, 324). Grassland, sclerophyllous vegetation and other shrubs in the Mediterranean are generally characterised by higher level of flammability, as opposed to broad-leaved forests (Corona et al., 2014; Della Rocca et al., 2018; Dimitrakopoulos, 2001; Dimitrakopoulos and Panov, 2001; Dimitrakopoulos and Papaioannou, 2001; Moreira et al., 2011). This result confirms the value of adopting annual

densities as a measure of fire occurrence, as it allows the evaluation of fire regime with the specific characteristics of land cover types.

The highest annual densities of number of fires and burned area are reported under the CLC class of burned areas (code 334). This class refers to natural woody vegetation affected by recent fires (less than one year), and includes damaged natural woody plants, sclerophyllous vegetation, transitional forest-shrub formations and areas with sparse vegetation (Kosztra et al., 2019).

Albeit to a lesser degree, heterogeneous agricultural areas (CLC classes 241, 242 and 243) appear to be widely affected by fires. In this land cover class, recorded events predominantly have an unintentional cause and are due to agricultural practices. In fact, inception occurs in agricultural land patches, where flames subsequently propagate to nearby natural and abandoned areas (Milazzo and Capone, 2010). Similar considerations apply to fires recorded in pastures (CLC class 231). Among permanent crops, olive groves (CLC class 223) are considerably affected by fires, due to their high flammability (Dimitrakopoulos and Papaioannou, 2001).

As a general trend, number of fires and total burned area appear to increase from cultivated land to broad-leaved forests, to shrubs and to sclerophyllous vegetation. Similar patterns were found elsewhere (Díaz-Delgado et al., 2004; Moreira et al., 2011; Mouillot et al., 2003). These results, along with spatial patterns of observed fire occurrence versus land systems in the region, support the identification of land cover as a key driver of fire spatial distribution (Bajocco and Ricotta, 2008; Carmo et al., 2011; Wells et al., 2004).

2.4.4. Influence of topography on fire occurrence and total burned area

The density of number of fires shows a marked increase with slope up to 25-30° (Figure 2.11a). The low number of fires recorded in plain areas is justified by the typical land cover in the coastal plains, dominated by orchards and horticulture, and reflects the observed densities of fire occurrence in the corresponding CLC classes (Figure 2.9). A decrease in fire occurrence is observed in slopes steeper than 30°. This may be explained by the fact that almost all fires are of anthropic origin (Lovreglio et al., 2010; Milazzo and Capone, 2010), and that the steepest slopes are less accessible (Oliveira et al., 2014).

Density of total burned area steadily increases with slope up to 20-25°, in a way similar to the number of fires (Figure 2.11b). However, values stabilise for steeper slopes. This different observation may be justified by the fact that fire containment efforts at steeper slopes are more difficult (Liang et al., 2012; Rodríguez y Silva et al., 2014), thus resulting in larger fires, as also observed in Figure 2.12a.

Aspect appears to control fire occurrence in the region, with South-West, South and South-East facing slopes being characterised by a higher density of number of fires and burned area (Figure 2.13). This result is common in Mediterranean ecosystems (Mouillot et al., 2003; Oliveira et al., 2014), where South-facing slopes are characterised by drier conditions due to a larger amount of solar radiation impinging on the surface, and where west facing slopes are exposed to the sun in the hours when maximum temperature is usually reached.

2.4.5. Influence of topography and land cover on fire behaviour characteristics

The influence of topography and land cover on fire behaviour characteristics appears to be limited, as opposed to observed influence on fire occurrence and total burned area. The reported dispersion of burned area across CLC classes (Figure 2.10a) shows a prevalence of larger fires in shrub and herbaceous vegetation associations (CLC classes 321, 323 and 324). At the other end of the spectrum, burned area in coniferous and mixed forests (classes 312 and 313) is more dispersed towards smaller fires. Similarly, in non-irrigated arable land (CLC class 211) and pastures (CLC class 231) burned area is dispersed towards larger values than in permanent crops (CLC classes 221, 222 and 223). Analogous patterns of burned area dispersion have been found elsewhere in the Mediterranean (Oliveira et al., 2014), and can be justified by the relatively larger patches with typically higher fuel loads characterising natural and seminatural land cover classes (Bajocco and Ricotta, 2008).

Overall, the interquartile dispersion of burned area across all land cover classes spans two orders of magnitude. On the other side, the interquartile dispersion of fire duration and rate of spread values covers less of an order of magnitude (Figure 2.12 b and c). This flattens the variability due to land cover, complicating the interpretation of results. Nevertheless, it is evident that in coniferous forest and mixed forest (CLC classes 312 and 313) rate of spread appears to be dispersed towards slightly lower values as opposed to all other land cover classes.

Fire behaviour appears to be independent of aspect (Figure 2.14). This means that aspect does not determine per se environmental conditions leading to observable differences in fire behaviour. On the other side, slope has a clear effect on burned area and fire duration, with increasing slopes leading to higher values (Figure 2.12 a and b). The fact that burned area and fire duration tends to increase with slope is likely due to the less efficient attack strategy in difficult terrain conditions (Rodríguez y Silva et al., 2014), leading to fires propagating freely and consuming larger patches of vegetation. Within its limited range of variability, rate of spread appears to increase up to slopes of 10-15° and to decrease for steeper slopes (Figure 2.12c). This ambiguous result can be justified by the fact that the measure of rate of spread proposed herein is the rate of advancement of fire perimeter. This quantity does not directly relate to the local rate of advancement of fire front, especially on steep slopes. The speed of advancement of fire front increases with slope only in the upslope direction, whereas in the downslope direction it decreases with increasing slope.

2.5. Conclusions

The first consideration that can be drawn from the observations described in this Chapter is on the annual variability of the geographic distribution of fire ignitions (Figure 2.8). Our findings are consistent with the widely acknowledged notion that spatial patterns of fire occurrence are controlled by anthropic and biophysical features of the landscape (Barbati et al., 2015; Duane et al., 2015; Lavorel et al., 2006; Ruffault and Mouillot, 2017). Indeed, it was found that land cover (Figure 2.9), slope (Figure 2.11) and aspect (Figure 2.13) are strong drivers of fire events in terms of both number of fires and total burned area. On the

other hand, interannual variability in the number of fires and total burned area is determined by variable factors such as weather (Ganteaume et al., 2013; Viegas and Viegas, 1994). In fact, weather controls fuel condition (Trenberth et al., 2014; Ustin et al., 2009; Williams and Abatzoglou, 2016; Zhang et al., 2015) and ultimately the probability of ignition and flames propagation (Finney, 2005; Finney et al., 2011; Hardy, 2005).

A second consideration can be drawn from noting that the interannual variability of fire behaviour, specifically of burned area, duration and rate of spread (Figure 2.5) is comparable or stronger than the variability induced by land cover (Figure 2.10) and terrain aspect (Figure 2.14). This points at weather forcing as a primary driver of fire characteristics. Indeed, weather variability through the year determines fuel condition, and thus fire behaviour (§1.3) and fire danger (§1.2.1). This consideration does not apply to variability in burned area and duration induced by terrain slope (Figure 2.12), where the observed marked increase of these characteristics with increasing slope can be justified by the difficulty in fire containment and suppression efforts in complex terrain conditions (Rodríguez y Silva et al., 2014).

3. Relating spatiotemporal patterns of forest fires burned area and duration to diurnal land surface temperature anomalies[1]

Abstract

Forest fires are a major source of ecosystem disturbance. Vegetation reacts to meteorological factors contributing to fire danger by reducing stomatal conductance, thus leading to an increase of canopy temperature. The latter can be detected by remote sensing measurements in the thermal infrared as a deviation of observed land surface temperature (LST) from climatological values, i.e. as an LST anomaly. A relationship is thus expected between LST anomaly and forest fires burned area and duration. These two characteristics are indeed controlled by a large variety of both static and dynamic factors related to topography, land cover, climate, weather (including those affecting LST), and anthropic activity. To investigate the predicting capability of remote sensing measurements, rather than constructing a comprehensive model, it would be relevant to determine whether anomalies of LST affect the probability distributions of burned area and fire duration. This research approached the outlined knowledge gap through the analysis of a dataset of forest fires in Campania (Italy) covering years 2003-2011 against remote sensing estimates of LST anomaly. An LST climatology was first computed from time series of daily Aqua-MODIS LST data (product MYD11A1, collection 6) over the longest available sequence of complete annual datasets (2003-2017), through the harmonic analysis of time series (HANTS) algorithm. HANTS was also used to create individual annual models of LST data, to minimize the effect of varying observation geometry and cloud contamination on LST estimates while retaining its seasonal variation. LST anomalies where thus quantified as the difference between LST annual models and LST climatology. Fire data were intersected with LST anomaly maps to associate each fire with the LST anomaly value observed at its position on the day before the event. Further to this step, the closest probability distribution function describing burned area and fire duration were identified against a selection of parametric

[1] Based on: Maffei, C., Alfieri, S.M., Menenti, M., 2018. Relating spatiotemporal patterns of forest fires burned area and duration to diurnal land surface temperature anomalies. Remote Sens. 10, 1777. https://doi.org/10.3390/rs10111777

models through the maximization of the Anderson-Darling goodness-of-fit. Parameters of the identified distributions conditional to LST anomaly where then determined along their confidence intervals. Results show that in the study area log-transformed burned area is described by a normal distribution, whereas log-transformed fire duration is closer to a generalized extreme value (GEV) distribution. The parameters of these distributions conditional to LST anomaly show clear trends with increasing LST anomaly; significance of this observation was verified by means of a likelihood ratio test. This confirmed that LST anomaly is a covariate of both burned area and fire duration. Therefore, it was observed that conditional probabilities of extreme events appear to increase with increasing positive deviations of LST from its climatology values. This confirms the stated hypothesis that LST anomaly affects forest fires burned area and duration, and highlights the informative content of time series of LST with respect to fire danger.

3.1. Introduction

Forest fires are a source of significant ecosystem damage at global scale, as they affect the biogeochemical cycle, are a source of atmospheric emissions, alter the net carbon balance, disturb forest structure, and cause long-term changes in soil properties (Certini, 2005; Harvey et al., 2016; Lehsten et al., 2009; Seidl et al., 2014; Thonicke et al., 2008; van der Werf et al., 2010). Fires also condition anthropic activities as they threaten human lives, have a negative effect on quality of life, and cause economic losses (Montagné-Huck and Brunette, 2018; Reisen et al., 2015; Viegas, 2009). Increasing concern derives from the observation that climate change is negatively affecting spatial and temporal patterns of fire disturbance (Frank et al., 2015; Liu et al., 2010; Seidl et al., 2017; Williams and Abatzoglou, 2016).

In Mediterranean ecosystems, prolonged droughts and heat waves create the preconditions for increases in frequency and intensity of forest fires (Gudmundsson et al., 2014; Lindner et al., 2010), the underlying mechanism being the reduction of live and dead fuels moisture content as a response of the soil-plant system to increased vapor-pressure deficit (Trenberth et al., 2014; Williams and Abatzoglou, 2016; Zhang et al., 2015). Vegetation response varies with species as well as with forest structure and soil/terrain characteristics, and it is determined by transpiration (Arnold et al., 1998; Douglass, 1967; Swift et al., 1975). The moisture of dead fuels, which include the organic elements of forest litter such as senescent grasses, dry leaves, small twigs and compacted organic material in the topsoil, is affected by weather variations as well, and it is regulated through evaporation (Aguado et al., 2007; Liu, 2017; Viney, 1991). The moisture content of both alive and dead fuels are thus affected by weather forcing, and indeed vegetation stress status has been found to be related to some meteorological drought indices, which in turn are related to moisture content of the largest size classes of dead fuels (Arpaci et al., 2013; Gudmundsson et al., 2014; Keetch and Byram, 1968; Merzouki and Leblon, 2011; Pellizzaro et al., 2007a; Weber and Nkemdirim, 1998).

The vegetation transpiration regulation mechanism reacts to water stress conditions by reducing stomatal conductance, thus leading to an increase of canopy temperature (Hsiao,

1973; Schulze et al., 1973; Zweifel et al., 2009). This phenomenon can be detected by satellite measurements in the thermal infrared, and has been widely used in the development of methodologies based on the satellite retrieval of land surface temperature (LST) to map vegetation stress conditions (Jackson et al., 1981; Kalma et al., 2008; Karnieli et al., 2010; Liu et al., 2016; Nemani and Running, 1989). As moisture content has a direct relationship with live fuels ignitability and flames propagation (Chuvieco et al., 2014; Dimitrakopoulos and Papaioannou, 2001; Pellizzaro et al., 2007b; Rossa et al., 2016), a relationship between LST and forest fires may be expected (Chowdhury and Hassan, 2015a; Leblon, 2005; Sobrino et al., 2016). Indeed, several approaches use LST in association with optical spectral indices of vegetation greenness or moisture content to construct physically based or empirical fire danger rating systems (Abdollahi et al., 2018; Chowdhury and Hassan, 2015b; Chuvieco et al., 2004; Jang et al., 2006; Tien Bui et al., 2016; Yu et al., 2017). Some researchers used LST to model energy budgets (Leblon, 2005; Nolan et al., 2016b; Vidal et al., 1994) or to estimate heat energy of pre-ignition (Dasgupta et al., 2006) and predict fire occurrence.

Little research was conducted to relate LST to fire behaviour. Post-fire LST was used to quantify burnt severity either alone (Quintano et al., 2015; Veraverbeke et al., 2012; Vlassova et al., 2014) or in conjunction with optical data (Quintano et al., 2017; Zheng et al., 2016). Pre-event LST was used, along with other factors, to model burned area, but results were ambiguous (Chaparro et al., 2016). While evidence supports the hypothesis that higher surface temperature is associated with an increased fire occurrence (Manzo-Delgado et al., 2004; Matin et al., 2017; Pan et al., 2016), no such relationship was previously investigated against burned area or fire duration.

Burned area is indeed controlled by a large variety of both static and dynamic factors, essentially falling into five groups: topography, such as elevation, slope, south-westness (in the northern hemisphere) or north-westness (in the southern hemisphere); land cover, including vegetation type, composition, connectivity, fuel load, pyrodiversity; climate, e.g. annual average daily maximum and minimum temperature; weather (including active drivers of fuel moisture) such as cumulative antecedent precipitation, wind speed, relative humidity; anthropic activity, including land development, road density, distance to settlements, fire prevention strategies and efficiency of fire extinguishing actions (Barrett et al., 2016; Faivre et al., 2016, 2014; Falk et al., 2007; Fernandes et al., 2016; Littell et al., 2016; Moreno et al., 2011; Viegas and Viegas, 1994). While less studied, fire duration appears to be related to similar factors (Costafreda-Aumedes et al., 2016; Fischer et al., 2015; Gustafson et al., 2011; Lasslop and Kloster, 2017). Among these factors, only those affecting vegetation moisture are related to LST. To investigate the predicting capability of remote sensing measurements, rather than constructing a comprehensive model, it would be relevant to determine whether an increase in LST affects the probability distributions of burned area and fire duration. Since an increase of LST would be evaluated against an LST climatology, thus implicitly implying the evaluation of a delta or anomaly, the objective would in other terms be to assess if such an anomaly is a covariate of the two named fire characteristics.

The research described in this chapter followed from this line of reasoning and tried to verify if a relationship linking anomalies of LST to burned area and fire duration exists, thus exploring the identified knowledge gap. The analyses were performed on the study area of Campania, Italy, for which a dataset comprising more than 8800 fire events recorded between 2003 and 2011 was made available by local authorities.

The accomplishment of the stated objective first required the definition of a method for the quantification of LST anomalies. Crucial to this step was the prior modelling of an LST climatology. Indeed, multitemporal analysis was suggested as a mean to determine seasonal minima against which to assess LST values triggering fire occurrence (Julien et al., 2006; Khorchani et al., 2018; Manzo-Delgado et al., 2004; Stroppiana et al., 2014). To this purpose, the longest available time series of daily Aqua-MODIS LST data was processed with the Harmonic Analysis of Time Series (HANTS) algorithm (Roerink et al., 2000; Verhoef, 1996) to construct a daily pixel-wise climatology of LST. HANTS was also used to process annual time series of LST and create cloud- and noise-free annual models of daily LST. LST anomaly was finally evaluated as the difference between the LST annual models and the LST climatology.

Further steps required the analysis of the fire data towards the identification of the closest fitting probability density function describing burned area and fire duration. The fire database was then intersected with daily maps of LST anomaly, and each fire was associated with the corresponding LST anomaly value occurring at the same location on the day before the event. Parameters of the identified distributions conditional to LST anomaly were determined along their confidence intervals, and trends were identified (Hernandez et al., 2015). Finally, probability of extreme events conditional to LST anomaly were evaluated.

3.2. Materials and Methods

3.2.1. Study Area

A detailed description of the study area was provided in §2.2.1.

3.2.2. Data

MODIS LST data

A dataset of daily gridded Aqua-MODIS LST data (product MYD11A1, collection 6) from 2003 to 2017 retrieved from the Land Processes Distributed Active Archive Center (LP DAAC, https://e4ftl01.cr.usgs.gov/) was used for this research. MYD11 products are generated by an angle-dependent split-window algorithm exploiting the differential atmospheric absorption in MODIS bands 31 (11 µm) and 32 (12 µm) to determine LST values from radiance measurements of clear-sky pixels. The achieved mean LST error is typically within ±0.6 K, and the standard deviation of validation errors is typically less than 0.5 K (Wan, 2014).

Product MYD11A1 contains both diurnal (13:30) and nocturnal (1:30) LST measurements, along with corresponding quality assurance information. Preference was given to diurnal

rather than nocturnal data, and to Aqua-MODIS rather than Terra-MODIS, to capture canopy temperature variations due to water stress occurring at the hour of the day when maximum air temperature is approximatively achieved. Retrieved LST estimates were further masked against MYD11A1 pixel-wise quality assurance (QA) metadata, and only data marked as good quality (QA bits 1,0 = 00), i.e. retrieved at nominal radiometric and clear-sky conditions, were retained (Van Nguyen et al., 2015; Xu and Shen, 2013). However, this approach does not ensure that all cloud contaminated pixels are excluded from further processing (Ackerman et al., 2008).

Fire data

A dataset of about 8800 fires officially recorded in Campania between 2003 and 2011[2] was provided by the Forest Fire Protection Information Unit of Carabinieri, a law enforcement agency in charge of forest fires prevention, firefighting, arson investigations and prosecution, and burned area inventorying. The database details the presumed date and time of fire ignition, recorded date and time of fire extinction, geographic coordinates of burned area centroid, total burned area, and presumed causes. While Carabinieri record burnt scar perimeters on a fire-by-fire basis, according to conventional practices of field surveying with GPS receivers and desk digital cartography, these were not provided for this research. However, for the purpose of this study, this is not a source of concern on the positional accuracy of the provided centroids, as only 53 fires (0.87% of the fires in the dataset) are larger than 1 km^2, i.e. of a MODIS pixel in the thermal bands.

The dataset covered a range of fire seasons that were considered safe to critical in both number of fires and total burnt area. Most fires (84%) occur between June and September. About 99.8% of fires are of human origin (negligent or arson). On average, 980 fires are recorded each year, leading to the loss of more than 6160 hectares of natural areas, including 4190 ha of forests.

Fires in the database were intersected with the CORINE Land Cover (CLC) map (European Environment Agency, 2007) to select those occurred in natural areas only. CLC maps are produced at a nominal scale of 1:100.000, with a minimum mapping unit of 25 ha and minimum width of linear elements of 100 m, and are updated every six years. Fires occurred between 2003 and 2005 were intersected with CLC 2006, while fires between 2006 and 2011 were intersected with CLC 2012. A total of more than 6100 events occurred in land cover classes reported in Table 3.1 were used in this research, thus excluding events recorded on agricultural land.

Recorded burned area encompasses five orders of magnitude, while its average is 7.1 ha. The 95th percentile of burned area is 27.8 ha; this quantity was used as a reference for extreme events in the region. Analogously, mean fire duration is 9.4 hours, and the 95th percentile is 27.5 hours.

[2] This is a subset of the fire data used in Chapter 2 to characterise the fire regime in the study area.

3.2.3. Modelling temporal patterns of LST

The modelling of the LST climatology and of LST annual models was performed by means of the Harmonic Analysis of Time Series (HANTS) algorithm (Roerink et al., 2000; Verhoef, 1996). This method was initially proposed to fill in missing or cloudy observations and to remove outliers in time series of NDVI data by exploiting its periodic behaviour (Menenti et al., 1993; Verhoef et al., 1996). It was later successfully used on time series of LST (e.g. Alfieri et al., 2013; Menenti et al., 2016; Van Nguyen et al., 2015).

A temporal sequence of N images $I(x,y,t_i)$, $i = 1, 2, \ldots, N$, can be described as a Fourier series:

$$I(x,y,t_i) = a_0(x,y) + \sum_{j=1}^{M} a_j(x,y) \times \cos\left(\omega_j t_i - \varphi_j(x,y)\right) \quad (3.1)$$

where $I(x,y,t_i)$ is the LST retrieved from MODIS measurements at pixel longitude x, pixel latitude y, day t_i when the i^{th} image was taken, ω_j is the frequency of the j^{th} harmonic term in the Fourier series, M is the number of frequencies of the Fourier series, $a_j(x,y)$ and $\varphi_j(x,y)$ are the amplitude and phase of the j^{th} harmonic term. The harmonic frequencies are integer multiples of the base frequency:

$$\omega_j = (2\pi/L) \times j \quad (3.2)$$

where L is the length of the base period. Because the zero frequency has no phase, the amplitude related to the zero frequency $a_0(x,y)$ is equal to the average of all N observations of $I(x,y,t_i)$ (Menenti et al., 2016).

Table 3.1. CORINE Land Cover (CLC) classes used to select fires used in subsequent analyses.

CLC code	*Description*
231	Pastures
243	Land principally occupied by agriculture, with significant areas of natural vegetation
311	Broad-leaved forest
312	Coniferous forest
313	Mixed forest
321	Natural grassland
323	Sclerophyllous vegetation
324	Transitional woodland shrub
333	Sparsely vegetated areas
334	Burnt areas

HANTS handles the Fourier analysis as a least squares curve fitting problem within an iterative approach. In the first step, the least squares curve fitting is performed using all valid data in the series. In the second step, observations that deviate from the curve determined in the first iteration more than a pre-defined threshold (the fit error tolerance, FET) in the specified direction of rejection (lower values or higher values) are removed, and the remaining data are used to compute the least square curve fitting again. The iterations are repeated until either all the remaining observations are within the FET or the number of remaining data points becomes less than the specified degree of over determinedness (DOD) (Roerink et al., 2003).

3.2.4. Evaluation of land surface temperature anomaly

HANTS was used to decompose the time series of MODIS LST retrievals into their descriptive significant periodic components. Series comprising the first three harmonics were fit to the data with two different methods:

- HANTS was executed on yearly sequences 2003-2011 of daily LST data individually to construct annual models of daily LST (Xu and Shen, 2013). The objective of this approach was the removal of LST variability due to undetected cloud contamination and varying observation geometry while modelling LST annual variation. The result was a collection of new annual series of daily LST maps, one for each year being considered, computed from the identified harmonic components. These were used as representative of actual measurements.
- The algorithm was executed on the whole 2003-2017 data set, with a base period of one year, to construct a pixel-wise daily climatology of LST (Alfieri et al., 2013). The need of using this climatology as a basis for the calculation of thermal anomalies suggested its evaluation from the longest available sequence of complete annual datasets of daily MODIS LST data. The output of this process is a new series of daily LST maps computed from the identified harmonic components, representative of daily climatological values of LST.

A synthesis of the HANTS parameters adopted in the two approaches is reported in Table 3.2. In both, the base period is one year, and the number of frequencies is set to three. The direction of outliers' rejection was set as "Lo", thus leading to the removal of all data points that are more than FET lower than the fitted harmonics, according to the fact that cloud contamination in pixels causes an underestimation of LST. The development of the LST climatology is based on a more relaxed FET value, as opposed to annual models, to compensate for its inter-annual variability. The degree of over determinedness was dynamically adjusted on a per-pixel basis as the half of LST estimates marked as good quality in the QA of MYD11A1 product.

Figure 3.1 depicts one year of clear-sky Aqua-MODIS LST retrievals in a sample pixel within the study area, along with the corresponding LST annual model and the LST climatology. It can be observed that the annual model captures LST variation throughout the year, while filtering its variability. LST climatology, derived from the 2003-2017 series of daily LST data,

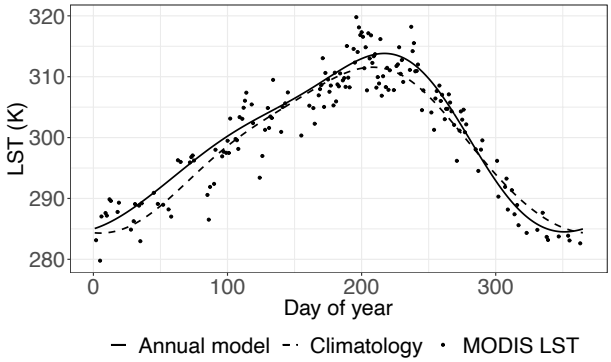


Figure 3.1. Aqua-MODIS LST data, LST annual model and LST climatology observed in year 2007 at pixel 40°50'40"N, 14°8'56"E.

shows a distinct pattern. In this example, the annual model of LST is higher than the LST climatology for most of the year.

A land surface temperature anomaly is hereby defined as the difference between LST annual models and the LST climatology. At a given day t_i the anomaly is positive when the LST annual model is higher that the LST climatology. In this sense, LST anomaly quantifies the deviation of LST from the climatology value expected in that pixel (Figure 3.1). The approach of using the LST annual model rather than the actual measurements of LST hinders the detection of LST variations occurring over a short period of time. Nevertheless, it quantifies the build-up of the LST anomaly throughout the dry season while filtering the variability in LST estimates due to observation geometry, residual cloud contamination and retrieval accuracy. This in turns allows the appreciation of LST anomalies with values below the accuracy allowed by the MYD11A1 algorithm, and provides measurements in dates when complete cloud cover is present (Alfieri et al., 2013).

Daily maps of LST anomaly were produced for the entire observation period between 2003 and 2011. These maps were intersected with fire data, so that each fire was associated with the value of the LST anomaly in the same location on the day before the event.

Table 3.2. Parameters used in HANTS algorithm to pre-process LST data. Computation of the LST climatology is based on a more relaxed FET value to compensate for its inter-annual variability.

HANTS parameters	*LST annual models*	*LST climatology*
Length of the base period (L)	1 year	1 year
Number of frequencies (M)	3	3
Direction of outliers' rejection	Lo	Lo
Fit error tolerance (FET)	4 K	6 K
Degree of over-determinedness (DOD)	Half of valid points	Half of valid points

3.2.5. Parametric distributions of burned area and fire duration

Burned area and fire duration relate to the difficulty of control of fires and to the damage they cause, and thus to fire danger (FAO, 1986; Walding et al., 2018). Prior to any investigation on the relationship between these fire characteristics and LST anomaly, their probability distributions were identified.

Several parametric distributions are reported in literature to fit burned area, including normal (Weber and Stocks, 1998), log-normal (Corral et al., 2008; Haydon et al., 2000), exponential (Baker, 1989; Cumming, 2001; Weber and Stocks, 1998), gamma (Cumming, 2001), generalized extreme value (Moritz, 1997), and Weibull (Reed and McKelvey, 2002). A limited number of papers report on parametric distributions of fire duration (e.g. Palma et al., 2007). The diversity of these results highlights that no one single model can be identified to describe burned area and fire duration distribution globally, due to the diversity of encompassed terrain, climate, ecology, forest and fire management practices (Cui and Perera, 2008; Reed and McKelvey, 2002), and that the closest fitting model needs to be identified on a regional basis.

In this study, both burned area and fire duration datasets were tested against the following parametric models:

- Normal

$$f(x|\mu,\sigma) = \frac{1}{\sqrt{2\pi}\sigma}\exp\left[-\frac{(x-\mu)^2}{2\sigma^2}\right] \quad (3.3)$$

- Log-normal

$$f(x|\mu,\sigma) = \frac{1}{\sqrt{2\pi}\sigma x}\exp\left[-\frac{(\ln x-\mu)^2}{2\sigma^2}\right] \quad (3.4)$$

- Exponential

$$f(x|\lambda) = \lambda\exp(-\lambda x) \quad (3.5)$$

- Gamma

$$f(x|a,s) = \frac{1}{s^a\Gamma(a)}x^{a-1}\exp(-x/s) \quad (3.6)$$

- Generalized extreme value (GEV)

$$f(x|a,b,s) = \frac{1}{b}\left[1+s\left(\frac{x-a}{b}\right)\right]^{-\frac{1}{s}-1}\exp\left\{-\left[1+s\left(\frac{x-a}{b}\right)\right]^{-\frac{1}{s}}\right\} \quad (3.7)$$

- Weibull

$$f(x|a,b) = \frac{a}{b}\left(\frac{x}{b}\right)^{a-1}\exp\left[-\left(\frac{x}{b}\right)^{-a}\right] \quad (3.8)$$

These models were fitted to burned area and fire duration data by minimizing the Anderson-Darling distance (Anderson and Darling, 1954):

$$AD = n \int_{-\infty}^{+\infty} \frac{[F_n(x) - F(x)]^2}{F(x)[1 - F(x)]} dF(x) \quad (3.9)$$

where $F(x)$ is the model cumulative distribution function and $F_n(x)$ is the empirical cumulative distribution of the sample. The maximum goodness-of-fit criterion with Anderson-Darling distance gives more weight to the tails of the distribution. The closest fitting model for each of the two variables was identified as the one providing the minimum Anderson-Darlin distance.

3.2.6. Conditional distribution of fire characteristics

The parameters of the closest fitting distributions identified for burned area and fire duration conditional to LST anomaly were evaluated by dividing the values attained by this covariate at fire locations the day previous to the event into ten bins each corresponding to a decile, following the approach proposed in (Hernandez et al., 2015). In accordance with the analyses performed under the previous section, conditional parameters were determined with the maximum goodness-of-fit criterion, while their corresponding 95% confidence intervals were determined by means of 1000 bootstrap parameter estimations. Significance of the variation of observed distribution parameters across the decile bins of LST anomaly were finally verified through a likelihood ratio test where the likelihood of the model describing the entire dataset was compared against the sum of the likelihoods of the ten models in each bin.

3.3. Results

3.3.1. Evaluation of land surface temperature anomaly

LST in the study area exhibits significant inter-annual variability, as demonstrated by the two selected maps extracted from LST annual models of years 2007 and 2011 on the same date (Figure 3.2). However, LST maps are not indicative of deviations from a climatology. Indeed, maps of LST anomaly on the same dates show significantly different spatial patterns (Figure 3.3).

In the proposed selected dates, Figure 3.3 also reports fires occurred in the following day, represented with circles proportional to burned area. Fires occurring where a higher LST anomaly is reported result in a larger burned area, albeit such a qualitative evaluation varies with the chosen dates. Similar considerations could be drawn for fire duration, but for the sake of brevity these are not shown.

Maps of LST anomaly were sampled at each fire location on the day before the event. Average LST anomaly is 1.3 K, and 77% of fires occur when LST anomaly is positive, i.e. LST annual model value is higher than LST climatology value. On a monthly basis, this percentage varies between 69% and 88%, the only exception being December with 57%. A partial dependence of LST anomaly values from CLC classes can be noted, with coniferous forest and sclerophyllous vegetation showing a wider proportion of fires occurring when a negative LST anomaly is observed (Figure 3.4).

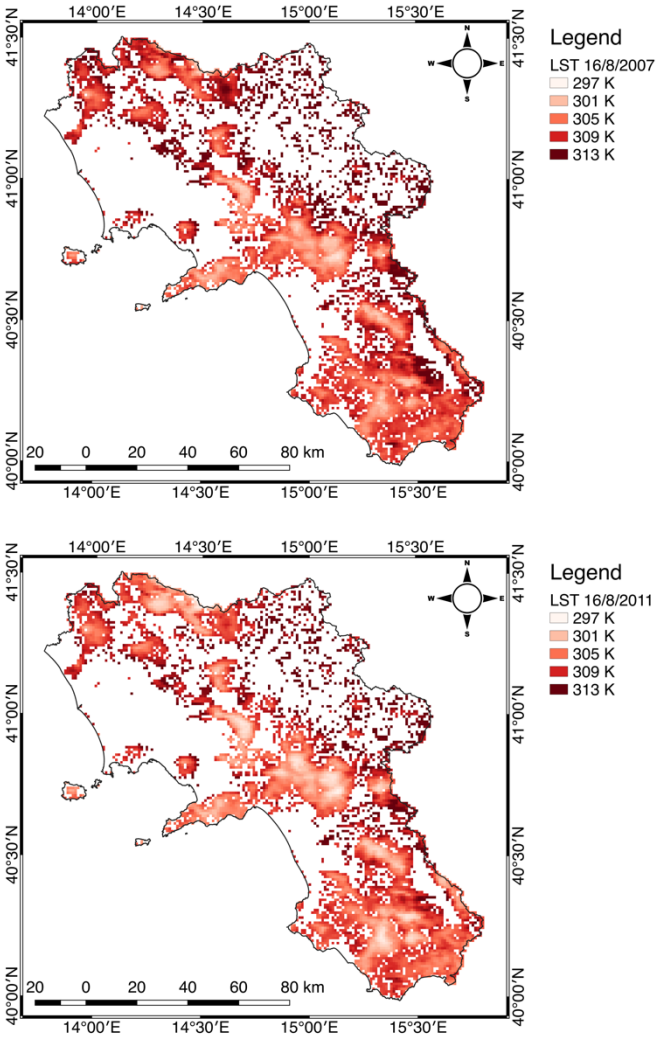


Figure 3.2. Selected maps of LST as derived from HANTS processing of annual time series: 16/8/2007 (top); 16/8/2011 (bottom).

3.3.2. Statistical models of burned area and fire duration

Burned area and fire duration range over several orders of magnitude and are strongly positively skewed. For this reason, they were preliminary scaled and converted to their base 10 logarithm, to have log-transformed positive values only. An initial investigation highlighted that log-transformed burned area and log-transformed fire duration show a linear correlation with a Pearson's correlation coefficient of 0.58 (Figure 3.5). While clearly

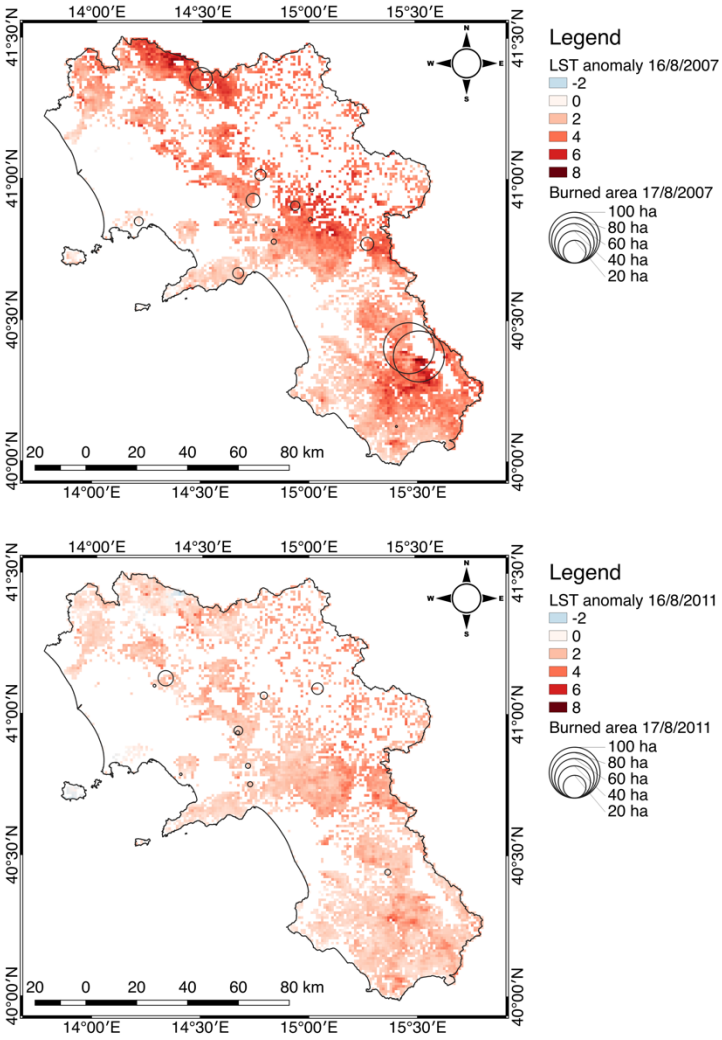


Figure 3.3. Selected maps of LST anomaly: 16/8/2007 with superimposed fires recorded on 17/8/2007 (top); 16/8/2011 with superimposed fires recorded on 17/8/2011 (bottom).

related, the relative weakness of this correlation confirms that the two fire behaviour characteristics are not redundant.

Figure 3.6 reports scatterplots of log-transformed burned area and log-transformed fire duration against corresponding LST anomaly. Pearson's correlation coefficients are 0.15 and 0.16 respectively, confirming that the observed large variability in these fire behaviour characteristics can't be explained by the sole LST anomaly, and indeed no trends can be clearly identified. To facilitate interpretation, data were subdivided in ten decile bins of LST anomaly, and mean log-transformed burned area and log-transformed fire duration were calculated in each bin. Results plotted in Figure 3.7 show clearer trends, with mean log-

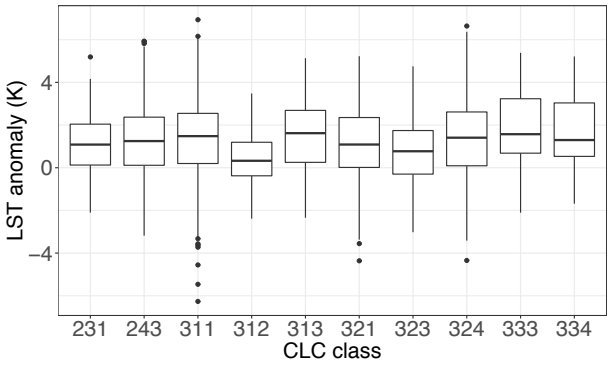


Figure 3.4. Boxplot of observed LST anomaly in each CLC class (Table 3.1).

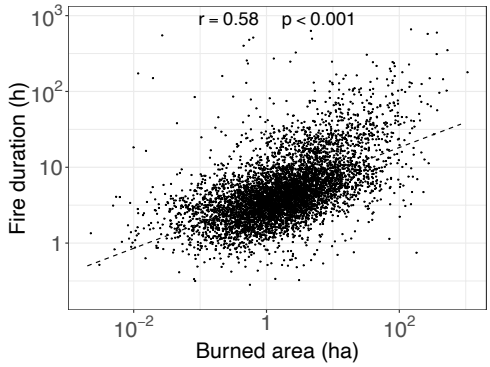


Figure 3.5. Scatterplot of log-transformed fire duration against log-transformed burned area.

transformed burned area increasing with increasing LST anomaly, confirming that the latter might be a covariate of this fire behaviour characteristic. A similar consideration may be drawn for log-transformed fire duration.

The parametric probability distributions listed in section §3.2.5 were fitted to log-transformed burned area and log-transformed fire duration using the maximum goodness-of-fit method. The corresponding Anderson-Darling distance reported in Table 3.3 show that log-transformed burned area is more closely described by a normal distribution, whereas log-transformed fire duration is closer to a GEV distribution. The corresponding Q-Q plots are reported in Figure 3.8.

3.3.3. Conditional distribution of burned area and fire duration

Parameters of the normal distribution of log-transformed burned area show a clear trend against LST anomaly (Figure 3.9). The sum of the likelihoods of the ten models fitted to burned area data in each bin was compared against the likelihood of the model describing the entire dataset by means of a likelihood ratio test. The null hypothesis in which the ten distributions are identical to the distribution describing all burned area data collectively was

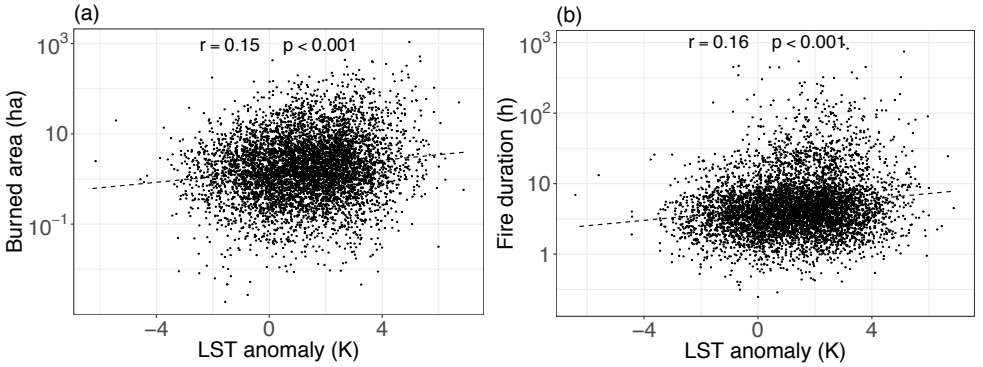


Figure 3.6. Scatterplot of log-transformed burned area (a) and log-transformed fire duration (b) against LST anomaly.

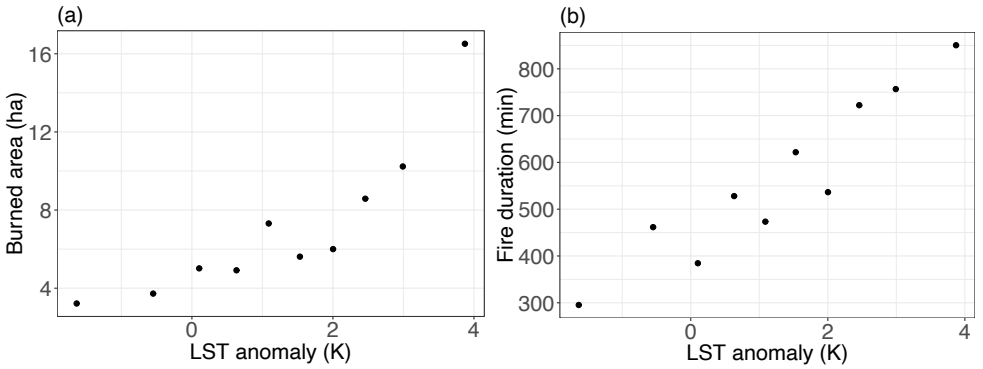


Figure 3.7. Mean burned area (a) and mean fire duration (b) in ten deciles of LST anomaly.

rejected at a significance level of p<0.05. A similar result was observed with the GEV distribution of log-transformed fire duration, where location, scale and shape exhibit a clear trend with LST anomaly (Figure 3.10), and the null hypothesis is rejected with p<0.05.

The retrieved conditional distributions (ten for each of the two fire characteristics, one in each of LST anomaly decile bins) were used to calculate the probability of fires larger than 27.8 ha (95th percentile of burned area) and the probability of fires lasting more than 27.5 hours (95th percentile of fire duration). Resulting plots (Figure 3.11) show that probability of large fires ranges from 1.8% in the first LST anomaly decile to 9.9% in the tenth decile, i.e. when LST anomaly increases from -1.6 to 3.9 K. Analogously, probability of fires lasting more than 27.5 hours ranges from 0.4% to 8.9%.

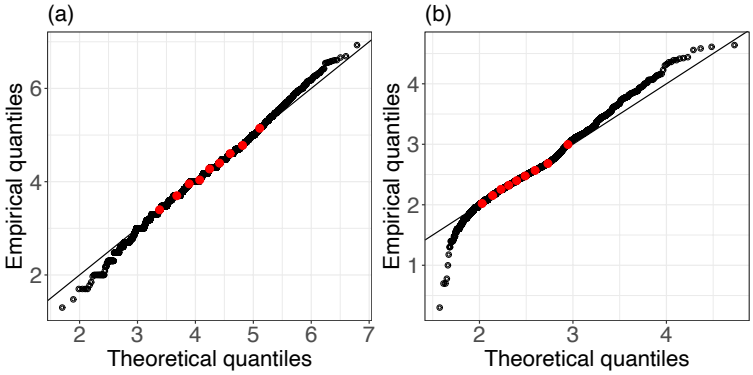


Figure 3.8. Q-Q plots of the normal distribution of log-transformed burned area (a) and of the generalized extreme value distribution of log-transformed fire duration (b). Red circles highlight the deciles of the distributions.

3.4. Discussion

A clear relationship exists in several ecosystems between forest fires and meteorological forcing (Gudmundsson et al., 2014; Lindner et al., 2010; Seidl et al., 2017; Trenberth et al., 2014; Williams and Abatzoglou, 2016; Zhang et al., 2015). Prolonged absence of rainfall and increased air temperatures, while creating the preconditions for forest fires, push vegetation towards water stress conditions to which it responds by reducing transpiration. This leads in turn to an increase of vegetation temperature, a phenomenon that can be detected by remote sensing measurements in the thermal infrared (Hsiao, 1973; Jackson et al., 1981; Kalma et al., 2008; Karnieli et al., 2010; Liu et al., 2016; Nemani and Running, 1989; Schulze et al., 1973; Zweifel et al., 2009). Rather than modelling a direct dependence, this study hypothesized that remote observations of LST, and more specifically deviations of LST values from a climatology, could be a covariate of burned area and fire duration of

Table 3.3. Anderson-Darling distance values for all tested distributions.

Model	*Log-transformed burned area*	*Log-transformed fire duration*
Normal	9.2	69.5
Log-normal	20.2	28.8
Exponential	1662	1711
Gamma	13.5	39.7
Generalized extreme value	13.5	15.1
Weibull	32.6	245

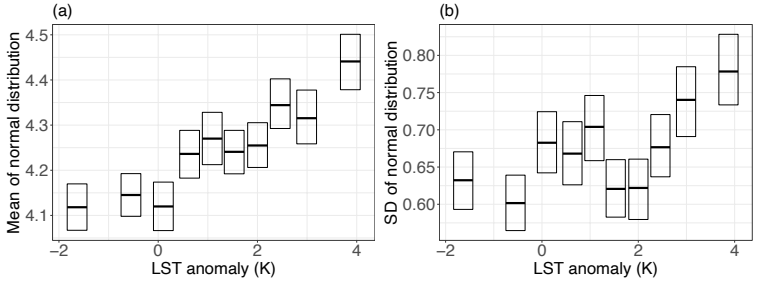


Figure 3.9. Plots of mean (a) and standard deviation (b) of normal distribution of log-transformed burned area, and their 95% confidence intervals, conditional to LST anomaly in 10 decile bins.

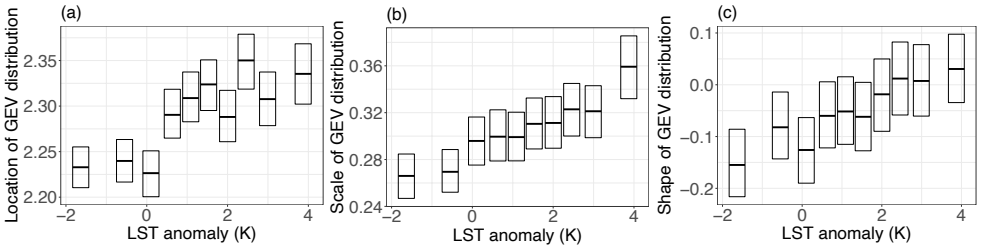


Figure 3.10. Plot of location (a), scale (b) and shape (c) of the generalized extreme value distribution of log-transformed fire duration, and their 95% confidence intervals, conditional to LST anomaly in 10 decile bins.

individual fires. Intuitively, prolonged events could eventually lead to larger burnt scars. Indeed, a correlation was found between log-transformed burned area and log-transformed fire duration (Figure 3.5), albeit its relative weakness supports the idea that these two quantities could be studied separately.

This research faced two substantial challenges. The first one was the identification of a suitable probability distribution model describing burned area and fire duration data in the study area. Several models are reported in cited literature (Baker, 1989; Corral et al., 2008; Cumming, 2001; Haydon et al., 2000; Moritz, 1997; Palma et al., 2007; Reed and McKelvey, 2002; Weber and Stocks, 1998), and indeed the diversity of these results highlights that no one single model can be identified to describe burned area probability distribution globally, and that a model should be adopted on a per-study basis (Cui and Perera, 2008; Reed and McKelvey, 2002). Among those tested herein, normal appears to be the closest fitting model for log-transformed burned area, and GEV for log-transformed fire duration. In both circumstances, the fitting was not perfect towards the tails, as demonstrated by the relatively high Anderson-Darling distance (Table 3.3) and by the Q-Q plots (Figure 3.8). Indeed, the final extent of a fire and its duration are contributed by several factors related to topography, land cover, climate, weather, and anthropic action (including fire suppression activities). The complex and varied landscape in the study area, with significant variations of population density, topography, land use/land cover and land management practices across its extent (Chapter 2), along with the efficiency of the local fire prevention and management resources, created a unique combination of factors shaping the

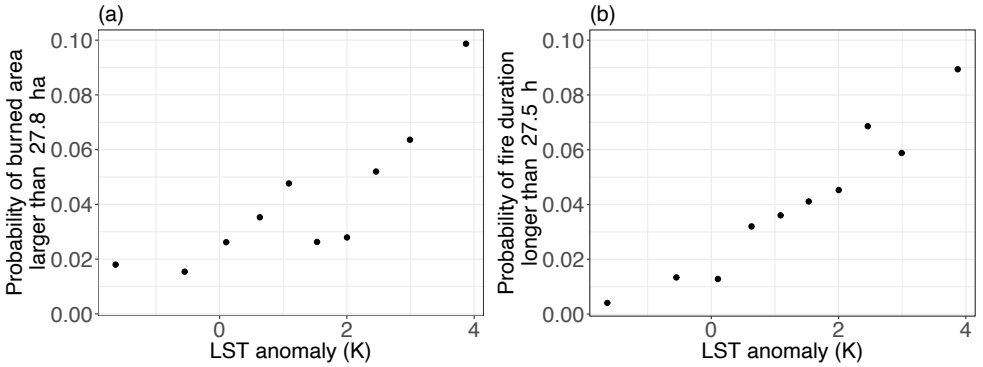


Figure 3.11. Estimated probability of burned area exceeding 27.8 ha, conditional to LST anomaly values in 10 decile bins (a); estimated probability of fire duration exceeding 27.5 hours, conditional to LST anomaly values in 10 decile bins (b).

probability distributions of fire characteristics that is not properly captured by the tested models.

The second challenge was the construction of a climatology of LST to use as a basis for the evaluation of the LST anomaly. The phenomenon to be indirectly detected as a deviation from the LST climatology is the reduction in stomatal conductance due to plant water stress. The need to acknowledge for its intra-annual variability excluded the opportunity to identify a seasonal mean on any base that is not over short periods of time. Indeed, the availability of daily diurnal Aqua-MODIS measurements over fifteen years allowed the calculation of an LST climatology on a daily basis. Rather than a daily average, the latter was the result of the modelling of the time series by means of the HANTS algorithm. This approach has the advantage to retain seasonal variability while filtering out disturbance sources such as undetected cloud contamination, which induces a bias by reducing the detected temperature, and the varying observation geometry (Menenti et al., 2016).

HANTS algorithm was also used to model annual LST series individually. This led to the definition of the LST anomaly as a deviation of the LST annual model from the LST climatology. While the use of the LST annual model instead of current measurements might hinder the detection of LST variations occurring over a short period of time, this approach has the advantage of still detecting the build-up of the LST anomaly throughout the dry season while leveraging the named effects of observation geometry and residual cloud contamination (Alfieri et al., 2013).

The LST climatology and the LST annual models were constructed using the same HANTS parameters, with the only exception of FET (Table 3.2). The need for a more relaxed FET in the LST climatology was justified by the need to account for the inter-annual variability of LST. While affecting the shape of the modelled curve, a lower FET in combination with the rejection of lower outliers would clearly determine a climatology characterized by generally higher LST values. The value of FET = 6 K was identified as a compromise between the need of constructing an LST climatology of general validity while still rejecting cloud-contaminated data in both cooler and warmer years.

Fire data were intersected with maps of LST anomaly, and each fire was associated with the LST anomaly value recorded at fire location on the day before the event. The underlying idea is that LST data is produced in near-real-time by ground receiving stations, allowing the mapping of fire danger forecast for the following day. The way LST anomaly was defined in this paper, i.e. as a deviation of LST annual model from LST climatology as opposed to the deviation of the actual MYD11A1 estimate, implies a slow day-to-day variation of LST anomaly. This in turn increases the temporal validity of produced LST anomaly maps up to a certain extent. Checking the effect of sampling in time at more days before the event was beyond the objectives of this research. However, it is here anticipated that tests performed on LST anomaly recorded five days before the event led to results similar to those reported herein.

Observed average LST anomaly is 1.3 K, while 23% of fires occur with a negative LST anomaly. The distribution of LST anomaly appears to be partially dependent on land cover class as reported in Figure 3.4. Negative values are proportionally more prevalent in coniferous forest and sclerophyllous vegetation than in other land cover classes. The observation of this dependence was expected from literature review (e.g. Barrett et al., 2016; Faivre et al., 2014) and does not affect the quality of further findings. Indeed, evaluations of burned area and fire duration were performed conditional to LST anomaly, i.e. leveraging out all other parameters. In effect, other factors such as accessibility of the zone, availability and effectiveness of the fire extinguishing means and the winds can heavily influence the occurrence of fires, the final burned area and event duration regardless of the previous LST anomaly, either positive or negative.

This study demonstrated the informative content of time series of LST. Indeed, LST anomaly was found to be a covariate of burned area and fire duration. Fire data were grouped in ten decile bins of the associated LST anomaly values and the parameters of the identified distributions along with their 95% confidence interval were evaluated in each of them. The choice of the number of bins was initially tested with a trial-and-error approach, towards the identification of a compromise between the clarity of observed trends and the amplitude of the distribution parameters confidence interval. As similar results were observed across a range from five to twenty bins, for the sake of objectiveness in the approach the number of ten was chosen as the most appropriate.

Mean and variance of the normal distribution describing log-transformed burned area both tend to increase with increasing LST anomaly values (Figure 3.9), likewise the location, scale, and shape parameters of the GEV distribution describing log-transformed fire duration (Figure 3.10). A likelihood ratio test confirmed that probability distribution models of burned area and fire duration conditional to LST anomaly are significantly different than the models describing the entire dataset. Along with the observed trends in parameters values, this result confirms the stated hypothesis that LST anomaly as defined in this chapter is a meaningful variable contributing to fire danger. It means that this quantity, along with its time-dependent nature, may be used pairwise other relevant parameters towards the statistical modelling of burned area and fire duration.

As a consequence of the variation of burned area and fire duration probability distributions conditional to LST anomaly, it is possible to plot and interpret how the probability of

extreme events evolves with increasing LST anomaly values. Indeed, end users such as forest managers and civil protection agencies are particularly interested in these probabilities to drive their preparedness activities (Preisler et al., 2004). The models constructed in the ten decile bins of LST anomaly demonstrate that the probability of a forest fire to result in a total burned area exceeding a given threshold (in our example, the 95th percentile of the dataset) significantly increases with increasing LST values (Figure 3.11a). A similar result was found for fire duration (Figure 3.11b), supporting the idea that maps of LST anomaly such as those in Figure 3.3 are useful to depict the contribution of LST to fire danger.

3.5. Conclusions

Vegetation response to meteorological factors contributing to fire danger – prolonged absence of rainfall and high air temperature – results in an increase of LST that can be detected by remote sensing measurements in the thermal infrared as a deviation from climatological values. This chapter demonstrates that such LST anomalies are a covariate of forest fires burned area and duration. While several studies demonstrated how a wide number of both static and dynamic factors related to topography, land cover, climate, weather, anthropic activity, and fire extinguishing strategies affect the probability distribution of these two fire behaviour characteristics, to the best of authors' knowledge no previous research was conducted to investigate the role of satellite measurements of LST.

The initial hypothesis was addressed by first identifying probability distributions functions describing available fire data. Among those tested, log-transformed burned area is closer to a normal distribution, while log-transformed fire duration is closer to a generalized extreme value distribution. The HANTS algorithm was then used to process time series of diurnal Aqua-MODIS LST measurements and construct a climatology against which anomalies of LST were quantified. Finally, parameters of the identified distributions conditional to LST anomaly where then evaluated, showing clear trends.

The observed variation of burned area and fire duration distributions conditional to LST anomaly demonstrate that increasing positive deviations of LST from the expected seasonal value correspond to an increasing probability of extreme events, i.e. of the final fire extent and duration exceeding a given threshold. This finding clearly identifies a practical mean to interpret maps of LST anomaly. As opposed to typical fire danger rating systems based on meteorological data, this remote sensing quantity has the advantage of claiming a higher spatial resolution. It is here highlighted that the identified relationships are preconditioning in nature, and do not predict actual fire occurrence. The latter is related to a different array of determinants relating to probability of a heat source leading to an ignition.

This study was performed ex post trough the evaluation of LST annual models against an LST climatology. This approach is observational in nature and not predictive. While the achievement of more generality of the proposed research would require investigations in a wider and diverse array of regions, strategies for the assessment of the LST anomaly up to

the current date need to be developed. However, this was beyond the objectives of this research.

4. A MODIS-based perpendicular moisture index to retrieve leaf moisture content of forest canopies[3]

Abstract

Moisture dictates vegetation susceptibility to fire ignition and propagation. Various spectral indices have been proposed for the estimation of equivalent water thickness (EWT), which is defined as the mass of liquid water per unit of leaf surface. However, fire models use live fuel moisture content (LFMC) as a measure of vegetation moisture. LFMC is defined as the ratio of the mass of the liquid water in a leaf over the mass of dry matter, and traditional spectral indices are not as effective as with EWT in capturing LFMC variability. The aim of this study was to explore the potential of the Moderate Resolution Imaging Spectroradiometer (MODIS) on board Terra and Aqua satellites in retrieving LFMC from top of the canopy reflectance, and to develop a new spectral index sensitive to this parameter. All the analyses were based on synthetic canopy spectra constructed by coupling the PROSPECT (leaf optical properties model) and SAIL (Scattering by Arbitrarily Inclined Leaves) radiative transfer models. Simulated top of the canopy spectra were then convolved to MODIS land bands 1-7 spectral response functions. All band pairs were evaluated to determine the subspace of MODIS measurements where the separability of points based on their value of LFMC was the highest. This led to the identification of isolines of LFMC in the plane defined by MODIS reflectance retrievals in bands 2 and 5; the isolines are straight and parallel, and ordered from lower to higher values of LFMC. This finding allowed the construction of a novel spectral index that is directly related to LFMC – the perpendicular moisture index (PMI). This index measures the distance of a point in the plane spanned by reflectance in MODIS bands 2 (0.86 μm) and 5 (1.24 μm) from a reference line, that of completely dry vegetation. Validation against simulated data showed that PMI exhibits a linear relationship with LFMC. When the vegetation cover is dense, the LFMC explains most of the variability in the PMI (r^2=0.70 when LAI>2; r^2=0.87 when LAI>4). When LAI is lower, the contribution of soil background to the measured reflectance increases, and the index underestimates LFMC. The PMI was also validated against the LOPEX93 (Leaf Optical

[3] Based on the "accepted manuscript" of the article published by Taylor & Francis Group: Maffei, C., Menenti, M., 2014. A MODIS-based perpendicular moisture index to retrieve leaf moisture content of forest canopies. Int. J. Remote Sens. 35, 1829–1845. https://doi.org/10.1080/01431161.2013.879348

Properties Experiment 1993) dataset of leaf optical and biophysical measurements, scaled to canopy reflectance with SAIL, showing acceptable results (r^2=0.56 when LAI>2; r^2=0.63 when LAI>4).

4.1. Introduction

Forest fires are a major threat to human life, economic development and the environment (FAO, 2007). Fire managers need timely and reliable danger maps to support them in the preventive allocation of resources (Carlson and Burgan, 2003; Chuvieco et al., 2010). Several factors contribute to fire danger, including the relative amount of fuels available for burning, their type and condition, specifically moisture content (FAO, 1986). Among these, fuel moisture is the most dynamic; it is also the most relevant, since it determines the forests' susceptibility to fire ignition and propagation (Rothermel, 1972). A higher moisture means a higher amount of heat needed to ignite a fuel, as more energy is necessary to evaporate water (Chuvieco et al., 2002). It also implies slower fire propagation, since part of the heat released by the flames is used to evaporate the water from the adjacent fuels (Verbesselt et al., 2002).

Field measurements are a reliable method for the estimation of vegetation moisture. However, these are impractical when the need is for cheap, fast and repeated monitoring of vast areas, as it would be required by decision makers at regional, national and international scale (San-Miguel-Ayanz et al., 2002). In this sense, remote sensing appears to be a promising technology, potentially providing daily updated maps of vegetation moisture to be used both for the evaluation of fire danger, to inform preparedness practices for the allocation of means and resources (Miller and Ager, 2013; Vakalis et al., 2004), and during the management of the emergency, for example to predict fire propagation scenarios and drive intervention activities (Ager et al., 2011; Papadopoulos and Pavlidou, 2011; Vakalis et al., 2004).

The evaluation of vegetation moisture from remote sensing measurements of reflected radiance in the solar spectrum relies on detailed studies of the optical properties of leaves (Gates et al., 1965; Gausman and Allen, 1973; Tucker, 1980; Woolley, 1971). A first measure of vegetation moisture is the equivalent water thickness (EWT), which denotes the content of water in leaf tissues. EWT is defined as the mass of water per unit area of leaf:

$$ETW = \frac{M_f - M_d}{A} \quad (4.1)$$

where M_f is the mass of the fresh leaf as measured in the field, M_d is the corresponding mass of the same leaf that has been oven dried, and A is leaf area. EWT is scaled to canopy level (EWT_c) by simple multiplication by leaf area index (LAI) (Ceccato et al., 2002b):

$$EWT_c = EWT \cdot LAI \quad (4.2)$$

EWT_c is thus the total amount of water in the canopy per unit area. A different measure of vegetation moisture is live fuel moisture content (LFMC), which expresses the percentage of mass of water in leaf tissues over the dry leaf mass:

$$LFMC = \frac{M_f - M_d}{M_d} \cdot 100 \quad (4.3)$$

Considering that dry matter content (DMC) is defined as:

$$DMC = \frac{M_d}{A} \quad (4.4)$$

it is clear that:

$$LFMC = \frac{EWT}{DMC} \cdot 100 \quad (4.5)$$

LFMC is thus a measure of water relative to DMC, and as such it is not scaled to canopy level through LAI. In many vegetation types, the mass of water exceeds that of the other leaf components, this meaning that LFMC values may be higher than 100%.

Both EWT and LFMC are valid measures of vegetation moisture, but they are not exchangeable, since a unique LFMC value can correspond to multiple EWT values, depending on leaf DMC. They are not even equivalent from a practical point of view, and the forest fire research community is specifically interested in LFMC maps (Carlson and Burgan, 2003; Hunt et al., 2013), since fire danger prediction tools and fire models depend on this measure of vegetation moisture (Andrews, 2007; Finney, 1998; Rothermel, 1991, 1972; Van Wagner, 1977; Yebra et al., 2013).

Analyses of leaf spectral signature sensitivity to EWT and DMC have shown that leaf reflectance is sensitive to leaf structure and to dry matter content in the near infrared (NIR, 0.7-1.1 µm), and to leaf structure, EWT and DMC in the SWIR (Ceccato et al., 2001; Seelig et al., 2008). Since SWIR reflectance doesn't provide an absolute measure of EWT, vegetation moisture spectral indices take into account NIR reflectance as a normalising factor against leaf structure and DMC (Ceccato et al., 2002b; Gao, 1996; Hardisky et al., 1983; Hunt and Rock, 1989). When calculated from remote sensing measurements of canopy reflectance, these spectral indices are actually sensitive to EWT_c, and thus they are inherently responsive to LAI (Colombo et al., 2008; Dasgupta and Qu, 2009). The sensitivity to LAI is indeed a general characteristic of spectral indices based on SWIR wavelengths (Bowyer and Danson, 2004; Dawson et al., 1999; Mousivand et al., 2014), negatively affecting the estimation of vegetation moisture (Wang et al., 2008; Zarco-Tejada et al., 2003).

Spectral indices for the estimation of EWT (or EWT_c) generally do not provide the same level of accuracy in estimating LFMC (Caccamo et al., 2012; Carlson and Burgan, 2003; Danson and Bowyer, 2004; Davidson et al., 2006; Maki et al., 2004; Yilmaz et al., 2008), although some exceptions are reported in literature, due to species-specific conditions (Sow et al., 2013; Verbesselt et al., 2007, 2002). Indeed, LFMC does not cause unambiguous spectral features in vegetation reflectance (Gao and Goetz, 1990; Peñuelas et al., 1993), while EWT and DMC affect vegetation spectra independently (Ceccato et al., 2002b; Verbesselt et al., 2007). Although this complicates any effort to retrieve LFMC from radiance measurements in the optical domain (Cohen, 1991; Lee et al., 2007), some successful experiments are reported in literature. Methods based on the inversion of a radiative transfer model (RTM),

i.e. on the inversion of the equation linking leaf biochemical and canopy biophysical characteristics to vegetation optical properties (Jacquemoud et al., 2000; Zarco-Tejada et al., 2003), address the estimation of LFMC by first exploiting the independent effect of EWT and DMC on vegetation reflectance to retrieve them separately, and then by calculating LFMC accordingly. The applicability of this method is limited by the fact that water absorption masks the effect of DMC, this leading to computation strategies where species specific values of DMC were used to constrain the inversion algorithm (Riaño et al., 2005) or where extensive field work on specific land covers was used to parameterise the look-up table used in the retrieval process (Yebra and Chuvieco, 2009c, 2009b). More practical approaches, i.e. not based on prior information of the observed surface, exploited the high dimensionality of hyperspectral measurements to retrieve LFMC with partial least squares regression (Li et al., 2007) and with wavelet analysis (Cheng et al., 2011). A computationally simpler approach is the Water Index (Peñuelas et al., 1997, 1993), which is based on the ratio of narrowband reflectance measurements around the leaf liquid water absorption feature at 970 nm; this index proved to be generally more effective than broadband indices in retrieving LFMC (Danson and Bowyer, 2004).

The objective of this work was to understand to what extent spectral measurements from the Moderate Resolution Imaging Spectroradiometer (MODIS) on board Terra and Aqua satellites are able to capture the effect of LFMC variability on vegetation reflectance and whether this can be translated into a simple spectral index. Spectral indices have a clear advantage over RTM inversion methods (Dasgupta et al., 2007), since their simplicity allows for the near-real time processing of remote sensing data at ground stations and the fast delivery of produced maps to the users (Chen et al., 2005). To achieve the stated objective, methodologies introduced by other authors (Ceccato et al., 2002b; Dasgupta and Qu, 2009; Huete, 1988) for the development of spectral indices may be followed. Basically, a dataset of reflectance measurements from MODIS is first simulated. The effect of LFMC variability on simulated reflectance is then characterised. When clear patterns of spectral variation emerge, a spectral index can be constructed maximising its sensitivity to LFMC and, where possible, minimising the effect of other disturbing factors. Accuracy in LFMC retrieval is then evaluated against a validation dataset.

4.2. Materials and methods

4.2.1. Simulation of canopy reflectance spectra with PROSPECT and SAIL

Simulated top of the canopy (TOC) reflectance data were produced coupling PROSPECT (leaf optical properties model) and SAIL (Scattering by Arbitrarily Inclined Leaves) models (Jacquemoud et al., 2009). PROSPECT (Feret et al., 2008; Jacquemoud and Baret, 1990) is a radiative transfer model (RTM) that simulates spectral reflectance and transmittance of plant leaves. Four parameters are required: chlorophyll a+b concentration C_{ab} (in µg/cm^2), EWT (in g/cm^2), DMC (in g/cm^2), and a leaf structural parameter N. With this model a wide range of leaf spectra can be simulated, corresponding to a variety of physiological conditions. Leaf reflectance and transmittance were scaled to TOC reflectance by using SAIL model (Verhoef, 1984; Verhoef et al., 2007), which requires information on leaf area index,

leaf angle distribution, hot-spot size, background spectrum, view geometry, and illumination geometry.

To evaluate our approach against independent data, a validation dataset based on LOPEX93 (Leaf Optical Properties Experiment 1993) database was used (Hosgood et al., 1995). The database includes leaf reflectance, leaf transmittance, EWT and DMC measurements for 335 samples from 67 plant species. Leaf spectral measurements were scaled to TOC reflectance using the SAIL model.

4.2.2. Simulation of MODIS reflectance data

This research focused on the Moderate Resolution Imaging Spectroradiometer (MODIS) on board Terra (EOS AM-1) and Aqua (EOS PM-1) NASA satellites. Although other instruments perform measurements in the NIR and SWIR spectral ranges, MODIS exhibits a unique compromise among spatial resolution, radiometric characteristics, and revisit time, allowing the frequent mapping of surface properties at regional scale. Moreover, MODIS data are open access, and can be downlinked and processed at ground stations for the near real-time delivery of derived products.

Each MODIS system views the entire Earth's surface almost on a daily basis, acquiring data in 36 spectral bands ranging from the optical to the thermal domains. The 20 spectral bands in the reflective range have been designed for various land, ocean, and atmosphere applications, with ground resolution of 250 m for bands 1 and 2, 500 m for bands 3-7, and 1000 m for the other bands. This study focussed on land bands 1-7, providing radiance measurements in the visible, the near infrared, and in three spectral bands in the shortwave infrared (Barnes et al., 2003).

All spectra produced by PROSPECT + SAIL were converted to MODIS reflectance using the instrument's spectral sampling specifications of bands 1-7 (Xiong et al., 2006). Simulated datasets were finally perturbed with gaussian noise (Zarco-Tejada et al., 2003) to account for signal-to-noise ratio (SNR) of MODIS bands (Barnes et al., 1998).

4.2.3. Development and validation of a spectral index

The identification and characterisation of the effect of LFMC variability on MODIS measurements, and the development of a spectral index sensitive to this vegetation parameter, were based on the following steps (Figure 4.1).

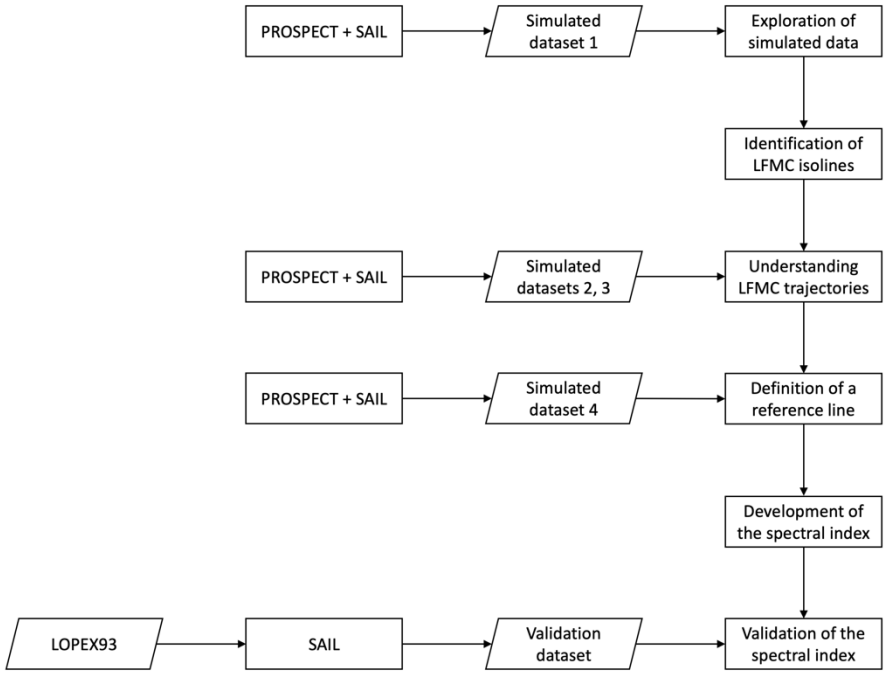


Figure 4.1. Flow chart showing how the various data sets are used towards the definition and validation of a spectral index sensitive to LFMC.

Simulation of reflectance measurements

An initial dataset (here referred to as dataset 1) consisting of 1000 spectra, 100 for each of the LFMC values between 50 and 500% in increments of 50%, was constructed. Input parameters to PROSPECT and SAIL models were chosen from random uniform distributions, limited sets of values or fixed values, as specified in Table 4.1 and Table 4.2. The adopted ranges were chosen to be wide enough to embrace a number of vegetation types and physiological conditions (Bowyer and Danson, 2004; Ceccato et al., 2002b, 2001; Cheng et al., 2006; Colombo et al., 2008; Danson and Bowyer, 2004; Dasgupta et al., 2007; Hao and Qu, 2007; Riaño et al., 2005; Yebra et al., 2008; Yebra and Chuvieco, 2009c; Zarco-Tejada et al., 2003).

To simulate the values of LFMC in the specified increments, for each value of LFMC, EWT was first randomly chosen according to ranges in Table 4.1; the corresponding DMC value was then computed accordingly. The pair of values EWT + DMC was retained only if the calculated DMC was within the ranges in Table 4.1, otherwise a new couple of values was iteratively generated until the given constraints were met.

Exploration of simulated data

The points of dataset 1 were projected on all the possible spectral planes whose axes are couples of MODIS bands 1-7, to identify the planes where clusters of points with the same value of LFMC exhibit the highest separability. The separability of clusters was assessed by means of the Jeffries-Matusita (JM) distance (Richards, 2013). The JM distance is a statistical separability index whose value is asymptotic to $\sqrt{2}$, this meaning that two clusters with $JM = \sqrt{2}$ can be discriminated with an accuracy of 100%. The plane allowing the best average pairwise JM distance among groups of points with the same value of LFMC was selected. Vegetation parameters other than LFMC causing the observed variability were

Table 4.1. Values of the parameters adopted to run PROSPECT model. C_{ab} denotes chlorophyll a+b concentration, EWT is the equivalent water thickness, DMC is the dry matter content, and N is a leaf structural parameter. U(a, b) denotes that the value of the parameter was randomly chosen from a continuous uniform distribution with parameters a and b.

	N	*C_{ab} (µg/cm^2)*	*EWT (g/cm^2)*	*DMC (g/cm^2)*
Dataset 1	U(1, 3)	U(20, 60)	U(0.01, 0.07)	U(0.004, 0.04)
Dataset 2	1.5	40	U(0.01, 0.07)	0.004 to 0.04 in increments of 0.006
Dataset 3	1.5	40	0.01 to 0.07 in increments of 0.01	U(0.004, 0.04)
Dataset 4	U(1, 3)	U(20, 60)	0	U(0.004, 0.04)

Table 4.2. Values of the parameters adopted to run SAIL model. LAI denotes the leaf area index, and ALA the average leaf inclination angle. U(a, b) denotes that the value of the parameter was randomly chosen from a continuous uniform distribution with parameters a and b. Observation geometry is set accordingly to MODIS specifications with random view angle along the scan line.

	LAI	*ALA*	*Hot-spot size*	*Soil spectrum*	*Sun zenith angle (°)*
Dataset 1	U(0.5, 7)	U(45, 75)	0.001	Dark to medium	U(40, 60)
Dataset 2	4	60	0.001	Medium	45
Dataset 3	4	60	0.001	Medium	45
Dataset 4	U(0.5, 7)	U(45, 75)	0.001	Dark to medium	U(40, 60)
Validation dataset	U(0.5, 7)	U(45, 75)	0.001	Dark to medium	U(40, 60)

recognised, and their effect on reflectance measurements was explored. It was expected that LAI might have a relevant role in this sense, where lower LAI values mean more exposed soil contributing to observed reflectance.

Identification of LFMC isolines

Isolines of LFMC were identified, and the effect of LAI variability on the displacement, in the selected plane, of points representing reflectance measurements was evaluated.

Understand LFMC trajectories

The direction of displacement of reflectance measurements when LFMC varies was analysed: since LFMC may vary as a consequence of variations in EWT and DMC, the displacements due to variations of these two parameters were explored by means of simulated datasets 2 and 3 (Table 4.1 and Table 4.2). In dataset 2 all parameters of the RTM models were fixed to a single value, except for DMC that was fixed to values between 0.004 and 0.04 g/cm^2 in increments of 0.006, while EWT was randomly chosen between 0.01 and 0.07 g/cm^2. This dataset consists of 25 spectra for each value of DMC, totalling 175 spectra. In dataset 3 the same fixed values of dataset 2 were chosen, with EWT varying in increments of 0.01 g/cm^2 between 0.01 and 0.07 and DMC randomly chosen between 0.004 and 0.04 g/cm^2. This dataset consists of 175 spectra, 25 for each value of EWT.

Definition of a reference line

Once isolines of LFMC are identified, and direction of displacement of points as an effect of LFMC variations are understood, a reference line against which to construct the index is needed. Dataset 4 was used to identify the line corresponding to the spectral measurements of completely dry vegetation. To simulate this dataset (Table 4.1 and Table 4.2), all PROSPECT and SAIL parameters were randomly chosen, except for EWT, which was fixed to 0 g/cm^2 (LFMC=0%).

Development of the spectral index

A spectral index for the quantification of LFMC was defined so that in the selected spectral plane its variation corresponded to a displacement perpendicular to isolines of LFMC (Verstraete and Pinty, 1996).

Validation of the spectral index

The validation of the proposed index was performed against both the simulated dataset and the validation dataset based on LOPEX93. To construct the latter, leaf spectral measurements were scaled to TOC reflectance using the SAIL model: for each LOPEX93

sample three different TOC spectra were generated, adopting random parameters of the radiative transfer model as for dataset 1 (Table 4.2). A total of 1005 TOC spectral measurements based on LOPEX93 data were generated.

4.3. Results

4.3.1. Exploration of simulated MODIS reflectance data

Simulated points from dataset 1 were projected in all possible spectral planes obtained from couples of MODIS land bands. In each plane, separability of clusters of points with the same value of LFMC was evaluated by calculating the average pairwise JM distance.

Some pairs of bands show that groups of points with the same LFMC value can be identified, and namely band 2 (0.86 µm, further indicated as B2) – band 5 (1.24 µm, B5) and band 2 – band 6 (1.64 µm, B6). The dispersion of each group causes clusters to overlap with its neighbours; nevertheless, in these couple of bands, clusters separability is maximum among all possible band couples (average pairwise JM distance is 0.57 and 0.50 for B2-B5 and B2-B6 respectively). No similar consideration could be drawn from all the other possible band combinations.

Bands 2, 5 and 6 correspond to NIR and SWIR wavelengths that are used in the cited spectral indices of vegetation moisture. Since variations in LFMC lead to observable variations of vegetation reflectance, there is evidence supporting further analyses towards the definition of a spectral index. Besides the better separability of groups of points with the same LFMC value in band combination B2-B5 as compared to B2-B6, the following considerations will be based solely on the B2-B5 plane as most detectors of Aqua-MODIS band 6 were damaged at launch (Barnes et al., 2003; Wang et al., 2006; Xiong et al., 2009), thus limiting the applicability of any result based on measurements in this band. Nevertheless, although not shown, most of the results reported in this study could be repeated for the B2-B6 band combination.

The observed average pairwise JM distance (0.57 in the B2-B5 spectral plane) implies a considerable overlapping of clusters of points with the same value of LFMC. When the average pairwise JM distance is calculated by considering only points characterised by higher values of LAI, clusters separability increases considerably, and specifically JM=0.90 when LAI>2, JM=1.13 when LAI>4.

The calculation of linear regressions for each cluster (Table 4.3) shows that points with the same value of LFMC cluster along straight lines. When a subset of points with higher LAI is used, regressions are stronger (Table 4.4). With decreasing values of LAI, more background soil is exposed, and points shift towards the soil line, i.e. towards lower reflectance values in band 2 and higher in band 5. This results in the larger dispersion of all points, as compared to those with LAI>2 and LAI>4.

Higher values of LAI imply both a closer alignment of points with the same value of LFMC to a straight line, and a better separability of these clusters. Such lines shift towards lower

NIR and higher SWIR reflectance values with decreasing LFMC (Table 4.3 and Table 4.4). These considerations clearly hint at the existence of isolines of LFMC.

4.3.2. Sensitivity of MODIS spectral reflectance to vegetation moisture

By noting the slopes and 95% confidence intervals of regression lines in Table 4.3 and Table 4.4, it can be concluded that LFMC isolines are parallel. This observation is always true when LFMC<200% and stays valid for higher values of LFMC only for increasing values of LAI. However, before a spectral index can be defined, trajectories of LFMC variations must be understood. To this end, datasets 2 and 3 were produced, where all PROSPECT and SAIL parameters were kept constant, with the only exception of EWT and DMC. In dataset 2 DMC assumes a few fixed values while EWT varies freely; in dataset 3 EWT assumes a few fixed values while DMC varies freely. These datasets were designed to show trajectories of LFMC when only one of the two parameters EWT and DMC varies.

Figure 4.2 shows the regression lines (continuous) of points with constant value of DMC (trajectories of LFMC when only EWT varies) and regression lines (dashed) of points with constant value of EWT (trajectories of LFMC when only DMC varies). The variations in LFMC only due to a change in EWT mainly affect SWIR reflectance: an increase of EWT corresponds to a decrease in the reflectance in band 5 and to a limited variation in the NIR reflectance. When EWT is fixed and LFMC varies because of a variation in DMC, both NIR and SWIR reflectance change, and decrease with increasing dry matter content.

Table 4.3. Coefficient of determination, slope, intercept and corresponding 95% confidence intervals of regression lines of simulated reflectance measurements in the B2-B5 plane, in dependence of LFMC values. All regressions are significant with p<0.001.

LFMC	r^2	*Slope*	*Intercept*
50	0.85	0.88±0.07	0.011±0.018
100	0.81	0.83±0.08	0.011±0.022
150	0.79	0.90±0.09	-0.024±0.026
200	0.82	0.86±0.08	-0.023±0.026
250	0.73	0.78±0.09	-0.001±0.031
300	0.76	0.72±0.08	0.018±0.029
350	0.61	0.65±0.10	0.027±0.037
400	0.56	0.62±0.11	0.033±0.040
450	0.72	0.67±0.08	0.011±0.032
500	0.52	0.51±0.10	0.071±0.038

Provided that in the real-world variations in LFMC might occur due to variations in both EWT and in DMC, these findings lead to the consideration that no predictable trajectories of LFMC exist in the B2-B5 plane. In turn, this implies that in the construction of a spectral index any direction of the displacement vector is equivalent to the others, as long as it crosses LFMC isolines. Maximum sensitivity is achieved when measuring LFMC variation perpendicularly to its isolines (Verstraete and Pinty, 1996). Since LFMC isolines are parallel straight lines, the desired spectral index must measure the displacement of points along a straight direction.

4.3.3. Development and validation of a spectral index sensitive to LFMC

A new spectral index was developed, based on the findings in the previous sections, to measure LFMC. Since the isolines are parallel, there is no preference among them, and it is correct to evaluate LFMC variations perpendicularly to them as the distance of the measured reflectance from an a priori identified reference line (Figure 4.3). With the obvious need to construct an index that is a measure of LFMC, such line can be assumed to be that of completely dry vegetation, i.e. LFMC=0% and EWT=0 as derived from dataset 4 for values of LAI>4. This distance is called Perpendicular Moisture Index (PMI), and it is calculated as:

$$PMI = -0.73 \cdot (R_5 - 0.94 \cdot R_2 - 0.0028) \quad (4.6)$$

Table 4.4. Coefficient of determination, slope, intercept and corresponding 95% confidence intervals of regression lines of subsets of simulated reflectance measurements in the B2-B5 plane characterised by LAI>2 and LAI>4, in dependence of LFMC values. All regressions are significant with p<0.001.

	LAI > 2			*LAI > 4*		
LFMC	*r^2*	*Slope*	*Intercept*	*r^2*	*Slope*	*Intercept*
50	0.95	0.94±0.05	-0.011±0.012	0.99	0.95±0.02	-0.019±0.006
100	0.97	0.92±0.04	-0.027±0.011	0.99	0.94±0.03	-0.038±0.008
150	0.97	0.96±0.04	-0.054±0.012	0.99	0.92±0.03	-0.040±0.009
200	0.96	0.96±0.04	-0.070±0.014	0.99	0.95±0.03	-0.072±0.011
250	0.95	0.94±0.05	-0.073±0.017	0.97	0.96±0.05	-0.085±0.018
300	0.90	0.93±0.07	-0.070±0.027	0.97	0.98±0.06	-0.110±0.023
350	0.85	0.84±0.08	-0.059±0.030	0.96	0.94±0.05	-0.107±0.021
400	0.83	0.83±0.09	-0.058±0.033	0.96	0.96±0.06	-0.122±0.022
450	0.90	0.83±0.06	-0.067±0.025	0.96	0.91±0.05	-0.110±0.023
500	0.81	0.83±0.09	-0.073±0.039	0.96	0.94±0.06	-0.131±0.027

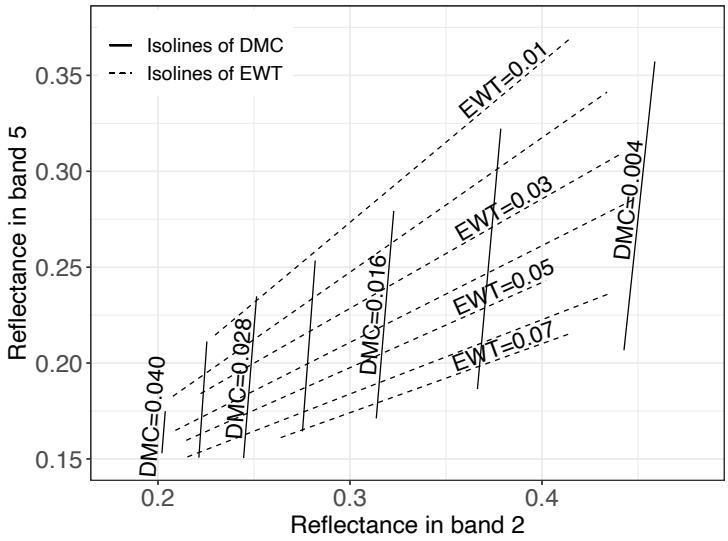


Figure 4.2. Trajectories of LFMC variations when only one of the two parameters EWT and DMC is allowed to vary freely.

where R_2 and R_5 are reflectance values measured in bands 2 and 5 respectively.

The PMI is larger for larger values of LFMC. However, from the results in the previous sections it can be anticipated that its predictive power is dependent on the density of vegetation cover. The exposure of the soil background shifts points towards the soil line, i.e. towards isolines with lower LFMC. Thus, it can be expected that with a reduction in LAI the index underestimates LFMC.

The PMI was initially validated against simulated values of LFMC (dataset 1), separately considering all data, data with LAI>2, and data with LAI>4. All regressions laws are linear, and the PMI can explain increasing percentages of LFMC variability with increasing values of LAI, being the coefficient of determination 0.32, 0.70 and 0.87 respectively for all data, data with LAI>2, and data with LAI>4.

Subsequent independent validation was performed against LOPEX93 data scaled to canopy reflectance with SAIL model. In this dataset, the regression laws are logarithmic, and lower performance is observed as compared with validation against dataset 1; coefficients of determination are 0.39, 0.56 and 0.63 respectively for all data, data with LAI>2, and data with LAI>4.

4.4. Discussion

Vegetation moisture is the main source of variability in the SWIR (Gates et al., 1965; Gausman and Allen, 1973; Tucker, 1980; Woolley, 1971). In its contribution to vegetation reflectance, the EWT plays the role of state variable of the radiative transfer equations (Feret et al., 2008; Jacquemoud et al., 2009; Jacquemoud and Baret, 1990). This justifies the

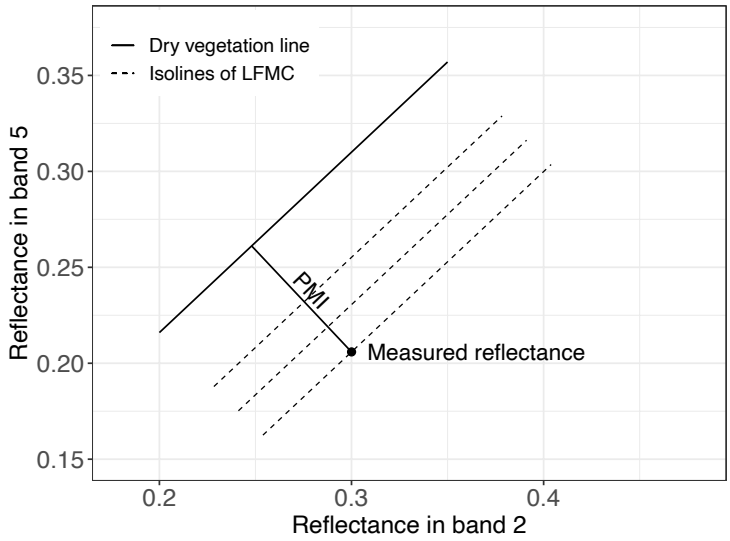


Figure 4.3. Graphical representation of the measurement performed by the perpendicular moisture index (PMI).

success of some spectral indices in retrieving this measure of vegetation moisture (Ceccato et al., 2002b; Gao, 1996; Hardisky et al., 1983; Hunt and Rock, 1989). However, the forest fires research community is interested in estimates of LFMC (Andrews, 2007; Carlson and Burgan, 2003; Finney, 1998; Hunt et al., 2013; Rothermel, 1991, 1972; Van Wagner, 1977; Yebra et al., 2013), which actually is the ratio of EWT and DMC, two independent state variables of the same equations. This has been seen as a complication in the retrieval of LFMC from spectral indices based on broadband remote sensing measurements in the optical domain (Ceccato et al., 2002b; Cohen, 1991; Gao and Goetz, 1990; Lee et al., 2007; Peñuelas et al., 1993; Verbesselt et al., 2007). Nevertheless, the value of an environmental variable can indeed be estimated if it results in an observable variation in vegetation reflectance that can be distinguished from other factors (Verstraete and Pinty, 1996).

The research reported herein tried to solve the problem of LFMC estimation from MODIS measurements by first identifying how LFMC variations affect the reflectance in the spectral space of the seven land bands, and then deriving an index formula so that its isolines are intersected by displacement of points that occur when this property changes. Evidence is shown that the planes obtained by combining band 2 (0.86 μm) with bands 5 (1.24 μm) and 6 (1.64 μm) provide clear separability for groups of points characterised by the same LFMC value.

These observations are in line with previous analyses of reflectance sensitivity to vegetation parameters (Bowyer and Danson, 2004; Dawson et al., 1999; Mousivand et al., 2014). DMC and EWT largely affect vegetation reflectance in the NIR and SWIR wavelengths (Ceccato et al., 2002b, 2001). The more evident effect of LFMC variation in band combinations 2-5 and 2-6, as compared to those based on band 7, is due to the fact that reflectance sensitivity to

EWT and DMC is weaker at longer SWIR wavelengths (Bowyer and Danson, 2004; Mousivand et al., 2014).

Focussing on MODIS bands 2 and 5, points representative of vegetation whose LFMC is constant lie on straight and parallel lines, at least for high LAI values (Table 4.3 and Table 4.4). Lines of decreasing values of LFMC are shifted towards lower reflectance values in band 2 and higher in band 5. This means that a point in this spectral space is displaced when LFMC changes. To detect and quantify such displacement, the PMI measures the distance of reflectance points from a reference line, that of completely dry vegetation (LFMC = 0%).

The PMI is a measure of LFMC. The LAI appears to be the main factor influencing the quality of the relationship between the PMI and LFMC. Good results are achievable on a wide range of LFMC values when LAI>2, which is a typical condition in a large variety of vegetation associations prone to fires (Asner et al., 2003). With decreasing values of LAI, the accuracy in the PMI vs LFMC relationship decreases. This is explained by the fact that reflectance in the SWIR is largely affected by this factor (Bowyer and Danson, 2004; Mousivand et al., 2014), and indeed the sensitivity to LAI is a characteristic that the PMI shares with the existing vegetation moisture spectral indices (Wang et al., 2008; Zarco-Tejada et al., 2003).

Dispersion of points away from the observed isolines for lower LAI values is towards lower reflectance in band 2 and higher reflectance in band 5. This is due to the fact that most soils show reflectance values in MODIS band 5 higher than in band 2 (Gao, 1996), while dense green vegetation exhibits the opposite behaviour. When LAI diminishes, more soil is exposed to sensor view and contributes to TOC reflectance, thus causing the displacement of points toward lower NIR and higher SWIR reflectance.

Table 4.3 and Table 4.4 show that the coefficient of determination of the regression lines of reflectance measurements in the B2-B5 plane for each simulated LFMC value (isolines of LFMC) decreases with increasing values of LFMC, and that this effect is more evident with lower values of LAI. Recalling that an increase in LFMC can be due to either an increase in leaf EWT or a reduction in DMC can explain this result. Indeed, the first cause implies a reduction in SWIR reflectance (Mousivand et al., 2014), and thus an increase of reflectance contrast between the leaves and the background soil, while the second increases both NIR and SWIR reflectance (Mousivand et al., 2014), increasing reflectance contrast in the NIR. Clearly, greater contrast results in a larger displacement of points towards the soil line when LAI diminishes.

The soil line and the dry vegetation line appear to be parallel in our experiments. This means that it is not possible to introduce modifications to the index in order to make it robust to LAI variations; nevertheless, this finding can be taken into account within the framework of the specific application (Seelig et al., 2008). Both the reduction of LAI and the reduction of LFMC have the same effect in the B2-B5 plane, i.e. points are shifted towards the dry vegetation reference line. This means that when LAI is lower, the PMI underestimates vegetation moisture. This can be considered safe when the application of the PMI is in the field of fire prevention (Gunes and Kovel, 2000; Minas et al., 2012; Mohamed Shaluf, 2008), where a missed alarm may have worse consequences than a false alarm.

All the analyses leading to the development of the PMI were based on simulated data. For the validation of the PMI, an independent TOC reflectance dataset was constructed based on LOPEX93 optical measurements scaled to canopy using SAIL radiative transfer model. The scaling did not consider species-specific values of canopy parameters. Indeed, any consideration on the dependence of vegetation spectral properties on LFMC variability that individual species exhibit was beyond the scope of our research. The coarse resolution of MODIS instruments (250-500 m in the land reflective bands) does not capture the horizontal and vertical distribution of species within a pixel. LFMC is a property beard at leaf level, and the scaling of LOPEX93 data to canopy level was a mean to evaluate the performance of PMI against real leaf data in a variety of simulated canopy structures.

4.5. Conclusions

Broadband spectral indices of vegetation moisture developed so far are sensitive to EWT. These spectral indices cannot be used to produce fire danger maps and the execution of fire propagation models, since these require the quantification of LFMC.

Specific patterns of points emerge in the plane of MODIS reflectance measurements in bands 2 and 5 when LFMC is kept constant and all other leaf, soil and canopy factors contributing to the observed reflectance vary freely. Points characterised by the same value of LFMC lay along straight parallel lines, i.e. isolines of LFMC exist in the B2-B5 plane. Dispersion of points away from these lines occurs at lower values of LAI.

Isolines of LFMC are parallel lines, ordered so that a reduction of LFMC results in an increase in SWIR reflectance and a reduction in NIR reflectance. This led to the construction of the perpendicular moisture index (PMI). In a way similar to that of the perpendicular vegetation index (Richardson and Wiegand, 1977) in the red-NIR plane, the PMI measures the distance of a reflectance point in the plane spanned by MODIS bands 2 and 5 from a reference line, that of completely dry vegetation. In this sense, the PMI is an explicit measure of LFMC.

In this work, the PMI was developed from a simulated dataset of vegetation reflectance, scaling leaf reflectance data to canopy level in the first place with an approach similar to that followed by Ceccato et al. (2002) for the definition of the global vegetation moisture index (GVMI). However, as compared to traditional vegetation moisture spectral indices, the PMI is specifically designed to be sensitive to LFMC.

The PMI shows linear correlation with LFMC in the simulated ranges, and logarithmic correlation with real leaf measurements scaled to canopy with the SAIL radiative transfer model. The strength of the correlation is dependent on the density of the vegetation cover, as expressed in terms of LAI. This characteristic is in common with all spectral indices based on measurements in the SWIR. Nevertheless, good results are achievable when LAI>2. When LAI<2, the exposure of soil background to sensor view results in an underestimate of LFMC by the PMI. When interpreted with consideration to fire danger mapping, this limitation might result in false alarms, but not in missed alarms.

5. Predicting forest fires burned area and rate of spread from pre-fire multispectral satellite measurements[4]

Abstract

Operational forest fire danger rating systems rely on the recent evolution of meteorological variables to estimate dead fuel condition. Further combining the latter with meteorological and environmental variables, they predict fire occurrence and spread. In this study, live fuel condition was retrieved from MODIS multispectral measurements in the near infrared and shortwave infrared. Next, these retrievals were combined with an extensive dataset on forest fires in Campania (13595 km^2), Italy, to determine how live fuel condition affects the probability distribution functions of fire behaviour characteristics. Accordingly, the specific objective of this study was to develop and evaluate a new approach to estimate the probability distribution functions of fire burned area, duration, and rate of spread as a function of the Perpendicular Moisture Index (PMI), whose value decreases with decreasing live fuel moisture content (LFMC). To this purpose, available fire data was intersected with MODIS 8-day composited reflectance data and, for comparison purposes, with Fire Weather Index (FWI) System components maps from global meteorological reanalyses, so to associate each fire event with the corresponding pre-fire PMI observation and current FWI System values. Fires were then grouped in ten decile bins of PMI and of the FWI System components, and the conditional probability distribution functions of burned area, fire duration and rate of spread were determined in each bin. Distributions of burned area and rate of spread vary across PMI decile bins, while no significant difference was observed for fire duration. Further testing this result with a likelihood ratio test confirmed that PMI is a covariate of burned area and rate of spread, but not of fire duration. By comparison, all FWI System components are a covariate of burned area and fire duration, but not of rate of spread. However, for burned area, the alternative model conditional to PMI retains a higher likelihood. An extreme event was defined as a fire whose burned area (respectively rate of spread) exceeds the 95^{th} percentile of the frequency distribution of recorded fires. The probability distribution functions in the ten decile bins of PMI were combined to obtain a

[4] Based on: Maffei, C., Menenti, M., 2019. Predicting forest fires burned area and rate of spread from pre-fire multispectral satellite measurements. ISPRS J. Photogramm. Remote Sens. 158, 263–278. https://doi.org/10.1016/j.isprsjprs.2019.10.013

conditional probability distribution function, which was then used to predict the probability of extreme fires, as defined. It was found that the probability of extreme events steadily increases with decreasing PMI. Overall, at the end of the dry season the probability of extreme events is about the double than at the beginning. These results may be used to produce frequently updated maps of the probability of extreme events given a PMI map retrieved from e.g. MODIS reflectance data.

5.1. Introduction

Wildfires are a widespread factor of ecosystem disturbance (Bond et al., 2005), causing invaluable human casualties, negative effects on carbon sequestration and substantial economic loss (FAO, 2007; Montagné-Huck and Brunette, 2018; Pellegrini et al., 2018). Scientific evidence supports the hypothesis that climate change may alter fire dynamics through the direct and indirect effects it exerts on fuel moisture and availability (Pausas and Ribeiro, 2013; Seidl et al., 2017; Williams and Abatzoglou, 2016) and ultimately on the probability distribution of dependent variables such as fire occurrence, burned area and rate of spread (Flannigan et al., 2016; Podschwit et al., 2018; Syphard et al., 2018).

Fire behaviour is determined by a diverse array of static and dynamic factors (Barrett et al., 2016; Faivre et al., 2016; Falk et al., 2007; Lasslop and Kloster, 2017; Littell et al., 2016; Viegas and Viegas, 1994). Among these, weather is an active driver of fuel moisture (Ustin et al., 2009), which in turn affects ignition delay (and thus ease of inception) and flames propagation (Chuvieco et al., 2009; Rothermel, 1972). Indeed, fire danger models rely on meteorological input to process indicators of fuel water content and assess fire behaviour.

The National Fire Danger Rating System used in the United States is a collection of fuel condition and fire behaviour indicators computed from meteorological measurements, fuel models, climate class and slope (Burgan, 1988; Deeming et al., 1977). Fuel condition components are a collection of descriptors of the water content of two classes of live fuels and four classes of dead fuels. The McArthur Forest Fire Danger Index used in Australia works along similar principles, but only contains one drought index related to dead fuels moisture (Griffiths, 1999; Keetch and Byram, 1968; McArthur, 1967). The Fire Weather Index (FWI) System is based on the progressive processing of meteorological measurements for the production of three dead fuels moisture codes and three fire behaviour indices, and does not include any model of live fuels moisture (Van Wagner, 1987).

The role of live fuels moisture is indeed crucial in predicting fire behaviour, as it can inhibit or promote the spread of fires (Rossa et al., 2016; Rossa and Fernandes, 2017; Ustin et al., 2009). Nevertheless, its value is not adequately represented by fire danger models as it depends, further to the variability of meteorological conditions, also on plant response to it, which is species and landscape specific (Ruffault et al., 2018). This opens to the adoption of Earth observation technologies in fire danger mapping (Leblon, 2005; Stow et al., 2006; Yebra et al., 2018, 2013), as water in leaf tissues affects the radiometric properties of live fuels in a distinguishable way, that can be captured by optical sensors (Bowyer and Danson, 2004; Buitrago Acevedo et al., 2018, 2017; Hunt and Rock, 1989; Mousivand et al., 2014). Pixel-based mapping of fire danger would then be made possible by the wide availability of

instruments providing daily global coverage, such as MODIS on board Terra and Aqua satellites, VIIRS on Suomi NPP and NOAA-20, and SLSTR on Sentinel-3A and -3B.

Several approaches were proposed for the use of remote sensing to evaluate fire danger. A few authors related indirect estimates of plant water stress to forest fires, e.g. through the analysis of time series of optical spectral indices (Bajocco et al., 2015; Burgan et al., 1998; Maselli et al., 2003), land surface temperature (LST) (Maffei et al., 2018; Menenti et al., 2016), or an integration of both (Jang et al., 2006; Pan et al., 2016). A more direct method is the inversion of radiative transfer models for the estimation of water content in vegetation (Cheng et al., 2014; Verrelst et al., 2015; Zarco-Tejada et al., 2003), but it needs extensive ground measurements to constrain the solutions space (Quan et al., 2015; Riaño et al., 2005; Yebra et al., 2018; Yebra and Chuvieco, 2009a). A different approach is the use of spectral indices for the estimation of moisture content, such as the Normalised Difference Water Index (NDWI) (Gao, 1996), the Global Vegetation Moisture Index (GVMI) (Ceccato et al., 2002b), and the Perpendicular Moisture Index (PMI) (Maffei and Menenti, 2014).

NDWI and GVMI have been reported in literature as predictors of fire occurrence. NDWI was used along with remotely sensed LST and atmospheric columnar water vapour to predict fire danger (Abdollahi et al., 2018), while time series of this index documented the seasonality of fire occurrence and demonstrated good forecasting capabilities (Huesca et al., 2014, 2009). GVMI was used along with LST, normalised difference vegetation index (NDVI), topography, land cover and human settlements to predict fire occurrence (Pan et al., 2016), although in specific land cover types other spectral indices had a better performance (Cao et al., 2013).

Both NDWI and GVMI were designed to evaluate canopy water content measured as equivalent water thickness (EWT, see §§ 1.5.2 and 4.1). EWT has a direct effect on the optical properties of vegetation, and indeed it is a parameter of leaf radiative transfer models such as PROSPECT (Feret et al., 2008; Jacquemoud and Baret, 1990). The more recently introduced PMI (Maffei and Menenti, 2014) was specifically constructed as sensitive to live fuel moisture content (LFMC, see §§ 1.5.2 and 4.1). This quantity expresses water content as a percentage of dry leaf mass. LFMC, along with the corresponding dead fuel moisture content, is a parameter in fire propagation models (Andrews et al., 2013; Finney, 1998; Rothermel, 1991, 1972), and affects probability distribution of burned area and rate of spread (Flannigan et al., 2016; Podschwit et al., 2018). The accuracy of a spectral index in retrieving biophysical quantities is typically assessed against field measurements (Gao et al., 2015; Ullah et al., 2014). However, in the context of the identified need to improve fire danger models through the estimation of LFMC (Ruffault et al., 2018), it would be relevant to investigate the effectiveness of PMI based estimation of LFMC in predicting fire behaviour characteristics that contribute to fire danger such as burned area, duration and spread (Dasgupta et al., 2007), and to evaluate its performance against traditional and trusted fire weather danger rating systems.

The objective of this study was to develop and evaluate a new approach to estimate the probability distribution functions of fire burned area, duration, and rate of spread as a function of pre-fire PMI. To this aim, a dataset of ten years of forest fires recorded in the

study area of Campania, Italy, was used along PMI maps computed from MODIS reflectance data. The effectiveness of PMI as a covariate of fire behaviour characteristics was then compared against FWI System components retrieved from global meteorological reanalysis data. Finally, probability of extreme events conditional to ignition as a function of PMI was evaluated.

5.2. Materials and methods

5.2.1. Study area

A detailed description of the study area was provided in §2.2.1.

5.2.2. Data

MODIS reflectance data

Satellite reflectance data used in this study is the 8-day composited Aqua-MODIS product (MYD09A1) collection 6 at 500 m resolution (Vermote et al., 1997; Vermote and Vermeulen, 1999). Granules covering months June to September of years 2002-2011 were downloaded from NASA's Land Processes Distributed Active Archive Centre, resulting in a dataset of 163 granules. Retrieved reflectance data were masked against MYD09A1 quality assurance layer, to ensure only the highest quality retrievals are retained. These correspond to band quality assurance bits = 0000 (highest reflectance band quality) and state quality assurance bits 0,1 = 00 (cloud state is clear) (Vermote et al., 2015).

Fire data

The Forest Fire Protection Information Unit of Carabinieri provided a database of 9127 fires that occurred in Campania between 2002 and 2011[5]. The dataset details for each event, among other information, cartographic coordinates, date and time of initial spread and fire extinction, and final burned area. 913 fires are recorded on average each year, with a mean burned area of 6.2 ha (Table 5.1). Year 2007 appears to be exceptional in terms of mean burned area (14.7 ha), as this is more than the triple of the mean burned area of all other years (4.2 ha). In this sense year 2011 is representative of baseline mean burned area, although characterised by a high fire occurrence. 99.8% of fires are of anthropic source, either arson or unintentional. The phenomenon peaks in the summer season, with 82% of fires recorded between June and September.

Fires in the dataset were selected for further analyses based on land cover and month of the year. To this purpose, data points were first intersected with a CORINE Land Cover (CLC) map (European Environment Agency, 2007) to select fires that occurred in natural areas only (Table 5.2). CLC maps are updated every six years since 2000, so fires were intersected with the closest prior land cover map. Finally, only fires occurring between June and

[5] This is a subset of the fire data used in Chapter 2 to characterise the fire regime in the study area.

September were selected, leading to a final number of 5005 fires retained for subsequent analyses.

This research focussed on burned area, fire duration and rate of spread as fire behaviour characteristics potentially related to remote sensing observations of vegetation moisture and meteorological fire danger indices. While burned area is explicitly available as a field in the provided database, the latter two variables were computed from data. Fire duration was evaluated as the difference, in hours, between fire inception and extinction. Rate of spread was calculated from burned area and fire duration in the simplified assumption of a circular fire growing at a constant rate in every direction throughout its duration on a flat and uniform surface.

Burned area, fire duration and rate of spread span over several orders of magnitude, and their distributions appear to be extremely skewed. Prior to any further analysis and to facilitate model fitting, their observations were log-transformed base 10 and shifted, so to have positive values only.

The Fire Weather Index (FWI) System

The Fire Weather Index (FWI) System is a collection of six indicators, computed from daily measurements of 24-hour cumulated precipitation, wind speed, relative humidity and air temperature to represent the effect of dead fuels moisture content and of wind on fire behaviour in a standardised fuel type and in no slope conditions (Van Wagner, 1987). It is composed of: Fine Fuel Moisture Code (FFMC), Duff Moisture Code (DMC) and Drought Code (DC), which are representative of the moisture content of three different classes of dead fuels; Initial Spread Index (ISI), providing a measure of rate of spread, independently

Table 5.1. Summary statistics of fires recorded in the study area between 2002 and 2011.

Year	*Number of fires*	*Mean burned area (ha)*	*Proportion of fires exceeding 95th percentile of burned area*
2002	310	3.8	1.9 %
2003	1323	4.1	2.3 %
2004	803	3.9	2.5 %
2005	669	2.9	1.2 %
2006	423	4.1	3.5 %
2007	1757	14.7	13.4 %
2008	776	4.4	3.6 %
2009	895	5.8	5.6 %
2010	537	3.7	1.9 %
2011	1634	4.2	3.0 %

of the variable quantity of fuels; Build-Up Index (BUI), a descriptor of the fuels available for combustion; Fire Weather Index (FWI), a comprehensive indicator related to fire intensity. Further details on the FWI System were provided in §1.4.3.

In this research, FWI layers were retrieved from the Global Fire Weather Database (Field et al., 2015). These layers are computed from NASA Modern Era Retrospective Analysis for Research and Applications version 2 global meteorological reanalyses of air temperature, relative humidity, wind speed and precipitation (Molod et al., 2015), and distributed at a resolution of 0.25° × 0.25° (about 21×28 km^2 at the latitude of the study area).

5.2.3. The Perpendicular Moisture Index

The Perpendicular Moisture Index (PMI) was developed from the observation that in a plane reporting MODIS reflectance at 0.86 μm (band 2) and 1.24 μm (band 5), isolines of LFMC are straight and parallel (Maffei and Menenti, 2014). The PMI is thus evaluated as the distance of reflectance points from a reference line:

$$PMI = -0.73 \cdot \left(R_{1.24\mu m} - 0.94 \cdot R_{0.86\mu m} - 0.028\right) \quad (5.1)$$

In this sense, PMI is a direct measure of LFMC, with higher values corresponding to higher moisture content.

Table 5.2. CORINE Land Cover (CLC) classes associated with fires for subsequent analyses.

CLC code	*Description*
231	Pastures
243	Land principally occupied by agriculture, with significant areas of natural vegetation
311	Broad-leaved forest
312	Coniferous forest
313	Mixed forest
321	Natural grassland
323	Sclerophyllous vegetation
324	Transitional woodland shrub
333	Sparsely vegetated areas
334	Burnt areas

5.2.4. Parametric distributions of fire characteristics

To evaluate the distribution of fire behaviour characteristics conditional to PMI and FWI System components, parametric distributions describing burned area, fire duration and rate of spread in the study area were first identified. Tested distributions were selected from existing literature (Baker, 1989; Corral et al., 2008; Cumming, 2001; Haydon et al., 2000; Moritz, 1997; Reed and McKelvey, 2002; Weber and Stocks, 1998), and included normal, log-normal, exponential, gamma, generalised extreme value (GEV) and Weibull. Available fire data were fitted to the named distribution through the minimisation of the Anderson-Darling distance (Anderson and Darling, 1954), and the closest fitting model for each fire characteristic was retained as a basis for further analyses (Hernandez et al., 2015; Maffei et al., 2018).

5.2.5. Conditional distributions of fire characteristics

PMI maps were produced from available MYD09A1 data and sampled at fire locations on the compositing period prior to the event. Similarly, maps of the six FWI System components were sampled on the day of the event. This resulted in each fire in the database being associated with the corresponding PMI recorded in the raster cell where it occurred in the antecedent 8-day MODIS compositing period as well with the corresponding daily value of the six FWI System components in the respective raster cell.

To understand whether PMI and the six FWI System components may be considered a covariate of fire characteristics, their observations were divided in ten decile bins. The parameters of the corresponding distributions were then retrieved in each bin with the Anderson-Darling maximum goodness of fit criterion, and their 95% confidence intervals were determined by means of 1000 bootstrap estimations (Hernandez et al., 2015; Maffei et al., 2018).

To assess the significance of observed distribution parameters across the decile bins, a likelihood ratio test was performed comparing, for PMI and for each of the FWI System components, the sum of the likelihoods of the ten models fitted in the individual bins (alternative models) to the likelihood of the unconditional model fitting all log-transformed burned area, fire duration and rate of spread data (null models). Test significance was set at 0.05.

5.2.6. Probability of extreme events conditional to ignition

The identified conditional probability distribution functions were further used to evaluate the probability of extreme events conditional to ignition as a function of PMI. Probabilities were computed by modelling the dependence of the corresponding distribution parameters on PMI. In this study, an event was considered extreme if it exceeded the 95^{th} percentile of burned area, fire duration and rate of spread values observed in the study area. The 95^{th} percentile of burned area of summer fires in natural areas is 30.0 ha, of fire duration is 28.2 h, of rate of spread is 48.4 m/h.

5.3. Results

5.3.1. Temporal and spatial variability of PMI

Maps of PMI exhibit significant inter- and intra-annual variability, as for example the four PMI maps representing compositing periods 4-11 July and 5-12 August of years 2007 and 2011 (Figure 5.1). Spatial patterns of PMI in the 5-12 August period show lower values as compared to 4-11 July in both years, corresponding to lower LFMC. Moreover, both compositing periods show in 2007 lower values than the corresponding periods in 2011.

To synthetically visualise seasonal evolution, median PMI was computed in each of the selected land cover classes (Table 5.2) across the dry season of years 2002 to 2011. While maps are characterised by a continuity of values, discretised in raster cells, this synthesis approach has the advantage of highlighting differences across land cover classes in observed PMI values (and indirectly LFMC). A consistent reduction of PMI, corresponding to a reduction in LFMC, is observed throughout the dry season for all classes in all years, as for example in 2007 and 2011 (Figure 5.2). The dynamic of such reduction shows inter-annual variability, as it can be here noticed with the higher medians (higher LFMC) recorded in 2011.

The observed diverse median values recorded in each CLC class are reflected in the PMI values recorded at fire locations (Figure 5.3). Indeed, lower PMI observations (and thus lower LFMC) are recorded at fires occurring in pastures and natural grasslands. Conversely, fires tend to be recorded with higher PMI values (higher LFMC) in broad leaved, coniferous, and mixed forests.

5.3.2. Probability models of fire characteristics

Log-transformed burned area, fire duration and rate of spread were fitted to normal, log-normal, exponential, gamma, GEV and Weibull distributions, and the corresponding Anderson-Darling statistics are reported in Table 5.3. Normal is the closest fitting distribution of log-transformed burned area, while GEV is the closest model for log-transformed fire duration and Weibull for log-transformed rate of spread. The corresponding Q-Q plots are reported in Figure 5.4.

5.3.3. Conditional distributions of fire characteristics

The mean of the normal distribution of log-transformed burned area conditional to PMI in ten decile bins shows a significant ($p<0.001$) decreasing ($r^2=0.80$) trend with increasing PMI (Figure 5.5a). The variation of standard deviation appears non-significant when evaluated against a linear model, and the confidence intervals of this parameter are consistent with a constant value across most PMI bins (Figure 5.5b). For log-transformed fire duration, no significant trend was observed in location and shape of GEV distribution conditional to PMI,

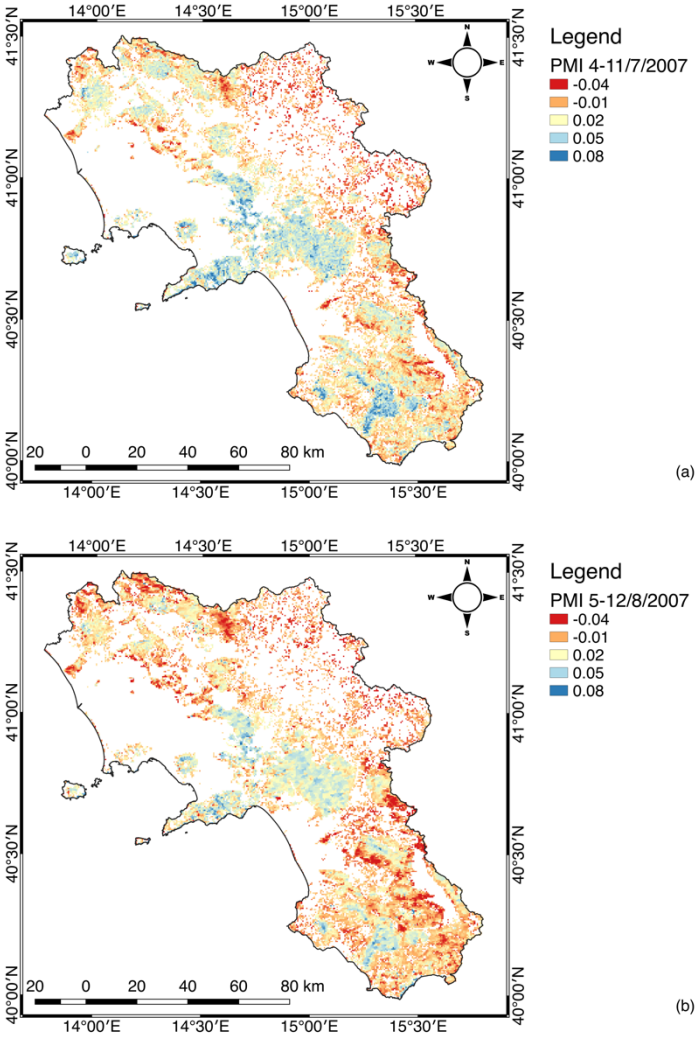


Figure 5.1. Selected PMI maps derived from Aqua-MODIS 8-day reflectance composites showing intra- and inter-annual variability: 4-11 July 2007 (a), 5-12 August 2007 (b), 4-11 July 2011 (c), 5-12 August 2011 (d).

and a weak increasing trend (r^2=0.53, $p<0.05$) in scale (Figure 5.6). Both scale and shape of the Weibull distribution of log-transformed rate of spread show significant ($p<0.001$) decreasing trends (r^2=0.96 and r^2=0.84 respectively) with increasing PMI (Figure 5.7). These observations support the idea that PMI is a covariate of burned area and rate of spread, while its contribution to fire duration probability distribution is weak or not significant.

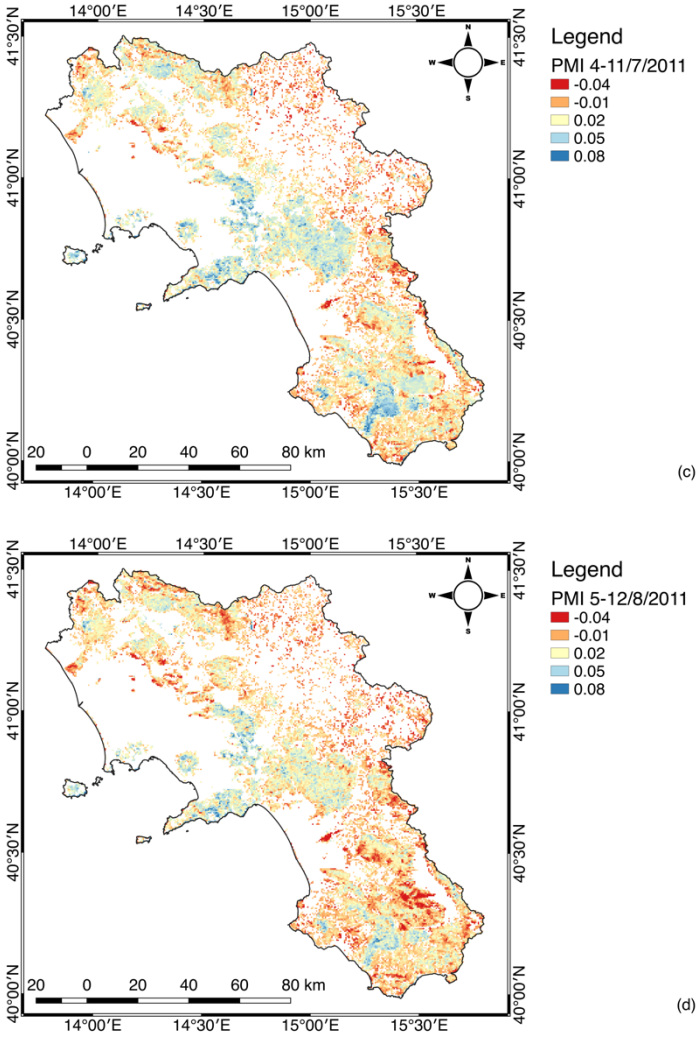


Figure 5.1. (continued)

The variability of the parameters of the normal distribution of burned area in ten decile bins of FWI System components support the idea that all six components are a covariate of burned area (Figure 5.8). Mean increases linearly with all components with $p<0.001$ and r^2 ranging between 0.84 and 0.96, substantially covering the same range of values covered against PMI. A significant linear variation of the standard deviation is observed only with DMC and BUI ($p<0.001$ and $p<0.01$ respectively). Similar observations can be drawn for fire duration, with location, scale, and shape of GEV distribution varying linearly with the respective FWI System components with significance at least $p<0.001$ for location and at least $p<0.05$ for scale and shape (Figure 5.9). The contribution of FWI System components to the variability of the Weibull distribution of log-transformed rate of spread is less evident

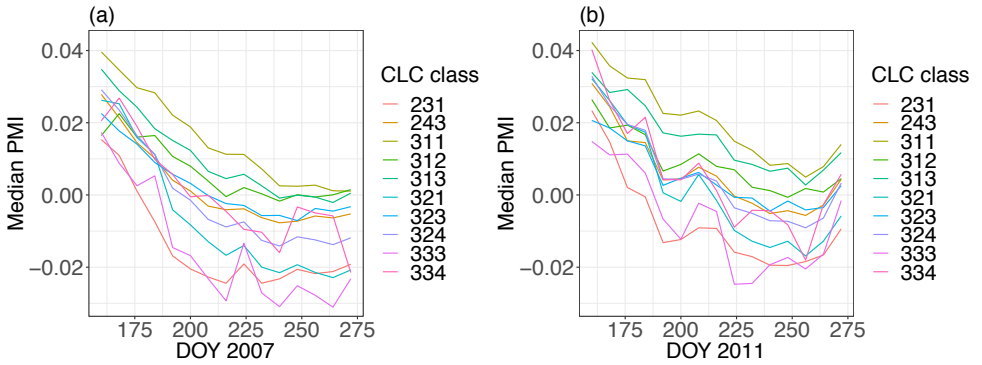


Figure 5.2.Evolution of the median PMI value in CLC classes (Table 5.2) during the dry season in two selected years: 2007 (a), 2011 (b).

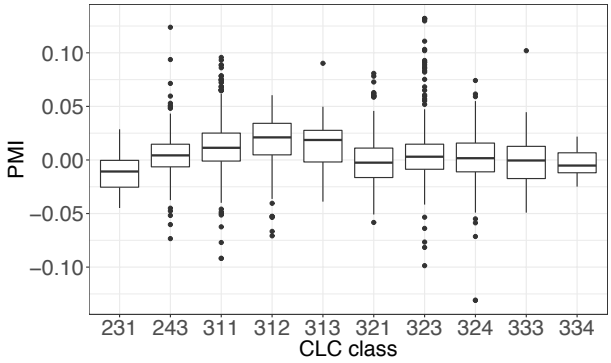


Figure 5.3. Boxplot of PMI observed at fire location in each CLC class (Table 5.2).

as compared against the other fire behaviour characteristics (Figure 5.10). Scale shows significant trends only conditional to DC (r^2=0.59, p<0.01) and BUI (r^2=0.67, p<0.01), while shape shows significant trends conditional to DMC (r^2=0.50, p<0.05), DC (r^2=0.66, p<0.01) and BUI (r^2=0.46, p<0.05) only. Moreover, the observed trends show limited sensitivity as compared to PMI (Figure 5.7).

The likelihood ratio test (Table 5.4) confirms that all models conditional to PMI and to the six FWI System components (alternative models) allow the rejection of the null model fitting all log-transformed burned area data. Among the alternative models, PMI ensures the highest summed likelihood. The test confirms that the alternative fire duration model conditional to PMI fails to reject the null model, while DMC shows the highest summed likelihood among the FWI System components. FFMC, DMC and DC fail to reject the null model of rate of spread, while PMI ensures the alternative model with the highest likelihood. These results confirm PMI is a covariate of burned area and rate of spread, but not of fire duration.

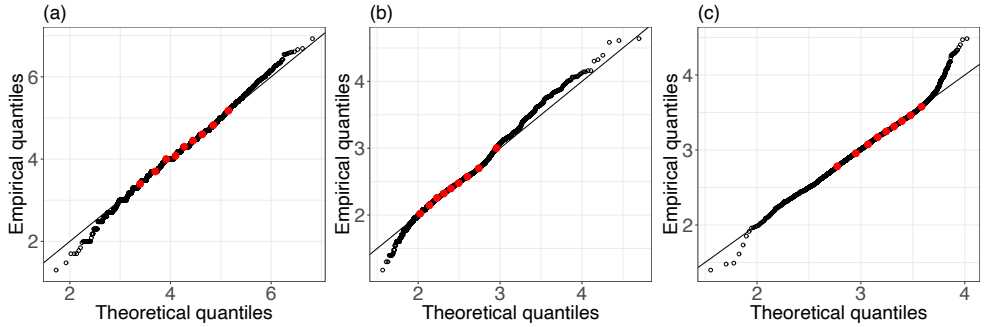


Figure 5.4 Q-Q plots of the normal distribution of log-transformed burned area (a), of the GEV distribution of log-transformed fire duration (b) and of the Weibull distribution of log-transformed rate of spread (c). Red circles indicate the deciles of the distributions.

5.3.4. Probability of extreme events conditional to ignition

From the observations above, a linear relationship was adopted to model the dependence of the mean of the normal distribution of log-transformed burned area on PMI, while for the standard deviation the constant value of the general model was adopted (Figure 5.5). For log-transformed rate of spread, a linear model was adopted for both scale and shape of the Weibull distribution (Figure 5.7). The resulting conditional probabilities over a range of PMI values are plotted in Figure 5.11. With decreasing PMI (and thus decreasing LFMC) the probability of a fire larger than 30 ha conditional to ignition increases from 1.8% to 7.4%. Similarly, the probability of a rate of spread higher than 48.4 m/h conditional to ignition raises from 1.2% to 10.5%.

Table 5.3. Anderson-Darling statistic values for tested distributions. Lower values indicate a closer fit.

Model	*Log-transformed burned area*	*Log-transformed fire duration*	*Log-transformed rate of spread*
Normal	7.2	52.3	20.3
Log-normal	16.7	20.4	40.8
Exponential	1347	1387	1559
Gamma	11.0	28.7	33.1
Generalised Extreme Value (GEV)	10.5	10.5	39.6
Weibull	25.2	134	8.2

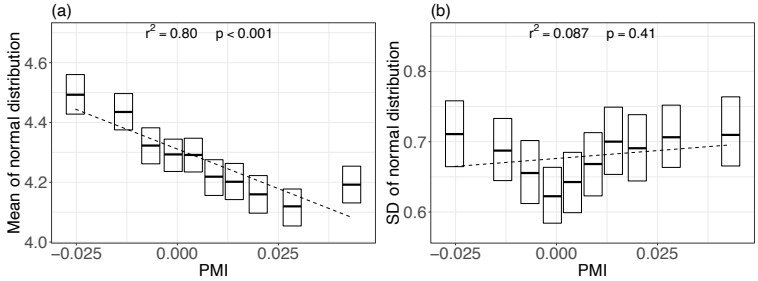


Figure 5.5. Plots of mean (a) and standard deviation (b) of normal distribution of log-transformed burned area, and their 95% confidence intervals, in ten decile bins of PMI. Regression lines refer to the estimated parameters.

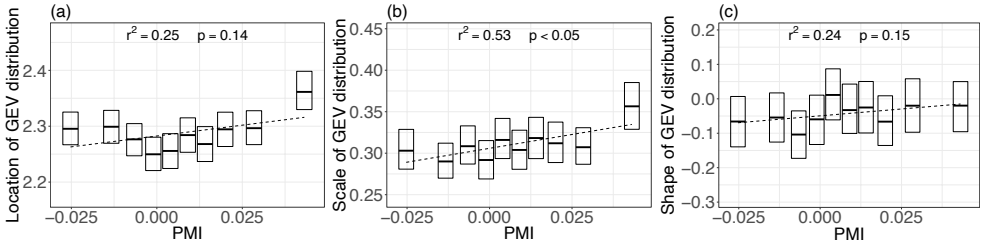


Figure 5.6. Plots of location (a), scale (b) and shape (c) of GEV distribution of log-transformed fire duration, and their 95% confidence intervals, in ten decile bins of PMI. Regression lines refer to the estimated parameters.

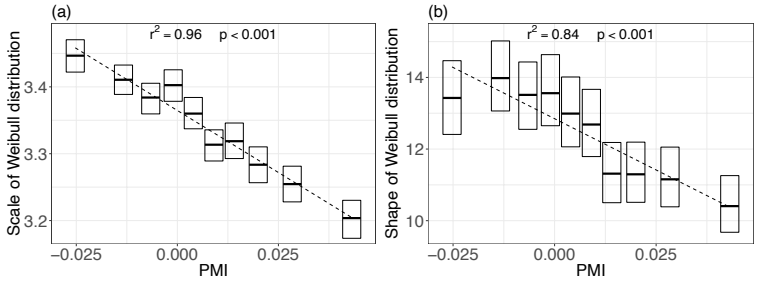


Figure 5.7. Plots of scale (a) and shape (b) of Weibull distribution of log-transformed rate of spread, and their 95% confidence intervals, in ten decile bins of PMI. Regression lines refer to the estimated parameters.

5.4. Discussion

This study had the stated objective of developing and evaluating a new approach to estimate the probability distribution functions of fire behaviour characteristics as a function of PMI. Those investigated in this study, as allowed by the available fire data, included rate of spread, burned area and duration. With climate change altering weather patterns

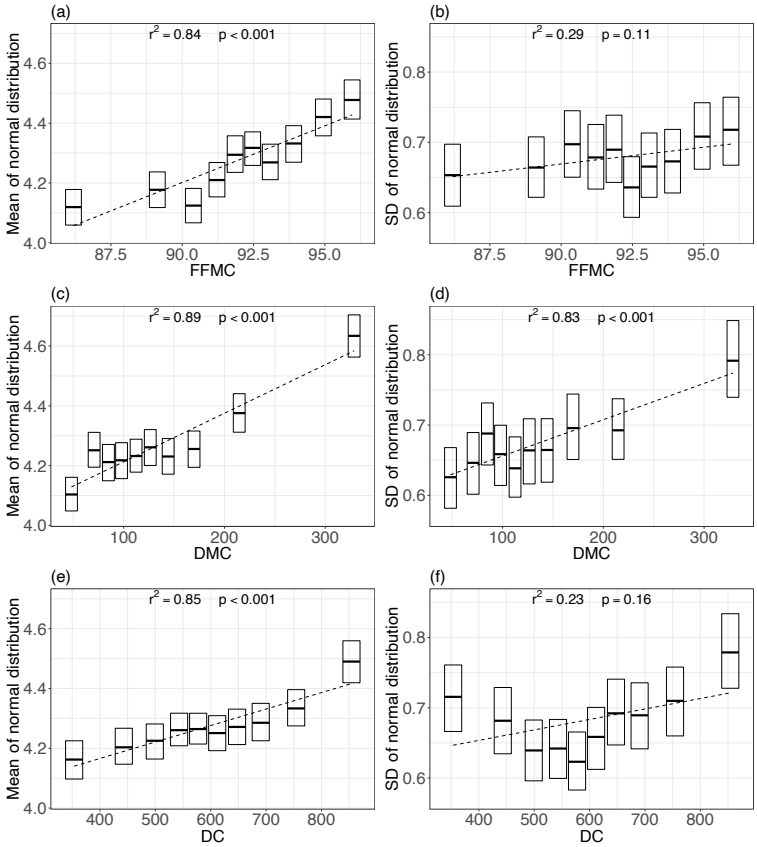


Figure 5.8. Plots of mean and standard deviation of normal distribution of log-transformed burned area, and their 95% confidence intervals, in ten decile bins of the Fire Weather Index (FWI) System components: FFMC (a, b), DMC (c, d), DC (e, f), ISI (g, h), BUI (i, j), FWI (k, l). Regression lines refer to the estimated parameters.

worldwide, and ultimately affecting fire regimes (Seidl et al., 2017), there is an increasing need to improve fire danger rating models and use synergistically the information they deliver (Chowdhury and Hassan, 2015a; Ruffault et al., 2018; Yebra et al., 2013). To support their preparedness activities, fire managers are interested in predicting fire occurrence and behaviour. Our approach, as based on probabilities of event properties rather than on their deterministic modelling, suits the need to predict fire danger.

Precondition for fire occurrence is the ease of ignition, which is determined by dead fuel moisture content (Aguado et al., 2007; Bianchi and Defossé, 2014; de Groot et al., 2005). Operational fire danger rating systems estimate this parameter from meteorological measurements (Burgan, 1988; Deeming et al., 1977; Keetch and Byram, 1968; McArthur, 1967; Van Wagner, 1987). Fire behaviour depends on a diverse array of factors, among which the moisture content of both dead and live fuels plays a significant role as it directly affects flame propagation (Rothermel, 1972). Vegetation moisture content is determined

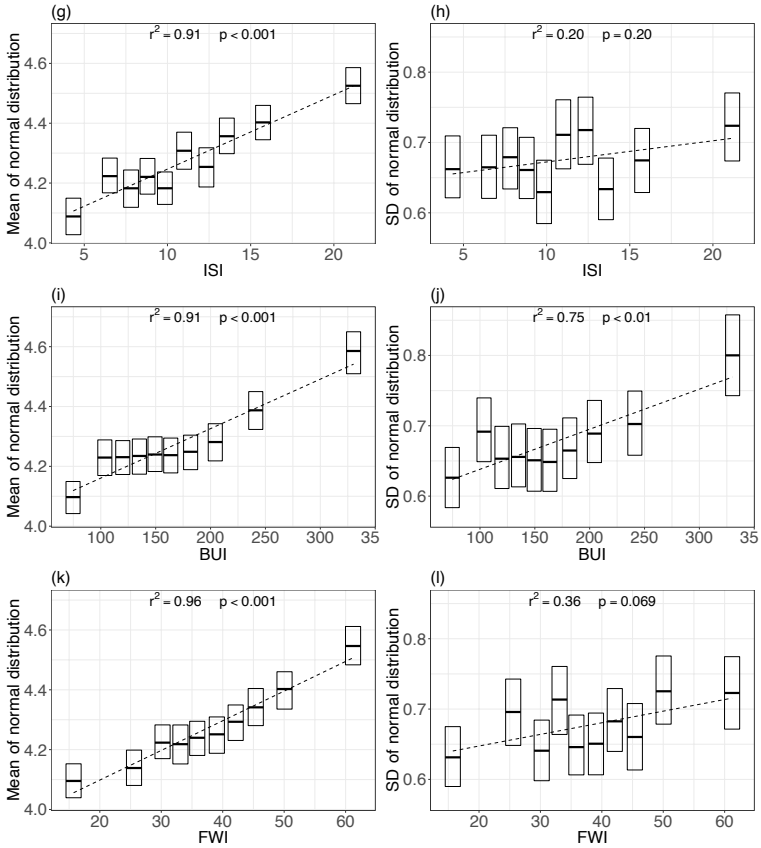


Figure 5.8. (continued)

by plant active response to weather conditions as regulated by transpiration, and by dry mass changes associated with phenology, both processes being species specific. For this reason, the simplified approach for the estimation of LFMC in fire danger models results in lack of generality (Jolly and Johnson, 2018; Nolan et al., 2018; Pellizzaro et al., 2007b; Ruffault et al., 2018).

In this research the Perpendicular Moisture Index (PMI) was used as a measure of LFMC. Indeed, remote sensing measurements in the near infrared and in the shortwave infrared allow for the quantification of water content in leaf tissues (Gates et al., 1965; Gausman and Allen, 1973; Tucker, 1980; Woolley, 1971). Among the various broadband spectral indices of vegetation moisture, the focus on the PMI is motivated by its initial development with respect to general spectral index development methods (Ceccato et al., 2002b; Dasgupta and Qu, 2009; Huete, 1988; Verstraete and Pinty, 1996) maximising its sensitivity to LFMC variations (Maffei and Menenti, 2014). This feature allows for its use along with existing fire danger models. Our approach is opposed to that of the Wildland Fire Assessment System services of the US Forest Service, which is based on the processing of time series of the NDVI for the evaluation of relative greenness (Preisler et al., 2009).

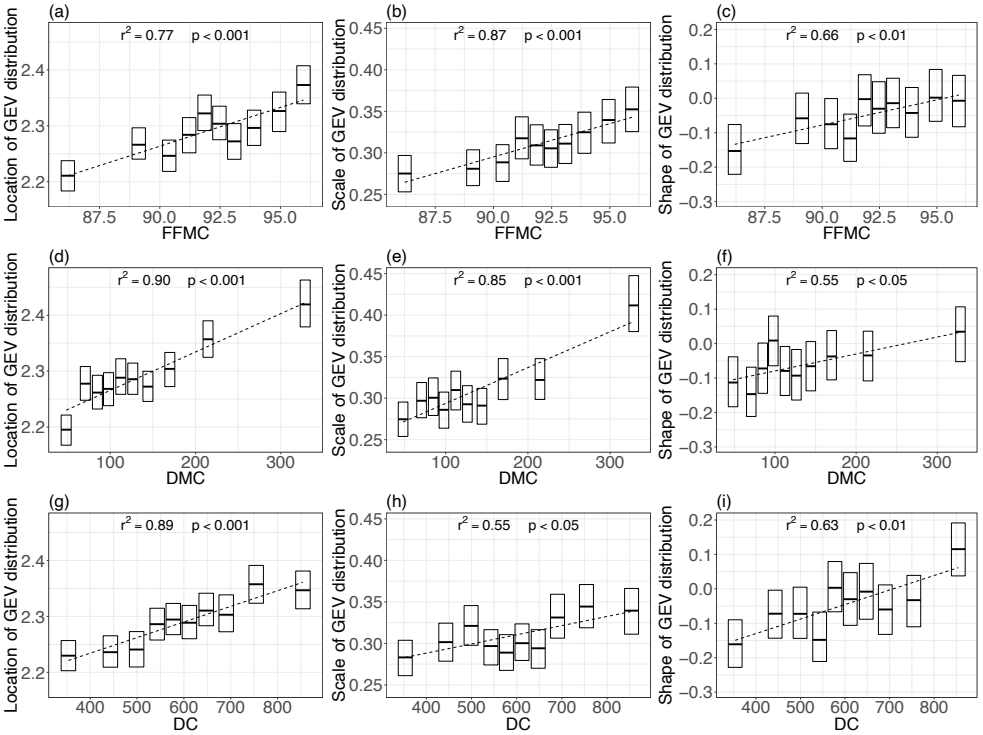


Figure 5.9. Plots of location, scale, and shape of GEV distribution of log-transformed fire duration, and their 95% confidence intervals, in ten decile bins of the Fire Weather Index (FWI) System components: FFMC (a, b, c), DMC (d, e, f), DC (g, h, i), ISI (j, k, l), BUI (m, n, o), FWI (p, q, r). Regression lines refer to the estimated parameters.

Indeed, the Fire Potential Index produced by the Wildland Fire Assessment System is a predictor of fire occurrence, and is not integrated in fire behaviour components of the National Fire Danger Rating System (Chowdhury and Hassan, 2015a).

The analyses were conducted in the study area of Campania (13595 km^2), an Italian region characterised by the diversity of its landscape and listed as one of the most fire prone in the Mediterranean (Chapter 2). Fire data was provided by Carabinieri, a law enforcement agency, and as such it can be considered official and correct. Provided data points correspond to the centroid of the burned area, but the exact burnt scar perimeters were not part of the dataset. While in general this might arise concerns on positional accuracy of the available coordinates against gridded MODIS reflectance composites, it must be observed that fire regime is dominated by many small fires, and indeed only 4.5% of fires in the database resulted in a burned area larger of a 500 × 500 m^2 MODIS pixel, and 0.7% larger than 1 km^2. This means that positional accuracy of fire data is substantially of the same order of magnitude of positional accuracy of MODIS data (Wolfe et al., 2002). Adding to this, because of the coarse MODIS resolution, the PMI value associated with each fire does not correspond to the PMI value of the specific vegetation patch where fire was ignited. This is not relevant for the purpose of this study, as the retrieved PMI was hereby

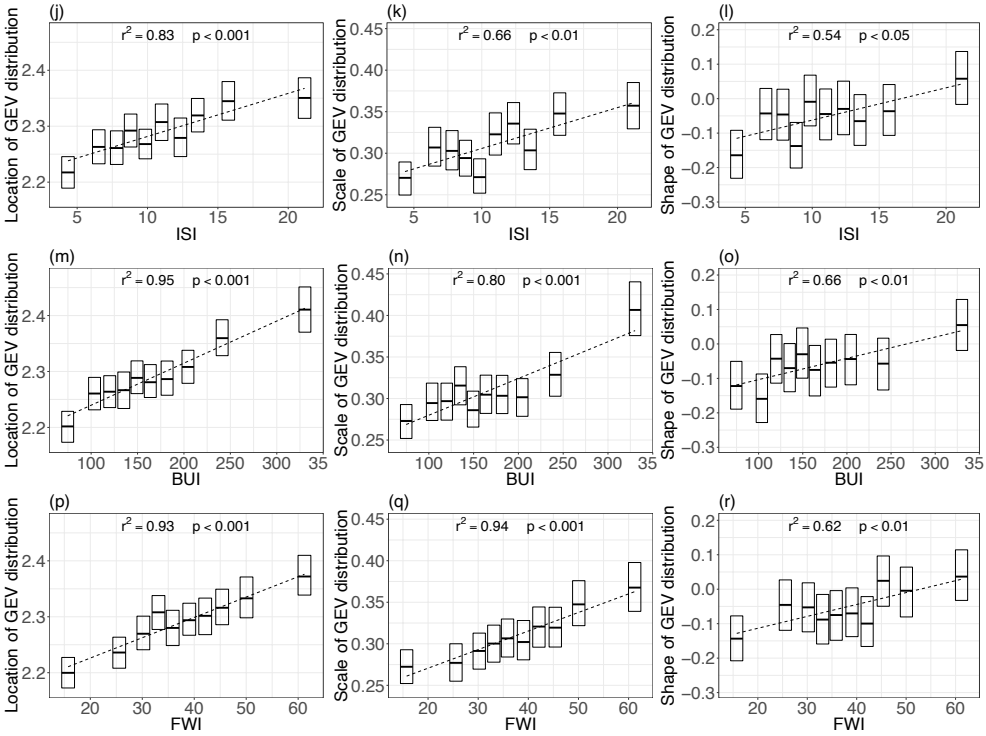


Figure 5.9. (continued)

regarded as a measure of the environmental conditions in the cell including the centroid of the burned area (Pyne et al., 1996). This is consistent with our use of PMI values to estimate the parameters of the probability distribution functions of fire characteristics applying to a cell, rather than for the construction of deterministic models linking satellite observations of LFMC to burned area and rate of advancement of flames.

For its nature, the fires dataset does not contain information on fire behaviour. However, it reports burned area and duration, while rate of spread was computed from these factors under the simplified assumption of a circular fire growing at a constant rate in every direction throughout its duration on a flat and uniform surface. Rate of spread is generally defined as "the relative activity of a fire in extending its horizontal dimensions", and the way it is expressed depends on the intended use of this information (FAO, 1986). As used in this research, rate of spread is the rate of advancement of fire perimeter, in metres per hour. This quantity does not directly relate to the local rate of advancement of flames. Indeed, the latter is affected by several factors including land cover, topography, and winds. As defined in this study, rate of spread is rather a measure of the average growth rate of a fire and, in this sense, it is considered for its contribution to the difficulty to control fires, and ultimately fire danger. In fact, fire danger models are aimed at segmenting landscape in fire danger classes and not at modelling the propagation of flames.

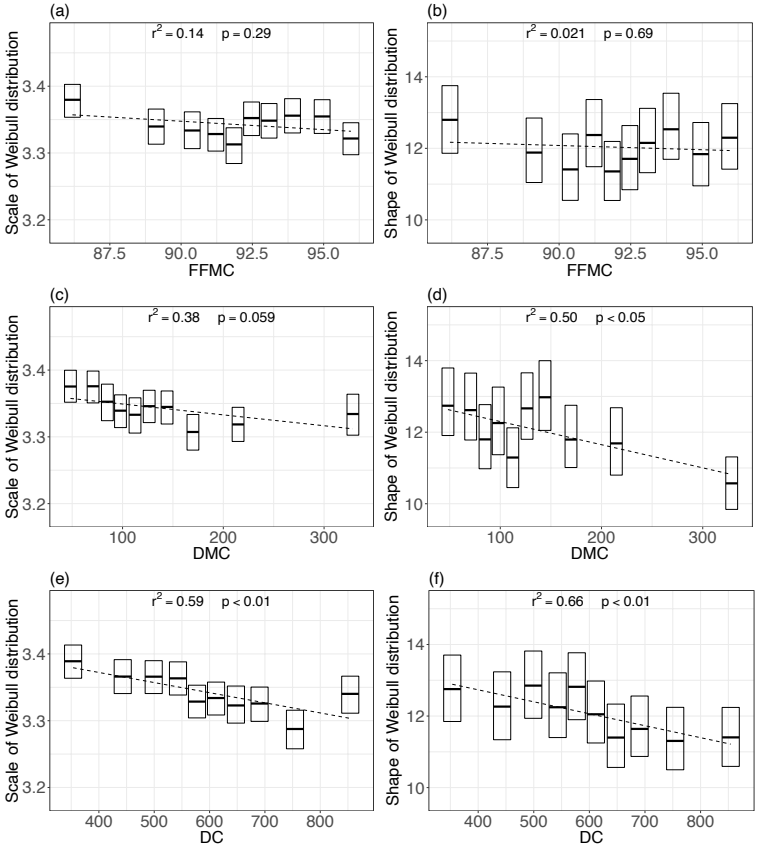


Figure 5.10. Plots of scale and shape of Weibull distribution of log-transformed rate of spread, and their 95% confidence intervals, in ten decile bins of the Fire Weather Index (FWI) System components: FFMC (a, b), DMC (c, d), DC (e, f), ISI (g, h), BUI (i, j), FWI (k, l). Regression lines refer to the estimated parameters.

Fires in the database were associated with the PMI values recorded in the pre-fire 8-day MODIS compositing period. The choice of sampling PMI from the antecedent compositing period was dictated by the need to ensure reflectance data is not contaminated by burnt scar, while simulating a typical operational scenario where this MODIS product would be used in the period building towards the availability of the following composite. The length of the compositing period and the use of the pre-fire composited granule do not pose a problem with regards to variations in LFMC. Indeed, vegetation moisture is not subject to abrupt changes over short periods of time (Leblon et al., 2001; Vicente-Serrano et al., 2013). With operational scenarios in mind, FWI maps were sampled on the day of the event, as this type of product is typically available on a daily basis and produced from weather forecasts.

Spatial patterns of PMI show clear seasonal and interannual variability, as for the example shown in Figure 5.1. Moreover, the temporal evolution of the median PMI per land cover

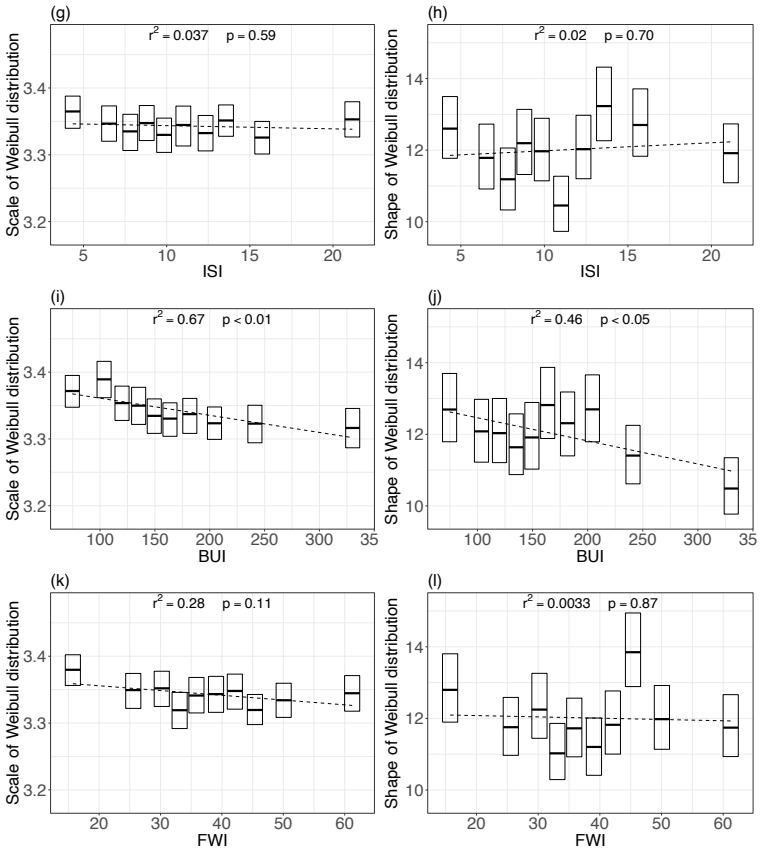


Figure 5.10. (continued)

class shows a steady decreasing trend throughout the dry season in each observation year, although at a different rate, with Figure 5.2 reporting the examples of years 2007 and 2011. This observation corresponds to a reduction of LFMC throughout the dry season, and is in line with findings on the seasonal evolution of LFMC in Mediterranean ecosystems (Nolan et al., 2018; Pellizzaro et al., 2007a, 2007b; Ruffault et al., 2018). The increase in PMI, and thus in LFMC, observed in September 2011 is likely due to abundant rainfall registered in the region (data from http://agricoltura.regione.campania.it/meteo/agrometeo.htm, last accessed 9th September 2021).

Fire events are recorded at PMI values that appear to depend on land cover classes (Figure 5.3). The highest PMI values, corresponding to higher LFMC, are observed in coniferous forests whereas the lowest values are observed in pastures. This result was expected (Barrett et al., 2016; Faivre et al., 2014) and it is due to the varying effect of species composition and structure on their flammability (Dimitrakopoulos, 2001; Dimitrakopoulos and Panov, 2001; Dimitrakopoulos and Papaioannou, 2001).

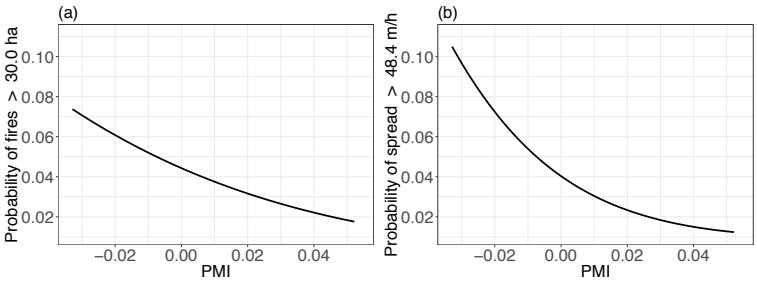


Figure 5.11. Modelled probability of extreme events, conditional to ignition, as a function of PMI: probability of fires larger than 30 ha (a); probability of rate of spread higher than 48.4 m/h (b).

This study is based on the initial identification of the probability distribution functions fitting available data on burned area, fire duration and rate of spread (Hernandez et al., 2015; Maffei et al., 2018). Several probability models fitting fire data are reported in literature (Baker, 1989; Corral et al., 2008; Cumming, 2001; Haydon et al., 2000; Moritz, 1997; Reed and McKelvey, 2002; Weber and Stocks, 1998). Indeed, fire behaviour is determined by a wide array of factors, most of which are related to the specific physical and environmental conditions of the area under investigation. This suggested the ad hoc identification of the probability distributions that best adapted to describe fire characteristics as shaped by the unique combination of landscape and environmental factors in Campania (Cui and Perera, 2008; Reed and McKelvey, 2002). It was found that log-transformed burned area is described by a normal distribution, log-transformed fire duration by a GEV distribution, and log-transformed rate of spread by a Weibull distribution.

The mean of the normal distribution of log-transformed burned area conditional to PMI shows a significant decreasing linear trend, whereas the standard deviation can safely be assumed to be constant (Figure 5.5). This would be expected, as a lower moisture content leads to a quicker propagation of flames and ultimately to a larger burned area (Rothermel, 1972). Likelihood ratio test (Table 5.4) confirms that the summed likelihood of the ten models constructed in decile bins of PMI (alternative model) allows the rejection with significance 0.05 of the null model where PMI is not a covariate of burned area. In other terms, the alternative model is a better probability model for observed burned area. Overall, these findings confirm that PMI is a covariate of burned area. Rate of spread shows similar results, with both parameters of the Weibull distribution conditional to PMI reporting decreasing trends (Figure 5.7) and the likelihood ratio test confirming rejection of the unconditional model (Table 5.4).

Scale is the only parameter of the GEV distribution of log-transformed fire duration exhibiting a significant trend across the ten decile bins of PMI, yet over a limited range of values (Figure 5.6). Indeed, confidence intervals of this parameter are consistent with a constant value across most PMI bins. In fact, the alternative (conditional) model fails to reject the null model (Table 5.4), and PMI can't be considered a covariate of fire duration.

These comments support the potential role of remote sensing measurements in contributing to fire danger mapping, as probability distributions of burned area and rate of

spread are clearly affected by PMI variability. This is the same effect that would be expected from the variability of fuel moisture content (Flannigan et al., 2016; Podschwit et al., 2018; Syphard et al., 2018). This potential was further assessed through comparison with FWI. The reanalysis data adopted in this study has a resolution of 0.25° × 0.25° (about 21×28 km^2 at the latitude of the study area), while operational services are available at a resolution of 10 km (San-Miguel-Ayanz et al., 2018). This results in a substantial lack of detail, as opposed to MODIS reflectance data available at 500 m resolution. However, resolution of this FWI data is still capable of capturing broad weather differences typically occurring in the study area, especially across its geomorphologic and climatic East-West gradient (Amato and Valletta, 2017; Fratianni and Acquaotta, 2017).

The mean of the normal distribution of log-transformed burned area conditional to the six FWI System components increases with all of them, while standard deviation can be assumed constant, as justified by most confidence intervals for all indices (Figure 5.8). All FWI System components were designed on individual scales, but with the clear meaning of higher values corresponding to higher danger. This finding implies that at increasing danger values the mean burned area of occurred fires was higher. The closer fit with fire behaviour indices can be explained by the fact that ISI, BUI and ultimately FWI combine information from drought indices and weather inputs, and thus tend to be better indicators of several aspects of forest fires (Van Wagner, 1987).

A similar observation can be drawn for log-transformed fire duration (Figure 5.9), where the variability of the parameters of the GEV distribution conditional to FWI System components justify increasing probability of longer fire duration with increasing danger, and where BUI and FWI show the closest fits. This is reflected in the corresponding likelihood ratio tests, with all conditional distributions (alternative models) rejecting the

Table 5.4. Results of the likelihood ratio test. Null model is the one fitting all data. Alternative model is the collection of ten models in decile bins of the candidate covariate. Significance level is 0.05. In bold the alternative models showing the highest likelihood for each fire characteristic.

	Burned area	*Duration*	*Rate of spread*
PMI	**Rejection**	Non-rejection	**Rejection**
FFMC	Rejection	Rejection	Non-rejection
DMC	Rejection	**Rejection**	Non-rejection
DC	Rejection	Rejection	Non-rejection
ISI	Rejection	Rejection	Rejection
BUI	Rejection	Rejection	Rejection
FWI	Rejection	Rejection	Rejection

null model, and the FWI System components showing to be a covariate of fire duration where PMI is not (Table 5.4).

The relationship between FWI System components and the parameters of the Weibull distribution of log-transformed rate of spread shows some ambiguities, with no trends against FFMC, ISI and FWI, and slightly decreasing trends against DMC, DC, and BUI (Figure 5.10). The latter result is counterintuitive, as is corresponds to a substantial decrease in rate of spread with increasing fire danger. Moreover, it contrasts with findings against PMI, where rate of spread increases with decreasing PMI (Figure 5.5). In fact, BUI is an indicator of fire behaviour and its value, along with its contributing factors DMC and DC, slowly increases throughout the dry season. This means that other seasonal dependent factors relevant to rate of spread, such as winds, might be having a predominant effect with BUI and the two moisture codes here acting as a proxy for them (Van Wagner, 1987).

The likelihood ratio tests on the probability models of rate of spread show that the alternative models conditional to FFMC, DMC and DC fail to reject the null model, as opposed to those conditional to ISI, BUI and FWI (Table 5.4). The most problematic are the alternative models conditional to ISI and FWI, which allow the rejection of the corresponding null models although conditional model parameters do not exhibit any significant trend. The result of the likelihood ratio test may be explained by an overfitting caused by the wide variability observed in the values of the conditional shape across the bins (Figure 5.10 h and l). Indeed, rejection of the null model does not directly imply that the alternative model is to be preferred. On the other side, the alternative model conditional to DC fails to reject null model, despite the significant trends observed in both shape and scale (Figure 5.10 e and f). In this case, it can be observed that a constant value fits most of the confidence intervals in both parameters. The latter comment also applies to BUI (Figure 5.10 i and j), although the corresponding alternative model allows for the rejection of the null model. Overall, these notes contrast with the net trend of parameters conditional to PMI and with their narrower confidence intervals (Figure 5.7). In fact, the alternative model conditional to PMI shows a likelihood higher than any FWI component (Table 5.4).

These results allow the computation of actionable information (Preisler et al., 2004) in the form of probability of extreme events conditional to ignition as a function of PMI (Figure 5.11). Clearly, forest fires in the study area are relatively small as compared to other areas worldwide. Yet defining as extreme events those that are above the 95^{th} percentile in terms of burned area or rate of spread is appropriate in this specific context, as it refers to the most demanding events the local authorities are faced with in terms of deployed resources for their containment in a highly anthropized and fragmented landscape. Bearing in mind that several other factors contribute to fire behaviour, and thus to the probability distribution functions of burned area and rate of spread, it is here observed an increasing probability of extreme events conditional to ignition with a reduction in PMI, and thus in LFMC. This is in line with expectations, and indirectly confirms the role of LFMC in driving fire behaviour (Nolan et al., 2016a; Pimont et al., 2019; Ruffault et al., 2018). When compared against the observed evolution of median PMI across the fire season (Figure 5.2),

the probability of extreme events at the end of the fire season is about the double than at the beginning.

5.5. Conclusions

This study demonstrated that satellite observations of LFMC by means of the PMI contribute to the prediction of the probability distributions of forest fires burned area and rate of spread, and that probability distribution functions conditional to PMI describe observations with a higher likelihood than the unconditional models. In other terms, it was demonstrated that PMI is a covariate of both burned area and rate of spread. Remote sensing measurements in the solar spectrum are thus a viable mean to complement existing fire danger mapping tools, contributing to the prediction of the probability of extreme events conditional to ignition.

Analyses described herein were performed on MODIS data. However, any sensor collecting measurements in the near infrared and shortwave infrared can be used to compute the PMI. Adding to MODIS, daily global observations are available from the two pairs of VIIRS and SLSTR sensors. This enables the daily availability of PMI maps at a resolution that is one order of magnitude higher than existing operational fire danger services based on meteorological data (Burgan, 1988; San-Miguel-Ayanz et al., 2012). Similar bands are also available in higher resolution sensors such as OLI on board Landsat 8 and MSI on Sentinel-2A and -2B, with resolutions of 30 and 10-20 m respectively. The development of an harmonised Landsat and Sentinel-2 reflectance product (Claverie et al., 2018) is indeed supporting the synergistic use of these platforms, towards a global mapping of vegetation properties contributing to fire danger at a spatial resolution that is three orders of magnitude higher than operational services, although with longer revisit times as compared to coarser resolution optical sensors.

The study was conducted on a specific study area, for which ad hoc probability distribution functions fitting fire data were identified. The need to determine site-specific statistical models is acknowledged in the scientific literature (Cui and Perera, 2008; Reed and McKelvey, 2002), suggesting that the applicability of a single global statistical model is unlikely. Nevertheless, the method developed in our study can be implemented elsewhere, as long as similar fire data is available to identify the local probability distribution functions. This is the case of several regional or national fire inventories that are either publicly available on the web, e.g. the Prométhée database in Mediterranean France, the Instituto da Conservação da Natureza e das Florestas (ICNF) fire inventory in Portugal, and the United States Geological Survey (USGS) fire occurrence data in the USA, or are provided upon request by relevant authorities, e.g. the Forest Fire Protection Information Unit of Carabinieri in Italy and the National Statistical Service in Greece. Such data, along satellite retrievals of PMI, would then serve as a basis for the construction of the local probability distribution functions of burned area and rate of spread conditional to PMI. This in turn would allow the mapping of the probability of events exceeding any given threshold, as deemed relevant by fire managers. From an application point of view, fire management and preparedness activities are conducted at regional scales, suggesting that the

implementation of regional models for the integration of satellite retrievals in fire danger mapping systems is a viable option.

6. Combining multi-spectral and thermal remote sensing to predict forest fire characteristics[6]

Abstract

Forest fires preparedness strategies require the assessment of spatial and temporal variability of fire danger. While several tools have been developed to predict fire occurrence and behaviour from weather data, it is acknowledged that fire danger models may benefit from direct assessment of live fuel condition, as allowed by Earth Observation technologies. In this study, the performance of pre-fire observations of land surface temperature (LST) anomaly and of the Perpendicular Moisture Index (PMI) in predicting fire characteristics was evaluated against the Fire Weather Index (FWI) System, a fire danger model adopted in several areas worldwide. To this purpose, a database of forest fires recorded in Campania (13,595 km^2), Italy, was combined with MODIS retrievals of LST anomaly and PMI, and with FWI maps from NASA's Global Fire Weather Database. Fires were grouped in decile bins of LST anomaly, PMI and FWI System components, and probability distribution functions of burned area, fire duration and rate of spread were fitted in each bin. The dependence of probability model parameters on LST anomaly, PMI and FWI System components was assessed by means of trend analysis (coefficient of determination and p-value of the linear fit, Sen's slope and Mann-Kendall test) and likelihood ratio test versus the corresponding unconditional probability model. Finally, the probability of an extreme event, conditional to ignition, was modelled as a function of LST anomaly and PMI. Results show that the probability distribution function of burned area has a strong dependence on both LST anomaly and PMI, that the probability distribution function of fire duration has a strong dependence on LST anomaly but not on PMI, and that the probability distribution function of rate of spread has a weak dependence on LST anomaly and a strong dependence on PMI. These results are in line with expectations from models of the combustion and flames propagation processes. Trend analyses and likelihood ratio tests showed that the FWI System components are good predictors of burned area and fire duration, but not of rate of spread. They also confirmed that, where LST anomaly and PMI are covariates of the

[6] Based on: Maffei, C., Lindenbergh, R., Menenti, M., 2021. Combining multi-spectral and thermal remote sensing to predict forest fire characteristics. ISPRS J. Photogramm. Remote Sens. 181, 400-412. https://doi.org/10.1016/j.isprsjprs.2021.09.016

considered fire characteristic, their performance is similar or better than the FWI System components. Finally, the probability of an extreme event in terms of burned area as a joint function of LST anomaly and PMI shows a wider dynamic range than the same probability modelled as a function of these remote sensing variables individually.

6.1. Introduction

Governments, local authorities, forestry corps and civil protection agencies are faced with the need to manage forest fires and to implement preparedness strategies aimed at safeguarding the security of citizens and at preserving the services of the biomes being affected (Carlson and Burgan, 2003; Fernández-Guisuraga et al., 2021; Mohamed Shaluf, 2008; Oliveira et al., 2017). Preparedness encompasses all initiatives aimed at developing operational response in case of a fire (Gunes and Kovel, 2000; Minas et al., 2012; Mohamed Shaluf, 2008). It requires the assessment of spatial and temporal variability of fire risk, e.g. through maps of fuel type and amount, fire hazard and danger, vulnerability and value of natural resources and of anthropic assets (Mhawej et al., 2015; Miller and Ager, 2013; Oliveira et al., 2017; Thompson et al., 2015).

Several fire danger rating systems have been developed worldwide to support decision making (Allgöwer et al., 2003; Sirca et al., 2018). These are typically based on the evaluation of biophysical and environmental variables that control fire occurrence and behaviour, and on the provision of one or more time-dependent indices in the form of maps. Among them are the McArthur Forest Fire Danger Index (McArthur, 1967; Noble et al., 1980), the National Fire Danger Rating System of the US (Deeming et al., 1977) and the Fire Weather Index (FWI) System (Van Wagner, 1987). The latter has been effectively used to map fire danger in several areas worldwide, including Europe (de Groot and Flannigan, 2014; San-Miguel-Ayanz et al., 2012).

A common trait of fire danger indices is their dependence on meteorological input (Chuvieco, 2003). This is based on the fact that fire occurrence and behaviour are both controlled by live and dead fuel moisture content, which in turn are determined by the interaction of vegetation, litter and dead woody material in the topsoil with weather and topography (Andrews, 2007; Finney, 1998; Rothermel, 1991, 1972; Van Wagner, 1987; Yebra et al., 2013). Indeed, fire danger rating systems model fuel moisture content from meteorological measurements and then use computed values to produce one or more indices that serve as predictors of fire occurrence and behaviour. However, the use of modelled rather than measured fuel moisture content results in a certain degree of approximation due to the simplifying assumptions this implies, especially with respect to live fuels (Ruffault et al., 2018; Schunk et al., 2017). In fact, the link between live fuel moisture content (LFMC) and weather forcing is dependent on structural and physiological characteristics of plants which are species specific (Jolly and Johnson, 2018; Pellizzaro et al., 2007b). Nevertheless, LFMC is essential in predicting fire behaviour (Jolly, 2007; Rossa and Fernandes, 2017). From a source data perspective, most fire danger rating services are based either on values from point weather measurements, e.g. automated weather stations, and as such computed indices are only valid in a limited area around the point of

data collection (Chowdhury and Hassan, 2015a; Schlobohm and Brain, 2002; Walding et al., 2018), or from coarse resolution weather forecasts from meteorological services, leading to produced maps being at a scale that might not be suitable for fire management purposes at local level (Martell, 2007; North et al., 2015; San-Miguel-Ayanz et al., 2012).

Direct observation of LFMC has the potential to enable a better evaluation of fire occurrence and fire behaviour danger indices (Jolly, 2007; Rossa and Fernandes, 2017; Ruffault et al., 2018; Ustin et al., 2009). This outlines a clear opportunity for Earth Observation technologies, as they provide repeated and frequent observations of land surface conditions (Allgöwer et al., 2003; Ma et al., 2019; Yebra et al., 2013). Most approaches for the use of remote sensing data in fire danger mapping focussed on relating land surface temperature (LST), spectral indices of vegetation moisture content, radar backscatter or indirect measures of plant stress to danger indices and fire occurrence. Time series of the Normalised Difference Water Index (Gao, 1996) were found to be related to the seasonality of fire occurrence (Huesca et al., 2014, 2009). The Normalised Difference Water Index was also used in conjunction with satellite estimates of LST to predict fire danger (Abdollahi et al., 2018). The Global Vegetation Moisture Index (Ceccato et al., 2002a) was used in combination with LST and a few landscape factors to predict fire occurrence (Pan et al., 2016). Radar backscatter was related to vegetation moisture and fire danger (Abbott et al., 2007; Hunt et al., 2011; Leblon et al., 2002), although it is acknowledged that it is also affected by many other surface properties (Leblon et al., 2016).

Several studies have shown that time series of optical vegetation spectral indices and of LST, as proxies of plant water stress, are related to fire occurrence (Bajocco et al., 2015; Burgan et al., 1998; Chowdhury and Hassan, 2015b; Chuvieco et al., 2004; Maselli et al., 2003; Slingsby et al., 2020; Yu et al., 2017). LST was also used to model energy budgets (Leblon, 2005; Nolan et al., 2016b; Vidal et al., 1994) and to estimate heat energy of pre-ignition (Dasgupta et al., 2006) and predict fire occurrence. Fire occurrence was also related to LST anomaly (Manzo-Delgado et al., 2004; Matin et al., 2017; Pan et al., 2016), although there is no shared definition of this parameter.

Cited approaches for forest fire danger mapping from remote sensing measurements essentially focus on fire occurrence. However, fire danger models are meant not only to predict fire occurrence, but also to provide a measure of expected fire behaviour characteristics. In this sense, any attempt to respond to the identified need to improve fire danger models (Ruffault et al., 2018) would need an understanding of remote sensing potential in predicting fire characteristics either deterministically (Dasgupta et al., 2007) or probabilistically (Flannigan et al., 2016). The latter would be more suited to fulfil the need of fire managers, as their interest is in the prediction of the probability of extreme events (Finney, 2005; Flannigan et al., 2016; Mazzetti et al., 2009; Podschwit et al., 2018; Syphard et al., 2018).

Supporting this approach, recent studies found that the probability distribution functions of burned area and fire duration are related to pre-fire satellite observations of LST anomaly (Maffei et al., 2018), and that probability distribution functions of burned area and rate of spread are related to pre-fire satellite observations of the Perpendicular Moisture Index (PMI) (Maffei and Menenti, 2019, 2014). These initial results potentially enable the

prediction of the probability of an extreme event, conditional to ignition, as a function of remote sensing measurements. However, it was not documented whether LST anomaly is related to the probability distribution function of rate of spread, how LST anomaly and PMI compare to each other and against traditional fire danger tools such as the FWI System in predicting forest fire characteristics, whether LST anomaly and PMI can be considered independent and how they can be jointly used to improve the pre-fire prediction of the probability of extreme events. To consolidate initial results, further research was needed to:

- Understand how LST anomaly and PMI compare in predicting burned area, fire duration and rate of spread of fire events and assess whether they are independent.
- Quantitatively assess their performance against predictions arising from the FWI System.
- Establish an approach for their joint use in the prediction of the probability of extreme events.

To achieve these objectives, LST anomaly was compared against PMI trying to explain the biophysical nature of the predictive differences between these two remote sensing quantities. Their performance as predictors of burned area, fire duration and rate of spread was evaluated against the components of the FWI System by means of trend analysis and likelihood ratio tests. Finally, it was developed a model jointly using LST anomaly and PMI to predict those fire characteristics for which both are proved to be a strong covariate.

6.2. Materials and methods

6.2.1. Study area

A detailed description of the study area was provided in §2.2.1.

6.2.2. Data

MODIS land surface temperature and reflectance data

Remote sensing datasets used in this research were the Aqua-MODIS Level 3 collection 6 land surface temperature (MYD11A1) and surface reflectance (MYD09A1) products. Level 3 products are standardised science-ready geophysical variables mapped on a fixed global grid (Masuoka et al., 1998).

MYD11A1 contains daily gridded diurnal and nocturnal LST estimates at a conventional resolution of 1 km, along with quality assurance (QA) metadata. A complete time series of MYD11A1 granules covering years 2003 till 2017 was used in this research, only retaining pixel data marked as good quality (Maffei et al., 2018; Van Nguyen et al., 2015; Xu and Shen, 2013).

MYD09A1 is a product containing 8-day composited reflectance at 500m resolution (Vermote et al., 1997). Tiles between June to September of years 2003-2011 were retrieved

and, likewise LST, masked against QA to ensure only good quality reflectance estimates are retained (Maffei and Menenti, 2019; Vermote et al., 2015).

Fire event data

For this study, a database of fires recorded in Campania between 2003 and 2011[7] was provided by the Forest Fire Protection Information Unit of Carabinieri (Italian national gendarmerie). This law enforcement agency is in charge, among other responsibilities, of burned area inventorying. Available data is thus to be considered official. For each event it reports the coordinates of the centroid of burned area, fire start and end date and time, and final burned area. A distinct fire season can be noted in summer, as 82% of fires and 89% of burned area are recorded between June and September.

A subset of 4949 events was extracted from the database, consisting of all fires occurred in natural areas only from June to September 2003-2011. Burned area and fire duration were the only fire characteristic explicitly reported in the database. These allowed the calculation of rate of spread, hereby defined as the constant radial growth rate of an equivalent circular fire resulting in the given burned area and duration.

Fire Weather Index

The FWI System is based on the processing of daily readings of temperature, relative humidity, wind speed, and precipitation for the production of six fire danger indicators (Van Wagner, 1987). The Fine Fuel Moisture Code (FFMC), the Duff Moisture Code (DMC) and the Drought Code (DC) model the moisture content of dead forest fuels. The Initial Spread Index (ISI) is calculated from FFMC and wind speed. ISI is generally related to burned area. The Build-Up Index (BUI) is computed from DMC and DC to represent fuel consumption. The FWI is a comprehensive indicator calculated by combining ISI and BUI to synthesise all the fire danger indicators of the FWI System. FWI is related to the energy output rate of a fire. Further details on the FWI System were provided in §1.4.3.Daily layers of the FWI System components used in this study are those from NASA's Global Fire Weather Database (Field et al., 2015; Molod et al., 2015), available at a resolution of 0.25° × 0.25°.

6.2.3. Retrieval of land surface temperature anomaly

In this study, LST anomaly was evaluated against a reference climatology constructed from the time series of daily diurnal Aqua-MODIS LST (Alfieri et al., 2013) through the harmonic analysis of time series (HANTS) algorithm (Menenti et al., 2016, 1993). Through the modelling of LST periodic behaviour, HANTS is robust with respect to missing observations and allows the removal of outliers in time series due to cloud cover or active fires. In a similar way, HANTS was applied to individual yearly series of daily LST data 2003-2011 to

[7] This is a subset of the fire data used in Chapter 2 to characterise the fire regime in the study area.

model annual variability (Xu and Shen, 2013). Daily LST anomaly was then evaluated as the LST value in the annual models minus the value in the climatology (Maffei et al., 2018).

6.2.4. The Perpendicular Moisture Index (PMI)

LFMC is the percentage mass of water in leaf tissues over dry leaf mass. This key variable in fire danger assessment directly controls flames propagation (Andrews, 2007; Carlson and Burgan, 2003; Chuvieco et al., 2009; Finney, 1998; Hunt et al., 2013; Rothermel, 1991, 1972; Van Wagner, 1977; Yebra et al., 2013). The remote sensing proxy for LFMC used in this study is the Perpendicular Moisture Index (PMI) (Maffei and Menenti, 2014), a spectral index specifically designed to maximise its sensitivity to LFMC variability. Details on how the PMI was constructed were provided in Chapter 4.Note that higher values of PMI correspond to higher LFMC. PMI maps of the study area were produced from the retrieved Aqua-MODIS 8-day composited surface reflectance.

6.2.5. Conditional distributions of fire characteristics

The dispersion of burned area, fire duration and rate of spread is extremely skewed. Prior to analyses, these variables were scaled and log-transformed, so to have positive values only. This study is essentially based on the evaluation of the parameters of the probability distribution functions of fire characteristics. From the given dataset it was found that log-transformed burned area, fire duration and rate of spread follow normal, generalised extreme value (GEV) and Weibull distributions respectively (Maffei and Menenti, 2019).

Prior to further analyses, fires in the dataset were intersected with maps of LST anomaly, PMI and FWI System components in a GIS environment, so that each event was associated with the corresponding LST anomaly value recorded in the day previous to the event, the PMI value recorded in the previous 8-day compositing period, and the values of the FWI System components recorded on the day of the event (Maffei et al., 2018; Maffei and Menenti, 2019). Observations of PMI, LST anomaly and FWI System components associated with fires were grouped in their respective ten decile bins. The parameters of the normal distribution of log-transformed burned area, of the GEV distribution of log-transformed fire duration and of the Weibull distribution of log-transformed rate of spread were assessed in each bin through the minimisation of the Anderson-Darling statistic (Anderson and Darling, 1954). The corresponding 95% confidence intervals were then evaluated by means of 1000 bootstrap estimations.

Trends in the values of the parameters of the probability distributions with respect to LST anomaly, PMI and the FWI System components were assessed and compared by means of linear regressions (coefficient of determination and p-value), Sen's slope magnitude (Sen, 1968) and Mann-Kendall test (Kendall, 1975; Mann, 1945). A likelihood ratio test was adopted to evaluate the probability distribution functions conditional to LST anomaly, PMI and the FWI System components (alternative models) against the corresponding unconditional models fitting all data (null models). Significance was set at 0.05 for linear regressions, the Mann-Kendall test, and the likelihood ratio test.

6.2.6. Probability of extreme events conditional to ignition

An extreme event is hereby defined as a fire whose fire characteristic is larger than the 95th percentile of the values recoded in the database. The evaluation of the probability of extreme events conditional to ignition as a function of LST anomaly (alternatively PMI) builds on the conditional probability distribution functions identified in the previous section. The dependence of distribution parameters on LST anomaly (alternatively PMI) were modelled by means of linear regressions.

A similar approach was adopted to model the probability of extreme events as a function of both LST anomaly and PMI. The bidimensional space spanned by LST anomaly and PMI was partitioned into 100 bins determined by the previously defined decile intervals. The parameters of the probability distribution functions were evaluated in each bidimensional bin through the minimisation of the Anderson-Darling statistic. Their dependence on LST anomaly and PMI was then modelled by means of a multiple linear regression. The performance of the derived linear models was then assessed by using the leave-one-out cross-validation (LOOCV).

6.3. Results

6.3.1. Comparing LST anomaly and PMI performance in predicting fire characteristics

The scatterplot of LST anomaly and PMI values associated with fire events shows that these two remote sensing observations are substantially unrelated (Figure 6.1). This is reflected in the dispersion of burned area, fire duration and rate of spread in decile bins of LST anomaly and PMI (Figure 6.2). Burned area appears to be dispersed towards higher values with increasing LST anomaly and with decreasing PMI (lower LFMC). Dispersion of fire duration is towards higher values with increasing LST anomaly, whereas no trend is observed against PMI. Conversely, rate of spread appears to be dispersed towards lower values with increasing PMI (higher LFMC), while only a weak decreasing trend can be noted against LST anomaly.

The analysis of the probability distribution functions of burned area, fire duration and rate of spread in decile bins of LST anomaly and PMI (conditional distributions) further demonstrated that these two satellite observables are differently related to fire characteristics. The mean of the normal distribution of log-transformed burned area varies with both LST anomaly (r^2=0.81, $p<0.001$) and PMI (r^2=0.80, $p<0.001$), showing comparable Sen's slope magnitude (Figure 6.3, Table 6.1). Standard deviation follows a significant trend only against LST anomaly (r^2=0.52, $p<0.05$), whereas a constant value fits most confidence intervals of this parameter in decile bins of PMI. The latter is confirmed by trend analysis, as Mann-Kendall test fails to reject the null hypothesis.

Location, scale, and shape of the GEV distribution of log-transformed fire duration conditional to LST anomaly follow strong and significant increasing trends (r^2=0.78, 0.79 and 0.87 respectively, $p<0.001$) with increasing LST anomaly (Figure 6.4, Table 6.2). The parameter of the GEV distribution of log-transformed fire duration conditional to PMI

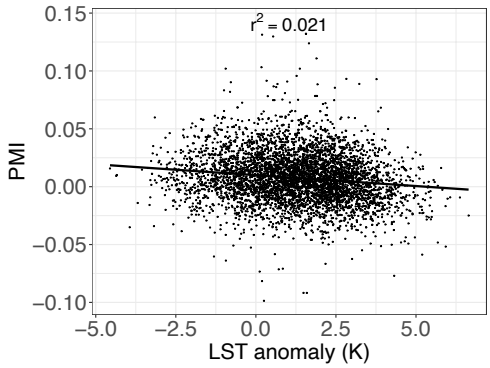


Figure 6.1. Scatterplot of PMI vs LST anomaly values associated with fire events.

showing a trend is scale (r^2=0.55, p<0.05). However, a constant value of scale would fit most confidence intervals, and indeed Mann-Kendall test fails to reject the null hypothesis for all three GEV parameters conditional to PMI, confirming the absence of a trend with significance 0.05.

Distribution of log-transformed rate of spread conditional to LST anomaly and PMI shows the opposite behaviour as compared to fire duration (Figure 6.5, Table 6.3). The scale and shape parameters of the Weibull distribution conditional to LST anomaly only show a weak decreasing trend (r^2=0.54 and 0.50 respectively), albeit significant (p<0.05). Sen's slope magnitude is low, yet the Mann-Kendall test allows the rejection of the null hypothesis, and the existence of a trend can be accepted with significance 0.05. Conversely, the scale and shape conditional to PMI show strong and significant decreasing trends (r^2=0.97 and 0.82 respectively, p<0.001) with increasing PMI (corresponding to increasing LFMC) and high Sen's slope magnitude.

The probability distribution functions of the three log-transformed fire characteristics conditional to LST anomaly and PMI allow the rejection of the null (unconditional) model in the likelihood ratio test (Table 6.4), confirming that LST anomaly is a covariate of all three fire characteristics. Similarly, probability models of log-transformed burned area and log-transformed rate of spread conditional to PMI allow the rejection of the unconditional model, whereas the corresponding conditional model of log-transformed fire duration does not. Comparing these findings against trends outlined in Figure 6.4 and in Table 6.2 leads to the conclusion that PMI is a covariate of burned area and rate of spread, but not of fire duration.

6.3.2. Assessing the performance of LST anomaly and PMI against the FWI System components

Trend analysis of the parameters of the probability distribution of log-transformed burned area, fire duration and rate of spread in decile bins of the FWI System components allows a comparison of the performance of pre-fire remote sensing retrievals of vegetation condition in predicting fire danger against a consolidated fire danger mapping tool based

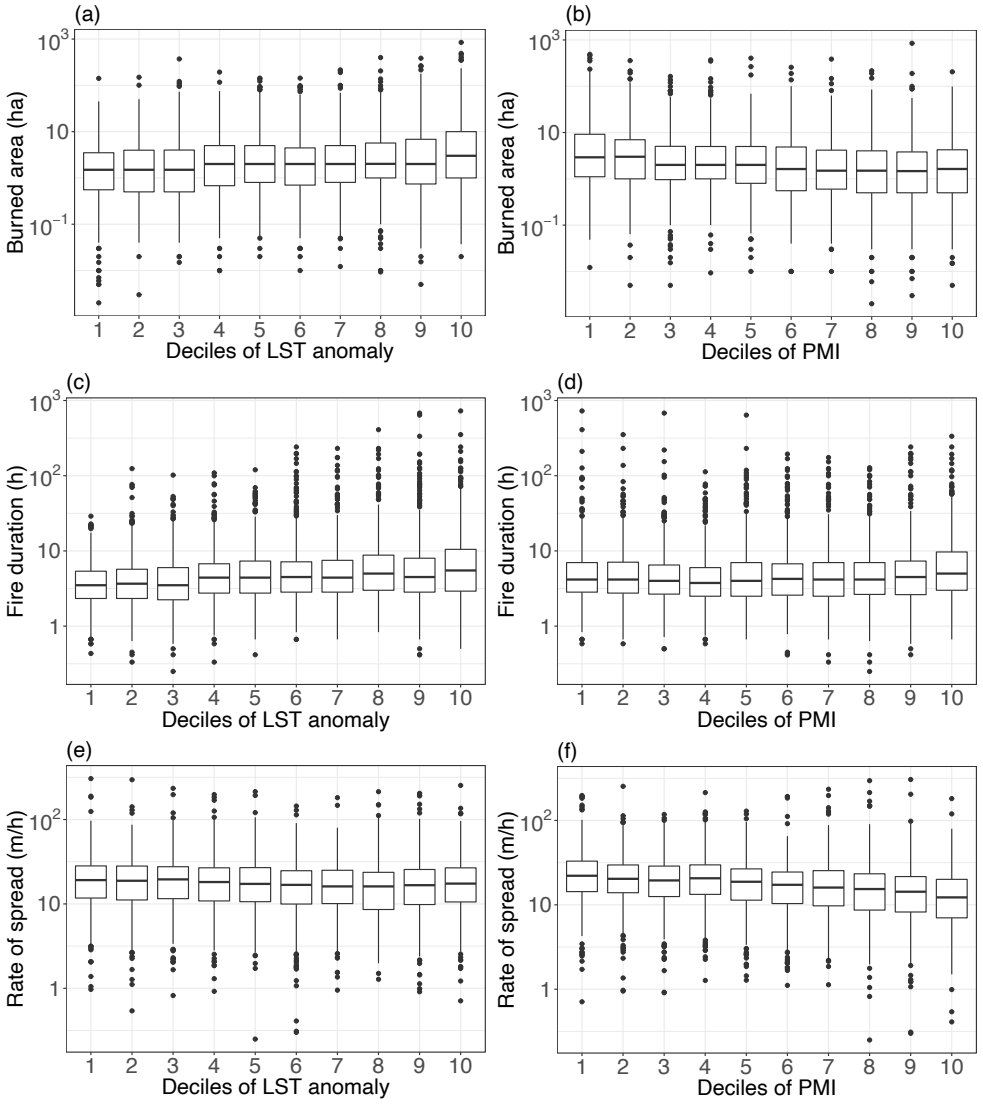


Figure 6.2. Boxplots of burned area, fire duration and rate of spread in decile bins of LST anomaly and PMI.

on meteorological data. The mean of the normal distribution of log-transformed burned area shows strong and significant ($p<0.001$) trends against all FWI System components, with Sen's slope magnitude values mostly comparable with those achieved by LST anomaly and PMI (Table 6.1). Conditional standard deviation is characterised by significant trends against FFMC, DMC and BUI, but only DMC's Mann-Kendall test allows the rejection of the null hypothesis, i.e. confirms that the alternative hypothesis of the existence of a trend can be accepted. These results are reflected in the likelihood ratio test (Table 6.4), as all alternative

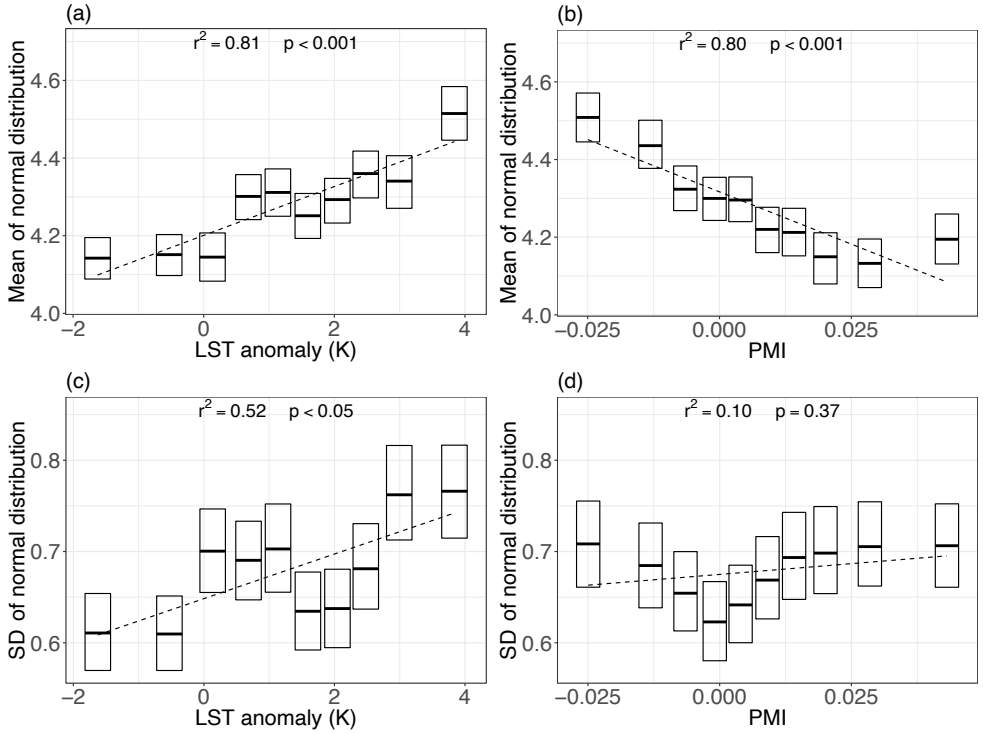


Figure 6.3. Mean and standard deviation of normal distribution of log-transformed burned area in decile bins of LST anomaly and PMI.

models conditional to FWI System components allow the rejection of the unconditional model.

Similar results were found with the parameters of the GEV distribution of log-transformed fire duration (Table 6.2). Location, scale, and shape show significant trends against all FWI System components with strength and Sen's slope magnitude substantially comparable with those against LST anomaly. Further, all conditional models allow the rejection of the unconditional model (Table 6.4).

The FWI System components do not appear to be good covariates of rate of spread. Scale of the Weibull distribution of log-transformed rate of spread shows significant ($p<0.01$) trends only against DC and BUI, although with lower strength and Sen's slope magnitude than PMI (Table 6.3). Shape shows significant ($p<0.05$) trends against DMC, DC, and BUI, but only DC's Mann-Kendall test rejects the null hypothesis of the absence of a trend. For both parameters, this contrasts with the strength and Sen's slope of the trends against PMI. While DC might still be considered a covariate of rate of spread, the corresponding conditional probability model does not allow the rejection of the unconditional model (Table 6.4).

6.3.3. Predicting the probability of extreme events conditional to ignition

As both LST anomaly and PMI are strong covariates of burned area and are not correlated, it was interesting to compare how the probability of extreme events conditional to ignition varies as a function of LST anomaly and PMI, both individually and jointly. The mean and the standard deviation of the normal distribution of log-transformed burned area were modelled as linear functions of LST anomaly according to regression lines identified in Figure 6.3. Similarly, the mean of the normal distribution of log-transformed burned area was modelled as a linear function of PMI, while standard deviation was kept constant. According to the available fire data, the 95th percentile of burned area is 30.0 ha. Plots of the probability of fires larger than 30.0 ha show a marked increase with increasing LST anomaly and decreasing PMI (Figure 6.6).

A similar approach was used to evaluate the probability of large fires as a joint function of LST anomaly and PMI. The derived linear model fitting the mean of the normal distribution of log-transformed burned area in the 100 bins determined by the decile intervals of LST anomaly and PMI has r^2=0.49 ($p<0.001$), whereas the corresponding linear model of the standard deviation has r^2=0.28 ($p<0.001$). The leave-one-out cross-validation coefficient of determination is 0.45 and 0.23 for the mean and the standard deviation respectively, showing relative robustness of their linear models as a function of LST anomaly and PMI.

Using as a reference the 2.5% - 97.5% percentile range of recorded LST anomaly and PMI values, probability of large fires conditional to ignition increased from 0.9% to 9.2% with LST anomaly ranging from -2.1 to 4.3 K and increases from 1.8% to 7.4% with PMI decreasing from 0.052 to -0.032. When the probability of fires exceeding 30.0 ha is modelled as a

Table 6.1. Trend analysis of the parameters of the normal distribution of log-transformed burned area across decile bins of LST anomaly, PMI and of the FWI System components, reporting coefficient of determination and p-value of the linear fit, Sen's slope, and Mann-Kendall test's result. Significance level of Mann-Kendall test is 0.05.

	Mean				*Standard deviation*			
	r^2	*p*	*Sen's slope*	*M-K test*	r^2	*p*	*Sen's slope*	*M-K test*
LST anomaly	0.81	***	0.033	Rejects	0.52	*	0.0124	Rejects
PMI	0.80	***	-0.038	Rejects	0.10	ns	0.0048	Fails
FFMC	0.82	***	0.036	Rejects	0.43	*	0.0050	Fails
DMC	0.89	***	0.028	Rejects	0.78	***	0.0093	Rejects
DC	0.81	***	0.017	Rejects	0.21	ns	0.0095	Fails
ISI	0.92	***	0.036	Rejects	0.21	ns	0.0043	Fails
BUI	0.91	***	0.025	Rejects	0.72	**	0.0075	Fails
FWI	0.96	***	0.034	Rejects	0.31	ns	0.0081	Fails

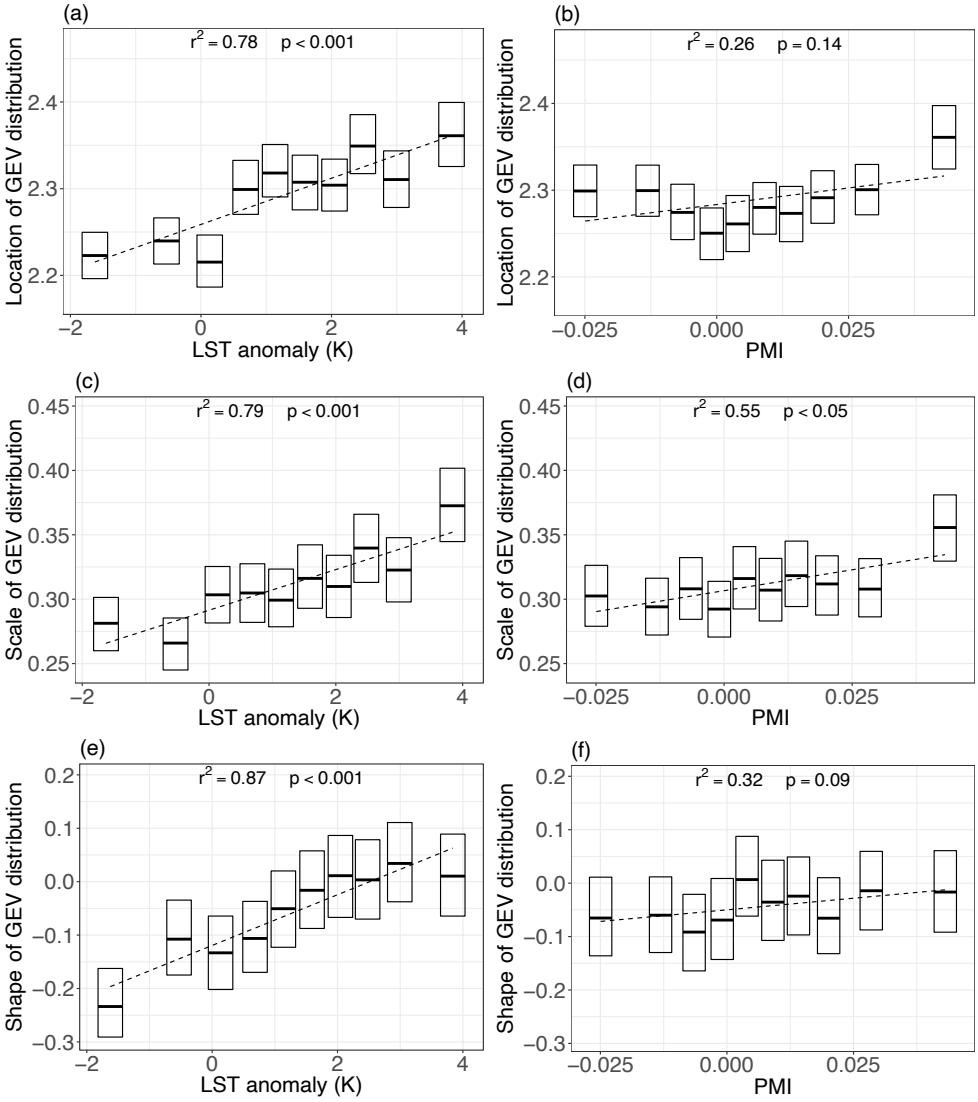


Figure 6.4. Location, scale, and shape of the GEV distribution of log-transformed fire duration in decile bins of LST anomaly and PMI.

function of both LST anomaly and PMI, modelled probabilities cover the wider range from 0.5% to 12.7% (Figure 6.7).

6.4. Discussion

This study stemmed from previous investigations on multi-spectral and thermal remote sensing of forest conditions for the prediction of some fire characteristics (Maffei et al., 2018; Maffei and Menenti, 2019). Its main objective was to compare LST anomaly and PMI capability to predict burned area, fire duration and rate of spread of actual fires such as those provided by the Forest Fire Protection Information Unit of Carabinieri, assess their performance against the FWI System components, evaluate and understand the independence of these two remote sensing observations of live fuel condition and establish an approach for their joint use in the prediction of extreme events. The PMI was designed to be a measure of LFMC (Maffei and Menenti, 2014), and as such it is related to the condition of green vegetation. LST anomaly was initially conceived as a measure of vegetation response to water stress (Alfieri et al., 2013; Maffei et al., 2018), and for this reason it was interpreted with reference to a physiological condition (Buitrago Acevedo et al., 2017; Chowdhury and Hassan, 2015a; Dasgupta et al., 2006; Leblon, 2005; Manzo-Delgado et al., 2004; Matin et al., 2017; Nolan et al., 2016b; Pan et al., 2016; Sobrino et al., 2016; Vidal et al., 1994). Indeed, when water stress attains certain levels it triggers plants transpiration regulation mechanism, and this results in a detectable increase of canopy temperature (Buitrago Acevedo et al., 2017; Hsiao, 1973; Jackson et al., 1981; Kalma et al., 2008; Karnieli et al., 2010; Liu et al., 2016; Nemani and Running, 1989; Schulze et al., 1973; Zweifel et al., 2009).

Table 6.2. Trend analysis of the parameters of the GEV distribution of log-transformed fire duration across decile bins of LST anomaly, PMI and of the FWI System components, reporting coefficient of determination and p-value of the linear fit, Sen's slope, and Mann-Kendall test's result. Significance level of Mann-Kendall test is 0.05.

	Location				*Scale*				*Shape*			
	r^2	*p*	*Sen's slope*	*M-K test*	r^2	*p*	*Sen's slope*	*M-K test*	r^2	*p*	*Sen's slope*	*M-K test*
LST an.	0.78	***	0.015	Rejects	0.79	***	0.0081	Rejects	0.87	***	0.027	Rejects
PMI	0.26	ns	0.006	Fails	0.55	*	0.0028	Fails	0.32	ns	0.006	Fails
FFMC	0.76	**	0.013	Rejects	0.85	***	0.0083	Rejects	0.70	**	0.012	Rejects
DMC	0.90	***	0.016	Rejects	0.83	***	0.0051	Rejects	0.44	*	0.014	Fails
DC	0.93	***	0.014	Rejects	0.53	*	0.0047	Fails	0.63	**	0.020	Rejects
ISI	0.83	***	0.012	Rejects	0.68	**	0.0086	Rejects	0.41	*	0.012	Fails
BUI	0.95	***	0.016	Rejects	0.80	***	0.0052	Rejects	0.57	*	0.012	Fails
FWI	0.93	***	0.012	Rejects	0.96	***	0.0087	Rejects	0.64	**	0.012	Fails

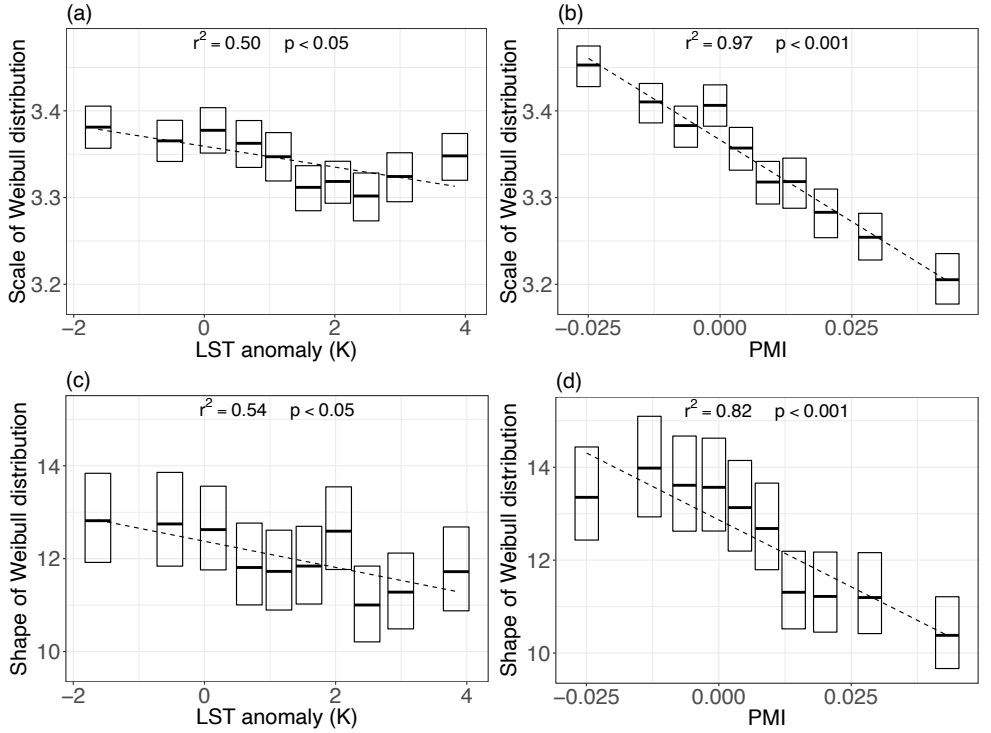


Figure 6.5. Scale and shape of the Weibull distribution of log-transformed rate of spread in decile bins of LST anomaly and PMI.

6.4.1. Considerations on spatial and temporal granularity of satellite data

Satellite imagery used in this research was at two different resolutions. MODIS optical bands to retrieve the PMI are available at a resolution of 500 m whereas thermal bands, from which LST anomaly is derived, are available at 1000 m. While the operational production of maps of probability of extreme events as a bivariate function of LST anomaly and PMI might require some consideration on the most suitable approach to combine data at different resolutions, from the point of view of the analyses herein this is not relevant. Indeed, each fire was associated with the pre-fire environmental condition (LST anomaly, alternatively PMI) of the cell in which it was located (1 and 0.25 km^2 respectively), independently of the resolution of the source dataset (Pyne et al., 1996). As it will be shortly discussed that these two variables are independent, there is no effect of the differing resolution on the characterisation of the pre-fire environmental conditions of the specific cell containing the fire.

The optical and thermal datasets were different also in terms of temporal structure. LST anomaly was derived from a daily climatology and an annual model of LST, both constructed by means of the HANTS algorithm (Alfieri et al., 2013; Menenti et al., 1993; Roerink et al.,

2000; Verhoef, 1996). In this sense, the daily temporal granularity of LST anomaly is inherent in the approach adopted to model it. On the other side, PMI was computed from the 8-day composited MODIS reflectance product. Composited products have the advantage of providing the best cloud free estimate of the pixel in a standardised grid while compensating for cloud cover and view angle. The coarser temporal granularity was not perceived as an obstacle as during the dry season LFMC only changes abruptly in correspondence of rainfalls (Ruffault et al., 2018) and the use of the prior compositing period in a predictive approach renders temporal sampling less critical. An alternative approach could have been to model PMI variability by means of the HANTS algorithm to gap-fill cloudy pixels and compensate for noise, while retaining a daily coverage, as reported in literature for LST and NDVI (Alfieri et al., 2013; Menenti et al., 2016, 1993; Verhoef, 1996). However, it is not known whether harmonic analysis is able to capture PMI variability with a reasonable number of harmonics with respect to the available number of observations (Zhou et al., 2015), and investigating this was beyond the objectives of this study.

Analyses reported herein are based on pre-fire satellite observations of LST anomaly and of PMI. Indeed, each fire was associated to the LST anomaly data from the previous day and to the PMI map of the previous 8-day compositing period. This ensures that results can be adopted in an operational scenario where current observations are used to predict fire characteristics in the following days. This is not inconsistent with the choice of associating fires with the same day value of the FWI System components. Indeed, FWI maps are available in advance as being produced from forecasts of weather conditions (San-Miguel-Ayanz et al., 2012).

Table 6.3. Trend analysis of the parameters of the Weibull distribution of log-transformed rate of spread across decile bins of LST anomaly, PMI and of the FWI System components, reporting coefficient of determination and p-value of the linear fit, Sen's slope, and Mann-Kendall test's result. Significance level of Mann-Kendall test is 0.05.

	Scale				*Shape*			
	r^2	*p*	*Sen's slope*	*M-K test*	r^2	*p*	*Sen's slope*	*M-K test*
LST anomaly	0.50	*	-0.0077	Rejects	0.54	*	-0.129	Rejects
PMI	0.97	***	-0.0254	Rejects	0.82	***	-0.419	Rejects
FFMC	0.18	ns	-0.0017	Fails	0.03	ns	0.032	Fails
DMC	0.38	ns	-0.0064	Rejects	0.41	*	-0.137	Fails
DC	0.66	**	-0.0098	Rejects	0.57	*	-0.173	Rejects
ISI	0.05	ns	-0.0009	Fails	0.01	ns	0.027	Fails
BUI	0.65	**	-0.0066	Rejects	0.52	*	-0.102	Fails
FWI	0.30	ns	-0.0026	Fails	0.01	ns	-0.025	Fails

6.4.2. LST anomaly and PMI as predictors of fire characteristics

LST anomaly appears to capture part of the variability in burned area and fire duration (Figure 6.2), with increasing values leading to larger fires and longer durations. This is reflected in the parameters of the corresponding conditional probability distribution functions. Both mean and standard deviation of normal distribution of log-transformed burned area conditional to LST anomaly show significant ($p<0.001$ and $p<0.05$ respectively) increasing trends (Figure 6.3) with a high Sen's slope magnitude (Table 6.1). Similarly, location, scale, and shape of the GEV distribution of log-transformed fire duration conditional to LST anomaly are characterised by strong (r^2=0.78, 0.79 and 0.87) and significant ($p<0.001$) trends with a high Sen's slope (Table 6.2). These results are further confirmed by the likelihood ratio test, with the conditional (alternative) models allowing the rejection of the unconditional (null) models for both fire characteristics (Table 6.4).

The dispersion of rate of spread in decile bins of the LST anomaly shows a weakly decreasing trend (Figure 6.2). This is reflected in both scale and shape of the corresponding Weibull distribution. Both parameters exhibit a significant ($p<0.05$) decreasing trend (Figure 6.5), albeit less significant and with a much lower Sen's slope magnitude as opposed to PMI (Table 6.3). The Mann-Kendall test confirms that the null hypothesis of absence of trend can be rejected, and the likelihood ratio test further confirms that the alternative model allows the rejection of the null model (Table 6.4). Nevertheless, the weakness of the trend and the relatively low Sen's slope magnitude implies that LST anomaly might not be considered a strong covariate for rate of spread.

Along the same line of reasoning, it can be noted that the dispersion of burned area and rate of spread varies across decile bins of PMI (Figure 6.2). Increasing values of PMI, corresponding to increasing LFMC, lead to a dispersion of burned area and rate of spread

Table 6.4. Results of the likelihood ratio test. Null model is the one fitting all data. Alternative model is the collection of ten models in decile bins of the candidate covariate. Significance level is 0.05. In bold the alternative models showing the highest likelihood for each fire characteristic.

	Burned area	*Duration*	*Rate of spread*
LST anomaly	**Rejects**	**Rejects**	Rejects
PMI	Rejects	Fails	**Rejects**
FFMC	Rejects	Rejects	Fails
DMC	Rejects	Rejects	Fails
DC	Rejects	Rejects	Fails
ISI	Rejects	Rejects	Rejects
BUI	Rejects	Rejects	Rejects
FWI	Rejects	Rejects	Rejects

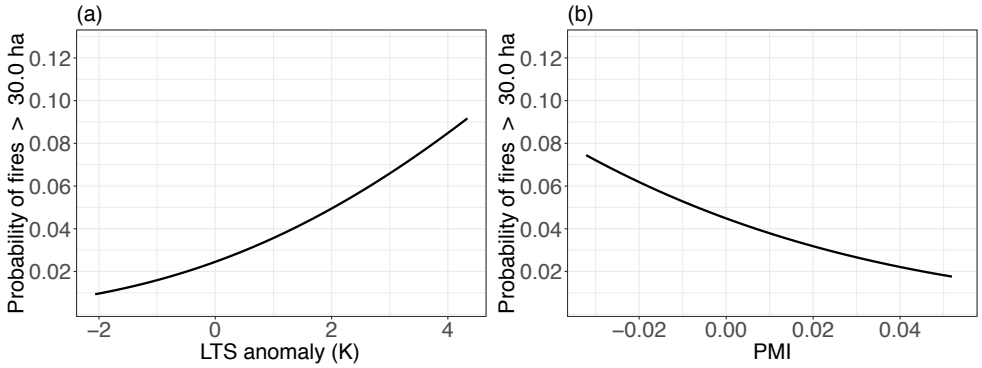


Figure 6.6. Modelled probability of fires larger than 30.0 ha (95th percentile of the values recorded in the study area), conditional to ignition, as a function of LST anomaly and PMI.

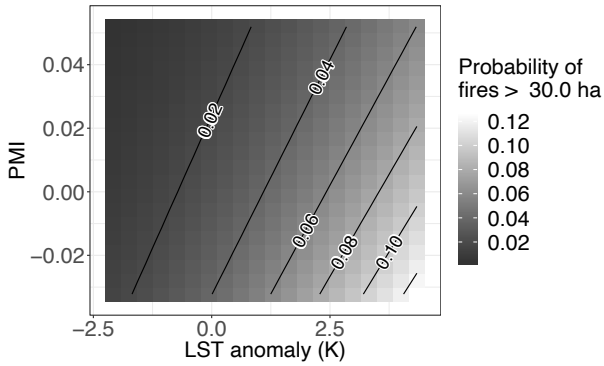


Figure 6.7. Modelled probability of fires larger than 30.0 ha (95th percentile of the values recorded in the study area), conditional to ignition, as a function of both LST anomaly and PMI. Solid lines indicate probability values.

towards lower values. This is further confirmed in the trends of the parameters of the corresponding probability distribution models. The mean of the normal distribution of log-transformed burned area has a strong (r^2=0.80) and significant (p<0.001) decreasing trend with PMI (Figure 6.3) with high Sen's slope magnitude (Table 6.1). As opposed to LST anomaly, standard deviation shows no trend, the Mann-Kendall test fails to reject the null hypothesis and a constant value would be appropriate to describe its variability. The likelihood ratio test confirms that this probability model conditional to PMI allows the rejection of the unconditional model. Both scale and shape of the Weibull distribution of log-transformed rate of spread show strong (r^2=0.97 and 0.82) and significant (p<0.001) trends against PMI (Figure 6.5), both characterised by a high Sen's slope magnitude (Table 6.3). The likelihood ratio test confirms the rejection of the corresponding null model (Table 6.4).

PMI doesn't appear to control fire duration. The dispersion of fire duration values doesn't vary across decile bins of PMI (Figure 6.2), and the only parameter of the GEV distribution

of log-transformed fire duration that shows a significant ($p<0.05$), yet weak trend is scale (Figure 6.4). Nevertheless, the Mann-Kendall test fails to reject the null hypothesis, and the absence of a trend can't be rejected (Table 6.2). Indeed, constant values would fit most confidence intervals across PMI bins (Figure 6.4) and the likelihood ratio test confirms that the conditional model fails to reject the null model (Table 6.4).

These results do not come unexpected. PMI was already demonstrated to be a good predictor of summer fires burned area and rate of spread in the region (Maffei and Menenti, 2019). Results based on LST anomaly were less obvious, as previous analyses focussed on burned area and fire duration only, and the evaluation was performed on events occurring all the year round (Maffei et al., 2018). That said, analyses herein confirm that LST anomaly is a predictor of burned area and fire duration of summer fires. It was also found that LST anomaly is not a strong covariate of rate of spread, albeit the existence of a relationship linking it to the corresponding probability distribution model cannot be ruled out.

6.4.3. Comparing the predictive performance of LST anomaly and PMI against the FWI System components

Trend analysis and likelihood ratio test were used to compare LST anomaly and PMI versus the FWI System components. This fire danger model was chosen as it proved to be adaptable to various biomes worldwide (de Groot and Flannigan, 2014; Dowdy et al., 2009; San-Miguel-Ayanz et al., 2012; Taylor and Alexander, 2006). LST anomaly and PMI perform as well as FWI in predicting burned area, with the mean of the normal distribution of log-transformed burned area showing strong and significant ($p<0.001$) trends and comparable Sen's slope magnitude (Table 6.1). While trends in the standard deviation are quite varying and not present in some covariates, all conditional models of log-transformed burned area allow the rejection of the null model (Table 6.4). Similar considerations lead to note that LST anomaly performs similarly to the FWI System components in predicting fire duration (Table 6.2). With respect to rate of spread, none of the FWI System components shows convincing trends of the conditional parameters of the Weibull distribution (Table 6.3). While an exception could be raised for DC, it must be noted that the corresponding conditional model fails to reject the unconditional (null) model (Table 6.4). It can thus be stated that, in the study area, multi-spectral remote sensing of LFMC (via the PMI) is a good predictor of rate of spread whereas the FWI System components are not.

6.4.4. Interpreting results against combustion and propagation processes

LST anomaly and PMI proved to be independent, as noted in Figure 6.1 and because of their different prediction capability with respect to fire duration and rate of spread. PMI is a spectral index exploiting the different effect of water content on the spectral properties of vegetation in the near infrared and in the shortwave infrared to provide a direct measure of LFMC (Maffei and Menenti, 2014). The clear relationship reported between PMI and the rate of spread has a direct physical interpretation, as LFMC controls flames propagation (Andrews et al., 2013; Finney, 1998; Rothermel, 1991, 1972; Wilson, 1990). The fact that

LST anomaly is not as good as a covariate of rate of spread suggests that the initial hypothesis of interpreting it as a measure of vegetation water stress, and indirectly of moisture content, is not able to explain results reported in this study.

LST anomaly is a measure of the deviation of the observed LST from its climatological value. While vegetation responds to water stress through a decrease in stomatal conductance which leads to an increase of its temperature, in Mediterranean environments characterised by prolonged dry summers this plant protection mechanism is actually triggered on a seasonal basis (Pellizzaro et al., 2007a, 2007b). This means that LST increase because of increased water stress might have already been accounted for into the LST climatology. LST anomaly may thus be unrelated to vegetation water stress condition and may be rather interpreted as a measure of excess enthalpy stored in fuels. This opens to a physically based interpretation of LST anomaly as a covariate of fire duration, a fire characteristic substantially unrelated to PMI. Several environment and anthropic factors have been found to affect fire duration (Costafreda-Aumedes et al., 2016; Fischer et al., 2015; Gustafson et al., 2011; Lasslop and Kloster, 2017), but from a fire behaviour point of view, duration is rather a measure of the probability of extinction, which is the resultant of heat fluxes between the flaming zone, the surrounding fuels and the atmosphere (Finney et al., 2013). Higher heat content in the fuels imply that less endothermic enthalpy is needed to sustain fire spread, this resulting in a lower probability of extinction (Albini, 1986, 1985; Wilson, 1990, 1985). The interpretation of LST anomaly as a measure of excess enthalpy thus justifies its effect on fire duration.

The weak decreasing trend observed between LST anomaly and rate of spread may be susceptible of a similar physical interpretation. Heat fluxes between burning material and the surrounding fuels are at the basis of flames propagation, and rate of spread is determined by the ratio between the heat flux received by the fuels from the heat source and the heat required to achieve ignition (Rothermel, 1972; Weber, 1991). While the latter is dependent on fuel moisture content, the former is determined by convective and radiative heat exchange (Albini, 1985; Baines, 1990). Convective heat exchange is dependent on temperature difference and on a heat exchange coefficient weakly dependent on the same temperature difference. A higher fuel temperature might thus lead to slower flames propagation. Clearly, LST anomaly values observed in this study can not be considered as a driver of the rate of spread as LFMC (as measured by PMI). Yet this interpretation may explain the observed weakly decreasing trends in rate of spread with increasing LST anomaly.

6.4.5. Joint use of LST anomaly and PMI for the prediction of extreme events

It was discussed that LST anomaly and PMI are good predictors of fire duration and rate of spread respectively, and this was justified through the outlined physical interpretation. Their independence was also noted. As these two remote sensing observations of fuel condition are both strong predictors of burned area, this opened an opportunity for their joint use for the evaluation of the probability of extreme events. Indeed, if burned area is considered as a resultant, among the other factors, of rate of spread and fire duration, it is

reasonable to expect that the joint use of LST anomaly and PMI may lead to better predictions. The adopted approach was to model the parameters of the probability distribution of log-transformed burned area as a function of these two remote sensing observables. Findings discussed herein reasonably allowed the use of linear models. From these, the probability of extreme events, conditional to ignition could be evaluated as a function of LST anomaly and PMI. Extreme events were here defined as those exceeding the 95th percentile of all burned area values recorded in the study area, that is 30 ha. The probability of fires larger than 30.0 ha conditional to ignition shows a ten-fold increase from 0.9% to 9.2% when LST anomaly increases from -2.1 to 4.3 K, and a four-fold increase from 1.8% to 7.4% when PMI decreases from 0.052 to -0.032 (Figure 6.6). Extending this line of reasoning, bivariate linear models were constructed for the mean and the standard deviation of the normal distribution of log-transformed burned area, leading to a model predicting the probability of extreme events, conditional to ignition, as a function of both LST anomaly and PMI. The joint model, when evaluated over the same range of LST anomaly and PMI values (-2.1 to 4.3 K and 0.052 to -0.032 respectively), shows that the probability of fires larger than 30.0 ha conditional to ignition varies between 0.5% and 12.7% (Figure 6.7), that is a 25-fold increase. The wider dynamic range attained confirms the stated hypothesis that the joint use of LST anomaly and PMI can lead to improved predictions.

6.5. Conclusion

Fire danger is defined as “the resultant, often expressed as an index, of both constant and variable factors affecting the inception, spread, and difficulty of control of fires and the damage they cause” (FAO, 1986). The concept of danger is semantically related to a human perception (Bachmann and Allgöwer, 2000). FAO definition, through the reference to difficulty of control, acknowledges fire behaviour and its resultants (such as burned area and fire duration) as components of fire danger (Allgöwer et al., 2003). Fire danger indices available to decision makers and fire managers reflect this and mainly focus on the prediction of fire occurrence – the inception and spread in FAO’s definition – and behaviour (Allgöwer et al., 2003; Sirca et al., 2018).

This study sits on the fire behaviour side of fire danger, in this being a novelty as a remote sensing application, and contributes to the identified need to improve fire danger models (Jolly, 2007; Jolly and Johnson, 2018; Nolan et al., 2018; Pellizzaro et al., 2007b; Rossa et al., 2016; Rossa and Fernandes, 2017; Ruffault et al., 2018; Schunk et al., 2017; Ustin et al., 2009) through an understanding of how pre-fire satellite observations of live fuel condition are related to fire characteristics such as burned area, fire duration and rate of spread. More specifically it was shown that LST anomaly is a strong covariate of fire duration and weak covariate of rate of spread, whereas PMI is a strong covariate of rate of spread. Both remote sensing quantities are strong predictors of burned area. Complementarity with the well consolidated FWI System, especially in terms of the prediction of rate of spread, was also shown. These findings are relevant as they allow the prediction of the probability of extreme events, conditional to ignition, as a function of pre-fire satellite observations of fuel condition. This has an immediate operational application, whereas fire managers are

interested in understanding whether emergency conditions are likely to arise, putting a pressure on response resources.

While LST anomaly and PMI can be used individually to predict the fire characteristics that they control, this study tested the advantage of their synergistic use in the prediction of burned area. This approach was supported by the demonstrated independence of LST anomaly and PMI. The probability of large fires conditional to ignition as a function of both LST anomaly and PMI covers a broader range of values as compared to the same probability evaluated as a function of these two remote sensing quantities individually. The outlined approach is clearly open to further integration with traditional fire danger indices such as the FWI, but this was outside the scope of this study.

A final consideration is on the wide availability of open access satellite remote sensing datasets whose increased accessibility allows the creation of operational services. This study was performed on MODIS data to cover the range of dates of available fire records. Nevertheless, it may be repeated with any satellite remote sensing data acquired in the near, shortwave, and thermal infrared domains. Among the others it is worth naming instruments such as VIIRS on board Suomi NPP and NOAA-20, and SLSTR on board the Sentinel-3 series. All named systems provide daily global coverage, and their data is in the open access domain.

7. Conclusions and recommendations

This chapter summarises research results presented in previous chapters and contextualises them against the research questions identified at the beginning of this thesis. It further discusses novelty of the proposed approach and potential impact in terms of user needs. Finally, recommendations for further research are given.

7.1. From research questions to results

The overarching objective of this study was to translate pre-fire optical and thermal remote sensing observations of forests into actionable information supporting fire preparedness. The research was developed in response to an identified need to improve existing fire danger models, mostly based on weather forecasts, and compensate for their lack of quantitative information on live fuel condition (Ruffault et al., 2018). Fire danger is a measure of constant and variable factors affecting the inception and spread of fires, and the difficulty to control fires, expressed in the form of an index (FAO, 1986). Fire danger models are used to predict the probability of extreme events, both in terms of fire occurrence and fire behaviour.

The most relevant biophysical property controlling fire inception and flame spread is live fuel moisture content (LFMC) (Pyne et al., 1996). LFMC also determines the radiometric properties of vegetation (Gates et al., 1965; Hsiao, 1973), which can be observed by spaceborne imaging spectroradiometers (Yebra et al., 2013). The use of remote sensing for the prediction of fire occurrence has already been documented (Cao et al., 2013; Huesca et al., 2014, 2009; Pan et al., 2016). However, no research was found in literature relating pre-fire remote sensing measurements to fire behaviour characteristics. These considerations raised the following research question: to what extent can remote sensing of forest condition be used to predict fire behaviour characteristics and assess the probability of extreme events?

To address the arising research question, an extensive dataset of actual fires recorded in Campania, Italy, by the Forest Fire Protection Information Unit of Carabinieri (Italian National Gendarmerie, §2.2.2) was combined with pre-fire optical and thermal Aqua-MODIS Level 3 land surface temperature and surface reflectance products to construct predictive models of burned area, fire duration and rate of spread. Defining the problem and structuring the approach identified five research sub-questions as outlined in §1.6.

Responses to these sub-questions are discussed below. In response to the main research question, results showed that pre-fire remote sensing observations of live fuel condition in the optical and thermal infrared domains are covariates of burned area, fire duration and rate of spread, i.e. they control the probability distribution functions of these fire characteristics. This allowed the modelling of the probability of extreme events, conditional to ignition, as a function of pre-fire remote sensing measurements, demonstrating the use of Earth Observation to generate actionable information useful for fire danger management.

Q1. Which characteristics of fire behaviour are probabilistically related to pre-fire land surface temperature (LST) anomalies?

This research question was addressed in Chapters 3 and 6. The daily land surface temperature (LST) anomaly was evaluated against a reference climatology (Alfieri et al., 2013) modelled through the harmonic analysis of time series (HANTS) algorithm (Menenti et al., 2016, 1993) of the longest series of daily diurnal Aqua-MODIS LST. Further, HANTS was used to model the annual variability of yearly series of daily LST data. This enabled to evaluate the LST anomaly as the difference between the LST value in the annual model and LST value in the climatology (Maffei et al., 2018).

Crucial to the probabilistic approach used in this study was the identification of the best fitting probability models describing burned area, fire duration and rate of spread. The probability distribution of fire characteristics is shaped by the unique combination of topography, land use/land cover, land management practices and human settlements characterising each region, and the adoption of models fitting data in other areas worldwide is not appropriate (Cui and Perera, 2008; Reed and McKelvey, 2002). Once the distributions of burned area, fire duration and rate of spread have been modelled, the study focussed on the evaluation of the corresponding probability models conditional to LST anomaly. In other words, the parameters of the distribution functions of these fire characteristics were modelled as a function of the LST anomaly. It was found that the LST anomaly is a covariate of burned area and fire duration, and that a higher LST anomaly shifts their corresponding distribution towards higher values. The trend of the parameters of the probability distribution of rate of spread as a function of LST anomaly is weak and decreasing, i.e. rate of spread tends to be distributed towards lower values with increasing LST anomaly. LST anomaly is thus strongly related to burned area and fire duration, and weakly related to rate of spread.

These results raise an important opportunity to map probability of extreme events, conditional to ignition, with pre-fire estimations of LST anomaly. In this study, an event is considered extreme if, say, its burned area exceeds the 95^{th} percentile of historical values in the region. Once the dependence of the parameters of the probability distribution of burned area and fire duration are modelled against LST anomaly, the probability of extreme events, conditional to ignition, is a function of LST anomaly. As expected, it was found that an increasing LST anomaly leads to increased probability of extreme events in terms of both burned area and fire duration.

The fact that the LST anomaly is a strong covariate of burned area and fire duration, and a weak covariate of rate of spread, and that against the latter it shows a decreasing trend, is susceptible of a physical interpretation. From a fire behaviour point of view, duration is related to the probability of flame extinction. The probability of extinction is determined by heat fluxes between the flaming zone, the surrounding fuels and the atmosphere, and higher heat content in the fuels results in a lower probability of extinction (Albini, 1986, 1985; Wilson, 1990, 1985). An interpretation of LST anomaly as a measure of excess enthalpy, i.e. heat content in fuels, would justify its observed effect on fire duration.

Similar reasoning may explain the weak decreasing trend observed between LST anomaly and rate of spread. Indeed, rate of spread is determined by the ratio between the heat fluxes towards the fuel and the heat of ignition (Rothermel, 1972; Weber, 1991). Heat of ignition is determined by fuel moisture content, whereas heat fluxes are due to convective and radiative heat exchange (Albini, 1985; Baines, 1990). As convective heat exchange between burning material and the surrounding fuels is dependent on temperature difference and on a heat exchange coefficient weakly dependent on the same temperature difference, a higher fuel heat content implies a slower heat exchange and might well explain the slower propagation of flames.

Q2. To what extent can LFMC be retrieved by means of a broadband spectral index?

This research question emerged from an assessment of, (i) existing remote sensing methods for the evaluation of vegetation water content and, (ii) the requirements of fire models. Remote sensing practitioners mostly focussed on water content measured in terms of equivalent water thickness (EWT), which is defined as the mass of water per unit leaf area. The interest in EWT was mainly driven by the fact that this measure of water content is a parameter of vegetation radiative transfer models (Jacquemoud et al., 2009). Fire propagation models are rather based on fuel moisture content, which is defined as the percentage ratio of the mass of water in fuel tissues over oven dried fuel mass (Finney, 1998). Remote sensing methods proposed so far for the evaluation of LFMC use the ratio of EWT and dry matter content, the latter being a further parameter of vegetation radiative transfer models. Model inversion for the assessment of EWT and dry matter content would thus allow for the quantification of LFMC (Zarco-Tejada et al., 2003). Satisfactory results can only be achieved, however, if the inversion is constrained through the prior parameterisation of the lookup table used in the retrieval process, and this requires extensive fieldwork (Yebra et al., 2018; Yebra and Chuvieco, 2009a, 2009b).

In Chapter 4, in a different approach, the objective was to construct a spectral index based on existing broadband optical sensors allowing for wider generality and computational simplicity. By means of simulated spectral data (Jacquemoud et al., 2009) convolved to MODIS bands (Xiong et al., 2006) it was found that isolines of LFMC could be identified in the spectral reflectance subspace of near infrared (0.86 μm) and shortwave infrared (1.24 μm) bands, and that these isolines are straight and parallel. This led to the construction of the Perpendicular Moisture Index (PMI), defined as the distance of reflectance points from a reference dry vegetation line. The PMI was validated by means a publicly available dataset

of vegetation reflectance and moisture content measurements (Hosgood et al., 1995), and it was found that PMI and LFMC are linked by a logarithmic relationship.

Q3. Which characteristics of fire behaviour are probabilistically related to pre-fire remote sensing estimates of LFMC?

This research question was addressed in Chapter 5, relying on the Perpendicular Moisture Index (PMI) developed in Chapter 4 as a remote sensing estimate of LFMC. Following the same approach adopted for LST anomaly, probability models of burned area, fire duration and rate of spread conditional to PMI were constructed to identify trends linking their corresponding parameters to pre-fire values of PMI. It was thus found that PMI is a covariate of burned area and rate of spread, but not of fire duration. More specifically, it was found that decreasing values of PMI, i.e. decreasing values of LFMC, lead to burned area and rate of spread being distributed towards higher values. From a fire management point of view, it means that the probability of extreme events in terms of burned area or rate of spread, conditional to ignition, increases with decreasing PMI. PMI is thus strongly related to burned area and rate of spread, and unrelated to fire duration.

These results have an immediate physical interpretation, as fire propagation is controlled by fuel moisture content. Indeed, heat transported by radiation and convection to the fuels close to the flaming area induces dehydration and pyrolysis, with release of volatiles. Dehydration further causes a reduction in fuels temperature of ignition that, in conjunction with increased fuel temperature, eventually leads to combustion and thus to the advancement of the fire front. Clearly, a lower moisture content facilitates this process, leading to a quicker propagation of flames. Indeed, the dependence of the rate of spread on fuel moisture content has been widely reported in literature (Andrews et al., 2013; Finney, 1998; Rothermel, 1991, 1972; Wilson, 1990).

Q4. To what extent may pre-fire remote sensing estimations of LST anomaly and LFMC be used synergistically to improve predictions of extreme events?

A sufficient condition for the construction of a model dependent on both LST anomaly and LFMC, the latter estimated by retrieving the perpendicular moisture index (PMI), is that these two quantities are independent. In chapter 6 it was found that LST anomaly and PMI are unrelated. The independence of these two measures of vegetation conditions is consistent with the nature of the biophysical features being observed. It was discussed how LST anomaly can be interpreted as a measure of excess enthalpy stored in fuels, and how this explains the clear relationship between LST anomaly and fire duration. On the other side, PMI was specifically designed to maximise the sensitivity to LFMC variability, and this is reflected in this spectral index being a predictor of the rate of spread. The assumption of burned area being the resultant of the rate of spread and fire duration may then justify how both LST anomaly and PMI are covariates of burned area.

These considerations opened an opportunity to jointly use pre-fire LST anomaly and PMI for the prediction of the probability of extreme events, conditional to ignition, in terms of

burned area. The approach was based on the identification of a correlation of the parameters of the probability distribution of burned area with LST anomaly and PMI both individually (univariate models) and jointly (bivariate model). The sensitivity of the corresponding probability of extreme events, conditional to ignition, to LST anomaly and PMI was then reviewed across the three models in terms of sensitivity, i.e. estimated range of variation. It was found that the bivariate model is more sensitive to the probability of extreme events, conditional to ignition, than either univariate model, over the same range of values of LST anomaly and PMI. This result is relevant from an operational perspective, as fire managers are interested in predicting when and where emergency conditions may arise, i.e. what are the odds that a possible fire might be difficult to control.

Q5. How do remote sensing predictions of fire behaviour compare against predictions enabled by traditional fire danger models such as the Fire Weather Index (FWI) System (Van Wagner, 1987)?

This research question was addressed in Chapters 5 and 6. Traditional fire danger indices are essentially based on the processing of meteorological input to produce a few indicators related to fire occurrence and behaviour. Among them, the Fire Weather Index (FWI) System proved to be flexible enough to be satisfactorily used in several areas worldwide, including Europe. The FWI System is a collection of three moisture codes and three indices representing the effect of moisture content of three classes of dead forest fuel and of wind on fire behaviour (Van Wagner, 1987). As it only models dead fuel, whereas remote sensing in both the optical and the thermal domain is rather sensitive to live fuel status, some complementarity is envisaged. Yet it is interesting to understand how FWI System components compare against LST anomaly and PMI in the prediction of burned area, fire duration and rate of spread.

The approach for this evaluation followed the same line of reasoning adopted for remote sensing observations of live fuel status, i.e. the parameters of the probability distribution functions of burned area, fire duration and rate of spread conditional to FWI System components were analysed to identify trends. It was found that all FWI System components control burned area, albeit to a different extent, and that similar results apply to fire duration. It was also found that the parameters of the probability distribution of rate of spread are insensitive to FWI System components.

Relative performance of the probability distribution models conditional to LST anomaly, PMI and the six FWI System components was assessed, and it was shown that models conditional to remote sensing observations are characterised by a higher likelihood. This result is not final, considering the stated complementarity of the remote sensing and meteorological approaches with fuel condition being observed by the former and modelled by the latter. Yet it must be remarked how, in the study area, remote sensing in the optical domain was a predictor of rate of spread, whereas FWI System components were not.

7.2. Novelty and impact

To the best of this author's knowledge, research outlined in this dissertation delivered a few major innovations in the landscape of remote sensing of forest fire danger. Novelty lays both in the metrics being developed for the assessment of live fuel condition and in the approach aiming at quantifying probabilities of extreme events, conditional to ignition, as a function of remote sensing measurements. By focussing on fire behaviour characteristics, it further marked a distance from existing studies on remote sensing for fire danger mapping, where the main interest was fire occurrence. In detail:

- This is the first time a study related pre-fire remote sensing observations of live fuel excess heat content and of LFMC to fire behaviour characteristics such as burned area, duration, and rate of spread.
- The choice of a novel probabilistic approach rather than a deterministic one allowed the construction of models for the prediction of the probability of extreme events, conditional to ignition.
- In the study area, optical and thermal remote sensing measurements were a predictor of rate of spread, whereas none of the FWI System components was. This shows the potential for using Earth Observation to improve existing fire danger mapping tools.
- All newly identified relationships are based on pre-fire remote sensing observations of vegetation condition, hence demonstrating predicting capability.
- The perpendicular moisture index (PMI) is the first broadband spectral index designed to be sensitive to live fuel moisture content (LFMC). PMI was found to control the rate of spread, as it would be expected for LFMC by fire propagation models.
- The LST anomaly, as defined herein, was a predictor of fire duration. It is thus related to probability of flames extinction, as it would be expected for a measure of fuel heat content.

These accomplishments have an immediate impact as they allow the production of actionable information useful to fire preparedness and the pre-emptive management of fire suppression resources. The probabilistic approach proposed in this study is closer to the fire management needs, where the main concern is about the odds of facing complex operational scenarios associated with extreme events (Gunes and Kovel, 2000; North et al., 2015; Oliveira et al., 2017; Thompson et al., 2015). The fact that all results reported herein refer to pre-fire remote sensing observations of live fuel condition may allow the production of predictive maps. The complementarity of remote sensing and traditional meteorological fire danger indices with regards to both fuel condition and fire behaviour characteristic carries added value to fire managers. Once the local best fitting probability distribution function of forest fire characteristics has been identified, the relatively simple processing needed to produce maps of the probability of extreme events would allow an easy operationalisation of the proposed approach. Finally, the methodology may be replicated with other open Earth Observation data such as those provided by e.g. Sentinel-2 MSI and Sentinel-3 SLSTR, taking advantage of the long-term continuity of the Copernicus programme.

7.3. Outlook and recommendations

Like any endeavour aiming and expanding the knowledge base and at creating new tools, answers to research questions widen the horizon and open further questions. The first and most immediate would be: would the developed methodology work elsewhere? This research was performed in a relatively wide and diverse region in the middle of the Mediterranean. Extrapolation to other areas worldwide is not immediate for two main reasons. The first refers to the need to identify the probability model fitting burned area, fire duration and rate of spread. It was already discussed how transferring models from other areas would not be correct. Further, local environmental conditions and vegetation communities shape fuel composition and may alter the relationship between fire behaviour and remote sensing of fuel condition. It can be expected that separate regional predictive models may be created within the same methodological framework at the basis of this research. This is feasible as fire inventories in some of the most fire prone areas worldwide are either publicly available on the web, e.g. the Prométhée database in Mediterranean France, the Instituto da Conservação da Natureza e das Florestas (ICNF) fire inventory in Portugal, and the United States Geological Survey (USGS) fire occurrence data in the USA, or are provided upon request by relevant authorities, e.g. the Forest Fire Protection Information Unit of Carabinieri in Italy and the National Statistical Service in Greece. Nevertheless, the effectiveness of our approach would still need to be verified across different ecosystems/environment conditions and region extent.

The need to operationally implement the developed approach raises a further question: what would be a sensible strategy to evaluate the LST anomaly in near real time, with satellite observations being available till the date when the retrieval is required? In this study, LST anomaly was defined as the deviation of the LST annual model from the LST climatology. The use of an annual model based on the calendar year was observational in nature and not predictive. Strategies for the near real time assessment of the LST anomaly may be based on the evaluation of the LST annual model from one year of data up to the current day. An alternative could be using a shorter temporal sample of observations prior to the target date for each pixel, after filtering noise out, to estimate current LST. Both strategies would still make use of the LST climatology as defined in this thesis. However, understanding how such alternative metrics of LST anomaly are linked to fire characteristics would require further investigations.

The third question arising from this research is whether the same approach may be implemented using data from other sensor systems. This study focussed on MODIS on board of Aqua satellite for the purpose of ensuring the largest availability of satellite measurements covering the historical dataset of forest fires. Other space-borne imaging spectro-radiometers can provide similar radiometric data as those used in this work (near infrared, shortwave infrared, and thermal infrared), including VIIRS on board Suomi NPP and NOAA-20, and SLSTR on board the Sentinel-3 series.

A fourth research question immediately arising is whether the proposed approach would work for the prediction of fire behaviour characteristics other than burned area, duration, and rate of spread. Indeed, these were indirectly derived from the data available for this

research that did not contain further information on fire behaviour. Among several fire behaviour characteristics, it would be interesting to investigate fire intensity, as this is controlled by fuel amount and condition (De Luis et al., 2004; Vilà et al., 2001) and has been found to be related to FWI System components (Camia and Amatulli, 2009). A proxy for fire intensity is fire radiative power (Smith and Wooster, 2005; Wooster, 2003), which is a measure of the rate of radiant heat emitted from a fire and has the advantage of being widely available as part of the standard fire products retrieved from e.g. MODIS, VIIRS and SLSTR (Justice et al., 2002; Schroeder et al., 2014; Wooster et al., 2012).

A final area of development is on the integration of fire danger predictions based on Remote Sensing measurements with existing fire danger systems based on meteorological data. The complementarity of these two approaches has already been discussed in this chapter. Integration of optical and thermal observations of forest condition by means of a probabilistic framework led to improved predictions of burned area. It can thus be expected that further integration with the FWI System may be beneficial. More generally, it would be relevant to study other approaches to integrate meteorological and remote sensing measurements of the fire environment, specifically model based methodologies. The successful interpretation of the results of this dissertation in the light of the combustion and propagation processes would encourage further research in this direction.

The discussed reproducibility of the approach introduced by this study gives way to some recommendations beyond the developments prospected above, towards operational use of satellite remote sensing in fire danger mapping. The first and more relevant is to ensure that models linking remote sensing of forest condition to the probability of extreme events are adapted to the operational scenarios where they would be used. In addition to the discussed adaptation to the regional landscape characteristics, it would be specifically important to define with fire managers what is, from their point of view, the magnitude of an extreme event. In this study a conventional threshold was used, corresponding to the 95^{th} percentile of the historical values of fire behaviour characteristic of interest (e.g., burned area), but fire managers might want to advise otherwise.

Indeed, it is essential to work closely with end users to ensure data potential and limitations are properly understood. This study measured danger as the probability, conditional to ignition, of a fire characteristic of interest exceeding a threshold value. Other mechanisms of representation could be considered, such as a multiplier against a baseline probability, thus giving an immediate measure of increasing danger during the dry season. In fact, any remote sensing fire danger monitoring service should be meant to support an informed and sound decision-making process, and attention should be paid to the point of view of the user on data usage and interpretation, which might not necessarily coincide with that of the scientist or of the service provider.

Finally, the author firmly believes in the key role of open-source software and open-access data as innovation enablers. They ensure savings on licensing costs, reproducibility, and support from a wide community of programmers worldwide. This entire study was based on open data and software, and its operationalisation has no implied need to use commercial solutions.

References

Abatzoglou, J.T., Williams, A.P., Barbero, R., 2019. Global emergence of anthropogenic climate change in fire weather indices. Geophys. Res. Lett. 46, 326–336. https://doi.org/10.1029/2018GL080959

Abbott, K.N., Leblon, B., Staples, G.C., Maclean, D.A., Alexander, M.E., 2007. Fire danger monitoring using RADARSAT-1 over northern boreal forests. Int. J. Remote Sens. 28, 1317–1338. https://doi.org/10.1080/01431160600904956

Abdollahi, M., Islam, T., Gupta, A., Hassan, Q.K., 2018. An advanced forest fire danger forecasting system: integration of remote sensing and historical sources of ignition data. Remote Sens. 10, 923. https://doi.org/10.3390/rs10060923

Abouali, M., 2021. MATLAB Implementation of Harmonic ANalysis of Time Series (HANTS).

Ackerman, S.A., Holz, R.E., Frey, R., Eloranta, E.W., Maddux, B.C., McGill, M., 2008. Cloud detection with MODIS. Part II: validation. J. Atmos. Ocean. Technol. 25, 1073–1086. https://doi.org/10.1175/2007JTECHA1053.1

Adab, H., Devi Kanniah, K., Beringer, J., 2016. Estimating and up-scaling fuel moisture and leaf dry matter content of a temperate humid forest using multi resolution remote sensing data. Remote Sens. 8, 961. https://doi.org/10.3390/rs8110961

Ager, A.A., Vaillant, N.M., Finney, M.A., 2011. Integrating fire behavior models and geospatial analysis for wildland fire risk assessment and fuel management planning. J. Combust. 2011, 1–19. https://doi.org/10.1155/2011/572452

Aguado, I., Chuvieco, E., Borén, R., Nieto, H., 2007. Estimation of dead fuel moisture content from meteorological data in Mediterranean areas. Applications in fire danger assessment. Int. J. Wildl. Fire 16, 390–397. https://doi.org/10.1071/WF06136

Albini, F.A., 1986. Wildland fire spread by radiation - a model including fuel cooling by natural convection. Combust. Sci. Technol. 45, 101–113. https://doi.org/10.1080/00102208608923844

Albini, F.A., 1985. A model for fire spread in wildland fuels by radiation. Combust. Sci. Technol. 42, 229–258. https://doi.org/10.1080/00102208508960381

Alfieri, S.M., De Lorenzi, F., Menenti, M., 2013. Mapping air temperature using time series analysis of LST: the SINTESI approach. Nonlinear Process. Geophys. 20, 513–527. https://doi.org/10.5194/npg-20-513-2013

Allgöwer, B., Carlson, J.D., van Wagtendonk, J.W., 2003. Introduction to fire danger rating and remote sensing - Will remote sensing enhance wildland fire danger rating?, in: Chuvieco, E. (Ed.), Wildland Fire Danger Estimation and Mapping - The Role of Remote Sensing Data. World Scientific, Singapore, pp. 1–19. https://doi.org/10.1142/9789812791177_0001

Amato, V., Valletta, M., 2017. Wine landscapes of Italy, in: Soldati, M., Marchetti, M. (Eds.), Landscapes and Landforms of Italy, World Geomorphological Landscapes. Springer International Publishing, Cham, pp. 523–536. https://doi.org/10.1007/978-3-319-26194-2

Andela, N., Morton, D.C., Giglio, L., Chen, Y., van der Werf, G.R., Kasibhatla, P.S., DeFries, R.S., Collatz, G.J., Hantson, S., Kloster, S., Bachelet, D., Forrest, M., Lasslop, G., Li, F., Mangeon, S., Melton, J.R., Yue, C., Randerson, J.T., 2017. A human-driven decline in global burned area. Science (80-.). 356, 1356–1362. https://doi.org/10.1126/science.aal4108

Anderegg, W.R.L., Trugman, A.T., Badgley, G., Anderson, C.M., Bartuska, A., Ciais, P., Cullenward, D., Field, C.B., Freeman, J., Goetz, S.J., Hicke, J.A., Huntzinger, D., Jackson, R.B., Nickerson, J., Pacala, S., Randerson, J.T., 2020. Climate-driven risks to the climate mitigation potential of forests. Science (80-.). 368, eaaz7005. https://doi.org/10.1126/science.aaz7005

Anderson, S.A.J., Anderson, W.R., 2009. Predicting the elevated dead fine fuel moisture content in gorse (Ulex europaeus L.) shrub fuels. Can. J. For. Res. 39, 2355–2368. https://doi.org/10.1139/X09-142

Anderson, T.W., Darling, D.A., 1954. A test of goodness of fit. J. Am. Stat. Assoc. 49, 765–769. https://doi.org/10.1080/01621459.1954.10501232

Andrews, P.L., 2007. BehavePlus fire modeling system: Past, present, and future, in: Proceedings of 7th Symposium on Fire and Forest Meteorology. American Meteorological Society, Bar Harbor, p. 13 p.

Andrews, P.L., Cruz, M.G., Rothermel, R.C., 2013. Examination of the wind speed limit function in the Rothermel surface fire spread model. Int. J. Wildl. Fire 22, 959–969. https://doi.org/10.1071/WF12122

Arnold, J.G., Srinivasan, R., Muttiah, R.S., Williams, J.R., 1998. Large area hydrologic modeling and assessment - Part I: Model development. J. Am. Water Resour. Assoc. 34, 73–89. https://doi.org/10.1111/j.1752-1688.1998.tb05961.x

Arpaci, A., Eastaugh, C.S., Vacik, H., 2013. Selecting the best performing fire weather indices for Austrian ecoregions. Theor. Appl. Climatol. 114, 393–406. https://doi.org/10.1007/s00704-013-0839-7

Asner, G.P., Scurlock, J.M.O., Hicke, J.A., 2003. Global synthesis of leaf area index observations: implications for ecological and remote sensing studies. Glob. Ecol. Biogeogr. 12, 191–205. https://doi.org/10.1046/j.1466-822X.2003.00026.x

Bachmann, A., Allgöwer, B., 2000. The need for a consistent wildfire risk terminology, in: Neuenschwander, L.F., Ryan, K.C., Gollberg, G.E. (Eds.), Crossing the Millennium: Integrating Spatial Technologies and Ecological Principles for a New Age in Fire Management. pp. 67–77.

Baines, P.G., 1990. Physical mechanisms for the propagation of surface fires. Math. Comput. Model. 13, 83–94. https://doi.org/10.1016/0895-7177(90)90102-S

Bajocco, S., De Angelis, A., Rosati, L., Ricotta, C., 2009. The relationship between temporal patterns of wildfires and phytoclimatic regions in Sardinia (Italy). Plant Biosyst. 143, 588–596. https://doi.org/10.1080/11263500903233037

Bajocco, S., Ferrara, C., Guglietta, D., Ricotta, C., 2019. Fifteen years of changes in fire ignition frequency in Sardinia (Italy): A rich-get-richer process. Ecol. Indic. 104, 543–548. https://doi.org/10.1016/j.ecolind.2019.05.030

Bajocco, S., Guglietta, D., Ricotta, C., 2015. Modelling fire occurrence at regional scale: does vegetation phenology matter? Eur. J. Remote Sens. 48, 763–775. https://doi.org/10.5721/EuJRS20154842

Bajocco, S., Koutsias, N., Ricotta, C., 2017. Linking fire ignitions hotspots and fuel phenology: The importance of being seasonal. Ecol. Indic. 82, 433–440. https://doi.org/10.1016/j.ecolind.2017.07.027

Bajocco, S., Pezzatti, G.B., Mazzoleni, S., Ricotta, C., 2010a. Wildfire seasonality and land use: when do wildfires prefer to burn? Environ. Monit. Assess. 164, 445–452. https://doi.org/10.1007/s10661-009-0905-x

Bajocco, S., Ricotta, C., 2008. Evidence of selective burning in Sardinia (Italy): which land-cover classes do wildfires prefer? Landsc. Ecol. 23, 241–248. https://doi.org/10.1007/s10980-007-9176-5

Bajocco, S., Rosati, L., Ricotta, C., 2010b. Knowing fire incidence through fuel phenology: A remotely sensed approach. Ecol. Modell. 221, 59–66. https://doi.org/10.1016/j.ecolmodel.2008.12.024

Baker, W.L., 1989. Landscape ecology and nature reserve design in the Boundary Waters Canoe Area, Minnesota. Ecology 70, 23–35. https://doi.org/10.2307/1938409

Barbati, A., Corona, P., D'amato, E., Cartisano, R., 2015. Is landscape a driver of short-term wildfire recurrence? Landsc. Res. 40, 99–108. https://doi.org/10.1080/01426397.2012.761681

Barnes, W.L., Pagano, T.S., Salomonson, V. V., 1998. Prelaunch characteristics of the Moderate Resolution Imaging Spectroradiometer (MODIS) on EOS-AM1. IEEE Trans. Geosci. Remote Sens. 36, 1088–1100. https://doi.org/10.1109/36.700993

Barnes, W.L., Xiong, X., Salomonson, V. V., 2003. Status of terra MODIS and aqua modis. Adv. Sp. Res. 32, 2099–2106. https://doi.org/10.1016/S0273-1177(03)90529-1

Barrett, K., Loboda, T., McGuire, A.D., Genet, H., Hoy, E., Kasischke, E., 2016. Static and dynamic controls on fire activity at moderate spatial and temporal scales in the Alaskan boreal forest. Ecosphere 7, e01572. https://doi.org/10.1002/ecs2.1572

Bartlein, P.J., Hostetler, S.W., Shafer, S.L., Holman, J.O., Solomon, A.M., 2008. Temporal and spatial structure in a daily wildfire-start data set from the western United States (1986–96). Int. J. Wildl. Fire 17, 8–17. https://doi.org/10.1071/WF07022

Bashfield, A., Keim, A., 2011. Continent-wide DEM creation for the European union, in: 34th International Symposium on Remote Sensing of Environment - The GEOSS Era: Towards Operational Environmental Monitoring.

Bianchi, L.O., Defossé, G.E., 2014. Ignition probability of fine dead surface fuels of native Patagonian forests or Argentina. For. Syst. 23, 129–138. https://doi.org/10.5424/fs/2014231-04632

Biermann, F., Bai, X., Bondre, N., Broadgate, W., Arthur Chen, C.-T., Dube, O.P., Erisman, J.W., Glaser, M., van der Hel, S., Lemos, M.C., Seitzinger, S., Seto, K.C., 2016. Down to Earth: Contextualizing the Anthropocene. Glob. Environ. Chang. 39, 341–350. https://doi.org/10.1016/j.gloenvcha.2015.11.004

Bond, W.J., Woodward, F.I., Midgley, G.F., 2005. The global distribution of ecosystems in a world without fire. New Phytol. 165, 525–538. https://doi.org/10.1111/j.1469-8137.2004.01252.x

Bourgeau-Chavez, L.L., Kasischke, E.S., Riordan, K., Brunzell, S., Nolan, M., Hyer, E., Slawski, J., Medvecz, M., Walters, T., Ames, S., 2007. Remote monitoring of spatial and temporal surface soil moisture in fire disturbed boreal forest ecosystems with ERS SAR imagery. Int. J. Remote Sens. 28, 2133–2162. https://doi.org/10.1080/01431160600976061

Bovio, G., Camia, A., 1997. Land zoning based on fire history. Int. J. Wildl. Fire 7, 249–258. https://doi.org/10.1071/WF9970249

Bowd, E.J., Banks, S.C., Strong, C.L., Lindenmayer, D.B., 2019. Long-term impacts of wildfire and logging on forest soils. Nat. Geosci. 12, 113–118. https://doi.org/10.1038/s41561-018-0294-2

Bowyer, P., Danson, F.M., 2004. Sensitivity of spectral reflectance to variation in live fuel moisture content at leaf and canopy level. Remote Sens. Environ. 92, 297–308. https://doi.org/10.1016/j.rse.2004.05.020

Bradshaw, L.S., Deeming, J.E., Burgan, R.E., Cohen, J.D., 1984. The 1978 National Fire-Danger Rating System: technical documentation, General Technical Report INT-169. Department of Agriculture, Forest Service, Intermountain Forest and Range Experiment Station, Odgen. https://doi.org/10.2737/INT-GTR-169

Brenkert–Smith, H., Champ, P.A., Flores, N., 2006. Insights into wildfire mitigation decisions

among wildland-urban interface residents. Soc. Nat. Resour. 19, 759–768. https://doi.org/10.1080/08941920600801207

Buitrago Acevedo, M.F., Groen, T.A., Hecker, C.A., Skidmore, A.K., 2017. Identifying leaf traits that signal stress in TIR spectra. ISPRS J. Photogramm. Remote Sens. 125, 132–145. https://doi.org/10.1016/j.isprsjprs.2017.01.014

Buitrago Acevedo, M.F., Skidmore, A.K., Groen, T.A., Hecker, C.A., 2018. Connecting infrared spectra with plant traits to identify species. ISPRS J. Photogramm. Remote Sens. 139, 183–200. https://doi.org/10.1016/j.isprsjprs.2018.03.013

Burgan, R.E., 1988. 1988 Revisions to the 1978 National Fire-Danger Rating System. U.S. Department of Agriculture, Forest Service, Southeastern Forest Experiment Station, Asheville.

Burgan, R.E., Klaver, R.W., Klaver, J.M., 1998. Fuel models and fire potential from satellite and surface observations. Int. J. Wildl. Fire 8, 159–170. https://doi.org/10.1071/WF9980159

Burns, M., Cheng, A.S., 2007. Framing the need for active management for wildfire mitigation and forest restoration. Soc. Nat. Resour. 20, 245–259. https://doi.org/10.1080/08941920601117348

Caccamo, G., Chisholm, L.A., Bradstock, R.A., Puotinen, M.L., Pippen, B.G., 2012. Monitoring live fuel moisture content of heathland, shrubland and sclerophyll forest in south-eastern Australia using MODIS data. Int. J. Wildl. Fire 21, 257–269. https://doi.org/10.1071/WF11024

Calkin, D.E., Thompson, M.P., Finney, M.A., 2015. Negative consequences of positive feedbacks in US wildfire management. For. Ecosyst. 2, 9. https://doi.org/10.1186/s40663-015-0033-8

Camia, A., Amatulli, G., 2009. Weather factors and fire danger in the Mediterranean, in: Chuvieco, E. (Ed.), Earth Observation of Wildland Fires in Mediterranean Ecosystems. Springer Berlin Heidelberg, Berlin, Heidelberg, pp. 71–82. https://doi.org/10.1007/978-3-642-01754-4_6

Cao, X., Cui, X., Yue, M., Chen, J., Tanikawa, H., Ye, Y., 2013. Evaluation of wildfire propagation susceptibility in grasslands using burned areas and multivariate logistic regression. Int. J. Remote Sens. 34, 6679–6700. https://doi.org/10.1080/01431161.2013.805280

Cardil, A., Salis, M., Spano, D., Delogu, G., Molina Terrén, D., 2014. Large wildland fires and extreme temperatures in Sardinia (Italy). iForest - Biogeosciences For. 7, 162–169. https://doi.org/10.3832/ifor1090-007

Carlson, J.D., Bradshaw, L.S., Nelson, R.M., Bensch, R.R., Jabrzemski, R., 2007. Application of the Nelson model to four timelag fuel classes using Oklahoma field observations: model evaluation and comparison with National Fire Danger Rating System algorithms. Int. J. Wildl. Fire 16, 204–2016. https://doi.org/10.1071/WF06073

Carlson, J.D., Burgan, R.E., 2003. Review of users' needs in operational fire danger estimation: The Oklahoma example. Int. J. Remote Sens. 24, 1601–1620. https://doi.org/10.1080/01431160210144651

Carlucci, M., Zambon, I., Colantoni, A., Salvati, L., 2019. Socioeconomic development, demographic dynamics and forest fires in Italy, 1961–2017: A time-series analysis. Sustainability 11, 1305. https://doi.org/10.3390/su11051305

Carmo, M., Moreira, F., Casimiro, P., Vaz, P., 2011. Land use and topography influences on wildfire occurrence in northern Portugal. Landsc. Urban Plan. 100, 169–176. https://doi.org/10.1016/j.landurbplan.2010.11.017

Castro, F.X., Tudela, A., Sebastià, M.T., 2003. Modeling moisture content in shrubs to predict fire risk in Catalonia (Spain). Agric. For. Meteorol. 116, 49–59. https://doi.org/10.1016/S0168-1923(02)00248-4

Catry, F.X., Rego, F.C., Bação, F., Moreira, F., 2009. Modeling and mapping wildfire ignition risk in Portugal. Int. J. Wildl. Fire 18, 921–931. https://doi.org/10.1071/WF07123

Ceccato, P., Flasse, S., Grégoire, J.-M., 2002a. Designing a spectral index to estimate vegetation water content from remote sensing data: Part 2. Validation and applications. Remote Sens. Environ. 82, 198–207. https://doi.org/10.1016/S0034-4257(02)00036-6

Ceccato, P., Flasse, S., Tarantola, S., Jacquemoud, S., Grégoire, J.-M., 2001. Detecting vegetation leaf water content using reflectance in the optical domain. Remote Sens. Environ. 77, 22–33. https://doi.org/10.1016/S0034-4257(01)00191-2

Ceccato, P., Gobron, N., Flasse, S., Pinty, B., Tarantola, S., 2002b. Designing a spectral index to estimate vegetation water content from remote sensing data: Part 1 Theoretical approach. Remote Sens. Environ. 82, 188–197. https://doi.org/10.1016/S0034-4257(02)00037-8

Certini, G., 2005. Effects of fire on properties of forest soils: a review. Oecologia 143, 1–10. https://doi.org/10.1007/s00442-004-1788-8

Chaparro, D., Vall-llossera, M., Piles, M., Camps, A., Rüdiger, C., Riera-Tatché, R., 2016. Predicting the extent of wildfires using remotely sensed soil moisture and temperature trends. IEEE J. Sel. Top. Appl. Earth Obs. Remote Sens. 9, 2818–2829. https://doi.org/10.1109/JSTARS.2016.2571838

Chen, D., Huang, J., Jackson, T.J., 2005. Vegetation water content estimation for corn and soybeans using spectral indices derived from MODIS near- and short-wave infrared bands. Remote Sens. Environ. 98, 225–236. https://doi.org/10.1016/j.rse.2005.07.008

Cheng, T., Rivard, B., Sánchez-Azofeifa, A., 2011. Spectroscopic determination of leaf water content using continuous wavelet analysis. Remote Sens. Environ. 115, 659–670. https://doi.org/10.1016/j.rse.2010.11.001

Cheng, T., Rivard, B., Sánchez-Azofeifa, A.G., Féret, J.-B., Jacquemoud, S., Ustin, S.L., 2014.

Deriving leaf mass per area (LMA) from foliar reflectance across a variety of plant species using continuous wavelet analysis. ISPRS J. Photogramm. Remote Sens. 87, 28–38. https://doi.org/10.1016/j.isprsjprs.2013.10.009

Cheng, Y.-B., Zarco-Tejada, P.J., Riaño, D., Rueda, C.A., Ustin, S.L., 2006. Estimating vegetation water content with hyperspectral data for different canopy scenarios: Relationships between AVIRIS and MODIS indexes. Remote Sens. Environ. 105, 354–366. https://doi.org/10.1016/j.rse.2006.07.005

Chowdhury, E.H., Hassan, Q.K., 2015a. Operational perspective of remote sensing-based forest fire danger forecasting systems. ISPRS J. Photogramm. Remote Sens. 104, 224–236. https://doi.org/10.1016/j.isprsjprs.2014.03.011

Chowdhury, E.H., Hassan, Q.K., 2015b. Development of a new daily-scale Forest Fire Danger Forecasting System using remote sensing data. Remote Sens. 7, 2431–2448. https://doi.org/10.3390/rs70302431

Chuvieco, E. (Ed.), 2009. Earth Observation of Wildland Fires in Mediterranean Ecosystems. Springer-Verlag, Berlin, Heidelberg. https://doi.org/10.1007/978-3-642-01754-4

Chuvieco, E. (Ed.), 2003. Wildland Fire Danger Estimation and Mapping. World Scientific, Singapore. https://doi.org/10.1142/5364

Chuvieco, E., Aguado, I., Jurdao, S., Pettinari, M.L., Yebra, M., Salas, J., Hantson, S., de la Riva, J., Ibarra, P., Rodrigues, M., Echeverría, M., Azqueta, D., Román, M. V., Bastarrika, A., Martínez, S., Recondo, C., Zapico, E., Martínez-Vega, F.J., 2014. Integrating geospatial information into fire risk assessment. Int. J. Wildl. Fire 23, 606–619. https://doi.org/10.1071/WF12052

Chuvieco, E., Aguado, I., Yebra, M., Nieto, H., Salas, J., Martín, M.P., Vilar, L., Martínez, J., Martín, S., Ibarra, P., de la Riva, J., Baeza, J., Rodríguez, F., Molina, J.R., Herrera, M.A., Zamora, R., 2010. Development of a framework for fire risk assessment using remote sensing and geographic information system technologies. Ecol. Modell. 221, 46–58. https://doi.org/10.1016/j.ecolmodel.2008.11.017

Chuvieco, E., Cocero, D., Riaño, D., Martin, P., Martínez-Vega, J., de la Riva, J., Pérez, F., 2004. Combining NDVI and surface temperature for the estimation of live fuel moisture content in forest fire danger rating. Remote Sens. Environ. 92, 322–331. https://doi.org/10.1016/j.rse.2004.01.019

Chuvieco, E., Riaño, D., Aguado, I., Cocero, D., 2002. Estimation of fuel moisture content from multitemporal analysis of Landsat Thematic Mapper reflectance data: applications in fire danger assessment. Int. J. Remote Sens. 23, 2145–2162. https://doi.org/10.1080/01431160110069818

Chuvieco, E., Wagtendonk, J., Riaño, D., Yebra, M., Ustin, S.L., 2009. Estimation of fuel conditions for fire danger assessment, in: Chuvieco, E. (Ed.), Earth Observation of Wildland Fires in Mediterranean Ecosystems. Springer Berlin Heidelberg, Berlin, Heidelberg, pp. 83–96. https://doi.org/10.1007/978-3-642-01754-4_7

Chuvieco, E., Yue, C., Heil, A., Mouillot, F., Alonso-Canas, I., Padilla, M., Pereira, J.M., Oom, D., Tansey, K., 2016. A new global burned area product for climate assessment of fire impacts. Glob. Ecol. Biogeogr. 25, 619–629. https://doi.org/10.1111/geb.12440

Claverie, M., Ju, J., Masek, J.G., Dungan, J.L., Vermote, E.F., Roger, J.-C., Skakun, S. V., Justice, C.O., 2018. The Harmonized Landsat and Sentinel-2 surface reflectance data set. Remote Sens. Environ. 219, 145–161. https://doi.org/10.1016/j.rse.2018.09.002

Cohen, W.B., 1991. Response of vegetation indices to changes in three measures of leaf water stress. Photogramm. Eng. Remote Sens. 57, 195–202.

Colombo, R., Meroni, M., Marchesi, A., Busetto, L., Rossini, M., Giardino, C., Panigada, C., 2008. Estimation of leaf and canopy water content in poplar plantations by means of hyperspectral indices and inverse modeling. Remote Sens. Environ. 112, 1820–1834. https://doi.org/10.1016/j.rse.2007.09.005

Corona, P., Ferrari, B., Cartisano, R., Barbati, A., 2014. Calibration assessment of forest flammability potential in Italy. iForest - Biogeosciences For. 7, 300–305. https://doi.org/10.3832/ifor1123-007

Corral, Á., Telesca, L., Lasaponara, R., 2008. Scaling and correlations in the dynamics of forest-fire occurrence. Phys. Rev. E 77, 016101. https://doi.org/10.1103/PhysRevE.77.016101

Costafreda-Aumedes, S., Cardil, A., Molina, D.M., Daniel, S.N., Mavsar, R., Vega-Garcia, C., 2016. Analysis of factors influencing deployment of fire suppression resources in Spain using artificial neural networks. iForest - Biogeosciences For. 9, 138–145. https://doi.org/10.3832/ifor1329-008

Cui, W., Perera, A.H., 2008. What do we know about forest fire size distribution, and why is this knowledge useful for forest management? Int. J. Wildl. Fire 17, 234–244. https://doi.org/10.1071/WF06145

Cumming, S.G., 2001. A parametric model of the fire-size distribution. Can. J. For. Res. 31, 1297–1303. https://doi.org/10.1139/x01-032

Cyr, D., Gauthier, S., Bergeron, Y., 2007. Scale-dependent determinants of heterogeneity in fire frequency in a coniferous boreal forest of eastern Canada. Landsc. Ecol. 22, 1325–1339. https://doi.org/10.1007/s10980-007-9109-3

Danson, F.M., Bowyer, P., 2004. Estimating live fuel moisture content from remotely sensed reflectance. Remote Sens. Environ. 92, 309–321. https://doi.org/10.1016/j.rse.2004.03.017

Dasgupta, S., Qu, J.J., 2009. Soil adjusted vegetation water content retrievals in grasslands. Int. J. Remote Sens. 30, 1019–1043. https://doi.org/10.1080/01431160802438548

Dasgupta, S., Qu, J.J., Hao, X., Bhoi, S., 2007. Evaluating remotely sensed live fuel moisture estimations for fire behavior predictions in Georgia, USA. Remote Sens. Environ. 108, 138–150. https://doi.org/10.1016/j.rse.2006.06.023

Dasgupta, S., Qu, Jj.J., Hao, X., 2006. Design of a Susceptibility Index for Fire Risk Monitoring. IEEE Geosci. Remote Sens. Lett. 3, 140–144. https://doi.org/10.1109/LGRS.2005.858484

Davidson, A., Wang, S., Wilmshurst, J., 2006. Remote sensing of grassland-shrubland vegetation water content in the shortwave domain. Int. J. Appl. Earth Obs. Geoinf. 8, 225–236. https://doi.org/10.1016/j.jag.2005.10.002

Dawson, T.P., Curran, P.J., North, P.R.J., Plummer, S.E., 1999. The propagation of foliar biochemical absorption features in forest canopy reflectance: a theoretical analysis. Remote Sens. Environ. 67, 147–159. https://doi.org/10.1016/S0034-4257(98)00081-9

de Groot, W.J., Flannigan, M.D., 2014. Climate change and early warning systems for wildland fire, in: Singh, A., Zommers, Z. (Eds.), Reducing Disaster: Early Warning Systems for Climate Change. Springer Netherlands, Dordrecht, pp. 127–151. https://doi.org/10.1007/978-94-017-8598-3_7

de Groot, W.J., Wardati, Wang, Y., 2005. Calibrating the Fine Fuel Moisture Code for grass ignition potential in Sumatra, Indonesia. Int. J. Wildl. Fire 14, 161–169. https://doi.org/10.1071/WF04054

De Luis, M., Baeza, M.J., Raventós, J., González-Hidalgo, J.C., 2004. Fuel characteristics and fire behaviour in mature Mediterranean gorse shrublands. Int. J. Wildl. Fire 13, 79–87. https://doi.org/10.1071/WF03005

Deeming, J.E., Burgan, R.E., Cohen, J.D., 1977. The National Fire Danger Rating System - 1978. U.S. Department of Agriculture, Forest Service, Intermountain Forest and Range Experiment Station, Ogden.

Delignette-Muller, M.L., Dutang, C., 2015. fitdistrplus : An R package for fitting distributions. J. Stat. Softw. 64. https://doi.org/10.18637/jss.v064.i04

Della Rocca, G., Danti, R., Hernando, C., Guijarro, M., Madrigal, J., 2018. Flammability of two Mediterranean mixed forests: study of the non-additive effect of fuel mixtures in laboratory. Front. Plant Sci. 9, 825. https://doi.org/10.3389/fpls.2018.00825

Di Gennaro, A., 2002. I sistemi di terre della Campania. S.EL.CA., Firenze.

Díaz-Delgado, R., Lloret, F., Pons, X., 2004. Spatial patterns of fire occurrence in Catalonia, NE, Spain. Landsc. Ecol. 19, 731–745. https://doi.org/10.1007/s10980-005-0183-1

Díaz-Delgado, R., Lloret, F., Pons, X., Terradas, J., 2002. Satellite evidence of decreasing resilience in Mediterranean plant communities after recurrent wildfires. Ecology 83, 2293–2303. https://doi.org/10.1890/0012-9658(2002)083[2293:SEODRI]2.0.CO;2

Dickson, B.G., Prather, J.W., Xu, Y., Hampton, H.M., Aumack, E.N., Sisk, T.D., 2006. Mapping the probability of large fire occurrence in northern Arizona, USA. Landsc. Ecol. 21, 747–761. https://doi.org/10.1007/s10980-005-5475-x

Dimitrakopoulos, A.P., 2001. A statistical classification of Mediterranean species based on

their flammability components. Int. J. Wildl. Fire 10, 113–118. https://doi.org/10.1071/WF01004

Dimitrakopoulos, A.P., Bemmerzouk, A.M., 2003. Predicting live herbaceous moisture content from a seasonal drought index. Int. J. Biometeorol. 47, 73–79. https://doi.org/10.1007/s00484-002-0151-1

Dimitrakopoulos, A.P., Panov, P.I., 2001. Pyric properties of some dominant Mediterranean vegetation species. Int. J. Wildl. Fire 10, 23–27. https://doi.org/10.1071/WF01003

Dimitrakopoulos, A.P., Papaioannou, K.K., 2001. Flammability assessment of Mediterranean forest fuels. Fire Technol. 37, 143–152. https://doi.org/10.1023/A:1011641601076

Douglass, J.E., 1967. Effects of species and arrangement of forests on evapotranspiration, in: Sopper, W.E., Lull, H.W. (Eds.), Proceedings of the International Symposium on Forest Hydrology. Pergamon, New York, pp. 451–461.

Dowdy, A.J., Mills, G.A., Finkele, K., de Groot, W., 2009. Australian fire weather as represented by the McArthur Forest Fire Danger Index and the Canadian Forest Fire Weather Index. Centre for Australian Weather and Climate Research, Melbourne.

Duane, A., Piqué, M., Castellnou, M., Brotons, L., 2015. Predictive modelling of fire occurrences from different fire spread patterns in Mediterranean landscapes. Int. J. Wildl. Fire 24, 407–418. https://doi.org/10.1071/WF14040

Dube, O.P., 2009. Linking fire and climate: Interactions with land use, vegetation, and soil. Curr. Opin. Environ. Sustain. 1, 161–169. https://doi.org/10.1016/j.cosust.2009.10.008

Ducci, D., Tranfaglia, G., 2008. Effects of climate change on groundwater resources in Campania (southern Italy). Geol. Soc. London, Spec. Publ. 288, 25–38. https://doi.org/10.1144/SP288.3

Eaton, J.W., Bateman, D., Hauberg, S., Wehbring, R., 2020. GNU Octave version 6.1.0 manual: a high-level interactive language for numerical computations.

Elia, M., Giannico, V., Spano, G., Lafortezza, R., Sanesi, G., 2020. Likelihood and frequency of recurrent fire ignitions in highly urbanised Mediterranean landscapes. Int. J. Wildl. Fire 29, 120–131. https://doi.org/10.1071/WF19070

European Environment Agency, 2007. CLC2006 Technical Guidelines, EEA Technical report. Office for Official Publications of the European Communities, Luxembourg. https://doi.org/10.2800/12134

Faivre, N.R., Jin, Y., Goulden, M.L., Randerson, J.T., 2016. Spatial patterns and controls on burned area for two contrasting fire regimes in Southern California. Ecosphere 7, e01210. https://doi.org/10.1002/ecs2.1210

Faivre, N.R., Jin, Y., Goulden, M.L., Randerson, J.T., 2014. Controls on the spatial pattern of wildfire ignitions in Southern California. Int. J. Wildl. Fire 23, 799–811.

https://doi.org/10.1071/WF13136

Falk, D.A., Miller, C., McKenzie, D., Black, A.E., 2007. Cross-scale analysis of fire regimes. Ecosystems 10, 809–823. https://doi.org/10.1007/s10021-007-9070-7

Fan, L., Wigneron, J.-P., Xiao, Q., Al-Yaari, A., Wen, J., Martin-StPaul, N., Dupuy, J.-L., Pimont, F., Al Bitar, A., Fernandez-Moran, R., Kerr, Y.H., 2018. Evaluation of microwave remote sensing for monitoring live fuel moisture content in the Mediterranean region. Remote Sens. Environ. 205, 210–223. https://doi.org/10.1016/j.rse.2017.11.020

FAO, 2007. Fire Management - Global Assessment 2006. Food and Agriculture Organization of the United Nations, Rome.

FAO, 1995. Planning for sustainable use of land resources - Towards a new approach. Food and Agriculture Organization of the United Nations, Rome.

FAO, 1986. Wildland fire management terminology. Food and Agriculture Organization of the United Nations, Rome.

Feret, J.-B., François, C., Asner, G.P., Gitelson, A.A., Martin, R.E., Bidel, L.P.R., Ustin, S.L., le Maire, G., Jacquemoud, S., 2008. PROSPECT-4 and 5: Advances in the leaf optical properties model separating photosynthetic pigments. Remote Sens. Environ. 112, 3030–3043. https://doi.org/10.1016/j.rse.2008.02.012

Fernandes, P.M., 2015. Empirical support for the use of prescribed burning as a fuel treatment. Curr. For. Reports 1, 118–127. https://doi.org/10.1007/s40725-015-0010-z

Fernandes, P.M., 2013. Fire-smart management of forest landscapes in the Mediterranean basin under global change. Landsc. Urban Plan. 110, 175–182. https://doi.org/10.1016/j.landurbplan.2012.10.014

Fernandes, P.M., Botelho, H.S., 2003. A review of prescribed burning effectiveness in fire hazard reduction. Int. J. Wildl. Fire 12, 117–128. https://doi.org/10.1071/WF02042

Fernandes, P.M., Monteiro-Henriques, T., Guiomar, N., Loureiro, C., Barros, A.M.G., 2016. Bottom-up variables govern large-fire size in portugal. Ecosystems 19, 1362–1375. https://doi.org/10.1007/s10021-016-0010-2

Fernández-Guisuraga, J.M., Suárez-Seoane, S., Calvo, L., 2021. Radiative transfer modeling to measure fire impact and forest engineering resilience at short-term. ISPRS J. Photogramm. Remote Sens. 176, 30–41. https://doi.org/10.1016/j.isprsjprs.2021.04.002

Ferrara, C., Salvati, L., Corona, P., Romano, R., Marchi, M., 2019. The background context matters: Local-scale socioeconomic conditions and the spatial distribution of wildfires in Italy. Sci. Total Environ. 654, 43–52. https://doi.org/10.1016/j.scitotenv.2018.11.049

Field, R.D., Spessa, A.C., Aziz, N.A., Camia, A., Cantin, A., Carr, R., de Groot, W.J., Dowdy, A.J., Flannigan, M.D., Manomaiphiboon, K., Pappenberger, F., Tanpipat, V., Wang, X.,

2015. Development of a Global Fire Weather Database. Nat. Hazards Earth Syst. Sci. 15, 1407–1423. https://doi.org/10.5194/nhess-15-1407-2015

Finney, M.A., 2005. The challenge of quantitative risk analysis for wildland fire. For. Ecol. Manage. 211, 97–108. https://doi.org/10.1016/j.foreco.2005.02.010

Finney, M.A., 2001. Design of regular landscape fuel treatment patterns for modifying fire growth and behavior. For. Sci. 47, 219–228. https://doi.org/10.1093/forestscience/47.2.219

Finney, M.A., 2000. Efforts at comparing simulated and observed fire growth patterns. USDA Forest Service, Missoula Fire Sciences Laboratory, Missoula.

Finney, M.A., 1998. FARSITE: Fire Area Simulator – Model development and evaluation. Ogden. https://doi.org/10.2737/RMRS-RP-4

Finney, M.A., Cohen, J.D., McAllister, S.S., Jolly, W.M., 2013. On the need for a theory of wildland fire spread. Int. J. Wildl. Fire 22, 25–36. https://doi.org/10.1071/WF11117

Finney, M.A., Grenfell, I.C., McHugh, C.W., Seli, R.C., Trethewey, D., Stratton, R.D., Brittain, S., 2011. A method for ensemble wildland fire simulation. Environ. Model. Assess. 16, 153–167. https://doi.org/10.1007/s10666-010-9241-3

Fiorucci, P., Gaetani, F., Minciardi, R., 2008. Regional partitioning for wildfire regime characterization. J. Geophys. Res. 113, F02013. https://doi.org/10.1029/2007JF000771

Fischer, M.A., Di Bella, C.M., Jobbágy, E.G., 2015. Influence of fuel conditions on the occurrence, propagation and duration of wildland fires: A regional approach. J. Arid Environ. 120, 63–71. https://doi.org/10.1016/j.jaridenv.2015.04.007

Flannigan, M.D., Wotton, B.M., Marshall, G.A., de Groot, W.J., Johnston, J., Jurko, N., Cantin, A.S., 2016. Fuel moisture sensitivity to temperature and precipitation: climate change implications. Clim. Change 134, 59–71. https://doi.org/10.1007/s10584-015-1521-0

Flatley, W.T., Lafon, C.W., Grissino-Mayer, H.D., 2011. Climatic and topographic controls on patterns of fire in the southern and central Appalachian Mountains, USA. Landsc. Ecol. 26, 195–209. https://doi.org/10.1007/s10980-010-9553-3

Frank, Dorothea, Reichstein, M., Bahn, M., Thonicke, K., Frank, David, Mahecha, M.D., Smith, P., van der Velde, M., Vicca, S., Babst, F., Beer, C., Buchmann, N., Canadell, J.G., Ciais, P., Cramer, W., Ibrom, A., Miglietta, F., Poulter, B., Rammig, A., Seneviratne, S.I., Walz, A., Wattenbach, M., Zavala, M.A., Zscheischler, J., 2015. Effects of climate extremes on the terrestrial carbon cycle: concepts, processes and potential future impacts. Glob. Chang. Biol. 21, 2861–2880. https://doi.org/10.1111/gcb.12916

Fratianni, S., Acquaotta, F., 2017. The climate of Italy, in: Soldati, M., Marchetti, M. (Eds.), Landscapes and Landforms of Italy, World Geomorphological Landscapes. Springer International Publishing, Cham, pp. 29–38. https://doi.org/10.1007/978-3-319-26194-2

Ganatsas, P., Antonis, M., Marianthi, T., 2011. Development of an adapted empirical drought index to the Mediterranean conditions for use in forestry. Agric. For. Meteorol. 151, 241–250. https://doi.org/10.1016/j.agrformet.2010.10.011

Ganteaume, A., Camia, A., Jappiot, M., San-Miguel-Ayanz, J., Long-Fournel, M., Lampin, C., 2013. A review of the main driving factors of forest fire ignition over europe. Environ. Manage. 51, 651–662. https://doi.org/10.1007/s00267-012-9961-z

Gao, B.-C., 1996. NDWI - A normalized difference water index for remote sensing of vegetation liquid water from space. Remote Sens. Environ. 58, 257–266. https://doi.org/10.1016/S0034-4257(96)00067-3

Gao, B.-C., Goetz, A.F.H., 1990. Column atmospheric water vapor and vegetation liquid water retrievals from airborne imaging spectrometer data. J. Geophys. Res. 95, 3549–3564. https://doi.org/10.1029/JD095iD04p03549

Gao, Y., Walker, J.P., Allahmoradi, M., Monerris, A., Ryu, D., Jackson, T.J., 2015. Optical sensing of vegetation water content: a synthesis study. IEEE J. Sel. Top. Appl. Earth Obs. Remote Sens. 8, 1456–1464. https://doi.org/10.1109/JSTARS.2015.2398034

Gates, D.M., Keegan, H.J., Schleter, J.C., Weidner, V.R., 1965. Spectral properties of plants. Appl. Opt. 4, 11–20. https://doi.org/10.1364/AO.4.000011

Gausman, H.W., Allen, W.A., 1973. Optical parameters of leaves of 30 plant species. Plant Physiol. 52, 57–62. https://doi.org/10.1104/pp.52.1.57

GDAL/OGR Contributors, 2021. GDAL/OGR Geospatial Data Abstraction software Library.

GRASS Development Team, 2020. Geographic Resources Analysis Support System (GRASS) Software.

Griffiths, D., 1999. Improved formula for the Drought Factor in McArthur's Forest Fire Danger Meter. Aust. For. 62, 202–206. https://doi.org/10.1080/00049158.1999.10674783

Gudmundsson, L., Rego, F.C., Rocha, M., Seneviratne, S.I., 2014. Predicting above normal wildfire activity in southern Europe as a function of meteorological drought. Environ. Res. Lett. 9, 084008. https://doi.org/10.1088/1748-9326/9/8/084008

Gunes, A.E., Kovel, J.P., 2000. Using GIS in emergency management operations. J. Urban Plan. Dev. 126, 136–149. https://doi.org/10.1061/(ASCE)0733-9488(2000)126:3(136)

Gustafson, E.J., Shvidenko, A.Z., Scheller, R.M., 2011. Effectiveness of forest management strategies to mitigate effects of global change in south-central Siberia. Can. J. For. Res. 41, 1405–1421. https://doi.org/10.1139/x11-065

Hao, X., Qu, J.J., 2007. Retrieval of real-time live fuel moisture content using MODIS measurements. Remote Sens. Environ. 108, 130–137. https://doi.org/10.1016/j.rse.2006.09.033

Hardisky, M.A., Klemas, V., Smart, R.M., 1983. The influence of soil salinity, growth form, and leaf moisture on the spectral radiance of Spartina alterniflora canopies.

Photogramm. Eng. Remote Sens. 49, 77–83.

Hardy, C.C., 2005. Wildland fire hazard and risk: Problems, definitions, and context. For. Ecol. Manage. 211, 73–82. https://doi.org/10.1016/j.foreco.2005.01.029

Harrison, S.P., Marlon, J.R., Bartlein, P.J., 2010. Fire in the Earth System, in: Dodson, J. (Ed.), Changing Climates, Earth Systems and Society. Springer Netherlands, Dordrecht, pp. 21–48. https://doi.org/10.1007/978-90-481-8716-4_3

Harvey, B.J., Donato, D.C., Turner, M.G., 2016. High and dry: post-fire tree seedling establishment in subalpine forests decreases with post-fire drought and large stand-replacing burn patches. Glob. Ecol. Biogeogr. 25, 655–669. https://doi.org/10.1111/geb.12443

Haydon, D.T., Friar, J.K., Pianka, E.R., 2000. Fire-driven dynamic mosaics in the Great Victoria Desert, Australia. Landsc. Ecol. 15, 373–381. https://doi.org/10.1023/A:1008138029197

Hernandez, C., Keribin, C., Drobinski, P., Turquety, S., 2015. Statistical modelling of wildfire size and intensity: a step toward meteorological forecasting of summer extreme fire risk. Ann. Geophys. 33, 1495–1506. https://doi.org/10.5194/angeo-33-1495-2015

Hofierka, J., Mitášová, H., Neteler, M., 2009. Geomorphometry in GRASS GIS, in: Hengl, T., Reuter, H.I. (Eds.), Geomorphometry: Concepts, Software, Applications. Elsevier, Amsterdam, pp. 387–410. https://doi.org/10.1016/S0166-2481(08)00017-2

Hosgood, B., Jacquemoud, S., Andreoli, G., Verdebout, J., Pedrini, A., Schmuck, G., 1995. Leaf Optical Properties Experiment 93 (LOPEX93). Joint Research Centre, Ispra.

Hsiao, T.C., 1973. Plant responses to water stress. Annu. Rev. Plant Physiol. 24, 519–570. https://doi.org/10.1146/annurev.pp.24.060173.002511

Huesca, M., Litago, J., Merino-de-Miguel, S., Cicuendez-López-Ocaña, V., Palacios-Orueta, A., 2014. Modeling and forecasting MODIS-based Fire Potential Index on a pixel basis using time series models. Int. J. Appl. Earth Obs. Geoinf. 26, 363–376. https://doi.org/10.1016/j.jag.2013.09.003

Huesca, M., Litago, J., Palacios-Orueta, A., Montes, F., Sebastián-López, A., Escribano, P., 2009. Assessment of forest fire seasonality using MODIS fire potential: a time series approach. Agric. For. Meteorol. 149, 1946–1955. https://doi.org/10.1016/j.agrformet.2009.06.022

Huete, A.R., 1988. A soil-adjusted vegetation index (SAVI). Remote Sens. Environ. 25, 295–309. https://doi.org/10.1016/0034-4257(88)90106-X

Hunt, E.R., Li, L., Yilmaz, M.T., Jackson, T.J., 2011. Comparison of vegetation water contents derived from shortwave-infrared and passive-microwave sensors over central Iowa. Remote Sens. Environ. 115, 2376–2383. https://doi.org/10.1016/j.rse.2011.04.037

Hunt, E.R., Rock, B.N., 1989. Detection of changes in leaf water content using near- and middle-infrared reflectances. Remote Sens. Environ. 30, 43–54.

https://doi.org/10.1016/0034-4257(89)90046-1

Hunt, E.R., Ustin, S.L., Riaño, D., 2013. Remote sensing of leaf, canopy, and vegetation water contents for satellite environmental data records, in: Qu, J., Powell, A., Sivakumar, M. (Eds.), Satellite-Based Applications on Climate Change. Springer, Dordrecht, pp. 335–357. https://doi.org/10.1007/978-94-007-5872-8_20

Hurteau, M.D., North, M., 2010. Carbon recovery rates following different wildfire risk mitigation treatments. For. Ecol. Manage. 260, 930–937. https://doi.org/10.1016/j.foreco.2010.06.015

Jackson, R.D., Idso, S.B., Reginato, R.J., Pinter, P.J., 1981. Canopy temperature as a crop water stress indicator. Water Resour. Res. 17, 1133–1138. https://doi.org/10.1029/WR017i004p01133

Jacquemoud, S., Bacour, C., Poilvé, H., Frangi, J.-P., 2000. Comparison of four radiative transfer models to simulate plant canopies reflectance direct and inverse mode. Remote Sens. Environ. 74, 471–481. https://doi.org/10.1016/S0034-4257(00)00139-5

Jacquemoud, S., Baret, F., 1990. PROSPECT: A model of leaf optical properties spectra. Remote Sens. Environ. 34, 75–91. https://doi.org/10.1016/0034-4257(90)90100-Z

Jacquemoud, S., Verhoef, W., Baret, F., Bacour, C., Zarco-Tejada, P.J., Asner, G.P., François, C., Ustin, S.L., 2009. PROSPECT+SAIL models: A review of use for vegetation characterization. Remote Sens. Environ. 113, S56–S66. https://doi.org/10.1016/j.rse.2008.01.026

Jang, J., Viau, A.A., Anctil, F., 2006. Thermal-water stress index from satellite images. Int. J. Remote Sens. 27, 1619–1639. https://doi.org/10.1080/01431160500509194

Jolly, W.M., 2007. Sensitivity of a surface fire spread model and associated fire behaviour fuel models to changes in live fuel moisture. Int. J. Wildl. Fire 16, 503–509. https://doi.org/10.1071/WF06077

Jolly, W.M., Johnson, D.M., 2018. Pyro-ecophysiology: shifting the paradigm of live wildland fuel research. Fire 1, 8. https://doi.org/10.3390/fire1010008

Julien, Y., Sobrino, J.A., Verhoef, W., 2006. Changes in land surface temperatures and NDVI values over Europe between 1982 and 1999. Remote Sens. Environ. 103, 43–55. https://doi.org/10.1016/j.rse.2006.03.011

Justice, C.O., Giglio, L., Korontzi, S., Owens, J., Morisette, J.T., Roy, D., Descloitres, J., Alleaume, S., Petitcolin, F., Kaufman, Y.J., 2002. The MODIS fire products. Remote Sens. Environ. 83, 244–262. https://doi.org/10.1016/S0034-4257(02)00076-7

Kalma, J.D., McVicar, T.R., McCabe, M.F., 2008. Estimating land surface evaporation: A review of methods using remotely sensed surface temperature data. Surv. Geophys. 29, 421–469. https://doi.org/10.1007/s10712-008-9037-z

Karnieli, A., Agam, N., Pinker, R.T., Anderson, M., Imhoff, M.L., Gutman, G.G., Panov, N.,

Goldberg, A., 2010. Use of NDVI and land surface temperature for drought assessment: merits and limitations. J. Clim. 23, 618–633. https://doi.org/10.1175/2009JCLI2900.1

Keetch, J.J., Byram, G.M., 1968. A Drought Index for Forest Fire Control, U.S.D.A. Forest Service Reseaech Paper SE-38. U.S. Department of Agriculture, Forest Service, Southeastern Forest Experiment Station, Asheville, NC.

Kendall, M.G.., 1975. Rank correlation methods, 4th ed. ed. Oxford University Press, New York.

Kharuk, V.I., Kasischke, E.S., Yakubailik, O.E., 2007. The spatial and temporal distribution of fires on Sakhalin Island, Russia. Int. J. Wildl. Fire 16, 556. https://doi.org/10.1071/WF05009

Khorchani, M., Vicente-Serrano, S.M., Azorín-Molina, C., Garcia, M., Martin-Hernandez, N., Peña-Gallardo, M., El Kenawy, A., Domínguez-Castro, F., 2018. Trends in LST over the peninsular Spain as derived from the AVHRR imagery data. Glob. Planet. Change 166, 75–93. https://doi.org/10.1016/j.gloplacha.2018.04.006

Konings, A.G., Rao, K., Steele-Dunne, S.C., 2019. Macro to micro: microwave remote sensing of plant water content for physiology and ecology. New Phytol. 223, 1166–1172. https://doi.org/10.1111/nph.15808

Kosztra, B., Büttner, G., Hazeu, G., Arnold, S., 2019. Updated CLC illustrated nomenclature guidelines. European Environment Agency, Wien.

Krebs, P., Pezzatti, G.B., Mazzoleni, S., Talbot, L.M., Conedera, M., 2010. Fire regime: history and definition of a key concept in disturbance ecology. Theory Biosci. 129, 53–69. https://doi.org/10.1007/s12064-010-0082-z

Kuhn, M., 2021. caret: Classification and Regression Training.

Lasaponara, R., Santulli, A., Telesca, L., 2005. Time-clustering analysis of forest-fire sequences in southern Italy. Chaos, Solitons & Fractals 24, 139–149. https://doi.org/10.1016/j.chaos.2004.07.025

Lasslop, G., Coppola, A.I., Voulgarakis, A., Yue, C., Veraverbeke, S., 2019. Influence of Fire on the Carbon Cycle and Climate. Curr. Clim. Chang. Reports 5, 112–123. https://doi.org/10.1007/s40641-019-00128-9

Lasslop, G., Kloster, S., 2017. Human impact on wildfires varies between regions and with vegetation productivity. Environ. Res. Lett. 12, 115011. https://doi.org/10.1088/1748-9326/aa8c82

Latham, D., Williams, E., 2001. Lightning and forest fires, in: Johnson, E.A., Miyanishi, K. (Eds.), Forest Fires. Elsevier, pp. 375–418. https://doi.org/10.1016/B978-012386660-8/50013-1

Lavorel, S., Flannigan, M.D., Lambin, E.F., Scholes, M.C., 2006. Vulnerability of land systems to fire: Interactions among humans, climate, the atmosphere, and ecosystems. Mitig.

Adapt. Strateg. Glob. Chang. 12, 33–53. https://doi.org/10.1007/s11027-006-9046-5

Leblon, B., 2005. Monitoring forest fire danger with remote sensing. Nat. Hazards 35, 343–359. https://doi.org/10.1007/s11069-004-1796-3

Leblon, B., Alexander, M.E., Chen, J., White, S., 2001. Monitoring fire danger of northern boreal forests with NOAA-AVHRR NDVI images. Int. J. Remote Sens. 22, 2839–2846. https://doi.org/10.1080/01431160121183

Leblon, B., Kasischke, E., Alexander, M.E., Doyle, M., Abbott, M., 2002. Fire danger monitoring using ERS-1 SAR images in the case of northern boreal forests. Nat. Hazards 27, 231–255. https://doi.org/10.1023/A:1020375721520

Leblon, B., San-Miguel-Ayanz, J., Bourgeau-Chavez, L., Kong, M., 2016. Remote sensing of wildfires, in: Baghdadi, N., Zribi, M. (Eds.), Land Surface Remote Sensing. Elsevier, London, pp. 55–95. https://doi.org/10.1016/B978-1-78548-105-5.50003-7

Lee, K.-S., Kook, M.-J., Shin, J.-I., Kim, S.-H., Kim, T.-G., 2007. Spectral characteristics of forest vegetation in moderate drought condition observed by laboratory measurements and spaceborne hyperspectral data. Photogramm. Eng. Remote Sens. 73, 1121–1127. https://doi.org/10.14358/PERS.73.10.1121

Lehsten, V., Tansey, K., Balzter, H., Thonicke, K., Spessa, A., Weber, U., Smith, B., Arneth, A., 2009. Estimating carbon emissions from African wildfires. Biogeosciences 6, 349–360. https://doi.org/10.5194/bg-6-349-2009

Li, L., Ustin, S.L., Riaño, D., 2007. Retrieval of fresh leaf fuel moisture content using Genetic Algorithm Partial Least Squares (GA-PLS) modeling. IEEE Geosci. Remote Sens. Lett. 4, 216–220. https://doi.org/10.1109/LGRS.2006.888847

Liang, J., Calkin, D.E., Gebert, K.M., Venn, T.J., Silverstein, R.P., 2012. Factors influencing large wildland fire suppression expenditures. Int. J. Wildl. Fire 21, 650–659. https://doi.org/10.1071/wf07010_co

Lindner, M., Maroschek, M., Netherer, S., Kremer, A., Barbati, A., Garcia-Gonzalo, J., Seidl, R., Delzon, S., Corona, P., Kolström, M., Lexer, M.J., Marchetti, M., 2010. Climate change impacts, adaptive capacity, and vulnerability of European forest ecosystems. For. Ecol. Manage. 259, 698–709. https://doi.org/10.1016/j.foreco.2009.09.023

Littell, J.S., Peterson, D.L., Riley, K.L., Liu, Y., Luce, C.H., 2016. A review of the relationships between drought and forest fire in the United States. Glob. Chang. Biol. 22, 2353–2369. https://doi.org/10.1111/gcb.13275

Liu, Y., 2017. Responses of dead forest fuel moisture to climate change. Ecohydrology 10, e1760. https://doi.org/10.1002/eco.1760

Liu, Y., Stanturf, J., Goodrick, S., 2010. Trends in global wildfire potential in a changing climate. For. Ecol. Manage. 259, 685–697. https://doi.org/10.1016/j.foreco.2009.09.002

Liu, Y., Wu, C., Peng, D., Xu, S., Gonsamo, A., Jassal, R.S., Altaf Arain, M., Lu, L., Fang, B.,

Chen, J.M., 2016. Improved modeling of land surface phenology using MODIS land surface reflectance and temperature at evergreen needleleaf forests of central North America. Remote Sens. Environ. 176, 152–162. https://doi.org/10.1016/j.rse.2016.01.021

Lloret, F., Calvo, E., Pons, X., Díaz-Delgado, R., 2002. Wildfires and landscape patterns in the Eastern Iberian Peninsula. Landsc. Ecol. 17, 745–759. https://doi.org/10.1023/A:1022966930861

Lovreglio, R., Leone, V., Giaquinto, P., Notarnicola, A., 2010. Wildfire cause analysis: four case-studies in southern Italy. iForest - Biogeosciences For. 3, 8–15. https://doi.org/10.3832/ifor0521-003

Lozano, F.J., Suárez-Seoane, S., De Luis, E., 2010. Effects of wildfires on environmental variability: a comparative analysis using different spectral indices, patch metrics and thematic resolutions. Landsc. Ecol. 25, 697–710. https://doi.org/10.1007/s10980-010-9453-6

Lu, D., Chen, Q., Wang, G., Liu, L., Li, G., Moran, E., 2016. A survey of remote sensing-based aboveground biomass estimation methods in forest ecosystems. Int. J. Digit. Earth 9, 63–105. https://doi.org/10.1080/17538947.2014.990526

Ma, S., Zhou, Y., Gowda, P.H., Dong, J., Zhang, G., Kakani, V.G., Wagle, P., Chen, L., Flynn, K.C., Jiang, W., 2019. Application of the water-related spectral reflectance indices: A review. Ecol. Indic. 98, 68–79. https://doi.org/10.1016/j.ecolind.2018.10.049

Maffei, C., Alfieri, S.M., Menenti, M., 2018. Relating spatiotemporal patterns of forest fires burned area and duration to diurnal land surface temperature anomalies. Remote Sens. 10, 1777. https://doi.org/10.3390/rs10111777

Maffei, C., Menenti, M., 2019. Predicting forest fires burned area and rate of spread from pre-fire multispectral satellite measurements. ISPRS J. Photogramm. Remote Sens. 158, 263–278. https://doi.org/10.1016/j.isprsjprs.2019.10.013

Maffei, C., Menenti, M., 2014. A MODIS-based perpendicular moisture index to retrieve leaf moisture content of forest canopies. Int. J. Remote Sens. 35, 1829–1845. https://doi.org/10.1080/01431161.2013.879348

Maki, M., Ishiahra, M., Tamura, M., 2004. Estimation of leaf water status to monitor the risk of forest fires by using remotely sensed data. Remote Sens. Environ. 90, 441–450. https://doi.org/10.1016/j.rse.2004.02.002

Mann, H.B., 1945. Nonparametric tests against trend. Econometrica 13, 245–259. https://doi.org/10.2307/1907187

Manzo-Delgado, L., Aguirre-Gómez, R., Álvarez, R., 2004. Multitemporal analysis of land surface temperature using NOAA-AVHRR: preliminary relationships between climatic anomalies and forest fires. Int. J. Remote Sens. 25, 4417–4424. https://doi.org/10.1080/01431160412331269643

Martell, D.L., 2007. Forest fire management, in: Weintraub, A., Romero, C., Bjørndal, T.,

Epstein, R., Miranda, J. (Eds.), Handbook of Operations Research in Natural Resources. Springer US, Boston, MA, pp. 489–509. https://doi.org/10.1007/978-0-387-71815-6_26

Maselli, F., Romanelli, S., Bottai, L., Zipoli, G., 2003. Use of NOAA-AVHRR NDVI images for the estimation of dynamic fire risk in Mediterranean areas. Remote Sens. Environ. 86, 187–197. https://doi.org/10.1016/S0034-4257(03)00099-3

Masuoka, E., Fleig, A., Wolfe, R.E., Patt, F., 1998. Key characteristics of MODIS data products. IEEE Trans. Geosci. Remote Sens. 36, 1313–1323. https://doi.org/10.1109/36.701081

Matin, M.A., Chitale, V.S., Murthy, M.S.R., Uddin, K., Bajracharya, B., Pradhan, S., 2017. Understanding forest fire patterns and risk in Nepal using remote sensing, geographic information system and historical fire data. Int. J. Wildl. Fire 26, 276–286. https://doi.org/10.1071/WF16056

Matthews, S., 2014. Dead fuel moisture research: 1991–2012. Int. J. Wildl. Fire 23, 78–92. https://doi.org/10.1071/WF13005

Mazzetti, P., Nativi, S., Angelini, V., Verlato, M., Fiorucci, P., 2009. A grid platform for the European Civil Protection e-Infrastructure: the forest fires use scenario. Earth Sci. Informatics 2, 53–62. https://doi.org/10.1007/s12145-009-0025-8

McArthur, A.G., 1967. Fire behaviour in Eucalypt forests. Australia Forestry and Timber Bureau, Canberra.

McFarlane, B.L., McGee, T.K., Faulkner, H., 2011. Complexity of homeowner wildfire risk mitigation: an integration of hazard theories. Int. J. Wildl. Fire 20, 921–931. https://doi.org/10.1071/WF10096

Menenti, M., Azzali, S., Verhoef, W., van Swol, R., 1993. Mapping agroecological zones and time lag in vegetation growth by means of Fourier analysis of time series of NDVI images. Adv. Sp. Res. 13, 233–237. https://doi.org/10.1016/0273-1177(93)90550-U

Menenti, M., Malamiri, H.R.G., Shang, H., Alfieri, S.M., Maffei, C., Jia, L., 2016. Observing the response of terrestrial vegetation to climate variability across a range of time scales by time series analysis of land surface temperature, in: Ban, Y. (Ed.), Multitemporal Remote Sensing. Springer International Publishing, Cham, pp. 277–315. https://doi.org/10.1007/978-3-319-47037-5_14

Merzouki, A., Leblon, B., 2011. Mapping fuel moisture codes using MODIS images and the Getis statistic over western Canada grasslands. Int. J. Remote Sens. 32, 1619–1634. https://doi.org/10.1080/01431160903586773

Mhawej, M., Faour, G., Adjizian-Gerard, J., 2015. Wildfire likelihood's elements: A literature review. Challenges 6, 282–293. https://doi.org/10.3390/challe6020282

Michetti, M., Pinar, M., 2019. Forest fires across Italian regions and implications for climate change: A panel data analysis. Environ. Resour. Econ. 72, 207–246. https://doi.org/10.1007/s10640-018-0279-z

Milazzo, A., Capone, M., 2010. Incendi Boschivi 2009. Corpo Forestale dello Stato, Rome.

Miller, C., Ager, A.A., 2013. A review of recent advances in risk analysis for wildfire management. Int. J. Wildl. Fire 22, 1–14. https://doi.org/10.1071/WF11114

Minas, J.P., Hearne, J.W., Handmer, J.W., 2012. A review of operations research methods applicable to wildfire management. Int. J. Wildl. Fire 21, 189–196. https://doi.org/10.1071/WF10129

Modugno, S., Balzter, H., Cole, B., Borrelli, P., 2016. Mapping regional patterns of large forest fires in wildland-urban Interface areas in Europe. J. Environ. Manage. 172, 112–126. https://doi.org/10.1016/j.jenvman.2016.02.013

Mohamed Shaluf, I., 2008. Technological disaster stages and management. Disaster Prev. Manag. An Int. J. 17, 114–126. https://doi.org/10.1108/09653560810855928

Molod, A., Takacs, L., Suarez, M., Bacmeister, J., 2015. Development of the GEOS-5 atmospheric general circulation model: evolution from MERRA to MERRA2. Geosci. Model Dev. 8, 1339–1356. https://doi.org/10.5194/gmd-8-1339-2015

Montagné-Huck, C., Brunette, M., 2018. Economic analysis of natural forest disturbances: A century of research. J. For. Econ. 32, 42–71. https://doi.org/10.1016/j.jfe.2018.03.002

Moreira, F., Catry, F.X., Rego, F., Bacao, F., 2010. Size-dependent pattern of wildfire ignitions in Portugal: when do ignitions turn into big fires? Landsc. Ecol. 25, 1405–1417. https://doi.org/10.1007/s10980-010-9491-0

Moreira, F., Vaz, P., Catry, F., Silva, J.S., 2009. Regional variations in wildfire susceptibility of land-cover types in Portugal: implications for landscape management to minimize fire hazard. Int. J. Wildl. Fire 18, 563–574. https://doi.org/10.1071/WF07098

Moreira, F., Viedma, O., Arianoutsou, M., Curt, T., Koutsias, N., Rigolot, E., Barbati, A., Corona, P., Vaz, P., Xanthopoulos, G., Mouillot, F., Bilgili, E., 2011. Landscape-wildfire interactions in southern Europe: Implications for landscape management. J. Environ. Manage. 92, 2389–2402. https://doi.org/10.1016/j.jenvman.2011.06.028

Moreno, J.M., Viedma, O., Zavala, G., Luna, B., 2011. Landscape variables influencing forest fires in central Spain. Int. J. Wildl. Fire 20, 678–689. https://doi.org/10.1071/WF10005

Morgan, P., Hardy, C.C., Swetnam, T.W., Rollins, M.G., Long, D.G., 2001. Mapping fire regimes across time and space: Understanding coarse and fine-scale fire patterns. Int. J. Wildl. Fire 10, 329–342. https://doi.org/10.1071/WF01032

Moritz, M.A., 1997. Analyzing Extreme disturbance events: Fire in Los Padres National Forest. Ecol. Appl. 7, 1252–1262. https://doi.org/10.2307/2641212

Mouillot, F., Ratte, J.-P., Joffre, R., Moreno, J.M., Rambal, S., 2003. Some determinants of the spatio-temporal fire cycle in a mediterranean landscape (Corsica, France). Landsc. Ecol. 18, 665–674. https://doi.org/10.1023/B:LAND.0000004182.22525.a9

Mousivand, A., Menenti, M., Gorte, B., Verhoef, W., 2014. Global sensitivity analysis of the spectral radiance of a soil–vegetation system. Remote Sens. Environ. 145, 131–144. https://doi.org/10.1016/j.rse.2014.01.023

Nelson, R.M., 2000. Prediction of diurnal change in 10-h fuel stick moisture content. Can. J. For. Res. 30, 1071–1087. https://doi.org/10.1139/x00-032

Nemani, R.R., Running, S.W., 1989. Estimation of regional surface resistance to evapotranspiration from NDVI and thermal-IR AVHRR data. J. Appl. Meteorol. 28, 276–284. https://doi.org/10.1175/1520-0450(1989)028<0276:EORSRT>2.0.CO;2

Nicholls, N., Lucas, C., 2007. Interannual variations of area burnt in Tasmanian bushfires: relationships with climate and predictability. Int. J. Wildl. Fire 16, 540–546. https://doi.org/10.1071/WF06125

Nieto, H., Aguado, I., Chuvieco, E., Sandholt, I., 2010. Dead fuel moisture estimation with MSG–SEVIRI data. Retrieval of meteorological data for the calculation of the equilibrium moisture content. Agric. For. Meteorol. 150, 861–870. https://doi.org/10.1016/j.agrformet.2010.02.007

Noble, I.R., Bary, G.A. V., Gill, A.M., 1980. McArthur's fire-danger meters expressed as equations. Austral Ecol. 5, 201–203. https://doi.org/10.1111/j.1442-9993.1980.tb01243.x

Nolan, R.H., Boer, M.M., Resco de Dios, V., Caccamo, G., Bradstock, R.A., 2016a. Large-scale, dynamic transformations in fuel moisture drive wildfire activity across southeastern Australia. Geophys. Res. Lett. 43, 4229–4238. https://doi.org/10.1002/2016GL068614

Nolan, R.H., Hedo, J., Arteaga, C., Sugai, T., Resco de Dios, V., 2018. Physiological drought responses improve predictions of live fuel moisture dynamics in a Mediterranean forest. Agric. For. Meteorol. 263, 417–427. https://doi.org/10.1016/j.agrformet.2018.09.011

Nolan, R.H., Resco de Dios, V., Boer, M.M., Caccamo, G., Goulden, M.L., Bradstock, R.A., 2016b. Predicting dead fine fuel moisture at regional scales using vapour pressure deficit from MODIS and gridded weather data. Remote Sens. Environ. 174, 100–108. https://doi.org/10.1016/j.rse.2015.12.010

North, M.P., Stephens, S.L., Collins, B.M., Agee, J.K., Aplet, G., Franklin, J.F., Fulé, P.Z., 2015. Reform forest fire management. Science (80-.). 349, 1280–1281. https://doi.org/10.1126/science.aab2356

Oliveira, S., Laneve, G., Fusilli, L., Eftychidis, G., Nunes, A., Lourenço, L., Sebastián-López, A., 2017. A common approach to foster prevention and recovery of forest fires in Mediterranean Europe, in: Fuerst-Bjeliš, B. (Ed.), Mediterranean Identities - Environment, Society, Culture. IntechOpen, London, pp. 337–361. https://doi.org/10.5772/intechopen.68948

Oliveira, S., Moreira, F., Boca, R., San-Miguel-Ayanz, J., Pereira, J.M.C., 2014. Assessment of

fire selectivity in relation to land cover and topography: a comparison between Southern European countries. Int. J. Wildl. Fire 23, 620–630. https://doi.org/10.1071/WF12053

Oliveira, S., Oehler, F., San-Miguel-Ayanz, J., Camia, A., Pereira, J.M.C., 2012. Modeling spatial patterns of fire occurrence in Mediterranean Europe using Multiple Regression and Random Forest. For. Ecol. Manage. 275, 117–129. https://doi.org/10.1016/j.foreco.2012.03.003

Palma, C.D., Cui, W., Martell, D.L., Robak, D., Weintraub, A., 2007. Assessing the impact of stand-level harvests on the flammability of forest landscapes. Int. J. Wildl. Fire 16, 584–592. https://doi.org/10.1071/WF06116

Pan, J., Wang, W., Li, J., 2016. Building probabilistic models of fire occurrence and fire risk zoning using logistic regression in Shanxi Province, China. Nat. Hazards 81, 1879–1899. https://doi.org/10.1007/s11069-016-2160-0

Papadopoulos, G.D., Pavlidou, F.-N., 2011. A comparative review on wildfire simulators. IEEE Syst. J. 5, 233–243. https://doi.org/10.1109/JSYST.2011.2125230

Parisien, M.-A., Moritz, M.A., 2009. Environmental controls on the distribution of wildfire at multiple spatial scales. Ecol. Monogr. 79, 127–154. https://doi.org/10.1890/07-1289.1

Parker, R.J., Boesch, H., Wooster, M.J., Moore, D.P., Webb, A.J., Gaveau, D., Murdiyarso, D., 2016. Atmospheric CH4 and CO2 enhancements and biomass burning emission ratios derived from satellite observations of the 2015 Indonesian fire plumes. Atmos. Chem. Phys. 16, 10111–10131. https://doi.org/10.5194/acp-16-10111-2016

Parra, A., Moreno, J.M., 2017. Post-fire environments are favourable for plant functioning of seeder and resprouter Mediterranean shrubs, even under drought. New Phytol. 214, 1118–1131. https://doi.org/10.1111/nph.14454

Parson, A., Robichaud, P.R., Lewis, S.A., Napper, C., Clark, J.T., 2010. Field guide for mapping post-fire soil burn severity. Fort Collins. https://doi.org/10.2737/RMRS-GTR-243

Pausas, J.G., Llovet, J., Rodrigo, A., Vallejo, R., 2008. Are wildfires a disaster in the Mediterranean basin? – A review. Int. J. Wildl. Fire 17, 713. https://doi.org/10.1071/WF07151

Pausas, J.G., Paula, S., 2012. Fuel shapes the fire-climate relationship: evidence from Mediterranean ecosystems. Glob. Ecol. Biogeogr. 21, 1074–1082. https://doi.org/10.1111/j.1466-8238.2012.00769.x

Pausas, J.G., Ribeiro, E., 2013. The global fire-productivity relationship. Glob. Ecol. Biogeogr. 22, 728–736. https://doi.org/10.1111/geb.12043

Pellegrini, A.F.A., Ahlström, A., Hobbie, S.E., Reich, P.B., Nieradzik, L.P., Staver, A.C., Scharenbroch, B.C., Jumpponen, A., Anderegg, W.R.L., Randerson, J.T., Jackson, R.B., 2018. Fire frequency drives decadal changes in soil carbon and nitrogen and ecosystem productivity. Nature 553, 194–198. https://doi.org/10.1038/nature24668

Pellizzaro, G., Cesaraccio, C., Duce, P., Ventura, A., Zara, P., 2007a. Relationships between seasonal patterns of live fuel moisture and meteorological drought indices for Mediterranean shrubland species. Int. J. Wildl. Fire 16, 232–241. https://doi.org/10.1071/WF06081

Pellizzaro, G., Duce, P., Ventura, A., Zara, P., 2007b. Seasonal variations of live moisture content and ignitability in shrubs of the Mediterranean Basin. Int. J. Wildl. Fire 16, 633–641. https://doi.org/10.1071/WF05088

Peñuelas, J., Filella, I., Biel, C., Serrano, L., Savé, R., 1993. The reflectance at the 950–970 nm region as an indicator of plant water status. Int. J. Remote Sens. 14, 1887–1905. https://doi.org/10.1080/01431169308954010

Peñuelas, J., Piñol, J., Ogaya, R., Filella, I., 1997. Estimation of plant water concentration by the reflectance Water Index WI (R900/R970). Int. J. Remote Sens. 18, 2869–2875. https://doi.org/10.1080/014311697217396

Pimont, F., Ruffault, J., Martin-StPaul, N.K., Dupuy, J.-L., 2019. Why is the effect of live fuel moisture content on fire rate of spread underestimated in field experiments in shrublands? Int. J. Wildl. Fire 28, 127–137. https://doi.org/10.1071/WF18091

Piñol, J., Filella, I., Ogaya, R., Peñuelas, J., 1998. Ground-based spectroradiometric estimation of live fine fuel moisture of Mediterranean plants. Agric. For. Meteorol. 90, 173–186. https://doi.org/10.1016/S0168-1923(98)00053-7

Podschwit, H.R., Larkin, N.K., Steel, E.A., Cullen, A., Alvarado, E., 2018. Multi-model forecasts of very-large fire occurences during the end of the 21st century. Climate 6, 100. https://doi.org/10.3390/cli6040100

Pohlert, T., 2020. trend: Non-parametric trend tests and change-point detection.

Preisler, H.K., Brillinger, D.R., Burgan, R.E., Benoit, J.W., 2004. Probability based models for estimation of wildfire risk. Int. J. Wildl. Fire 13, 133–142. https://doi.org/10.1071/WF02061

Preisler, H.K., Burgan, R.E., Eidenshink, J.C., Klaver, J.M., Klaver, R.W., 2009. Forecasting distributions of large federal-lands fires utilizing satellite and gridded weather information. Int. J. Wildl. Fire 18, 508516. https://doi.org/10.1071/WF08032

Pugh, T.A.M., Arneth, A., Kautz, M., Poulter, B., Smith, B., 2019. Important role of forest disturbances in the global biomass turnover and carbon sinks. Nat. Geosci. 12, 730–735. https://doi.org/10.1038/s41561-019-0427-2

Pyne, S.J., Andrews, P.L., Laven, R.D., 1996. Introduction to Wildland Fire, 2nd ed. John Wiley & Sons, Inc., New York.

QGIS Development Team, 2021. QGIS Geographic Information System.

Quan, X., He, B., Li, X., Liao, Z., 2016. Retrieval of grassland live fuel moisture content by parameterizing radiative transfer model with interval estimated LAI. IEEE J. Sel. Top. Appl. Earth Obs. Remote Sens. 9, 910–920.

https://doi.org/10.1109/JSTARS.2015.2472415

Quan, X., He, B., Li, X., Tang, Z., 2015. Estimation of grassland live fuel moisture content from ratio of canopy water content and foliage dry biomass. IEEE Geosci. Remote Sens. Lett. 12, 1903–1907. https://doi.org/10.1109/LGRS.2015.2437391

Quintano, C., Fernández-Manso, A., Calvo, L., Marcos, E., Valbuena, L., 2015. Land surface temperature as potential indicator of burn severity in forest Mediterranean ecosystems. Int. J. Appl. Earth Obs. Geoinf. 36, 1–12. https://doi.org/10.1016/j.jag.2014.10.015

Quintano, C., Fernandez-Manso, A., Roberts, D.A., 2017. Burn severity mapping from Landsat MESMA fraction images and Land Surface Temperature. Remote Sens. Environ. 190, 83–95. https://doi.org/10.1016/j.rse.2016.12.009

R Core Team, 2020. R: A language and environment for statistical computing.

Reed, W.J., McKelvey, K.S., 2002. Power-law behaviour and parametric models for the size-distribution of forest fires. Ecol. Modell. 150, 239–254. https://doi.org/10.1016/S0304-3800(01)00483-5

Reisen, F., Duran, S.M., Flannigan, M., Elliott, C., Rideout, K., 2015. Wildfire smoke and public health risk. Int. J. Wildl. Fire 24, 1029–1044. https://doi.org/10.1071/WF15034

Riaño, D., Vaughan, P., Chuvieco, E., Zarco-Tejada, P.J., Ustin, S.L., 2005. Estimation of fuel moisture content by inversion of radiative transfer models to simulate equivalent water thickness and dry matter content: Analysis at leaf and canopy level. IEEE Trans. Geosci. Remote Sens. 43, 819–826. https://doi.org/10.1109/TGRS.2005.843316

Richards, J.A., 2013. Remote Sensing Digital Image Analysis. Springer Berlin Heidelberg, Berlin, Heidelberg. https://doi.org/10.1007/978-3-642-30062-2

Richardson, A.J., Wiegand, C.L., 1977. Distinguishing vegetation from soil background information. Photogramm. Eng. Remote Sens. 43, 1541–1552.

Ricotta, C., Arianoutsou, M., Díaz-Delgado, R., Duguy, B., Lloret, F., Maroudi, E., Mazzoleni, S., Moreno, J.M., Rambal, S., Vallejo, R., Vázquez, A., 2001. Self-organized criticality of wildfires ecologically revisited. Ecol. Modell. 141, 307–311. https://doi.org/10.1016/S0304-3800(01)00272-1

Ricotta, C., Avena, G., Marchetti, M., 1999. The flaming sandpile: self-organized criticality and wildfires. Ecol. Modell. 119, 73–77. https://doi.org/10.1016/S0304-3800(99)00057-5

Ricotta, C., Micozzi, L., Bellelli, M., Mazzoleni, S., 2006. Characterizing self-similar temporal clustering of wildfires in the Cilento National Park (Southern Italy). Ecol. Modell. 197, 512–515. https://doi.org/10.1016/j.ecolmodel.2006.03.029

Rodrigues, M., Costafreda-Aumedes, S., Comas, C., Vega-García, C., 2019. Spatial stratification of wildfire drivers towards enhanced definition of large-fire regime zoning and fire seasons. Sci. Total Environ. 689, 634–644.

https://doi.org/10.1016/j.scitotenv.2019.06.467

Rodríguez y Silva, F., Molina Martínez, J.R., González-Cabán, A., 2014. A methodology for determining operational priorities for prevention and suppression of wildland fires. Int. J. Wildl. Fire 23, 544. https://doi.org/10.1071/WF13063

Roerink, G.J., Menenti, M., Soepboer, W., Su, Z., 2003. Assessment of climate impact on vegetation dynamics by using remote sensing. Phys. Chem. Earth 28, 103–109. https://doi.org/10.1016/S1474-7065(03)00011-1

Roerink, G.J., Menenti, M., Verhoef, W., 2000. Reconstructing cloudfree NDVI composites using Fourier analysis of time series. Int. J. Remote Sens. 21, 1911–1917. https://doi.org/10.1080/014311600209814

Rollins, M.G., Morgan, P., Swetnam, T., 2002. Landscape-scale controls over 20th century fire occurrence in two large Rocky Mountain (USA) wilderness areas. Landsc. Ecol. 17, 539–557. https://doi.org/10.1023A:1021584519109

Rossa, C.G., Fernandes, P.M., 2017. On the effect of live fuel moisture content on fire-spread rate. For. Syst. 26, eSC08. https://doi.org/10.5424/fs/2017263-12019

Rossa, C.G., Veloso, R., Fernandes, P.M., 2016. A laboratory-based quantification of the effect of live fuel moisture content on fire spread rate. Int. J. Wildl. Fire 25, 569–573. https://doi.org/10.1071/WF15114

Rothermel, R.C., 1991. Predicting behavior and size of crown fires in the northern Rocky Mountains. U.S. Department of Agriculture, Forest Service, Ogden. https://doi.org/10.2737/INT-RP-438

Rothermel, R.C., 1972. A mathematical model to predicting fire spread in wildland fuels. Odgen.

Ruffault, J., Martin-StPaul, N., Pimont, F., Dupuy, J.-L., 2018. How well do meteorological drought indices predict live fuel moisture content (LFMC)? An assessment for wildfire research and operations in Mediterranean ecosystems. Agric. For. Meteorol. 262, 391–401. https://doi.org/10.1016/j.agrformet.2018.07.031

Ruffault, J., Mouillot, F., 2017. Contribution of human and biophysical factors to the spatial distribution of forest fire ignitions and large wildfires in a French Mediterranean region. Int. J. Wildl. Fire 26, 498–508. https://doi.org/10.1071/WF16181

Saatchi, S.S., Moghaddam, M., 2000. Estimation of crown and stem water content and biomass of boreal forest using polarimetric SAR imagery. IEEE Trans. Geosci. Remote Sens. 38, 697–709. https://doi.org/10.1109/36.841999

Salis, M., Arca, B., Alcasena-Urdiroz, F., Massaiu, A., Bacciu, V., Bosseur, F., Caramelle, P., Dettori, S., Fernandes de Oliveira, A.S., Molina-Terren, D., Pellizzaro, G., Santoni, P.-A., Spano, D., Vega-Garcia, C., Duce, P., 2019. Analyzing the recent dynamics of wildland fires in Quercus suber L. woodlands in Sardinia (Italy), Corsica (France) and Catalonia (Spain). Eur. J. For. Res. 138, 415–431. https://doi.org/10.1007/s10342-019-01179-1

San-Miguel-Ayanz, J., Barbosa, P., Schmuck, G., Liberta, G., Schulte, E., 2002. Towards a coherent forest fire information system in Europe: The European Forest Fire Information System (EFFIS), in: Viegas, D.X. (Ed.), Forest Fire Research & Wildland Fire Safety. Millpress, Coimbra, p. 13.

San-Miguel-Ayanz, J., Durrant, T., Boca, R., Libertà, G., Branco, A., de Rigo, D., Ferrari, D., Maianti, P., Artés Vivancos, T., Costa, H., Lana, F., Löffler, P., Nuijten, D., Ahlgren, A.C., Leray, T., 2018. Forest Fires in Europe, Middle East and North Africa 2017. Luxembourg. https://doi.org/10.2760/663443

San-Miguel-Ayanz, J., Durrant, T., Boca, R., Libertà, G., Branco, A., de Rigo, D., Ferrari, D., Maianti, P., Artés Vivancos, T., Oom, D., Pfeiffer, H., Nuijten, D., Leray, T., 2019. Forest Fires in Europe, Middle East and North Africa 2018. Ispra. https://doi.org/10.2760/1128

San-Miguel-Ayanz, J., Moreno, J.M., Camia, A., 2013. Analysis of large fires in European Mediterranean landscapes: Lessons learned and perspectives. For. Ecol. Manage. 294, 11–22. https://doi.org/10.1016/j.foreco.2012.10.050

San-Miguel-Ayanz, J., Schulte, E., Schmuck, G., Camia, A., Strobl, P., Liberta, G., Giovando, C., Boca, R., Sedano, F., Kempeneers, P., McInerney, D., Withmore, C., de Oliveira, S.S., Rodrigues, M., Durrant, T., Corti, P., Oehler, F., Vilar, L., Amatulli, G., 2012. Comprehensive Monitoring of Wildfires in Europe: The European Forest Fire Information System (EFFIS), in: Tiefenbacher, J. (Ed.), Approaches to Managing Disaster - Assessing Hazards, Emergencies and Disaster Impacts. InTech, Rijeka, pp. 87–108. https://doi.org/10.5772/28441

Saura-Mas, S., Lloret, F., 2007. Leaf and shoot water content and leaf dry matter content of Mediterranean woody species with different post-fire regenerative strategies. Ann. Bot. 99, 545–554. https://doi.org/10.1093/aob/mcl284

Schlobohm, P., Brain, J., 2002. Gaining an understanding of the National Fire Danger Rating System. National Wildfire Coordinating Group, Boise.

Schroeder, W., Oliva, P., Giglio, L., Csiszar, I.A., 2014. The new VIIRS 375 m active fire detection data product: Algorithm description and initial assessment. Remote Sens. Environ. 143, 85–96. https://doi.org/10.1016/j.rse.2013.12.008

Schulze, E.-D., Lange, O.L., Kappen, L., Buschbom, U., Evenari, M., 1973. Stomatal responses to changes in temperature at increasing water stress. Planta 110, 29–42. https://doi.org/10.1007/BF00386920

Schunk, C., Leuchner, M., Menzel, A., 2014. Evaluation of a system for automatic dead fine fuel moisture measurements, in: Advances in Forest Fire Research. Imprensa da Universidade de Coimbra, pp. 1115–1123. https://doi.org/10.14195/978-989-26-0884-6_121

Schunk, C., Wastl, C., Leuchner, M., Menzel, A., 2017. Fine fuel moisture for site- and species-specific fire danger assessment in comparison to fire danger indices. Agric. For. Meteorol. 234–235, 31–47. https://doi.org/10.1016/j.agrformet.2016.12.007

Seelig, H. -D., Hoehn, A., Stodieck, L.S., Klaus, D.M., Adams III, W.W., Emery, W.J., 2008. The assessment of leaf water content using leaf reflectance ratios in the visible, near-, and short-wave-infrared. Int. J. Remote Sens. 29, 3701–3713. https://doi.org/10.1080/01431160701772500

Seidl, R., Schelhaas, M.-J., Rammer, W., Verkerk, P.J., 2014. Increasing forest disturbances in Europe and their impact on carbon storage. Nat. Clim. Chang. 4, 806–810. https://doi.org/10.1038/nclimate2318

Seidl, R., Thom, D., Kautz, M., Martin-Benito, D., Peltoniemi, M., Vacchiano, G., Wild, J., Ascoli, D., Petr, M., Honkaniemi, J., Lexer, M.J., Trotsiuk, V., Mairota, P., Svoboda, M., Fabrika, M., Nagel, T.A., Reyer, C.P.O., 2017. Forest disturbances under climate change. Nat. Clim. Chang. 7, 395–402. https://doi.org/10.1038/nclimate3303

Sen, P.K., 1968. Estimates of the regression coefficient based on Kendall's tau. J. Am. Stat. Assoc. 63, 1379–1389. https://doi.org/10.1080/01621459.1968.10480934

Shive, K.L., Sieg, C.H., Fulé, P.Z., 2013. Pre-wildfire management treatments interact with fire severity to have lasting effects on post-wildfire vegetation response. For. Ecol. Manage. 297, 75–83. https://doi.org/10.1016/j.foreco.2013.02.021

Sirca, C., Salis, M., Arca, B., Duce, P., Spano, D., 2018. Assessing the performance of fire danger indexes in a Mediterranean area. iForest - Biogeosciences For. 11, 563–571. https://doi.org/10.3832/ifor2679-011

Slijepcevic, A., Anderson, W.R., Matthews, S., Anderson, D.H., 2015. Evaluating models to predict daily fine fuel moisture content in eucalypt forest. For. Ecol. Manage. 335, 261–269. https://doi.org/10.1016/j.foreco.2014.09.040

Slingsby, J.A., Moncrieff, G.R., Wilson, A.M., 2020. Near-real time forecasting and change detection for an open ecosystem with complex natural dynamics. ISPRS J. Photogramm. Remote Sens. 166, 15–25. https://doi.org/10.1016/j.isprsjprs.2020.05.017

Smith, A.M.S., Wooster, M.J., 2005. Remote classification of head and backfire types from MODIS fire radiative power and smoke plume observations. Int. J. Wildl. Fire 14, 249–254. https://doi.org/10.1071/WF05012

Sobrino, J.A., Del Frate, F., Drusch, M., Jiménez-Muñoz, J.C., Manunta, P., Regan, A., 2016. Review of thermal infrared applications and requirements for future high-resolution sensors. IEEE Trans. Geosci. Remote Sens. 54, 2963–2972. https://doi.org/10.1109/TGRS.2015.2509179

Sow, M., Mbow, C., Hély, C., Fensholt, R., Sambou, B., 2013. Estimation of herbaceous fuel moisture content using vegetation indices and land surface temperature from MODIS data. Remote Sens. 5, 2617–2638. https://doi.org/10.3390/rs5062617

Stephenson, A.G., 2002. evd: Extreme Value Distributions. R News 2.

Stevens-Rumann, C.S., Kemp, K.B., Higuera, P.E., Harvey, B.J., Rother, M.T., Donato, D.C., Morgan, P., Veblen, T.T., 2018. Evidence for declining forest resilience to wildfires

under climate change. Ecol. Lett. 21, 243–252. https://doi.org/10.1111/ele.12889

Stow, D., Niphadkar, M., Kaiser, J., 2006. Time series of chaparral live fuel moisture maps derived from MODIS satellite data. Int. J. Wildl. Fire 15, 347–360. https://doi.org/10.1071/WF05060

Stroppiana, D., Antoninetti, M., Brivio, P.A., 2014. Seasonality of MODIS LST over Southern Italy and correlation with land cover, topography and solar radiation. Eur. J. Remote Sens. 47, 133–152. https://doi.org/10.5721/EuJRS20144709

Swift, L.W., Swank, W.T., Mankin, J.B., Luxmoore, R.J., Goldstein, R.A., 1975. Simulation of evapotranspiration and drainage from mature and clear-cut deciduous forests and young pine plantation. Water Resour. Res. 11, 667–673. https://doi.org/10.1029/WR011i005p00667

Syphard, A.D., Sheehan, T., Rustigian-Romsos, H., Ferschweiler, K., 2018. Mapping future fire probability under climate change: Does vegetation matter? PLoS One 13, e0201680. https://doi.org/10.1371/journal.pone.0201680

Tanase, M.A., Panciera, R., Lowell, K., Aponte, C., 2015. Monitoring live fuel moisture in semiarid environments using L-band radar data. Int. J. Wildl. Fire 24, 560–572. https://doi.org/10.1071/WF14149

Tansey, K., Grégoire, J.-M., Stroppiana, D., Sousa, A., Silva, J., Pereira, J.M.C., Boschetti, L., Maggi, M., Brivio, P.A., Fraser, R., Flasse, S., Ershov, D., Binaghi, E., Graetz, D., Peduzzi, P., 2004. Vegetation burning in the year 2000: Global burned area estimates from SPOT VEGETATION data. J. Geophys. Res. 109, D14S03. https://doi.org/10.1029/2003JD003598

Taylor, S.W., Alexander, M.E., 2006. Science, technology, and human factors in fire danger rating: the Canadian experience. Int. J. Wildl. Fire 15, 121–135. https://doi.org/10.1071/WF05021

Telesca, L., Amatucci, G., Lasaponara, R., Lovallo, M., Rodrigues, M.J., 2007a. Space–time fractal properties of the forest-fire series in central Italy. Commun. Nonlinear Sci. Numer. Simul. 12, 1326–1333. https://doi.org/10.1016/j.cnsns.2005.12.003

Telesca, L., Amatulli, G., Lasaponara, R., Lovallo, M., Santulli, A., 2007b. Identifying spatial clustering properties of the 1997–2003 Liguria (Northern Italy) forest-fire sequence. Chaos, Solitons & Fractals 32, 1364–1370. https://doi.org/10.1016/j.chaos.2005.11.075

Telesca, L., Amatulli, G., Lasaponara, R., Lovallo, M., Santulli, A., 2005. Time-scaling properties in forest-fire sequences observed in Gargano area (southern Italy). Ecol. Modell. 185, 531–544. https://doi.org/10.1016/j.ecolmodel.2005.01.009

Telesca, L., Lasaponara, R., 2010. Analysis of time-scaling properties in forest-fire sequence observed in Italy. Ecol. Modell. 221, 90–93. https://doi.org/10.1016/j.ecolmodel.2009.01.019

Telesca, L., Lasaponara, R., 2006. Emergence of temporal regimes in fire sequences. Phys.

A Stat. Mech. its Appl. 360, 543–547. https://doi.org/10.1016/j.physa.2005.04.045

Thompson, M.P., Haas, J.R., Gilbertson-Day, J.W., Scott, J.H., Langowski, P., Bowne, E., Calkin, D.E., 2015. Development and application of a geospatial wildfire exposure and risk calculation tool. Environ. Model. Softw. 63, 61–72. https://doi.org/10.1016/j.envsoft.2014.09.018

Thonicke, K., Venevsky, S., Sitch, S., Cramer, W., 2008. The role of fire disturbance for global vegetation dynamics: coupling fire into a Dynamic Global Vegetation Model. Glob. Ecol. Biogeogr. 10, 661–677. https://doi.org/10.1046/j.1466-822X.2001.00175.x

Tien Bui, D., Thi Le, K.-T., Nguyen, V.C., Le, H.D., Revhaug, I., 2016. Tropical forest fire Susceptibility Mapping at the Cat Ba National Park area, Hai Phong City, Vietnam, using GIS-based kernel logistic regression. Remote Sens. 8, 347. https://doi.org/10.3390/rs8040347

Tøttrup, C., 2014. EU-DEM statistical validation report. European Environment Agency, Copenhagen.

Trenberth, K.E., Dai, A., van der Schrier, G., Jones, P.D., Barichivich, J., Briffa, K.R., Sheffield, J., 2014. Global warming and changes in drought. Nat. Clim. Chang. 4, 17–22. https://doi.org/10.1038/nclimate2067

Tucker, C.J., 1980. Remote sensing of leaf water content in the near infrared. Remote Sens. Environ. 10, 23–32. https://doi.org/10.1016/0034-4257(80)90096-6

Tuia, D., Lasaponara, R., Telesca, L., Kanevski, M., 2008. Emergence of spatio-temporal patterns in forest-fire sequences. Phys. A Stat. Mech. its Appl. 387, 3271–3280. https://doi.org/10.1016/j.physa.2008.01.057

Tuia, D., Lasaponara, R., Telesca, L., Kanevski, M., 2007. Identifying spatial clustering phenomena in forest-fire sequences. Phys. A Stat. Mech. its Appl. 376, 596–600. https://doi.org/10.1016/j.physa.2006.10.102

Turco, M., Bedia, J., Di Liberto, F., Fiorucci, P., von Hardenberg, J., Koutsias, N., Llasat, M.-C., Xystrakis, F., Provenzale, A., 2016. Decreasing fires in Mediterranean Europe. PLoS One 11, e0150663. https://doi.org/10.1371/journal.pone.0150663

Turco, M., Llasat, M.C., von Hardenberg, J., Provenzale, A., 2013. Impact of climate variability on summer fires in a Mediterranean environment (northeastern Iberian Peninsula). Clim. Change 116, 665–678. https://doi.org/10.1007/s10584-012-0505-6

Ullah, S., Skidmore, A.K., Ramoelo, A., Groen, T.A., Naeem, M., Ali, A., 2014. Retrieval of leaf water content spanning the visible to thermal infrared spectra. ISPRS J. Photogramm. Remote Sens. 93, 56–64. https://doi.org/10.1016/j.isprsjprs.2014.04.005

Ustin, S.L., Riaño, D., Koltunov, A., Roberts, D.A., Dennison, P.E., 2009. Mapping fire risk in Mediterranean ecosystems of California: vegetation type, density, invasive species, and fire frequency, in: Earth Observation of Wildland Fires in Mediterranean Ecosystems. Springer Berlin Heidelberg, Berlin, Heidelberg, pp. 41–53. https://doi.org/10.1007/978-3-642-01754-4_4

Vacchiano, G., Foderi, C., Berretti, R., Marchi, E., Motta, R., 2018. Modeling anthropogenic and natural fire ignitions in an inner-alpine valley. Nat. Hazards Earth Syst. Sci. 18, 935–948. https://doi.org/10.5194/nhess-18-935-2018

Vakalis, D., Sarimveis, H., Kiranoudis, C.T., Alexandridis, A., Bafas, G., 2004. A GIS based operational system for wildland fire crisis management II. System architecture and case studies. Appl. Math. Model. 28, 411–425. https://doi.org/10.1016/j.apm.2003.10.006

van der Werf, G.R., Randerson, J.T., Giglio, L., Collatz, G.J., Mu, M., Kasibhatla, P.S., Morton, D.C., Defries, R.S., Jin, Y., van Leeuwen, T.T., 2010. Global fire emissions and the contribution of deforestation, savanna, forest, agricultural, and peat fires (1997-2009). Atmos. Chem. Phys. 10, 11707–11735. https://doi.org/10.5194/acp-10-11707-2010

Van Nguyen, O., Kawamura, K., Trong, D.P., Gong, Z., Suwandana, E., 2015. Temporal change and its spatial variety on land surface temperature and land use changes in the Red River Delta, Vietnam, using MODIS time-series imagery. Environ. Monit. Assess. 187, 464. https://doi.org/10.1007/s10661-015-4691-3

van Rossum, G., de Boer, J., 1991. Interactively testing remote servers using the Python programming language. CWI Q. 4, 283–303.

Van Wagner, C.E., 1987. Development and structure of the Canadian Forest Fire Weather Index System. Canadian Forestry Service, Ottawa.

Van Wagner, C.E., 1977. Conditions for the start and spread of crown fire. Can. J. For. Res. 7, 23–34. https://doi.org/10.1139/x77-004

van Zyl, J.J., 2001. The Shuttle Radar Topography Mission (SRTM): a breakthrough in remote sensing of topography. Acta Astronaut. 48, 559–565. https://doi.org/10.1016/S0094-5765(01)00020-0

Veraverbeke, S., Dennison, P., Gitas, I., Hulley, G., Kalashnikova, O., Katagis, T., Kuai, L., Meng, R., Roberts, D., Stavros, N., 2018. Hyperspectral remote sensing of fire: State-of-the-art and future perspectives. Remote Sens. Environ. 216, 105–121. https://doi.org/10.1016/j.rse.2018.06.020

Veraverbeke, S., Verstraeten, W.W., Lhermitte, S., Van De Kerchove, R., Goossens, R., 2012. Assessment of post-fire changes in land surface temperature and surface albedo, and their relation with fire-burn severity using multitemporal MODIS imagery. Int. J. Wildl. Fire 21, 243–256. https://doi.org/10.1071/WF10075

Verbesselt, J., Fleck, S., Coppin, P., 2002. Estimation of fuel moisture content towards fire risk assessment: a review, in: Viegas, D.X. (Ed.), Forest Fire Research & Wildland Fire Safety. pp. 1–11.

Verbesselt, J., Somers, B., Lhermitte, S., Jonckheere, I., van Aardt, J., Coppin, P., 2007. Monitoring herbaceous fuel moisture content with SPOT VEGETATION time-series for fire risk prediction in savanna ecosystems. Remote Sens. Environ. 108, 357–368.

https://doi.org/10.1016/j.rse.2006.11.019

Verhoef, W., 1996. Application of Harmonic Analysis of NDVI Time Series (HANTS), in: Azzali, S., Menenti, M. (Eds.), Fourier Analysis of Temporal NDVI in the Southern African and American Continents. Wageningen, pp. 19–24.

Verhoef, W., 1984. Light scattering by leaf layers with application to canopy reflectance modeling: The SAIL model. Remote Sens. Environ. 16, 125–141. https://doi.org/10.1016/0034-4257(84)90057-9

Verhoef, W., Jia, L., Xiao, Q., Su, Z., 2007. Unified optical-thermal four-stream radiative transfer theory for homogeneous vegetation canopies. IEEE Trans. Geosci. Remote Sens. 45, 1808–1822. https://doi.org/10.1109/TGRS.2007.895844

Verhoef, W., Menenti, M., Azzali, S., 1996. A colour composite of NOAA-AVHRR-NDVI based on time series analysis (1981-1992). Int. J. Remote Sens. 17, 231–235. https://doi.org/10.1080/01431169608949001

Vermote, E.F., El Saleous, N., Justice, C.O., Kaufman, Y.J., Privette, J.L., Remer, L., Roger, J.C., Tanré, D., 1997. Atmospheric correction of visible to middle-infrared EOS-MODIS data over land surfaces: background, operational algorithm and validation. J. Geophys. Res. Atmos. 102, 17131–17141. https://doi.org/10.1029/97JD00201

Vermote, E.F., Roger, J.-C., Ray, J.P., 2015. MODIS surface reflectance user's guide - Collection 6.

Vermote, E.F., Vermeulen, A., 1999. MODIS ATBD - Atmospheric correction algorithm: spectral reflectances (MOD09).

Verrelst, J., Camps-Valls, G., Muñoz-Marí, J., Rivera, J.P., Veroustraete, F., Clevers, J.G.P.W., Moreno, J., 2015. Optical remote sensing and the retrieval of terrestrial vegetation bio-geophysical properties - A review. ISPRS J. Photogramm. Remote Sens. 108, 273–290. https://doi.org/10.1016/j.isprsjprs.2015.05.005

Verstraete, M.M., Pinty, B., 1996. Designing optimal spectral indexes for remote sensing applications. IEEE Trans. Geosci. Remote Sens. 34, 1254–1265. https://doi.org/10.1109/36.536541

Vicente-Serrano, S.M., Gouveia, C., Camarero, J.J., Beguería, S., Trigo, R., López-Moreno, J.I., Azorín-Molina, C., Pasho, E., Lorenzo-Lacruz, J., Revuelto, J., Morán-Tejeda, E., Sanchez-Lorenzo, A., 2013. Response of vegetation to drought time-scales across global land biomes. Proc. Natl. Acad. Sci. 110, 52–57. https://doi.org/10.1073/pnas.1207068110

Vidal, A., Pinglo, F., Durand, H., Devaux-Ros, C., Maillet, A., 1994. Evaluation of a temporal fire risk index in mediterranean forests from NOAA thermal IR. Remote Sens. Environ. 49, 296–303. https://doi.org/10.1016/0034-4257(94)90024-8

Viegas, D.X. (Ed.), 2009. Recent forest fire related accidents in Europe. Office for Official Publications of the European Communities, Luxembourg. https://doi.org/10.2788/50781

Viegas, D.X., Piñol, J., Viegas, M.T., Ogaya, R., 2001. Estimating live fine fuels moisture content using meteorologically-based indices. Int. J. Wildl. Fire 10, 223–240. https://doi.org/10.1071/WF01022

Viegas, D.X., Viegas, M.T., 1994. A relationship between rainfall and burned area for Portugal. Int. J. Wildl. Fire 4, 11–16. https://doi.org/10.1071/WF9940011

Vilà, M., Lloret, F., Ogheri, E., Terradas, J., 2001. Positive fire-grass feedback in Mediterranean Basin woodlands. For. Ecol. Manage. 147, 3–14. https://doi.org/10.1016/S0378-1127(00)00435-7

Viney, N.R., 1991. A review of fine fuel moisture modelling. Int. J. Wildl. Fire 1, 215–234. https://doi.org/10.1071/WF9910215

Vlassova, L., Pérez-Cabello, F., Mimbrero, M.R., Llovería, R.M., García-Martín, A., 2014. Analysis of the relationship between land surface temperature and wildfire severity in a series of Landsat images. Remote Sens. 6, 6136–6162. https://doi.org/10.3390/rs6076136

Walding, N.G., Williams, H.T.P., McGarvie, S., Belcher, C.M., 2018. A comparison of the US National Fire Danger Rating System (NFDRS) with recorded fire occurrence and final fire size. Int. J. Wildl. Fire 27, 99–113. https://doi.org/10.1071/WF17030

Wan, Z., 2014. New refinements and validation of the collection-6 MODIS land-surface temperature/emissivity product. Remote Sens. Environ. 140, 36–45. https://doi.org/10.1016/j.rse.2013.08.027

Wang, L., Qu, J.J., Hao, X., Zhu, Q., 2008. Sensitivity studies of the moisture effects on MODIS SWIR reflectance and vegetation water indices. Int. J. Remote Sens. 29, 7065–7075. https://doi.org/10.1080/01431160802226034

Wang, L., Qu, J.J., Xiong, X., Hao, X., Xie, Y., Che, N., 2006. A new method for retrieving band 6 of Aqua MODIS. IEEE Geosci. Remote Sens. Lett. 3, 267–270. https://doi.org/10.1109/LGRS.2006.869966

Weber, L., Nkemdirim, L., 1998. Palmer's Drought Indices Revisited. Geogr. Ann. Ser. A, Phys. Geogr. 80, 153–172.

Weber, M.G., Stocks, B.J., 1998. Forest fires in the boreal forests of Canada, in: Moreno, J.M. (Ed.), Large Forest Fires. Backhuys Publishers, Leiden, pp. 215–233.

Weber, R.O., 1991. Modelling fire spread through fuel beds. Prog. Energy Combust. Sci. 17, 67–82. https://doi.org/10.1016/0360-1285(91)90003-6

Wells, M.L., O'Leary, J.F., Franklin, J., Michaelsen, J., McKinsey, D.E., 2004. Variations in a regional fire regime related to vegetation type in San Diego County, California (USA). Landsc. Ecol. 19, 139–152. https://doi.org/10.1023/B:LAND.0000021713.81489.a7

Wickham, H., 2016. ggplot2: Elegant Graphics for Data Analysis. Springer-Verlag, New York.

Williams, A.P., Abatzoglou, J.T., 2016. Recent advances and remaining uncertainties in resolving past and future climate effects on global fire activity. Curr. Clim. Chang.

Reports 2, 1–14. https://doi.org/10.1007/s40641-016-0031-0

Wilson, R.A., 1990. Reexamination of Rothermel's fire spread equations in no-wind and no-slope conditions. U.S. Department of Agriculture, Forest Service, Odgen.

Wilson, R.A., 1985. Observations of extinction and marginal burning states in free burning porous fuel beds. Combust. Sci. Technol. 44, 179–193. https://doi.org/10.1080/00102208508960302

Wolfe, R.E., Nishihama, M., Fleig, A.J., Kuyper, J.A., Roy, D.P., Storey, J.C., Patt, F.S., 2002. Achieving sub-pixel geolocation accuracy in support of MODIS land science. Remote Sens. Environ. 83, 31–49. https://doi.org/10.1016/S0034-4257(02)00085-8

Woolley, J.T., 1971. Reflectance and transmittance of light by leaves. Plant Physiol. 47, 656–662. https://doi.org/10.1104/pp.47.5.656

Wooster, M.J., 2003. Fire radiative energy for quantitative study of biomass burning: derivation from the BIRD experimental satellite and comparison to MODIS fire products. Remote Sens. Environ. 86, 83–107. https://doi.org/10.1016/S0034-4257(03)00070-1

Wooster, M.J., Xu, W., Nightingale, T., 2012. Sentinel-3 SLSTR active fire detection and FRP product: Pre-launch algorithm development and performance evaluation using MODIS and ASTER datasets. Remote Sens. Environ. 120, 236–254. https://doi.org/10.1016/j.rse.2011.09.033

Wulder, M.A., Coops, N.C., Roy, D.P., White, J.C., Hermosilla, T., 2018. Land cover 2.0. Int. J. Remote Sens. 39, 4254–4284. https://doi.org/10.1080/01431161.2018.1452075

Xiong, X., Che, N., Barnes, W.L., 2006. Terra MODIS on-orbit spectral characterization and performance. IEEE Trans. Geosci. Remote Sens. 44, 2198–2206. https://doi.org/10.1109/TGRS.2006.872083

Xiong, X., Chiang, K., Sun, J., Barnes, W.L., Guenther, B., Salomonson, V. V., 2009. NASA EOS Terra and Aqua MODIS on-orbit performance. Adv. Sp. Res. 43, 413–422. https://doi.org/10.1016/j.asr.2008.04.008

Xu, Y., Shen, Y., 2013. Reconstruction of the land surface temperature time series using harmonic analysis. Comput. Geosci. 61, 126–132. https://doi.org/10.1016/j.cageo.2013.08.009

Yang, X., Yu, Y., Hu, H., Sun, L., 2018. Moisture content estimation of forest litter based on remote sensing data. Environ. Monit. Assess. 190, 421. https://doi.org/10.1007/s10661-018-6792-2

Yebra, M., Chuvieco, E., 2009a. Generation of a species-specific look-up table for fuel moisture content assessment. IEEE J. Sel. Top. Appl. Earth Obs. Remote Sens. 2, 21–26. https://doi.org/10.1109/JSTARS.2009.2014008

Yebra, M., Chuvieco, E., 2009b. Linking ecological information and radiative transfer models to estimate fuel moisture content in the Mediterranean region of Spain: Solving the

ill-posed inverse problem. Remote Sens. Environ. 113, 2403–2411. https://doi.org/10.1016/j.rse.2009.07.001

Yebra, M., Chuvieco, E., 2009c. Generation of a species-specific look-up table for fuel moisture content assessment. IEEE J. Sel. Top. Appl. Earth Obs. Remote Sens. 2, 21–26. https://doi.org/10.1109/JSTARS.2009.2014008

Yebra, M., Chuvieco, E., Riaño, D., 2008. Estimation of live fuel moisture content from MODIS images for fire risk assessment. Agric. For. Meteorol. 148, 523–536. https://doi.org/10.1016/j.agrformet.2007.12.005

Yebra, M., Dennison, P.E., Chuvieco, E., Riaño, D., Zylstra, P., Hunt, E.R., Danson, F.M., Qi, Y., Jurdao, S., 2013. A global review of remote sensing of live fuel moisture content for fire danger assessment: Moving towards operational products. Remote Sens. Environ. 136, 455–468. https://doi.org/10.1016/j.rse.2013.05.029

Yebra, M., Quan, X., Riaño, D., Rozas Larraondo, P., van Dijk, A.I.J.M., Cary, G.J., 2018. A fuel moisture content and flammability monitoring methodology for continental Australia based on optical remote sensing. Remote Sens. Environ. 212, 260–272. https://doi.org/10.1016/j.rse.2018.04.053

Yilmaz, M.T., Hunt, E.R., Jackson, T.J., 2008. Remote sensing of vegetation water content from equivalent water thickness using satellite imagery. Remote Sens. Environ. 112, 2514–2522. https://doi.org/10.1016/j.rse.2007.11.014

Yool, S., 2009. Broad-scale monitoring of live fuel moisture. Geogr. Compass 3, 1703–1716. https://doi.org/10.1111/j.1749-8198.2009.00267.x

Yu, B., Chen, F., Li, B., Wang, L., Wu, M., 2017. Fire risk prediction using remote sensed products: a case of Cambodia. Photogramm. Eng. Remote Sens. 83, 19–25. https://doi.org/10.14358/PERS.83.1.19

Zarco-Tejada, P.J., Rueda, C.A., Ustin, S.L., 2003. Water content estimation in vegetation with MODIS reflectance data and model inversion methods. Remote Sens. Environ. 85, 109–124. https://doi.org/10.1016/S0034-4257(02)00197-9

Zhang, K., Kimball, J.S., Nemani, R.R., Running, S.W., Hong, Y., Gourley, J.J., Yu, Z., 2015. Vegetation greening and climate change promote multidecadal rises of global land evapotranspiration. Sci. Rep. 5, 15956. https://doi.org/10.1038/srep15956

Zheng, Z., Zeng, Y., Li, S., Huang, W., 2016. A new burn severity index based on land surface temperature and enhanced vegetation index. Int. J. Appl. Earth Obs. Geoinf. 45, 84–94. https://doi.org/10.1016/j.jag.2015.11.002

Zhou, J., Jia, L., Menenti, M., 2015. Reconstruction of global MODIS NDVI time series: Performance of Harmonic ANalysis of Time Series (HANTS). Remote Sens. Environ. 163, 217–228. https://doi.org/10.1016/j.rse.2015.03.018

Zumbrunnen, T., Bugmann, H., Conedera, M., Bürgi, M., 2008. Linking forest fire regimes and climate - A historical analysis in a dry inner alpine valley. Ecosystems 12, 73–86. https://doi.org/10.1007/s10021-008-9207-3

Zweifel, R., Rigling, A., Dobbertin, M., 2009. Species-specific stomatal response of trees to drought - a link to vegetation dynamics? J. Veg. Sci. 20, 442–454. https://doi.org/10.1111/j.1654-1103.2009.05701.x

About the author



Carmine Maffei received the *Diploma di Laurea* (MSc) in Aerospace Engineering from the University of Naples Federico II, Italy, in 2001, after defending a dissertation on the classification of forest species from airborne hyperspectral remote sensing datasets. He joined Delft University of Technology in 2009 as a guest PhD candidate in the Department of Geoscience and Remote Sensing to conduct a study titled "Remote sensing-based prediction of forest fire characteristics", supervised by Prof. Massimo Menenti and Dr Roderik Lindenbergh.

In 2001 he worked on a short contract at the Royal Holloway, University of London (Egham, United Kingdom). From 2001 to 2004, he worked at the Institute for Agricultural and Forest Systems in the Mediterranean (Ercolano, Italy), part of the National Research Council. From 2004 to 2006, he worked in the Department of Engineering at the University of Sannio (Benevento, Italy). From 2006 to 2014, he worked at MARSec, Mediterranean Agency for Remote Sensing and Environmental Control (Benevento, Italy). From 2014 to 2017, he worked at BENECON, Regional Competence Centre for the Cultural Heritage, the Ecology, and the Economy (Frignano, Italy). He is currently with the University of Leicester (United Kingdom), where he instigates and leads strategic partnerships and multi-disciplinary, multi-stakeholder innovation projects, leveraging national and international programmes linking skills and businesses to accelerate the growth of the Earth Observation downstream services industry. His research interests are in the optical and thermal remote sensing of land, radiative transfer models of the soil-plant-atmosphere system, time series analysis, statistical modelling, and data science.

Mr Maffei is member of IEEE Geoscience and Remote Sensing Society, Remote Sensing & Photogrammetry Society, *Associazione Italiana Telerilevamento* (Italian Society of Remote Sensing), and International Association of Wildland Fire. He served, among the others, in the Board of the Space Technology Applications from Research (STAR) programme and in the Advisory Board of the East Midlands Centre of Excellence in Satellite Applications (EMCoE).

List of publications

Articles in peer-reviewed journals

[*]**Maffei, C.**, Lindenbergh, R., Menenti, M., 2021. Combining multi-spectral and thermal remote sensing to predict forest fire characteristics. ISPRS J. Photogramm. Remote Sens. 181, 400-412. https://doi.org/10.1016/j.isprsjprs.2021.09.016

Li, J., Zhao, Y., Bates, P., Neal, J., Tooth, S., Hawker, L., **Maffei, C.**, 2020. Digital Elevation Models for topographic characterisation and flood flow modelling along low-gradient, terminal dryland rivers: a comparison of spaceborne datasets for the Río Colorado, Bolivia. J. Hydrol. 591, 125617. https://doi.org/10.1016/j.jhydrol.2020.125617

Saulino, L., Rita, A., Migliozzi, A., **Maffei, C.**, Allevato, E., Garonna, A.P., Saracino, A., 2020. Detecting burn severity across Mediterranean forest types by coupling medium spatial resolution satellite imagery and field data. Remote Sens. 12, 741. https://doi.org/10.3390/rs12040741

[*]**Maffei, C.**, Menenti, M., 2019. Predicting forest fires burned area and rate of spread from pre-fire multispectral satellite measurements. ISPRS J. Photogramm. Remote Sens. 158, 263-278. https://doi.org/10.1016/j.isprsjprs.2019.10.013

[*]**Maffei, C.**, Alfieri, S.M., Menenti, M., 2018. Relating spatiotemporal patterns of forest fires burned area and duration to diurnal land surface temperature anomalies. Remote Sens. 10, 1777. https://doi.org/10.3390/rs10111777

Li, J., Yang, X., **Maffei, C.**, Tooth, S., Yao, G., 2018. Applying independent component analysis on Sentinel-2 imagery to characterize geomorphological responses to an extreme flood event near the non-vegetated Río Colorado terminus, Salar de Uyuni, Bolivia. Remote Sens. 10, 725. https://doi.org/10.3390/rs10050725

[*]**Maffei, C.**, Menenti, M., 2014. An application of the perpendicular moisture index for the prediction of fire hazard. EARSeL eProc. 13, 13-19. https://doi.org/10.12760/01-2014-1-02

[*] Related to this dissertation.

[*]**Maffei, C.**, Menenti, M., 2014. A MODIS-based perpendicular moisture index to retrieve leaf moisture content of forest canopies. Int. J. Remote Sens. 35, 1829-1845. https://doi.org/10.1080/01431161.2013.879348

[*]**Maffei, C.**, Alfieri, S.M., Menenti, M., 2013. Characterising fire hazard from temporal sequences of thermal infrared MODIS measurements. EARSeL eProc. 12, 1-7. https://doi.org/10.12760/01-2013-1-01

Leone, A.P., Menenti, M., Buondonno, A., Letizia, A., **Maffei, C.**, Sorrentino, G., 2007. A field experiment on spectrometry of crop response to soil salinity. Agric. Water Manag. 89, 39-48. https://doi.org/10.1016/j.agwat.2006.12.004

Book chapters

Maffei, C., 2018. The city and its volcano: remote sensing of the July 2016 large fire in Vesuvius National Park, in: Gambardella, C., Listokin, D. (Eds.), Development and Preservation in Large Cities: An International Perspective. La Scuola di Pitagora Editrice, Napoli, pp. 417-427.

[*]Menenti, M., Ghafarian Malamiri, H.R., Shang, H., Alfieri, S.M., **Maffei, C.**, Jia, L., 2016. Observing the response of terrestrial vegetation to climate variability across a range of time scales by time series analysis of land surface temperature, in: Ban, Y. (Ed.), Multitemporal Remote Sensing: Methods and Applications. Springer International Publishing, Cham, pp. 277-315. https://doi.org/10.1007/978-3-319-47037-5_14

Leone, A.P., Calabrò, G., Coppola, E., **Maffei, C.**, Menenti, M., Tosca, M., Vella, M., Buondonno, A., 2008. Prediction of soil properties with VIS-NIR-SWIR reflectance spectroscopy and artificial neural networks: A case study on three pedoenvironments of the Campania Region, Italy, in: Dazzi, C., Costantini, E. (Eds.), The Soils of Tomorrow: Soils Changing in a Changing World. Catena Verlag, Reiskirchen, pp. 689-702.

Articles in international conference proceedings

Gambardella, C., Pisacane, N., Avella, A., Argenziano, P., **Maffei, C.**, 2016. Low-cost aerial nadir photography and fast georeferencing, in: Han, B., Fan, H., Lin, J., Luo, X. (Eds.), International Conference on Geometry and Graphics ICGG 2016, 137.

Addabbo, P., di Bisceglie, M., Focareta, M., Galdi, C., **Maffei, C.**, Ullo, S.L., 2015. Combination of Landsat and EROS-B satellite images with GPS and LiDAR data for land monitoring. A case study: the Sant'Arcangelo Trimonte dump, in: IEEE International Geoscience and Remote Sensing Symposium IGARSS 2015, pp. 882-885. https://doi.org/10.1109/IGARSS.2015.7325906

[*] Related to this dissertation.

Gambardella, C., Pisacane, N., Avella, A., Argenziano, P., **Maffei, C.**, 2015. Pompei: Multi-scalar multi-sensor nD surveying, in: International Multidisciplinary Scientific GeoConference SGEM 2015, pp. 1119-1126. https://doi.org/10.5593/SGEM2015/B21/S10.143

Gambardella, C., Pisacane, N., Avella, A., Argenziano, P., **Maffei, C.**, 2015. Airborne remote sensing activities in Albania for multitemporal vegetation monitoring, in: International Multidisciplinary Scientific GeoConference SGEM 2015, pp. 957-964. https://doi.org/10.5593/SGEM2015/B21/S10.122

[*]**Maffei, C.**, Gambardella, C., Menenti, M., 2015. Remote sensing evaluation of fire hazard: towards operational tools for improving the security of citizens and protecting the environment, in: Piscitelli, M. (Ed.), Heritage and Technology: Mind Knowledge Experience, pp. 1632-1639.

Addabbo, P., di Bisceglie, M., Focareta, M., **Maffei, C.**, Ullo, S.L., 2015. Integration of satellite observations and ground-based measurements for landfill monitoring, in: IEEE Metrology for Aerospace 2015, pp. 411-415. https://doi.org/10.1109/metroaerospace.2015.7180692

[*]**Maffei, C.**, Bonora, L., Maselli, F., Mangiavillano, A., Menenti, M., 2014. The MODIS-based perpendicular moisture index as a tool for mapping fire hazard: indirect validation in three areas of the Mediterranean, in: Viegas, D.X. (Ed.), Advances in Forest Fire Research, pp. 1017-1023. https://doi.org/10.14195/978-989-26-0884-6_110

[*]**Maffei, C.**, Alfieri, S.M., Menenti, M., 2014. Time series of land surface temperature from daily MODIS measurements for the prediction of fire hazard, in: Viegas, D.X. (Ed.), Advances in Forest Fire Research, pp. 1024-1029. https://doi.org/10.14195/978-989-26-0884-6_111

[*]**Maffei, C.**, Menenti, M., 2013. Remote sensing estimation of vegetation moisture for the prediction of fire hazard, in: Lasaponara, R., Masini, N., Biscione, M. (Eds.), 33rd EARSeL Symposium – Towards Horizon 2020: Earth Observation and Social Perspectives, pp. 731-739.

[*]**Maffei, C.**, Menenti, M., 2012. The potential of remote sensing measurements of canopy reflectance for the evaluation of live fuel moisture content and fire hazard mapping, in: Spano, D., Bacciu, V., Salis, M., Sirca, C. (Eds.), Modelling Fire Behaviour and Risk, pp. 9-14.

[*]**Maffei, C.**, Alfieri, S.M., Menenti, M., 2012. Characterising fire hazard from temporal sequences of thermal infrared MODIS measurements. in: Ban, Y. (Ed.), First International Workshop on Temporal Analysis of Satellite Images, pp. 275-281.

[*]**Maffei, C.**, Menenti, M., 2010. Fire risk assessment: the role of hyperspectral remote sensing, in: Lacoste-Francis, H. (Ed.), Hyperspectral Workshop 2010.

Maffei, C., Leone, A.P., Meoli, G., Calabrò, G., Menenti, M., 2007. Retrieval of canopy moisture content for dynamic fire risk assessment using simulated MODIS bands, in: Neale,

[*] Related to this dissertation.

C.M.U., Owe, M., D'Urso, G. (Eds.), Remote Sensing for Agriculture, Ecosystems, and Hydrology IX – Proceedings of SPIE, 6742, 674205. https://doi.org/10.1117/12.737779

Maffei, C., Leone, A.P., Vella, M., Meoli, G., Tosca, M., Menenti, M., 2007. Retrieval of vegetation moisture indicators for dynamic fire risk assessment with simulated MODIS radiance, in: IEEE International Geoscience and Remote Sensing Symposium IGARSS 2007, pp. 4648-4651. https://doi.org/10.1109/IGARSS.2007.4423894

Maffei, C., Leone, A.P., Vella, M., Meoli, G., Menenti, M., 2006. The use of MODIS-simulated spectral bands for monitoring plant water stress as a help for dynamic fire risk assessment, in: Owe, M., D'Urso, G., Neale, C.M.U., Gouweleeuw, B.T. (Eds.), Remote Sensing for Agriculture, Ecosystems, and Hydrology VIII – Proceedings of SPIE, 6359, 63590Q. https://doi.org/10.1117/12.689905

Maffei, C., Leone, A.P., Menenti, M., Pippi, I., Maselli, F., Antonelli, P., 2005. Retrieval of aerosol optical thickness from PROBA-CHRIS images acquired over a coniferous forest, in: Owe, M., D'Urso, G. (Eds.), Remote Sensing for Agriculture, Ecosystems, and Hydrology VII – Proceedings of SPIE, 5976, 59670J. https://doi.org/10.1117/12.627661

Menenti, M., Maselli, F., Chiesi, M., Benedetti, R., Cristofori, S., Guzzi, D., Magnani, F., Raddi, S., **Maffei, C.** (2004). Multi-angular hyperspectral observations of Mediterranean forest with PROBA-CHRIS, in: Shen, S.S., Lewis, P.E. (Eds.), Imaging Spectrometry X – Proceedings of SPIE, 5546, pp. 204-212. https://doi.org/10.1117/12.559348



ISBN 978-94-6384-275-4

TU Delft